

Yttrium-90 and Rhenium-188 Radiopharmaceuticals for Radionuclide Therapy



IAEA

International Atomic Energy Agency

IAEA RADIOISOTOPES AND RADIOPHARMACEUTICALS SERIES PUBLICATIONS

One of the main objectives of the IAEA Radioisotope Production and Radiation Technology programme is to enhance the expertise and capability of IAEA Member States in deploying emerging radioisotope products and generators for medical and industrial applications in order to meet national needs as well as to assimilate new developments in radiopharmaceuticals for diagnostic and therapeutic applications. This will ensure local availability of these applications within a framework of quality assurance.

Publications in the IAEA Radioisotopes and Radiopharmaceuticals Series provide information in the areas of: reactor and accelerator produced radioisotopes, generators and sealed sources development/production for medical and industrial uses; radiopharmaceutical sciences, including radiochemistry, radiotracer development, production methods and quality assurance/quality control (QA/QC). The publications have a broad readership and are aimed at meeting the needs of scientists, engineers, researchers, teachers and students, laboratory professionals, and instructors. International experts assist the IAEA Secretariat in drafting and reviewing these publications. Some of the publications in this series may also be endorsed or co-sponsored by international organizations and professional societies active in the relevant fields.

There are two categories of publications: the **IAEA Radioisotopes and Radiopharmaceuticals Series** and **IAEA Radioisotopes and Radiopharmaceuticals Reports**.

IAEA RADIOISOTOPES AND RADIOPHARMACEUTICALS SERIES

Publications in this category present guidance information or methodologies and analyses of long term validity, for example protocols, guidelines, codes, standards, quality assurance manuals, best practices and high level technological and educational material.

IAEA RADIOISOTOPES AND RADIOPHARMACEUTICALS REPORTS

In this category, publications complement information published in the IAEA Radioisotopes and Radiopharmaceuticals Series in areas of the: development and production of radioisotopes and generators for medical and industrial applications; and development, production and QA/QC of diagnostic and therapeutic radiopharmaceuticals. These publications include reports on current issues and activities such as technical meetings, the results of IAEA coordinated research projects, interim reports on IAEA projects, and educational material compiled for IAEA training courses dealing with radioisotope and radiopharmaceutical related subjects. In some cases, these reports may provide supporting material relating to publications issued in the IAEA Radioisotopes and Radiopharmaceuticals Series.

All of these publications can be downloaded cost free from the IAEA web site:

<http://www.iaea.org/Publications/index.html>

Further information is available from:

Marketing and Sales Unit
International Atomic Energy Agency
Vienna International Centre
PO Box 100
1400 Vienna, Austria

Readers are invited to provide feedback to the IAEA on these publications. Information may be provided through the IAEA web site, by mail at the address given above, or by email to:

Official.Mail@iaea.org

YTTRIUM-90 AND RHENIUM-188
RADIOPHARMACEUTICALS FOR
RADIONUCLIDE THERAPY

The following States are Members of the International Atomic Energy Agency:

AFGHANISTAN	GHANA	OMAN
ALBANIA	GREECE	PAKISTAN
ALGERIA	GUATEMALA	PALAU
ANGOLA	HAITI	PANAMA
ARGENTINA	HOLY SEE	PAPUA NEW GUINEA
ARMENIA	HONDURAS	PARAGUAY
AUSTRALIA	HUNGARY	PERU
AUSTRIA	ICELAND	PHILIPPINES
AZERBAIJAN	INDIA	POLAND
BAHAMAS	INDONESIA	PORTUGAL
BAHRAIN	IRAN, ISLAMIC REPUBLIC OF	QATAR
BANGLADESH	IRAQ	REPUBLIC OF MOLDOVA
BELARUS	IRELAND	ROMANIA
BELGIUM	ISRAEL	RUSSIAN FEDERATION
BELIZE	ITALY	RWANDA
BENIN	JAMAICA	SAN MARINO
BOLIVIA	JAPAN	SAUDI ARABIA
BOSNIA AND HERZEGOVINA	JORDAN	SENEGAL
BOTSWANA	KAZAKHSTAN	SERBIA
BRAZIL	KENYA	SEYCHELLES
BRUNEI DARUSSALAM	KOREA, REPUBLIC OF	SIERRA LEONE
BULGARIA	KUWAIT	SINGAPORE
BURKINA FASO	KYRGYZSTAN	SLOVAKIA
BURUNDI	LAO PEOPLE'S DEMOCRATIC REPUBLIC	SLOVENIA
CAMBODIA	LATVIA	SOUTH AFRICA
CAMEROON	LEBANON	SPAIN
CANADA	LESOTHO	SRI LANKA
CENTRAL AFRICAN REPUBLIC	LIBERIA	SUDAN
CHAD	LIBYA	SWAZILAND
CHILE	LIECHTENSTEIN	SWEDEN
CHINA	LITHUANIA	SWITZERLAND
COLOMBIA	LUXEMBOURG	SYRIAN ARAB REPUBLIC
CONGO	MADAGASCAR	TAJIKISTAN
COSTA RICA	MALAWI	THAILAND
CÔTE D'IVOIRE	MALAYSIA	THE FORMER YUGOSLAV REPUBLIC OF MACEDONIA
CROATIA	MALI	TOGO
CUBA	MALTA	TRINIDAD AND TOBAGO
CYPRUS	MARSHALL ISLANDS	TUNISIA
CZECH REPUBLIC	MAURITANIA, ISLAMIC REPUBLIC OF	TURKEY
DEMOCRATIC REPUBLIC OF THE CONGO	MAURITIUS	UGANDA
DENMARK	MEXICO	UKRAINE
DOMINICA	MONACO	UNITED ARAB EMIRATES
DOMINICAN REPUBLIC	MONGOLIA	UNITED KINGDOM OF GREAT BRITAIN AND NORTHERN IRELAND
ECUADOR	MONTENEGRO	UNITED REPUBLIC OF TANZANIA
EGYPT	MOROCCO	UNITED STATES OF AMERICA
EL SALVADOR	MOZAMBIQUE	URUGUAY
ERITREA	MYANMAR	UZBEKISTAN
ESTONIA	NAMIBIA	VENEZUELA, BOLIVARIAN REPUBLIC OF
ETHIOPIA	NEPAL	VIET NAM
FIJI	NETHERLANDS	YEMEN
FINLAND	NEW ZEALAND	ZAMBIA
FRANCE	NICARAGUA	ZIMBABWE
GABON	NIGER	
GEORGIA	NIGERIA	
GERMANY	NORWAY	

The Agency's Statute was approved on 23 October 1956 by the Conference on the Statute of the IAEA held at United Nations Headquarters, New York; it entered into force on 29 July 1957. The Headquarters of the Agency are situated in Vienna. Its principal objective is "to accelerate and enlarge the contribution of atomic energy to peace, health and prosperity throughout the world".

IAEA RADIOISOTOPES AND RADIOPHARMACEUTICALS SERIES No. 5

YTTRIUM-90 AND RHENIUM-188
RADIOPHARMACEUTICALS FOR
RADIONUCLIDE THERAPY

INTERNATIONAL ATOMIC ENERGY AGENCY
VIENNA, 2015

COPYRIGHT NOTICE

All IAEA scientific and technical publications are protected by the terms of the Universal Copyright Convention as adopted in 1952 (Berne) and as revised in 1972 (Paris). The copyright has since been extended by the World Intellectual Property Organization (Geneva) to include electronic and virtual intellectual property. Permission to use whole or parts of texts contained in IAEA publications in printed or electronic form must be obtained and is usually subject to royalty agreements. Proposals for non-commercial reproductions and translations are welcomed and considered on a case-by-case basis. Enquiries should be addressed to the IAEA Publishing Section at:

Marketing and Sales Unit, Publishing Section
International Atomic Energy Agency
Vienna International Centre
PO Box 100
1400 Vienna, Austria
fax: +43 1 2600 29302
tel.: +43 1 2600 22417
email: sales.publications@iaea.org
<http://www.iaea.org/books>

© IAEA, 2015

Printed by the IAEA in Austria

January 2015

STI/PUB/1662

IAEA Library Cataloguing in Publication Data

Yttrium-90 and Rhenium-188 radiopharmaceuticals for radionuclide therapy. —

Vienna : International Atomic Energy Agency, 2015.

p. ; 24 cm. — (IAEA radioisotopes and radiopharmaceuticals series, ISSN 2077-6462 ; no. 5)

STI/PUB/1662

ISBN 978-92-0-103814-2

Includes bibliographical references.

1. Radionuclide generators.
2. Radioisotopes.
3. Radiopharmaceuticals.
4. Yttrium — Isotopes — Therapeutic use.
5. Rhenium — Isotopes — Therapeutic use. I. International Atomic Energy Agency. II. Series.

IAEAL

14-00942

FOREWORD

The IAEA helps to promote and support the development of new, more effective approaches to cancer treatment. Radionuclide therapy is a versatile nuclear medicine application using ionizing radiation for the treatment of various degenerative diseases including cancer. In contrast to radiation therapeutic methods, which use an external ion beam source, internal radionuclide therapy is performed by the intravenous administration of radionuclides conjugated to a molecular substrate. In contrast to chemotherapy, radionuclide therapy requires very low mass amounts of the targeting compound. The therapeutic effect is achieved by the ionizing radiation of the radionuclide and not by the pharmacological effect of the carrier molecule. The therapeutically effective radiation dose is determined by the physical characteristics of the radionuclide. Results show that radionuclides with long range beta emission, such as ^{188}Re and ^{90}Y , are the most efficient agents for irradiation of larger tumours.

Another advantage of radionuclide therapy compared with other types of cancer therapy is the possibility to determine selective accumulation in the targeted tissue by imaging using single photon computed tomography or positron emission tomography after the injection of diagnostic compounds that are structurally identical to the therapeutic counterpart. These non-invasive imaging methods also allow dose calculation prior to therapy, staging and monitoring of therapeutic efficacy.

The success of radionuclide therapy depends not only on the selection of an appropriate radionuclide but also on the pharmacodynamic and pharmacokinetic properties of the radiolabelled targeting vehicle. As the most sensitive non-invasive modality currently available for the detection and mapping of disease specific biomarkers, nuclear medicine plays a strategic role at the forefront of this trend. Many of these biomarkers or their natural ligands can be translated into potential imaging agents. These agents can be used to demonstrate the presence of appropriate molecular targets, or, when labelled with beta or gamma emitting radionuclides, will also be suitable for targeted radiotherapy.

Following a coordinated research project (CRP) focused on therapeutic radiopharmaceuticals, a CRP titled Development of Radiopharmaceuticals based on ^{188}Re and ^{90}Y for Radionuclide Therapy was initiated, aimed at stimulating research on the use of these two high energy beta emitters for developing new therapeutic radiopharmaceuticals. Emphasis was also given to the development of reliable and efficient quality control methods for determination of the radionuclidic purity of the radionuclide solutions employed in the production of the final therapeutic agents. Results of these investigations and some important experimental protocols are described in this report, which also includes a general introduction to the principles and concepts of radionuclide therapy.

The contributions of R. Mikołajczak (Poland) and M. Kameswaran (India) in compiling and editing this publication are gratefully acknowledged. The IAEA officer responsible for this publication was A. Duatti of the Division of Physical and Chemical Sciences.

EDITORIAL NOTE

This report does not address questions of responsibility, legal or otherwise, for acts or omissions on the part of any person.

Although great care has been taken to maintain the accuracy of information contained in this publication, neither the IAEA nor its Member States assume any responsibility for consequences which may arise from its use.

The use of particular designations of countries or territories does not imply any judgement by the publisher, the IAEA, as to the legal status of such countries or territories, of their authorities and institutions or of the delimitation of their boundaries.

The mention of names of specific companies or products (whether or not indicated as registered) does not imply any intention to infringe proprietary rights, nor should it be construed as an endorsement or recommendation on the part of the IAEA.

The authors are responsible for having obtained the necessary permission for the IAEA to reproduce, translate or use material from sources already protected by copyrights.

Material prepared by authors who are in contractual relation with governments is copyrighted by the IAEA, as publisher, only to the extent permitted by the appropriate national regulations.

This publication has been prepared from the original material as submitted by the authors. The views expressed do not necessarily reflect those of the IAEA, the governments of the nominating Member States or the nominating organizations.

The IAEA has no responsibility for the persistence or accuracy of URLs for external or third party Internet web sites referred to in this book and does not guarantee that any content on such web sites is, or will remain, accurate or appropriate

Guidance provided here, describing good practices, represents expert opinion but does not constitute recommendations made on the basis of a consensus of Member States.

CONTENTS

CHAPTER 1. INTRODUCTION	1
1.1. Background	1
1.2. Objectives	2
1.3. Summary of achievements	2
CHAPTER 2. FUNDAMENTAL CONCEPTS IN RADIONUCLIDE THERAPY	9
<i>K. Schomäcker</i>	
2.1. Introduction	9
2.2. Radionuclides	11
2.3. Vehicle molecules	14
2.4. Closing remarks	24
References to Chapter 2	26
CHAPTER 3. DEVELOPMENT OF RADIOPHARMACEUTICALS BASED ON ^{188}Re AND ^{90}Y FOR RADIONUCLIDE THERAPY AT IPEN-CNEN/SP	31
<i>J.A. Osso, Jr., G. Barrio, C.R.B.R. Dias, T.P. Brambilla, D.M. Dantas, K.N. Suzuki, A.B. Barbezan, N.P. Reis, T.A. Felix, M.F.S. Barboza, N.T. Fukumori, J. Mengatti</i>	
3.1. Strontium-90/yttrium-90 generators	31
3.2. Molecules labelled with ^{188}Re	44
References to Chapter 3	54
CHAPTER 4. EVALUATION OF THE $^{90}\text{Sr}/^{90}\text{Y}$ ELECTROCHEMICAL GENERATOR KAMADHENU AND USE OF ITS ^{90}Y ELUATE FOR LABELLING MABs	55
<i>A. Alberti, J. Comor, A. Cruz, R. Leyva, I. Hernández, A. Perera</i>	
4.1. Introduction	56
4.2. Materials and methods	56

4.3. Results	59
4.4. Conclusion	68
4.5. Recommendations and future work	69
References to Chapter 4	69
CHAPTER 5. PRECLINICAL EVALUATION OF ⁹⁰ Y LABELLED RITUXIMAB AND ERIC-1: TWO ANTIBODIES FOR TUMOUR THERAPY	70
<i>K. Schomäcker, T. Fischer</i>	
5.1. Experiments	71
References to Chapter 5	81
CHAPTER 6. DEVELOPMENT OF RADIOPHARMACEUTICALS BASED ON ¹⁸⁸ Re AND ⁹⁰ Y FOR RADIONUCLIDE THERAPY AT BARC	82
<i>U. Pandey, M. Kameswaran, S. Subramanian, R. Chakravarty, H.D. Sarma, G. Samuel, A. Dash, M. Venkatesh, M.R.A. Pillai</i>	
6.1. Validation of the EPC technique for determination of ⁹⁰ Sr contamination in ⁹⁰ Y eluted from ⁹⁰ Sr/ ⁹⁰ Y generator systems	82
6.2. Preparation and bioevaluation studies of ⁹⁰ Y labelled rituximab and TheraCIM antibodies	87
6.3. Yttrium-90 radiopharmaceuticals for liver cancer	99
References to Chapter 6	105
CHAPTER 7. DEVELOPMENT OF THERAPEUTIC RADIOPHARMACEUTICALS BASED ON ⁹⁰ Y BIOTIN	107
<i>L. Garaboldi, M. Chinol</i>	
7.1. Introduction	107
7.2. Materials and methods	109
7.3. Results	112

7.4. Discussion.....	114
7.5. Conclusion.....	117
References to Chapter 7.....	118
CHAPTER 8. LABELLING OF BIOTIN WITH ^{188}Re	120
<i>M. Pasquali, E. Janevik, L. Uccelli, A. Boschi,</i>	
<i>A. Duatti</i>	
8.1. Introduction.....	121
8.2. Design of ^{188}Re biotin complexes.....	122
8.3. Development of a kit formulation for biotinylated ^{188}Re complexes.....	125
8.4. Biological evaluation.....	128
8.5. Experiments.....	130
References to Chapter 8.....	132
CHAPTER 9. DEVELOPMENT OF RADIOPHARMACEUTICALS BASED ON ^{188}Re AND ^{90}Y FOR RADIONUCLIDE THERAPY IN POLAND.....	134
<i>D. Pawlak, T. Dziel, A. Muklanowicz, J.L. Parus,</i>	
<i>P. Garnuszek, W. Mikołajczak, M. Maurin,</i>	
<i>J. Pijarowska, A. Jaron, U. Karczmarczyk,</i>	
<i>E. Laszuk, A. Korsak, E. Jakubowska,</i>	
<i>E. Byszewska-Szpocinska, R. Mikołajczak</i>	
9.1. Determination of ^{90}Sr contamination in ^{90}Y eluate using solid phase extraction on a DGA column.....	134
9.2. Comparison of methods for chromatographic separation of DMSA complexes with $^{99\text{m}}\text{Tc}$ and ^{188}Re at (III) and (V) oxidation states; implications of product development (in collaboration with Vinča Institute of Nuclear Sciences, Belgrade, Serbia).....	137
9.3. Rhenium-188 radiolabelling of DPA ale (in collaboration with Division of Imaging Sciences, King's College London, UK).....	140
9.4. Development of a method for preparation of human serum albumin microspheres for labelling with ^{188}Re and ^{90}Y	147

9.5. Colloids for radiosynovectomy	155
9.6. Biotinylation of monoclonal antibodies and radiolabelling of biotin as a target and effector agent for pretargeting strategy in radioimmunotherapy of cancer.	163
References to Chapter 9	166

CHAPTER 10. DEVELOPMENT, PREPARATION AND QUALITY ASSURANCE OF RADIOPHARMACEUTICALS BASED ON ¹⁸⁸ Re AND ⁹⁰ Y FOR RADIONUCLIDE THERAPY: IN HOUSE PRODUCTION OF RADIOISOTOPES AT VINČA INSTUTE OF NUCLEAR SCIENCES	169
<i>D. Djokić, N.S. Nikolić, D.L. Janković, S.D. Vranješ-Djurić, D.Ž. Petrović</i>	

10.1. Introduction	169
10.2. Rhenium-188 labelled bone seeking and tumour specific agents for radionuclide therapy	170
10.3. Yttrium-90 labelled bone seeking and tumour specific agents for radionuclide therapy	177
10.4. Development of ⁹⁰ Sr/ ⁹⁰ Y generator systems	198
References to Chapter 10	204

CHAPTER 11. LOCAL DEVELOPMENT OF ⁹⁰ Y/ ⁹⁰ Sr GENERATORS AND ⁹⁰ Y RADIOPHARMACEUTICALS IN THE SYRIAN ARAB REPUBLIC	206
<i>T. Yassine, H. Mukhallalati</i>	

11.1. Introduction	206
11.2. Materials	207
11.3. Methods	208
11.4. Yttrium-90 MABs	215
11.5. Yttrium-90 EDTMP	221
11.6. FHMA labelling with ⁹⁰ Y	223
11.7. Conclusion	227
References to Chapter 11	227

CHAPTER 12. DEVELOPMENT OF $^{90}\text{Sr}/^{90}\text{Y}$ GENERATORS AND RADIOPHARMACEUTICALS USING ^{90}Y	229
<i>N. Poramatikul, J. Sangsuriyan, W. Sriweing, P. Kaeopookum, A. Chantawong, S. Yaset</i>	
12.1. Experiments	230
12.2. Results	233
12.3. Conclusion	237
References to Chapter 12	238
 CHAPTER 13. BIFUNCTIONAL BISPHTHONATE COMPLEXES OF $^{99\text{m}}\text{Tc}$ AND ^{188}Re FOR DIAGNOSIS AND THERAPY OF BONE METASTASES	239
<i>R.T.M. De Rosales, D.J. Berry, P.J. Blower</i>	
13.1. Introduction	239
13.2. Materials and results	242
13.3. Conclusion	258
References to Chapter 13	258
 CHAPTER 14. DEVELOPMENT OF $^{90}\text{Sr}/^{90}\text{Y}$ GENERATOR SYSTEMS BASED ON SLM TECHNIQUES FOR RADIOLABELLING OF THERAPEUTIC BIOMOLECULES WITH ^{90}Y	262
<i>N.T. Thu, D. Van Dong, B. Van Cuong, C. Van Khoa, V.T. Cam Hoa</i>	
14.1. Introduction	262
14.2. Materials	263
14.3. Methods	263
14.4. Results	268
14.5. Conclusion and suggestions	284
References to Chapter 14	284

ANNEX:	PROTOCOLS DEVELOPED UNDER THE COORDINATED RESEARCH PROJECT 'DEVELOPMENT OF THERAPEUTIC RADIOPHARMACEUTICALS BASED ON ¹⁸⁸ Re AND ⁹⁰ Y FOR RADIONUCLIDE THERAPY'	287
	CONTRIBUTORS TO DRAFTING AND REVIEW	301

Chapter 1

INTRODUCTION

1.1. BACKGROUND

The major goal of the coordinated research project (CRP) Development of Therapeutic Radiopharmaceuticals based on ^{188}Re and ^{90}Y for Radionuclide Therapy was to exploit advancements in radionuclide production technology, labelling and quality control methods employed in the preparation of ^{188}Re and ^{90}Y radiopharmaceuticals that have potential applications in the therapy of various cancers. To meet the requirements for future expansion and to sustain the growth of the application of radionuclide therapy, it is important to ensure and maintain a reliable supply of therapeutic radionuclides that have the required characteristics of high specific activity and high radionuclidic and chemical purity. Generator produced radionuclides are an attractive option for large scale, on-site availability of therapeutic radioisotopes. Therapeutic radiopharmaceuticals labelled with radionuclides withdrawn from locally produced generators can ensure the wide accessibility of this type of cancer treatment in Member States. Under a previous IAEA CRP Development of Generator Technologies for Therapeutic Radionuclides, relevant technologies for the production of $^{188}\text{W}/^{188}\text{Re}$ and $^{90}\text{Sr}/^{90}\text{Y}$ generators were transferred to Member States. Reactor produced ^{188}W was provided as a radiochemical to the participant groups. The optimization of elution parameters of the $^{188}\text{W}/^{188}\text{Re}$ generator to yield no carrier added ^{188}Re in high specific activity was an important achievement of the CRP. Protocols and quality control procedures were also developed for increasing the radionuclidic purity of ^{90}Y eluates. These procedures included column based extraction chromatography, supported liquid membrane (SLM) techniques and an electrochemical method for separating ^{90}Y from ^{90}Sr . The issue of ^{90}Sr estimation in ^{90}Y solutions has been addressed by devising a new analytical method based on extraction paper chromatography (EPC) coupled with liquid scintillation counting.

To be approved for routine checking of the quality of therapeutic radiopharmaceuticals administered to patients, the above methods would need further development and careful validation. In this context, this CRP was formulated to focus on further validation of quality control methods for ^{188}Re and ^{90}Y generator eluates, and, specifically, to focus on optimization of separation technologies of ^{90}Y from the parent radionuclide ^{90}Sr . A parallel programme was undertaken to investigate the design of new, site specific therapeutic radiopharmaceuticals prepared through the labelling of relevant biomolecules with ^{188}Re and ^{90}Y . In fact, there are a number of carrier molecules available that can

be advantageously used for the preparation of therapeutic radiopharmaceuticals that target different cancers. These comprise antibodies, peptides and small sized biomolecules. This programme was intended to support further acceleration of research prospects for developing ^{188}Re and ^{90}Y radiopharmaceuticals in Member States.

The first research coordination meeting (RCM) of the CRP was held at POLATOM, Warsaw, Poland, from 30 June to 4 July 2008. The meeting reviewed the work of the different participating laboratories and the drafted work plan. The second RCM of the CRP was held from 22 to 26 March 2010 at IAEA Headquarters in Vienna, Austria. The purpose of the meeting was to review the progress of the work done during the first 18 months, to make any necessary mid-term corrections and to formulate the work plan for the second half of the CRP. The last RCM of the CRP took place from 28 November to 2 December 2011 at IAEA Headquarters. During the meeting, the participant countries presented a comprehensive summary of their activities carried out within the whole period of the CRP and highlighted the main achievements. A critical analysis has been devoted to address problems and challenges that prevented full achievement of the expected outputs. Future perspectives and recommendations for promoting new projects in the field have also been extensively discussed.

1.2. OBJECTIVES

The overall objective of the CRP was linked to the main project 2.5.1.3. (2008–2009) Cost Effective Therapeutic Radiopharmaceuticals Development, which was aimed at finding solutions to meet the specific clinical needs of the developing world in the area of cancer treatment through the development of radioisotopic based techniques capable of promoting both the research and clinical application of locally produced radiopharmaceuticals. The specific objectives were to develop radiopharmaceuticals for targeted therapy using ^{188}Re and ^{90}Y and to study the performance of generators with long lived parent radionuclides, as well as to validate quality control procedures for estimating the purity of generator eluates.

1.3. SUMMARY OF ACHIEVEMENTS

1.3.1. Strontium-90/yttrium-90 generators

During this CRP, different types of equipment for recovering ^{90}Y from a $^{90}\text{Sr}/^{90}\text{Y}$ generator were developed and used by the participant groups. These

devices were designed to improve the radionuclidic purity of the resulting ^{90}Y , and, in particular, to obtain this therapeutic radionuclide almost free from its parent radionuclide ^{90}Sr .

An important achievement of the CRP was the development of the so-called $^{90}\text{Sr}/^{90}\text{Y}$ electrochemical generator first proposed by the participating group in India. That group first studied and developed an electrochemical generator using in house supplied ^{90}Y . Based on this scientific work, a prototype of this electrochemical generator was engineered and then supplied to the research group in Cuba for further development and performance optimization. Results obtained showed that the prototype could deliver $^{90}\text{YCl}_3$ with characteristics suitable for labelling of biomolecules such as peptides and antibodies. The various operation parameters, such as electrolyte composition, time of elution and number of purification steps, were tested and standardized, indicating that the system is reliable and reproducible. The generator operated almost 100 runs with activities up to 3.7 GBq (100 mCi). Following the same design, the group in Serbia developed a similar electrochemical generator that was tested using lower ^{90}Y activities.

The groups in the Syrian Arab Republic and Thailand employed extraction chromatography for purification of ^{90}Y generator eluates to yield high quality ^{90}Y . The group in the Syrian Arab Republic upgraded this generator system to allow it to operate up to 7.4 GBq (200 mCi). The final ^{90}Y was produced as a chloride salt in very high chemical and radionuclidic purity. It was further used for labelling peptides, antibodies and small molecules. The group in Thailand designed and fabricated a prototype of this type of generator and checked its performance with activities up to 3.7 GBq (100 mCi).

Generators developed using the SLM technology were employed by India and Viet Nam for routine elution of ^{90}Y . The group in Viet Nam assembled a semiautomatized generator that worked in a sequential mode with activities up to 3.7 GBq. The final ^{90}Y was recovered in the form of acetate salt suitable for further use in the labelling of molecules.

1.3.2. Quality control

A critical issue concerning the use of $^{90}\text{Sr}/^{90}\text{Y}$ generators for therapeutic applications is related to the availability of reliable methods for the determination of ^{90}Sr breakthrough in the final eluate. Because ^{90}Sr is a bone seeking radionuclide, the maximum permissible levels are extremely low and set up to 74 kBq (2 μCi) to prevent excessive body burden. This task is difficult to accomplish because both ^{90}Sr and ^{90}Y are pure β emitters with overlapping β spectra, and conventional techniques are not adequately sensitive for this purpose.

During this CRP, several groups dealt with the measurement of ^{90}Sr content in ^{90}Y samples using the following analytical methodologies:

- (a) EPC (Brazil, Cuba, India, Serbia, Syrian Arab Republic, Thailand, Viet Nam);
- (b) Extraction resin chromatography (Sr-Spec, DGA) (Poland, Syria);
- (c) Cation exchange paper chromatography (Wh P81) (Poland);
- (d) Measurement of the half-life of ^{90}Y with a β counter after allowing complete decay of ^{90}Y (Brazil, Cuba, Syrian Arab Republic);
- (e) Inductively coupled plasma optical emission spectroscopy (ICP OES) (Brazil, Thailand);
- (f) Inductively coupled plasma mass spectroscopy (ICP MS) (Syrian Arab Republic).

Work carried out by the groups in India and Thailand aimed at validating the EPC technology using, in particular, procedures described in the United States Pharmacopeia to validate their results. This method proved to be reliable and reproducible. Owing to limited access to key reagents needed for EPC, several participants investigated alternative solvents and solid supports that allowed for the achievement of good results. Hence, it is expected that the EPC method will prove to be very effective and will be widely applicable in Member States.

The extraction resin chromatographic method was validated in Poland, and a lowest detection limit (DL) of $3 \times 10^{-6}\%$ of ^{90}Sr was achieved in a sample containing 250 MBq of ^{90}Y .

A previously recommended method for indirectly assessing the presence of metallic impurities in ^{90}Y eluates rested on the analysis of results of the ^{90}Y labelling of the peptide 1,4,7,10-tetraazacyclododecane 1,4,7,10-tetraacetic acid (Tyr^3) octreotate (DOTATATE). High labelling yields associated with high specific activity provided robust evidence for a very low content of non-radioactive metals. Further validation studies carried out during the CRP strongly confirmed that this easy to use method constitutes a sensitive tool for qualitative assessment of the metallic purity of ^{90}Y eluates.

1.3.3. Yttrium-90 labelled antibodies

Labelling of various antibodies (rituximab, ERIC1, hR3) with ^{90}Y has been studied using 1,4,7,10-tetraazacyclododecane 1,4,7,10-tetraacetic acid (DOTA) and diethylenetetraminopenta acetic acid (DTPA) as chelating systems for the radiometal. Preliminary work was carried out on the characterization of the antibody after tethering the chelating group to its structure. This involved determination of the number of chelating groups per antibody molecule and

retention of the antibody's target specificity. After labelling, the stability of the resulting conjugate was tested both *in vitro* and *in vivo*, and its affinity for the target tissue, tumour accumulation and potential therapeutic efficacy were evaluated using experimental animal models. Standard procedures employed for this characterization were optimized and implemented by various research groups. In particular, the research groups in Cuba, Germany, India, Poland, the Syrian Arab Republic and Viet Nam, optimized the conjugation of the chelating system to the commercially available antibody rituximab using the bifunctional ligands 2-(4-isothiocyanatobenzyl) 1,4,7,10-tetraazacyclododecane 1,4,7,10-tetraacetic acid (p-SCN-Bn-DOTA), DOTA N-hydroxy succinimidyl (NHS) and DTPA. The group in Germany labelled the antibody ERIC1 with ^{90}Y as a potential candidate for the treatment of neuroblastoma and small cell lung cancer. Labelled ERIC1 was tested in animal models bearing neuroblastoma tumours. Biodistribution data showed high tumour accumulation and reproducible dose dependent tumour response. The optimal dose for complete tumour regression was found to correspond to 2 MBq/animal. The groups in Cuba, India and the Syrian Arab Republic presented preliminary results on labelling of the antibody hR3. Based on extensive experience in the field of antibody labelling, the group in Cuba also provided various protocols that included purification and quality control steps.

1.3.4. Yttrium-90 biotin pretargeting

The aim of this subproject was to demonstrate the advantages of the pretargeting approach when labelled antibodies are employed in cancer therapy. Preliminary work on this subject was performed to optimize the so-called three step pretargeting protocol based on the avidin biotin system in terms of the most appropriate concentration and time of administration of the various reagents.

The group in Italy conducted a preclinical evaluation of a new biotin DOTA conjugate labelled with ^{90}Y . Interestingly, the labelling was carried out using an automatic synthesis module, which afforded the final radiopharmaceutical in high radiochemical purity (RCP) and under sterile and pyrogen free conditions.

A remarkable result was reported by the group in Germany, which revealed that isolated tumour cells accumulated 20-fold higher radioactivity when a biotinylated antibody was employed as compared to a control using a non-biotinylated antibody. This group also performed extensive *in vivo* studies in tumour bearing mice, showing that the pretargeting approach is a promising technique to deliver high doses to the tumour with reduced side effects. Various additional parameters of this approach could still be finely tuned to optimize tumour to background ratios.

1.3.5. Yttrium-90 peptides

Within the scope of implementing the national capacity for local production of therapeutic radiopharmaceuticals, the groups in Serbia and Thailand performed labelling and quality control studies of the peptide based therapeutic agent ^{90}Y DOTATATE, which is currently under advanced clinical evaluation in Europe as a potential treatment for neuroendocrine tumours.

1.3.6. Yttrium-90 labelled particulates

Labelling of macroscopic aggregates still remains an attractive method for local delivery of therapeutic doses of radioactivity. A variety of particulates have been developed and labelled with ^{90}Y , including citrate colloids (Brazil, Poland), hydroxyapatite (HA) aggregates (Brazil, Serbia), human serum albumin (HSA) Sn(II) microspheres (Poland, Serbia, Viet Nam), ferric hydroxide colloids (Syrian Arab Republic), antimony sulphide colloids (Serbia), chromic phosphate colloids (Cuba), surface DOTA derivatized HSA microspheres (Poland and Viet Nam), ^{90}Y oxine lipiodol solutions (India) and plastic Bio-Rex 70 microparticles (India). Because particulate dimensions are crucial in determining the observed biological behaviour, many techniques have been employed to determine the size distribution of the resulting ^{90}Y labelled particles; these techniques include laser diffraction, scanned electron microscopy, optical counting and fractionated filtration. To determine the in vitro stability of labelled particulates, paper thin layer chromatography (TLC) with different eluents was employed as a quality control method after incubation in serum and under different challenging conditions followed by subsequent precipitation and centrifugation of the isolated particles. Groups in Brazil, India, Poland, Serbia and Viet Nam carried out in vivo biodistribution studies in animals to confirm in vivo stability. The first clinical studies were conducted in Brazil and Poland.

Interestingly, the group in Germany reported the observation that some common drugs routinely administered or co-administered to patients undergoing radiosynovectomy are capable of dissolving intra-articular injected ^{90}Y colloids, thus causing a fast washout of radioactivity from the inflamed site as a major drawback preventing achievement of the palliative effect.

1.3.7. Rhenium-188 biotin

A number of novel ^{188}Re labelled biotin conjugates were prepared by the Italian group following different molecular designs, but all were based on the characteristic ^{188}Re nitrido chemical motif. The resulting compounds exhibited high in vitro stability and in vivo inertness towards biotin degradation enzymes.

Binding affinity of these derivatives towards avidin was determined in vitro. Data indicated that affinity remained almost unchanged after labelling with respect to the free biotin. A model experiment aimed at elucidating the in vivo selective uptake by avidin was carried out in mice. This involved the preliminary intramuscular deposition of colloidal particles embedded with avidin, followed by intravenous injection of ^{188}Re labelled biotin. Biodistribution and imaging studies clearly showed that labelled biotin selectively concentrates in the area where avidin colloidal particles were previously distributed. A lyophilized ready to use kit formulation was successfully developed to allow easy on-site hospital preparation of this new therapeutic agent.

1.3.8. Rhenium-188 antibodies

The group in Brazil labelled the antibody rituximab with ^{188}Re following two different approaches: (i) by direct labelling with $[\text{}^{188}\text{ReO}_4]^-$ in the presence of Sn^{2+} as the reducing agent and after cleavage of the antibody's intrinsic disulphide bridges by mercaptoethanol and (ii) through the preliminary formation of the intermediate tricarbonyl metallic fragment $[\text{}^{188}\text{Re}(\text{CO})_3]^+$, which was reacted in turn with the histidine conjugated antibody. The results showed that the tricarbonyl route afforded a more stable radioconjugate with adequate characteristics for further biological evaluation in animal models.

1.3.9. Rhenium-188 bisphosphonates

A series of mononuclear ^{188}Re compounds incorporating a non-coordinated bisphosphonate moiety was prepared by the United Kingdom group using the ^{188}Re tricarbonyl metallic fragment as the labelling system and a dipicolylamine bisphosphonate derivative as the bifunctional ligand. The molecular structure of the resulting mononuclear complex (^{188}Re dipicolylamine alendronate (DPA ale)) was fully characterized. Affinity of the pendant bisphosphonate group for hydroxyapatite (HA) was tested using the structurally identical $^{99\text{m}}\text{Tc}$ analogue, and results showed higher retention of this complex on this inorganic matrix in comparison to the commercial bone seeking agent $^{99\text{m}}\text{Tc}$ methanediylbis(phosphonic acid) (MDP). A preliminary biological evaluation in normal rats demonstrated that ^{188}Re DPA ale concentrated in the skeleton, with the highest uptake in joints, thus confirming that this new agent exhibits strong affinity for bone tissue. Progress was also made in developing a second series of pendant bisphosphonate complexes of technetium and rhenium, comprising the technetium Re(V) nitride core coordinate by two dithiocarbamate ligands, each with a pendant bisphosphonate. Nano single photon emission computed tomography (SPECT) imaging in mice showed that $^{99\text{m}}\text{Tc}$ bis(bisphosphonate)

complex thus prepared shows bone affinity in mice, with bone uptake occurring more slowly but reaching a higher percentage of injected dose per gram weight (%ID/g) than ^{99m}Tc MDP by 150 min postinjection (p.i.); this continued to increase beyond 350 min thereafter, with no significant soft tissue uptake. Again, because of the well defined coordination chemistry, it is expected that the ^{188}Re complex will behave similarly. The two classes of bisphosphonate derivative have also shown outstanding affinity for binding to inorganic nanoparticulate materials (HA and superparamagnetic iron oxides), with potential applications in multimodality imaging and radionuclide therapy.

Preliminary results on the labelling and quality control of the classical bisphosphonate ligands (1-hydroxyethan-1,1-diyl)bis(phosphonic acid) (HEDP) (Serbia), MDP, ethylenediametetrametylenephosphoric acid (EDTMP) and clodronate (Brazil) with both ^{186}Re and ^{188}Re have been reported.

1.3.10. Rhenium-188(V) DMSA

The groups in Poland and Serbia investigated the production of the therapeutic agent $^{188}\text{Re(V)}$ dimercaptosuccinic acid (DMSA) previously proposed for the treatment of medullary carcinoma. The preparation route was devised through a modification of the existing kit formulation currently used for preparing the corresponding ^{99m}Tc analogue $^{99m}\text{Tc(V)}$ DMSA. Using this agent, the group in Serbia started a clinical trial involving a limited number of patients and presented the first results of this study.

Similarly, the group in Brazil conducted a few experiments on the labelling of DMSA with ^{188}Re using two alternative routes: (i) through a commercial kit formulation used for the preparation of the corresponding ^{99m}Tc analogue and (ii) through the oxalate method employed for the efficient reduction of the starting tetraoxo ^{188}Re anion.

Chapter 2

FUNDAMENTAL CONCEPTS IN RADIONUCLIDE THERAPY

K. SCHOMÄCKER

Department of Nuclear Medicine,
University of Cologne,
Cologne, Germany

Abstract

A short overview of the basic concepts and principles of radionuclide therapy is presented in this chapter. After introducing the most important radionuclides currently employed in therapeutic applications and new promising radioisotopes such as α emitters, this review covers the various types of vector molecules and biological approaches for targeting specific cancer cells. These applications include the use of receptor specific pharmacophores such as antibodies and peptides, and DNA targeting agents. The potential advantages of combining methods developed for radionuclide therapy with gene therapy and nanotechnology are also discussed.

2.1. INTRODUCTION

Cancer is now the second most common cause of death worldwide, and is on the rise. It therefore presents a profound human, social and economic problem and an enormous challenge to humankind [2.1]. The increase in malignant tumours has led to a dramatic surge in the development of new cancer treatments. This includes the radionuclide based therapies employed in nuclear medicine. Cancer patients are most commonly treated by external radiotherapy with ionizing radiation. In this approach, only a limited area around the primary tumour is treated through irradiation with high energy X rays. Targeted radionuclide therapy, on the other hand, is more like chemotherapy as it is a systemic treatment, brought about by injecting radioactive substances into the blood circulation. The radiopharmaceuticals suited for this purpose are vehicle molecule radionuclide constructs with high tumour affinity, which can transport toxic doses of radiation to the focus of the disease (tumours and metastases). The tumour specificity of the vehicle molecule is determined by its affinity to target structures (antigens, receptors, etc.). In this way, the ionizing radiation emitted by

radionuclides is used to kill cancer cells by damaging their DNA, thus causing tumours to shrink.

A radiopharmaceutical can be seen as an entity made up of a radionuclide and a vehicle molecule. An ideal radiopharmaceutical for therapeutic purposes must have especially high specificity, broad applicability, accurate targeting capacity and marked cytotoxic potential.

This means that the pharmaceutical should ideally:

- (a) Act exclusively in the cells of malignant tumours;
- (b) Reach all the cells of malignant tumours wherever they are localized;
- (c) Leave healthy tissues and organs unscathed while bringing maximum doses of radiation to the tumour;
- (d) Eliminate malignant tumour cells with great effectiveness.

Points (a)–(c) are determined chiefly by the choice of vehicle molecule, while the cytotoxic potential (d) depends essentially on the radiophysical properties of the radionuclide.

The biological action of a radiopharmaceutical is determined by the form of ionizing radiation emitted by the radionuclide [2.2]. While imaging procedures in nuclear medicine require radionuclides that will emit γ radiation that can penetrate the body, a different class of radionuclides possessing optimal relative biological effectiveness (RBE) is needed for radionuclide therapy. The RBE depends on linear energy transfer (LET), which is defined as the amount of energy transferred to material penetrated by an ionizing particle per unit distance, and is usually measured in kiloelectronvolts per micrometre. The LET is therefore greater when the energy of the ionizing radiation is lower and the distance penetrated is shorter. Thus, the LET is an indirect measure of the number of ionizations per unit of distance traversed and describes the action of any one form of radiation on biological material. As a consequence, comparable qualities of radiation with lower energy will have a shorter range in tissue and thus a higher LET and RBE. Radiation with a lower LET and RBE is described as sparsely ionizing in contrast to densely ionizing forms with higher LET and RBE. In principle, the radionuclides best suited for tumour therapy are those emitting densely ionizing radiation (short penetration into the tissue, with higher LET and RBE) such as α emitters or nuclides producing the Auger effect. These will also cause more intense radiation induced side effects on accumulation outside the tumour. In practice, β emitters that emit more sparsely ionizing radiation have become established as the nuclides of choice. With their directly ionizing electron radiation, they still offer a higher LET and RBE than γ radiation and represent an acceptable compromise between therapeutic efficacy and levels of adverse side effects.

A special characteristic of radiopharmaceuticals for therapeutic applications is that, in addition to their actual toxic radiation effects, they induce so-called bystander or, in the case of β emitters, crossfire effects [2.3–2.5]. This means that neighbouring tumour cells, not directly accessible to the radioactive molecule, can be destroyed. With some radioactive therapeutic agents, the cancerostatic properties produced by the vehicle molecule can be combined with the radiation damage induced by the radionuclide, resulting in a synergistic effect of substrate toxicity and radiation toxicity.

2.2. RADIONUCLIDES

2.2.1. Beta emitters

Although β emitters are normally classified as sparsely ionizing emitters, they are now applied for therapy routinely in clinical practice (see Table 2.1).

TABLE 2.1. SELECTED β EMITTERS FOR RADIONUCLIDE THERAPY

Radionuclide	$T_{1/2}$ ^a	$E_{\beta\max}$ ^b (keV)	$R_{\beta\max}$ ^c (mm)
Lu-177	6.7 d	497	1.8
Cu-67	61.9 h	575	2.1
I-131	8.0 d	606	2.3
Re-186	3.8 d	1077	4.8
Dy-165	2.3 h	1285	5.9
Sr-89	50.5 d	1491	7.0
P-32	14.3 d	1710	8.2
Ho-166	28.8 h	1854	9.0
Re-188	17.0 h	2120	10.4
Y-90	64.1 h	2284	11.3

^a Half-life.

^b Maximum energy of β particles emitted.

^c Maximum range of β particles emitted.

Over the last few decades, the nuclides ^{131}I and ^{90}Y have become well established in nuclear medicine for routine therapeutic applications. Samarium-153, a mixed emitter of β and γ radiation, and ^{89}Sr , a pure β emitter, are used for palliative treatment of bone metastases. Another highly promising radionuclide is ^{177}Lu , which is gradually replacing ^{90}Y for modern peptide based radioreceptor therapy [2.6].

There is no doubt that the feasibility of providing targeted radionuclide therapy anywhere in the world, including developing countries, depends on the availability of the well established β emitting radionuclides that are used routinely in clinical practice. Practicable generator systems for producing these are $^{90}\text{Sr}/^{90}\text{Y}$ and $^{188}\text{W}/^{188}\text{Re}$ generators [2.7, 2.8].

2.2.2. Alpha emitters

Alpha emitters should be able to restrict their toxic effect to a highly localized area. However, efforts still need to be made to prevent accumulations of the nuclide outside the tumour tissue. The range of α particles in soft tissue is only as much as a cell diameter (see Table 2.2).

This raises the exciting possibility that the advantages of cell specific molecular targeting could be combined with those of an effective form of radiation with a restricted focal range to achieve the goal of efficient treatment without side effects [2.9, 2.10]. The LET of α particles emitted, for instance by ^{211}At , is ~ 97 keV/ μm , which is 400 times higher than that of the high energy

TABLE 2.2. ALPHA EMITTERS FOR TARGETED RADIONUCLIDE THERAPY

Radionuclide	$T_{1/2}$ ^a	$E_{\alpha \text{ max}}$ ^b (MeV)	$R_{\alpha \text{ max}}$ ^c (μm)
At-211	2 h	6.79	60.7
Bi-212	61 min	7.80	75
Bi-213	46 min	8.32	84
Ac-225	10 d	6.83	61

^a Half-life.

^b Maximum energy of α particles emitted.

^c Maximum range of α particles emitted.

β particles emitted by ^{90}Y . Numerous studies on cell cultures have demonstrated that with just 1–10 hits by α particles per cell, the cell survival rate is already reduced to 37%. Furthermore, the action of α particles does not depend on the tissue becoming hypoxic, nor is it dependent on the dose rate or phase of the cell cycle.

Although the basic advantages of the radionuclides emitting α radiation have been recognized for some decades, clinical studies of this hugely promising targeted radiotherapy only recently began. The radionuclides of choice here are ^{211}At and ^{213}Bi . Both radionuclides are mostly used for the labelling of antibodies with high tumour affinity in the treatment of patients with leukaemia and brain tumours. Radium-223 has been tested for use in breast and prostate cancer, particularly in patients with bone metastases. Encouraging preliminary results with acceptable levels of activity outside the tumour have been reported [2.11, 2.12].

2.2.3. Radionuclides with the Auger effect

Auger electron emitting radionuclides have a particularly high RBE. On intracellular accumulation, the Auger effect occurs mostly within the cell because of the Auger electron's short range. The Auger effect is only actively destructive when it occurs within the cell, ideally within the DNA or close to it. For this reason, it can be assumed that only a few of the decays of radionuclides producing the Auger effect actually achieve cell destruction. Given this restricted subcellular field of action, it is reasonable to assume that radiopharmaceuticals based on the Auger effect, applied alone or in combination with radionuclides emitting other forms of radiation, could provide radiation therapy optimally tailored to the patient's specific individual needs [2.13].

It is worth noting that the radionuclides producing the Auger effect on electron capture (see Table 2.3) are often used for diagnostic purposes. This has raised concerns that these radionuclides, which are used on a massive scale, might be more radiotoxic than originally expected. Some groups are even considering therapeutic application of $^{99\text{m}}\text{Tc}$ [2.14, 2.15]. Because the majority of $^{99\text{m}}\text{Tc}$ radiopharmaceuticals do not accumulate intracellularly, there would be no concerns here.

TABLE 2.3. AUGER EMITTING RADIONUCLIDES WITH POTENTIAL FOR RADIONUCLIDE THERAPY

Radionuclide	$T_{1/2}$ ^a	N_{Aug} ^b	E_{Aug} ^c (μm)
Ga-67	3.26 d	4.7	6.264
Tc-99m	6.01 h	4.0	0.899
In-111	2.8 d	14.7	6.75
I-123	13.2 h	14.9	7.419
Tl-201	3.04 d	36.9	15.273
I-125	60.1 d	24.9	12.241

^a Half-life.

^b Number of Auger electrons emitted per decay.

^c Medium range of Auger electrons.

2.3. VEHICLE MOLECULES

The ability of vehicle molecules to transport relevant radionuclides into tumour cells or their vicinity can be based on various factors. The radioactive molecule itself may play a role in the metabolism of the target tissue. Compounds used as vehicles may be biologically active substances such as enzyme precursors, components of DNA, amino acids, melanin precursors, antibiotics, cytostatic or metal–ligand complexes, or substrates for tumour cell associated target structures such as antigens and receptors. Recent experimental approaches include attempts to induce or intensify the expression of structures identified as suitable target moieties by genetic modification. Vehicle molecules capable of transporting radionuclides right into tumour cells are of particular interest, as this will allow optimum results to be achieved with short range emitters, namely, maximum action with minimum side effects [2.16].

2.3.1. Exploitation of certain metabolic properties of tumour tissue

2.3.1.1. Iodide and phosphate

The best example of exploiting metabolic properties is the treatment of iodine accumulating thyroid tumours (as iodine metabolizing tissue) with radioactive sodium iodide ($^{131}\text{I-NaI}$), which is currently the most common form of metabolic tumour therapy with open radionuclides and has been in use since the 1940s (see Section 2.4). Another example, rarely used, is the treatment of malignant blood disorders (thrombocythaemia and polycythaemia vera). This exploits the fact that ^{32}P accumulates in the bone marrow of such patients, owing to an overproduction of certain blood cells, as the increased synthesis of nucleic acids raises phosphate consumption.

2.3.1.2. Bone seeking radiopharmaceuticals

Examples of bone seeking products are the radiopharmaceuticals used for palliative pain control in patients with skeletal metastases.

The substance previously applied for this was $\text{Na}_2\text{H}^{32}\text{PO}_4$, and the primary mechanism thought to underlie its action was the facilitated uptake of radiophosphorous into the DNA and ribonucleic acid (RNA). However, the side effects of the treatment raised concerns [2.17].

Following the identification of a series of radionuclides as bone seeking isotopes by Hamilton [2.18], Pecher [2.19] reported a raised concentration of strontium isotopes in the reactive zone of rapid bone growth around an osteogenic sarcoma. The mechanism by which these radionuclides were incorporated in ionic form was an ion exchange process involved in metabolism of the bone. Key research leading to the introduction of ^{89}Sr to routine clinical practice was performed by Firusian [2.20], who also demonstrated the superiority of this method of treatment over ^{32}P therapy. Kutzner et al. [2.21] carried out a clinical study on pain control using ^{90}Y citrate in patients with bone metastases from primary prostate cancer. The main product to become established in clinical practice was ^{153}Sm EDTMP, which becomes highly enriched in bone, particularly at points of growth and in bone lesions. The EDTMP chelate is responsible for the specific uptake into the newly formed bone matrix laid down by osteoblasts [2.22, 2.23]. However, the bone affinity of the radioactive lanthanides simply in ionic form has also been recognized for some time [2.24].

Although none of the ^{188}Re labelled bone pain palliation agents have yet been commercialized, ^{188}Re HEDP has been applied clinically in cancer patients. Here too, the ligand seems to play a more critical role in the incorporation process than the radionuclide [2.8].

2.3.1.3. Targeting of catecholamine producing tumours

Since the development of meta-[¹³¹I]-iodobenzylguanidine (¹³¹I MIBG) by Wieland et al. for nuclear medical procedures [2.25], this radiopharmaceutical has been the subject of intense debate in research journals. Metaiodobenzylguanidine (MIBG) is an analogue of norepinephrine containing the guanidine group of guanethidine. This is probably what enables it to use the same uptake and storage mechanisms as noradrenaline [2.26]. As a consequence of its biological behaviour, MIBG accumulates in various kinds of endocrine tumours, and is used chiefly in the treatment of neuroblastoma in children. The value of this therapeutic element in the framework of an intensive primary treatment is also the focus of intense clinical debate.

2.3.2. DNA targeting

Substances fundamentally suited for the killing of tumour cells would be components of DNA, preferably labelled with α emitters or Auger emitters. The basic effectiveness of this approach has been demonstrated many times in cell cultures. The problem lies in achieving sufficient selectivity on systemic administration [2.27].

Some interesting new approaches addressing this problem are offered by radionuclide based antisense therapy. Using the antisense technique, special RNA molecules can be applied that will diminish or completely block expression of a specific gene within the tumour cells. The antisense RNA (aRNA) is a single stranded RNA molecule that is complementary to messenger RNA (mRNA). The mRNA is transcribed from the non-coding strand (matrices strand) of the DNA. If the complementary strand is also transcribed, this produces an aRNA complementary to the mRNA. Through base pairing with the complementary mRNA, the aRNA blocks its translation within the cell. This technique is used to regulate the expression of individual genes. As a consequence, cellular functions involved in defence mechanisms against radiation damage such as apoptosis or DNA arrest can be down-regulated, which in turn intensifies radiation induced damage.

Balkin et al. developed a ¹⁷⁷Lu labelled anti-BCL2 peptide nucleic acid conjugate designed for dual modality non-Hodgkin lymphoma (NHL) therapy, that is, simultaneous down-regulation of BCL2 mediated resistance to apoptosis and delivery of cytotoxic internally emitted radiation [2.28]. Liu et al. reported that a three component nanoparticle, consisting of a targeting antibody, a transfecting peptide and an anti-RI alpha morpholino antisense oligomer labelled with Auger emitters, provided Auger electron mediated, antisense mediated, cytotoxicity of cells in culture [2.29].

2.3.3. Antibodies

The high specificity and affinity of antibodies to their antigens, that is, the ability antibodies have to react with a specific ‘partner’ (even when it is in very low concentrations and a wide range of other components are present in a millionfold excess), has led to their wide application in basic biochemical research, medical diagnostics and treatments including radioimmunotherapy [2.30].

On its surface, an antigen has a series of ‘foreign structures’ that the organism does not normally possess. Each of these antigen structures stimulates the proliferation of numerous, genetically distinct B lymphocytes. Each mature B cell then forms a clone (i.e. a population of genetically identical daughter cells), and each clone produces a specific antibody. The most diverse antibodies (immunoglobulins), which are carried in the blood serum, also originate from many different clones—in other words, they are polyclonal. Owing to their biochemical heterogeneity (in amino acid composition, particularly in the variable regions), they bind to various antigen structures with differing degrees of affinity. The problem of the diversity of antibodies, and, in particular, the question of whether somatic mutations play a role here, led Köhler and Milstein to perform an experimental study published in 1975 [2.31]. Their aim was to modify an antibody producing cell so that it would replicate itself continuously *in vitro*, thereby displaying any mutations that arose. They achieved this by fusing spleen cells with myeloma cells (cells of a lymphatic tumour) from a mouse of the same genetic type. This laid the foundation for a biological procedure, known today as hybridoma technology, which is used worldwide for the production of monoclonal antibodies (MAbs). It is usually only murine antibodies that are commonly available in a ready to use state. However, their application in humans is not unproblematic. The intramurine induced MAbs are recognized as foreign bodies by the human body and therefore frequently provoke the formation of human antimurine antibodies (HAMAs) after injection. This has complicated and delayed authorization from the United States Food and Drug Administration or the European Medicines Agency for clinical use.

Other factors standing in the way of a broad clinical acceptance of radioimmunotherapy are the fear of secondary malignancies or of myelodysplastic syndrome. It is relatively certain, however, that the risk of this outcome is no higher with radioimmunotherapy than it is with chemotherapy. A widely held concern in relation to radioimmunotherapy is that the haematological toxicity of the radionuclide might lower a patient’s tolerance to chemotherapy. However, studies have been performed that clearly demonstrate the exact opposite.

The stable coupling of metallic radionuclides has been optimized over the last 20 years. DTPA based and macrocyclic DOTA based chelators are mainly used for this purpose [2.32].

2.3.3.1. Haematological malignancies

Although radioimmunotherapy is still not sufficiently recognized as a standalone treatment for follicular lymphoma, an increasing number of clinical studies present evidence of a successful outcome when radioimmunotherapy is included in an overall therapy regime in combination with chemotherapy or, occasionally, with external radiation therapy. Radioimmunoconjugates bound to murine anti-CD20 antibodies for use in the treatment of NHL have been the most thoroughly investigated in clinical studies. The antibody conjugate ^{90}Y ibritumomab tiuxetan (Zevalin) is based on the precursor to rituximab developed in mice and has already been approved in the United States of America and Europe. Another example is ^{131}I tositumomab (Bexxar). It is an IgG2a anti-CD20 MAb derived from immortalized mouse cells.

The efficacy, particularly of Zevalin, has been sufficiently demonstrated in clinical studies. One study of 143 patients with relapsed or chemotherapy refractory, indolent NHL or transformed aggressive NHL [2.33] provides further convincing evidence. An important feature of this study was the randomization of the four weekly doses of rituximab versus ^{90}Y ibritumomab therapy. The overall response rate for the radioimmunoconjugate of 80%, combined with a complete remission rate of 30%, was significantly higher than the corresponding response rates of 56% and 16% recorded for rituximab alone. The tumour responses probably represent the combined result of the action of the unconjugated antibody and the targeted radiation therapy mediated by the antibodies.

There have also been reports from a few centres of successful therapeutic application of ^{131}I rituximab [2.34] for treatment of NHL. Some experience has been gained with clinical application of LYM-1, a mobile anti-HLA DR antibody investigated in the ^{131}I labelled form [2.35]. Further clinical tests have been carried out with an ^{131}I anti-CD45 antibody [2.36] and with ^{90}Y labelled epratuzumab (a humanized anti-CD22 immunoglobulin) [2.37].

New approaches for treating Hodgkin lymphoma have not produced very promising results as yet, and are still in the experimental phase [2.38].

As radioimmunotherapy with β emitting radionuclides raises the risk of myelosuppression, owing to the long range of β particles of the order of millimetres, alternative treatments have been developed using antibodies labelled with α emitters. The first clinical studies trialling such an approach with ^{213}Bi labelled anti-CD33 antibodies for treatment of myeloid leukaemia have now been published [2.39]. However, a limiting factor here is the short half-life of ^{213}Bi . Longer lived α emitters, such as ^{211}At or ^{225}Ac , with half-lives of 7.2 h and 10 d, respectively, offer a better basis for new treatments. Few studies have been carried out on radioimmunoconjugates labelled with Auger electron emitters. A study of internalizable anti-CD74 antibody, labelled with ^{67}Ga or ^{111}In , in Raji

cell cultures, presents one example. These investigations have shown ^{67}Ga to be markedly more effective than ^{111}In [2.40].

2.3.3.2. *Non-haematological malignancies*

Certain properties of solid tumours, such as a lack of sensitivity to radiation, antigen heterogeneity, tumour mass and raised interstitial pressure, which hinder the accumulation of macroglobulins within tumours, present fundamental obstacles to a radioimmunotherapeutic approach.

Clinical trials of new radioimmunotherapeutic approaches to the treatment of solid tumours have been halted at phase 1 or phase 2, because, although therapeutic effects have been demonstrated, the generally accepted criteria for objective proof of a response have not been fulfilled. One radioimmunoconjugate that has reached an advanced stage in clinical trials is pentumomab (R1549; Antisoma PLC), a radioimmunoconjugate with ^{90}Y labelled murine anti-HMFG1 (MUC-1) that is administered intraperitoneally for treatment of ovarian carcinomas [2.41]. Other radioimmunotherapeutic approaches for solid tumours have not yet passed the experimental stage. Preliminary trials with ^{90}Y labelled panitumumab (a humanized antibody) in models of head and neck cancer are worthy of mention here [2.42]. Encouraging results have also been obtained with an ^{131}I labelled antibody against surface antigens found on neuroblastomas or small cell lung carcinomas [2.43].

The intraperitoneal administration of labelled antibodies plays a significant role, particularly in an adjuvant situation or in the case of minimal residual disease in ovarian cancer. Intraperitoneal injection of a combination of taxol, interferon and the TAG72 antibody ^{177}Lu CC49 has been shown to achieve a response with relatively low bone marrow toxicity in a phase 1 study [2.44].

However, in a phase 3 study of patients, after a surgically defined complete remission from an ovarian carcinoma with treatment using ^{90}Y HMFG1, no extension of disease free survival could be shown in comparison to the control group [2.45].

Another example of focal application is in the treatment of brain tumours. Clinical trials have been conducted here with ^{131}I labelled antitenascin antibodies after surgical resection of advanced glioblastomas [2.46].

Investigations with ^{131}I iodine labelled humanized anti-CEACAM5 antibodies showed a marked therapeutic effect in 23 patients with colorectal metastases after resection of the liver [2.47]. Furthermore, a series of feasibility studies have been run on combined radiotherapy and chemotherapy [2.48–2.50].

Most radioimmunotherapeutic investigations are performed with fully intact antibodies. This is not just a consequence of simple production methods and a tendency to adhere to tried and tested handling protocols, but stems from the

fact that radioimmunoconstructs with complete antibodies display higher tumour uptake than those based on antibody fragments. The complete antibody has a longer half-life in the blood than antibody fragments, which gives the antibody a longer period of contact with the surface antigens on the tumour cells [2.51].

2.3.3.3. Pretargeted radioimmunotherapy

Tumour selectivity can be increased by means of bispecific antibodies; this is the principle behind multistage radioimmunotherapy in the form of so-called pretargeting. Here, the tumour tissue is first presented with a bispecific antibody. After the antibody has accumulated sufficiently on the tumour and after forced clearance of the antibody from the blood pool by a clearing agent, radioactively labelled therapeutic component with a higher affinity for the respective binding site of the bispecific antibody is applied. In the last step of this multistage process, radioactivity is finally brought selectively to the tumour cells while normal tissue is left unscathed. The ideal situation is to create an avidin, streptavidin or biotin binding site within the structure of the antibody. Biotin avidin binding constitutes one of the most stable bonds known. The respective binding partner can then be applied with a labelled therapeutic radionuclide. Promising preliminary results from clinical trials have already been reported. However, this radioimmunotherapeutic approach still needs fine tuning with regard to the setting of intervals between applications and optimal dosage of the active substances [2.52].

2.3.4. Radioreceptor therapy

In radiopeptide therapy, the receptor specific peptides are used as highly specific carriers to bring radionuclides directly to or into the cancer cells, so that these cells will be killed by their radiation. Peptide analogues can be bound to therapeutic radionuclides such as ^{177}Lu and ^{90}Y via chemical conjugators (chelators). Of these, the somatostatin analogues of the octreotide class have become the most fully established in clinical practice. Dosages are set individually according to the pretherapeutic diagnosis, particularly in the case of ^{68}Ga labelled analogues.

The therapeutic substance is administered slowly as an intravenous infusion. Within a few minutes after infusion, the radiopeptide docks at the receptor sites and can stay there for some days, irradiating the tumour cells and thereby destroying them. To avoid damage to the kidneys, through which the radioactive therapeutic substance is cleared, these are washed through immediately before and after the radionuclide injection with amino acid infusions. The therapy is generally repeated after a lengthy interval [2.53–2.55].

Another very promising form of radioreceptor therapy uses oestrogen receptors (ERs) as the target structure on tumour cells. ERs are intranuclear proteins that are expressed with high frequency in female breast and genital tumours. ERs bind oestrogens with high affinity and specificity and mediate an efficient concentration of the ligands in the cell nucleus. The ER hormone complex binds to specific 'responsive elements' of the DNA. Expression of ERs can be modulated reliably in biological models *in vivo* and *in vitro*. Because labelling with a radionuclide does not alter the affinity and specificity of the oestrogen for its receptor, oestrogen vehicles will carry radionuclides effectively and selectively into the cell nucleus of ER positive tumour cells.

ER ligands can therefore be used as vehicle molecules for radionuclides allowing radiation to be brought to that part of the cell, the DNA, which is most radiation sensitive. Hormone receptors, in this case ERs, can then act as a point of attack for cytotoxic radiopharmaceuticals with receptor affinity. Radiohormone therapy of this kind would also be effective for the treatment of genital carcinomas (e.g. ovarian cancer) where there is expression of sexual steroid receptors but no hormonal regulation, and, therefore, no responsiveness to conventional hormone therapy. Ideal radionuclides for this purpose would be Auger electron emitters, as their radiotoxic action is released at focal points within a very small space and can therefore be kept within the receptor positive cells or affected cell nucleus. Almost every decay of an Auger emitter within the DNA causes a double strand break and leads to irreparable and lethal cell damage. Auger emitters in extranuclear or extracellular locations are much less toxic [2.56–2.59].

2.3.5. Gene therapy approaches

In gene therapy approaches to targeted radionuclide therapy, the aim is to provoke genetic modifications in tumour cells to induce or strengthen expression of target structures on the tumour cells.

One example of this is the sodium iodide symporter (NIS), which is used therapeutically in radioiodine therapy for active transport of radioactive iodine into cells of the thyroid glands. If it were possible to provoke expression of NIS in extrathyroidal tumour tissue, such as mammary tumours or prostate carcinomas, then it would be possible to use radioiodine therapy against those tumours as well. The NIS is usually only found in thyroid, saliva, tear and lactating mammary glands. Limited therapeutic stimulation of NIS expression can be achieved through administration of various pharmaceuticals (e.g. retinoic acids). It is better to bring the NIS directly into the tumour tissue by artificial means. One possibility is to transfect tumour cells with the plasmids responsible for NIS

expression. However, the problem lies in transferring the promising results of the concept in cell cultures to the clinical situation [2.60, 2.61].

2.3.6. Colloids for RSO

The term radiosynoviorthesis (RSO) was first coined in 1968 by Delbarre et al. [2.62]. It describes the restoration (orthesis) of the synovia by means of radionuclides. Inflammatory synovial processes are suppressed through local application of radioactive substances, in this case β emitters in colloid form. The method is seen as an alternative to surgical synovectomy and can be referred to as radiosynovectomy or radiation synovectomy.

To be ideally suited for RSO, a radiopharmaceutical should have the following properties [2.63]. The β energy must penetrate and ablate the synovial tissue that is swollen by inflammation. The joint cartilage under the synovia and the skin covering it must not be damaged. The radionuclide must attach to particles that are small enough to be phagocytosed, but too large to escape from the joint before they are phagocytosed. A suitable particle size is 2–5 μm . The particles should be as biologically degradable as possible to avoid inducing tissue granulation.

Products of this type that are already commercially available and used routinely in clinical practice are the citrate colloids bearing ^{169}Er and ^{90}Y , and the ^{186}Re sulphide colloid. Yttrium-90 is also available as a silicate [2.64].

The role of citrate in radiopharmaceutical preparation is unclear. It may have been chosen for the traditional reason that citrate sounds somehow 'healthy'. Citrate ions can form relatively stable complexes with erbium and yttrium, which means that release of erbium or yttrium from the colloid and formation of the citrate salt should be dependent on time, position and citrate levels. These complexes, unlike the colloid products in which erbium is fixed, can leave the articular space and enter the blood circulation. This increases the radiotoxicity of the radiopharmaceuticals and demands critical review. Furthermore, the possible influence of co-injected contrast agents on the stability of ^{90}Y , ^{169}Er and ^{186}Re radiocolloids should be considered [2.65].

There is plenty of room for improvement of the radiopharmaceuticals for RSO, both with regard to chemical form (customized colloids of a defined diameter) and the radionuclide used [2.66, 2.67].

RSO offers a simple, localized and practicable treatment for inflammatory disorders of the joints. Inflammation of the synovia can be treated at an early stage by local application of radionuclides in colloid form. RSO has proved effective for pain relief in cases of more advanced inflammation (with onset of joint destruction). There are radiological indications of a suspension of

destructive processes within the joints under RSO, but no evidence of induction of repair processes within one year after radiation treatment.

2.3.7. Nanotechnology

Advances in the field of oncological nanotechnology have led to the development of nanoparticles suitable for the transport of therapeutically relevant radionuclides into targeted tumour tissue. Such nanoparticles include liposomes, fullerenes, iron oxide particles, polymers, dendrimers, quantum dots and carbon nanotubes.

With their extremely small size of <100 nm, nanoparticles offer the possibility of conjugation of radionuclides with binding sites or other targeted units. This innovative development can be expected to produce nanoparticles, which, being so small, can passively penetrate tumour tissue and transport cytotoxic radionuclides with high selectivity and minimal side effects to binding sites within tumours. There are currently thought to be two mechanisms for the transport of cytotoxic substances, such as radionuclides by nanoparticles into tumour tissue: (i) through passive incorporation specific to the target tissue or (ii) by docking alongside tumour specific target structures (antigens, receptors or sites of angiogenesis), which is a process mediated by targeting units with high tumour affinity.

There are currently three recognized generations of nanocarriers or nanoparticles: (i) a first generation for passive targeting, including fast uptake into the reticuloendothelial system (RES) of the liver and spleen as well as passive passage into tumour tissue; (ii) a second generation of nanoparticles comprising sterically stabilized, PEGylated nanocarriers (PEG = polyethylene glycol) that can bypass uptake through the RES, thereby prolonging the residence time in the blood and improving the chances of passive targeting through the enhanced permeability and retention effect in leaky tumour tissues; and (iii) a third generation of nanocarriers with bioconjugated targeting units (antibody peptides) and binding sites (e.g. DOTA structures) for metallic radionuclides on their surface. The challenges to be overcome for introduction of these three promising generations of nanoparticles lie in the synthesis of nanocarriers with stealth characteristics that would allow bypassing of the RES and longest possible residence time of the active agents in the blood, the production of multifunctional nanoparticles with improved tumour affinity and specificity, and the development of convincing strategies for their clinical testing prior to obtaining authorization [2.68].

The insertion of therapeutically active radionuclides either into or onto nanoparticles can take place by encapsulation in the particle or by attachment to existing binding sites on the surface of the particle. In principle, this would allow the combination of emitters with therapeutic and diagnostic functions as well as implementation in multiple imaging modalities (SPECT, positron emission tomography (PET), magnetic resonance imaging (MRI)) [2.69].

Examples of radionuclides for passive nanotargeting for therapeutic purposes are ^{131}I , ^{90}Y , ^{188}Re or ^{67}Cu encapsulated in liposomes. Coupling of ^{186}Re via N,N-bis(2-mercaptoethyl) dimethylethylenediamine to liposomes has also been attempted. Studies on parallel labelling of liposomes with ^{111}In and ^{188}Re form part of the drive towards combining therapy with diagnostics (theranostics). Over and above this, various approaches have been tried to achieve co-delivery of chemotherapeutic drugs and radionuclides for treatment and diagnosis by means of liposomes. Ting et al. [2.70] give a good overview of attempts to achieve state of the art multimodal targeting of tumours using radioactive nanoparticles with high tumour affinity. The following key investigations offer a fair picture of the current state of research:

- (a) Auger radiation induced, antisense mediated cytotoxicity of tumour cells using a three component streptavidin delivery nanoparticle with ^{111}In [2.71];
- (b) Intratumoural delivery of a theranostic metallofullerene (f-Gd₃N@C₈₀) labelled with ^{177}Lu and DOTA (^{177}Lu DOTA-f-GdN@C), allowing a possible combination of MRI and ^{177}Lu therapy [2.72];
- (c) Synthesis and investigation of cell uptake of a novel, dual modality ^{188}Re histidyl–glycyl–arginyl–glycyl–aspartic acid F–CdTe quantum dot probe for combination of therapeutic targeting of angiogenesis and MRI [2.73].

2.4. CLOSING REMARKS

Attempts to employ radionuclides in various chemical forms as tools in the fight against tumours have a history reaching back over 60 years. The use of radionuclides in their open form began in the late 1930s with attempts to treat blood diseases such as polycythaemia vera with the aid of ^{32}P labelled sodium hydrogen phosphate [2.74]. At the same time, ^{131}I sodium iodide was being trialled as a treatment for thyroid carcinoma [2.75]. Both procedures were based on the concept of metabolically mediated intracellular accumulation of radionuclides. Radioiodine treatment of thyroid disorders is the only treatment that has continued to be developed up to the present day and has become fully established in routine clinical practice. There has been no comparable breakthrough, despite intensive

research efforts, since then. However, a few partial successes are worthy of noting. Iodine-131 MIBG has now become established, at least as a radiopharmaceutical with a palliative action for routine treatment of childhood neuroblastomas. RSO can restore mobility to patients with painful joint disorders and makes the time spent waiting for an endoprosthesis more bearable. Intolerable pain from skeletal metastases can be relieved with β emitters, giving these patients a better quality of life.

However, sobering realities frequently have to be faced in nuclear medicine. Yttrium-90 Zevalin, a prize product on which great hopes were pinned, has not fulfilled investor expectations, in Europe at least. There has been a noticeable decline in this type of radionuclide therapy. The reasons lie in the relatively high price of radiopharmaceuticals, which can exceed €15 000, and the associated hesitancy of the user to undertake a somewhat complicated labelling procedure where wasteful mistakes could be made. The fact that most therapies require the collaboration of specialists in nuclear medicine with haemato-oncologists does not simplify the matter. Sometimes, a treatment is thwarted when the patient refuses consent for the procedure or the necessary blood tests involved.

The number of patients on radioiodine therapy wards has fallen in recent times, at least for those with benign thyroid disorders. Alternative plans for maintaining the demand for routine clinical services in the field of nuclear medicine are urgently required. There are grounds for hope. In recent years, impressive successes have been achieved with somatostatin analogues labelled with ^{177}Lu and ^{90}Y [2.76]. These, and other innovative approaches that have arisen from spectacular scientific advances in labelling technologies, genetics, proteomics, nanotechnology, molecular imaging and indeed computer technology, are all encouraging. Such advances were also crucial for the development of the novel therapeutic approaches described in this publication.

The future of nuclear medicine is in personalized medicine, in which the radionuclide used and the vehicle selected for any one pathological situation will be specifically tailored to the individual patient.

There is certainly room for improvement in the field with regard to translation of scientific advances to routine clinical applications (from bench to bedside). Finding ways to meet and deal with the ever increasing demands of pharmaceutical legislation and regulations for radiation protection so that these do not halt progress altogether is an urgent and pressing problem. There is no sense in dismissing these demands simply as bureaucratic obstacles and shutting our eyes to the issue. The internationally binding standards for good laboratory practice and good manufacturing practice are challenges that have to be faced in radiopharmacological research for the development of radioactive vehicles, particularly for therapeutic use. Obligatory adherence to these international

standards will be imposed with increasing insistence, also in developing countries, which is a good thing.

Radionuclide therapy opens up the possibility of bringing ionizing radiation directly into tumour tissue to achieve targeted eradication of cancer cells. This is, and will continue to be, an exciting challenge for nuclear medicine worldwide.

REFERENCES TO CHAPTER 2

- [2.1] FERLAY, J., et al., Estimates of worldwide burden of cancer in 2008: GLOBOCAN 2008, *Int. J. Cancer* **127** (2010) 12893.
- [2.2] PRESTON, R.J., Radiation biology: Concepts for radiation protection, *Health Phys.* **88** (2005) 545.
- [2.3] MAIRS, R.J., et al., Targeted radiotherapy: Microgray doses and the bystander effect, *Dose Response* **5** (2007) 204.
- [2.4] BRANS, B., et al., Clinical applications of newer radionuclide therapies, *Eur. J. Cancer* **42** (2006) 994.
- [2.5] KASSIS, A.I., Molecular and cellular radiobiological effects of Auger emitting radionuclides, *Radiat. Prot. Dosim.* **143** (2011) 241.
- [2.6] CREMONESI, M., et al., Recent issues on dosimetry and radiobiology for peptide receptor radionuclide therapy, *Q. J. Nucl. Med. Mol. Imaging* **55** (2011) 155.
- [2.7] WIKE, J.S., et al., Chemistry for commercial scale production of yttrium-90 for medical research, *Int. J. Radiat. Appl. Instrum. A* **41** (1990) 861.
- [2.8] LAMBERT, B., et al., Clinical applications of ¹⁸⁸Re-labelled radiopharmaceuticals for radionuclide therapy, *Nucl. Med. Commun.* **27** (2006) 223.
- [2.9] KIM, Y.S., BRECHBIEL, M.W., An overview of targeted alpha therapy, *Tumour Biol.* **33** (2012) 573.
- [2.10] CLAESSEON, K., et al., RBE of α -particles from ²¹¹At for complex DNA damage and cell survival in relation to cell cycle position, *Int. J. Radiat. Biol.* **87** (2011) 372.
- [2.11] MORGENSTERN, A., et al., Targeted alpha therapy with ²¹³Bi, *Curr. Radiopharm.* **4** (2011) 295.
- [2.12] VAIDYANATHAN, G., ZALUTSKY, M.R., Applications of ²¹¹At and ²²³Ra in targeted alpha-particle radiotherapy, *Curr. Radiopharm.* **4** (2011) 283.
- [2.13] HOWELL, R.W., Auger processes in the 21st century, *Int. J. Radiat. Biol.* **84** (2008) 959.
- [2.14] TAVARES, A.A., TAVARES, J.M., Evaluating ^{99m}Tc Auger electrons for targeted tumor radiotherapy by computational methods, *Med. Phys.* **37** (2010) 3551.
- [2.15] WENDISCH, M., et al., ^{99m}Tc reduces clonogenic survival after intracellular uptake in NIS-positive cells in vitro more than ¹³¹I, *Nuklearmed.* **49** (2010) 154.
- [2.16] DANCEY, G., BEGENT, R.H., MEYER, T., Imaging in targeted delivery of therapy to cancer, *Target Oncol.* **4** (2009) 201.
- [2.17] PAUWELS, E.K., STOKKEL, M.P., Radiopharmaceuticals for bone lesions. Imaging and therapy in clinical practice, *Q. J. Nucl. Med.* **45** (2001) 18.

- [2.18] HAMILTON, J.G., The metabolism of the fission products and the heaviest elements, *Radiology* **49** (1947) 325.
- [2.19] PECHER, C., Biological investigations with radioactive calcium and strontium, *Proc. Soc. Exp. Biol. Med.* **46** (1941) 86.
- [2.20] FIRUSIAN, N., Kinetics of radiostrontium, *Nucl. Med. (Stuttg.)* **13** (1974) 127.
- [2.21] KUTZNER, J., et al., Yttrium-90-therapy of bone metastases, *Dtsch. Med. Wochenschr.* **107** (1982) 1360.
- [2.22] TOEGEL, S., et al., Uptake of bone-seekers is solely associated with mineralisation! A study with ^{99m}Tc -MDP, ^{153}Sm -EDTMP and ^{18}F -fluoride on osteoblasts, *Eur. J. Nucl. Med. Mol. Imaging* **33** (2006) 491.
- [2.23] ROQUÉ, I., et al., Radioisotopes for metastatic bone pain, *Cochrane Database Syst. Rev.* **7** (2011) CD003347.
- [2.24] O'MARA, R.E., McAFEE, J.G., SUBRAMANIAN, G., Rare earth nuclides as potential agents for skeletal imaging, *J. Nucl. Med.* **10** (1969) 49.
- [2.25] WIELAND, D.M., WU, J.L., BROWN, L.E., Radiolabeled adrenergic neuron-blocking agents: Adrenomedullary imaging with ^{131}I -iodobenzylguanidine, *J. Nucl. Med.* **21** (1980) 349.
- [2.26] GRÜNWARD, F., EZZIDDIN, S., ^{131}I -metaiodobenzylguanidine therapy of neuroblastoma and other neuroendocrine tumors, *Semin. Nucl. Med.* **40** (2010) 153.
- [2.27] CORNELISSEN, B., VALLIS, K.A., Targeting the nucleus: An overview of Auger-electron radionuclide therapy, *Curr. Drug Discov. Technol.* **7** (2010) 263.
- [2.28] BALKIN, E.R., et al., In vitro evaluation of targeted antisense ^{177}Lu radiotherapy, *Anticancer Res.* **10** (2011) 3143.
- [2.29] LIU, X., et al., Auger-mediated cytotoxicity of cancer cells in culture by a ^{125}I -antisense oligomer delivered as a three-component streptavidin nanoparticle, *J. Biomed. Nanotechnol.* **6** (2010) 153.
- [2.30] SHARKEY, R.M., GOLDENBERG, D.M., Cancer radioimmunotherapy, *Immunotherapy* **3** (2011) 349.
- [2.31] KÖHLER, G., MILSTEIN, C., Continuous cultures of fused cells secreting antibody of proven defined specificity, *Nature* **256** (1975) 495.
- [2.32] BOSWELL, C.A., BRECHBIEL, M.W., Development of radioimmunotherapeutic and diagnostic antibodies: An inside-out view, *Nucl. Med. Biol.* **34** (2007) 757.
- [2.33] WITZIG, T.E., et al., Randomized controlled trial of yttrium-90-labeled ibritumomab tiuxetan radioimmunotherapy versus rituximab immunotherapy for patients with relapsed or refractory low-grade, follicular, or transformed B-cell non-Hodgkin's lymphoma, *J. Clin. Oncol.* **20** (2002) 2453.
- [2.34] TRAN, L., et al., The pharmacokinetics of ^{131}I -rituximab in a patient with CD20 positive non-Hodgkin lymphoma: Evaluation of the effect of radioiodination on the biological properties of rituximab, *Hum. Antib.* **20** (2011) 37.
- [2.35] SCHILLACI, O., et al., Effect of antilymphoma antibody, ^{131}I -Lym-1, on peripheral blood lymphocytes in patients with non-Hodgkin's lymphoma, *Cancer Biother. Radiopharm.* **22** (2007) 521.

- [2.36] PAGEL, J.M., et al., Allogeneic hematopoietic cell transplantation after conditioning with ¹³¹I-anti-CD45 antibody plus fludarabine and low-dose total body irradiation for elderly patients with advanced acute myeloid leukemia or high-risk myelodysplastic syndrome, *Blood* **114** (2009) 5444.
- [2.37] MATTES, M.J., et al., Therapy of advanced B-lymphoma xenografts with a combination of ⁹⁰Y-anti-CD22 IgG (epratuzumab) and unlabeled anti-CD20 IgG (veltuzumab), *Clin. Cancer Res.* **14** (2008) 6154.
- [2.38] DIETLEIN, M., et al., Development of anti-CD30 radioimmunoconstructs (RICs) for treatment of Hodgkin's lymphoma. Studies with cell lines and animal studies, *Nuklearmed.* **49** (2010) 97.
- [2.39] JURCIC, J.G., What happened to anti-CD33 therapy for acute myeloid leukemia? *Curr. Hematol. Malig. Rep.* **7** (2012) 65.
- [2.40] OCHAKOVSKAYA, R., et al., Therapy of disseminated B-cell lymphoma xenografts in severe combined immunodeficient mice with an anti-CD74 antibody conjugated with indium-111, gallium-67, or yttrium-90, *Clin. Cancer Res.* **7** (2001) 1505.
- [2.41] OEI, A.L., et al., Human anti-mouse IgM and IgG responses in ovarian cancer patients after radioimmunotherapy with ⁹⁰Y-muHMFG1, *Anticancer Res.* **28** (2008) 2721.
- [2.42] LIU, Z., et al., Epidermal growth factor receptor-targeted radioimmunotherapy of human head and neck cancer xenografts using ⁹⁰Y-labeled fully human antibody panitumumab, *Mol. Cancer Ther.* **9** (2010) 2297.
- [2.43] OTTO, C., et al., Localization of ¹³¹I-labelled monoclonal antibody ERIC1 in a subcutaneous xenograft model of neuroblastoma in SCID mice, *Nucl. Med. Commun.* **27** (2006) 171.
- [2.44] MEREDITH, R.F., et al., Intraperitoneal radioimmunochemotherapy of ovarian cancer: A phase I study, *Cancer Biother. Radiopharm.* **16** (2001) 305.
- [2.45] VERHEIJEN, R.H., et al., Phase III trial of intraperitoneal therapy with yttrium-90-labeled HMFG1 murine monoclonal antibody in patients with epithelial ovarian cancer after a surgically defined complete remission, *J. Clin. Oncol.* **24** (2006) 571.
- [2.46] REARDON, D.A., et al., A pilot study: ¹³¹I-antitenascin monoclonal antibody 81c6 to deliver a 44-Gy resection cavity boost, *Neuro. Oncol.* **10** (2008) 182.
- [2.47] LIERSCH, T., et al., Phase II trial of carcinoembryonic antigen radioimmunotherapy with ¹³¹I-labetuzumab after salvage resection of colorectal metastases in the liver: Five-year safety and efficacy results, *J. Clin. Oncol.* **23** (2005) 6763.
- [2.48] MEREDITH, R., et al., Predictors of long-term outcome from intraperitoneal radioimmunotherapy for ovarian cancer, *Cancer Biother. Radiopharm.* **27** (2012) 36.
- [2.49] JENSEN, A.D., et al., Phase II study of induction chemotherapy with TPF followed by radioimmunotherapy with cetuximab and intensity-modulated radiotherapy (IMRT) in combination with a carbon ion boost for locally advanced tumours of the oro-, hypopharynx and larynx-TPF-C-HIT, *BMC Cancer* **11** (2011) 182.
- [2.50] SHARKEY, R.M., et al., Combination radioimmunotherapy and chemoimmunotherapy involving different or the same targets improves therapy of human pancreatic carcinoma xenograft models, *Mol. Cancer Ther.* **10** (2011) 1072.
- [2.51] RUDNICK, S.I., ADAMS, G.P., Affinity and avidity in antibody-based tumor targeting, *Cancer Biother. Radiopharm.* **24** (2009) 155.

- [2.52] GOLDENBERG, D.M., et al., Multifunctional antibodies by the dock-and-lock method for improved cancer imaging and therapy by pretargeting, *J. Nucl. Med.* **49** (2008) 158.
- [2.53] BODEI, L., et al., Peptide receptor therapies in neuroendocrine tumors, *J. Endocrinol. Invest.* **32** (2009).
- [2.54] KWEKKEBOOM, D.J., DE HERDER, W.W., KRENNING, E.P., Somatostatin receptor-targeted radionuclide therapy in patients with gastroenteropancreatic neuroendocrine tumors, *Endocrinol. Metab. Clin. North Am.* **40** (2011) 173.
- [2.55] KUNIKOWSKA, J., et al., Clinical results of radionuclide therapy of neuroendocrine tumours with ^{90}Y -DOTATATE and tandem $^{90}\text{Y}/^{177}\text{Lu}$ -DOTATATE: Which is a better therapy option? *Eur. J. Nucl. Med. Mol. Imaging* **38** (2011) 1788.
- [2.56] SCHOMÄCKER, K., et al., "Investigations into biokinetics of I-123 diethylstilbestrol phosphate in tumour-bearing mice", *Radioactive Isotopes in Clinical Medicine and Research* (BERGMANN, H., SINZINGER, H., Eds), Birkhäuser Verlag, Basel (1997) 333.
- [2.57] SCHOMÄCKER, K., et al., Kinetics of receptor-mediated radiotoxicity of 16 alpha- ^{125}I -iodostradiol-3,17 beta, *Nuklearmed.* **37** (1998) 134.
- [2.58] FISCHER, T., SCHOMÄCKER, K., SCHICHA, H., Diethylstilbestrol (DES) labeled with Auger emitters: Potential radiopharmaceutical for therapy of estrogen receptor-positive tumors and their metastases? *Int. J. Radiat. Biol.* **84** (2008) 1112.
- [2.59] DeSOMBRE, E.R., et al., Therapy of estrogen receptor-positive micrometastases in the peritoneal cavity with Auger electron-emitting estrogens—theoretical and practical considerations, *Acta Oncol.* **39** (2000) 659.
- [2.60] KNOOP, K., et al., Image-guided, tumor stroma-targeted ^{131}I therapy of hepatocellular cancer after systemic mesenchymal stem cell-mediated NIS gene delivery, *Mol. Ther.* **19** (2011) 1704.
- [2.61] SERGANOVA, I., PONOMAREV, V., BLASBERG, R., Human reporter genes: Potential use in clinical studies, *Nucl. Med. Biol.* **34** (2007) 791.
- [2.62] DELBARRE, F., et al., Synoviorthesis with radioisotopes, *Presse Med.* **76** (1968) 1045.
- [2.63] DEUTSCH, E., BRODACK, J.W., DEUTSCH, K.F., Radiation synovectomy revisited, *Eur. J. Nucl. Med.* **20** (1993) 1113.
- [2.64] VAN DER ZANT, F.M., et al., Radiation synovectomy with yttrium-90, rhenium-186 and erbium-169: A systematic literature review with meta-analyses, *Clin. Exp. Rheumatol.* **27** (2009) 130.
- [2.65] SCHOMÄCKER, K., et al., Stability of radioactive colloids for radiation synovectomy: Influence of X-ray contrast agents, anaesthetics and glucocorticoids in vitro, *Nucl. Med. Commun.* **26** (2005) 1027.
- [2.66] KROPÁČEK, M., et al., Preparation and quality control of [^{166}Ho]-macroaggregates for radiosynoviorthesis, *Cancer Biother. Radiopharm.* **22** (2007) 450.
- [2.67] THOMAS, S., et al., ^{90}Y yttrium-hydroxyapatite: A new therapeutic option for radioactive synovectomy in haemophilic synovitis, *Haemophilia* **17** (2011) 985.
- [2.68] MUTHU, M.S., WILSON, B., Multifunctional radionanomedicine: A novel nanoplatform for cancer imaging and therapy, *Nanomedicine (Lond.)* **5** (2010) 169.

- [2.69] XIE, J., et al., PET/NIRF/MRI triple functional iron oxide nanoparticles, *Biomaterials* **31** (2010) 3016.
- [2.70] TING, G., et al., Nanotargeted radionuclides for cancer nuclear imaging and internal radiotherapy, *J. Biomed. Biotechnol.* **2010** (2010) 953537.
- [2.71] LIU, X., et al., Auger radiation-induced, antisense-mediated cytotoxicity of tumor cells using a 3-component streptavidin-delivery nanoparticle with ^{111}In , *J. Nucl. Med.* **50** (2009) 582.
- [2.72] BULTE, J.W., Science to practice: Can theranostic fullerenes be used to treat brain tumors? *Radiology* **261** (2011) 1.
- [2.73] LI, Z., et al., Synthesis and cell uptake of a novel dual modality ^{188}Re -HGRGD (D) F-CdTe QDs probe, *Talanta* **85** (2011) 936.
- [2.74] LAWRENCE, J.H., Nuclear physics and therapy: Preliminary report on a new method for the treatment of leukemia and polycythemia, *Radiology* **52** (1940) 51.
- [2.75] HERTZ, S., ROBERTS, A., Application of radioactive iodine in therapy of Graves' disease, *J. Clin. Invest.* **21** (1942) 624.
- [2.76] GIOVACCHINI G., et al., Peptide receptor radionuclide therapy with somatostatin analogues in neuroendocrine tumors, *Anticancer Agents Med. Chem.* **12** (2012) 526.

Chapter 3

DEVELOPMENT OF RADIOPHARMACEUTICALS BASED ON ^{188}Re AND ^{90}Y FOR RADIONUCLIDE THERAPY AT IPEN-CNEN/SP

J.A. OSSO, JR., G. BARRIO, C.R.B.R. DIAS, T.P. BRAMBILLA,
D.M. DANTAS, K.N. SUZUKI, A.B. BARBEZAN, N.P. REIS,
T.A. FELIX, M.F.S. BARBOZA, N.T. FUKUMORI, J. MENGATTI
Radiopharmacy Center,
Institute of Energetic and Nuclear Research,
IPEN-CNEN/SP,
São Paulo, Brazil

Abstract

The overall objectives of this CRP are the development of radiopharmaceuticals for targeted therapy using ^{188}Re and ^{90}Y to study the performance of generators with long lived parent radionuclides and to validate the quality control procedures for estimating the purity of generator eluents. The CRP is expected to enhance the capability in production of ^{90}Y and ^{188}Re radiopharmaceuticals to meet the increasing demand of therapeutic products for clinical applications, particularly in Brazil. Efforts have been made towards assembling $^{90}\text{Sr}/^{90}\text{Y}$ generators, performing quality control of ^{90}Y , labelling of DMSA(V), bisphosphonates and anti-CD20 with ^{188}Re , and labelling of HA with ^{90}Y .

3.1. STRONTIUM-90/YTTRIUM-90 GENERATORS

3.1.1. Strontium-90/yttrium-90 ion exchange chromatography generator

Two generators were prepared based on cation exchange resins in continuation of the work from the previous CRP on the development of generator technologies for therapeutic radionuclides [3.1–3.3]. The resin employed was Dowex 50WX8 (100–200 mesh), H^+ form, and the generators dimensions (see Fig. 3.1) were:

- (a) Generator G_1 : 10 cm high, 1 cm inner diameter;
- (b) Generator G_2 : 10 cm high, 0.5 cm inner diameter.

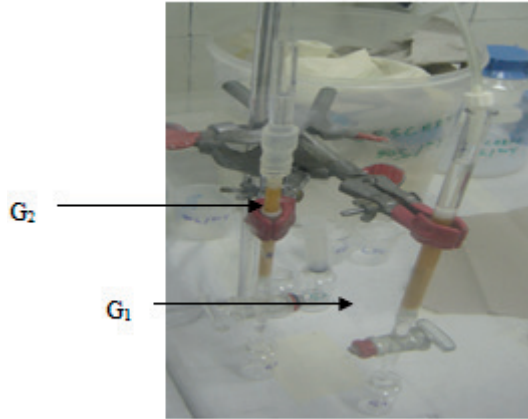


FIG. 3.1. Ion exchange generators.

The generators were assembled in a glovebox. The loading solution comprised 3 mCi of $^{90}\text{SrCl}_2$ in 1M HCl (from POLATOM). Elutions were performed with 0.003M and 0.03M ethylenediaminetetraacetic acid (EDTA) at pH4.5. Figure 3.2 shows the elution profiles of both generators, and Fig. 3.3 shows the elution efficiencies for both generators.

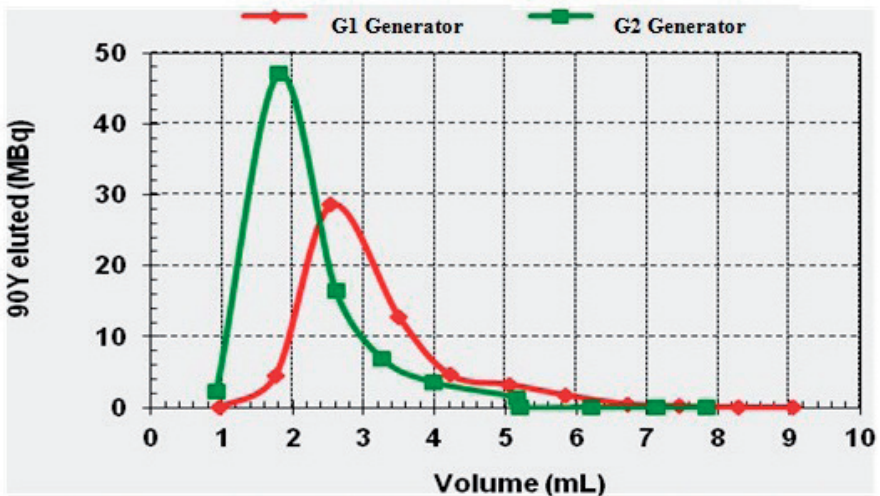


FIG. 3.2. Elution profiles for ion exchange generators.

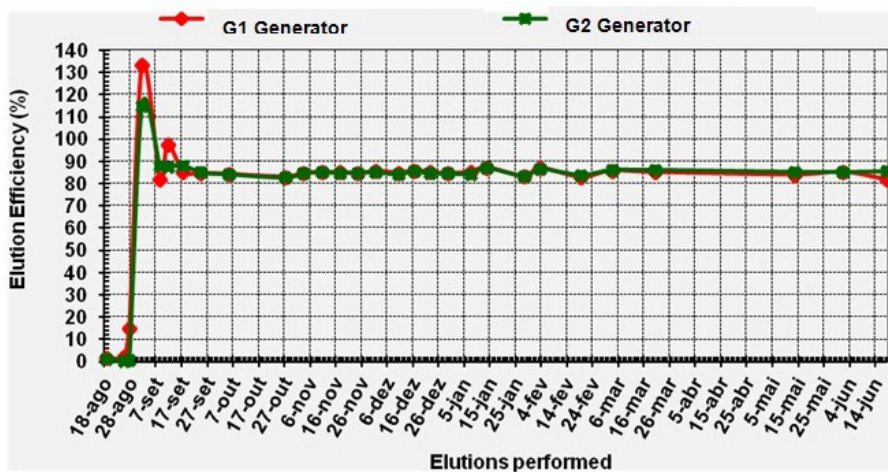


FIG. 3.3. Elution efficiencies for ion exchange generators.

Experiments were performed for EDTA destruction with nitric and perchloric acids. The mean efficiency values for both generators were $83\% \pm 1\%$ for 10 months of usage. The recovery of ^{90}Y in chloride form was $>95\%$ after three destruction processes.

3.1.2. Strontium-90/yttrium-90 electrochemical generator

The experiments were performed using a simple electrochemical device (see Fig. 3.4), with two platinum electrodes acting as the cathode and anode. A stabilized direct current power source (potentiostat unit) was used with the following characteristics: 15 V compliance, 15Ω resistance, 150 mA maximum current and 60 Hz impedance (Tectrol model TC 15-0015).

Initial experiments were performed using non-irradiated materials (strontium nitrate, $\text{Sr}(\text{NO}_3)_2$, and yttrium oxide, Y_2O_3) and radioactive tracers. These salts were irradiated at nuclear reactor IEA-R1m (Nuclear Energy Research Institute/National Nuclear Energy Commission (IPEN/CNEN-SP), Brazil), and produced ^{85}Sr and ^{88}Y as radiotracers. For electrolysis using non-irradiated materials, the analysis was performed by measuring the mass difference of $\text{Sr}(\text{NO}_3)_2$ and Y_2O_3 between the electrolysis, using a digital balance (Shimadzu model AU220D). The γ activities of ^{85}Sr and ^{88}Y were analysed using a high purity germanium (HPGe) detector (Canberra model 747).

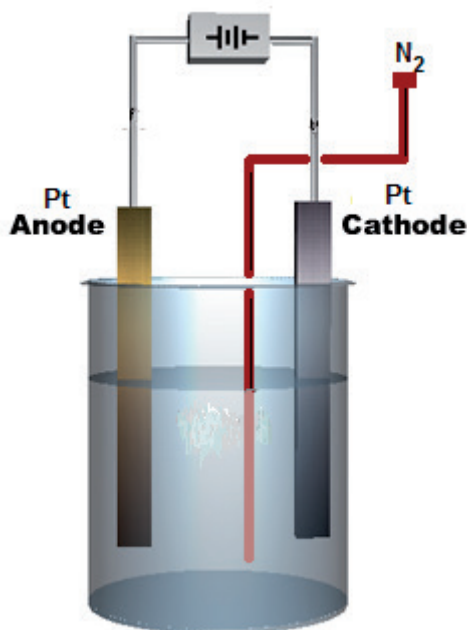


FIG. 3.4. Schematic diagram of the electrochemical device used in experiments.

The electrolysis was performed in two stages: the first one was aimed at electrodeposition of the desired element (yttrium) and the second one, called the recovery stage, was aimed at removal of yttrium from the electrode.

3.1.2.1. Electrolysis with non-irradiated materials

In the first stage, the electrodeposition stage, ~30 mL of a solution containing $\text{Sr}(\text{NO}_3)_2$ or Y_2O_3 in 1M HNO_3 was used. During the process, N_2 gas was gently bubbled into the electrolytic solution under continuous stirring using a magnetic stirrer.

The second stage, the recovery stage, was performed after removing the electrodes from the original solution and placing them in a fresh 0.001–1M HNO_3 solution. The polarity was reversed with constant potential and current for a period of 5–30 min. There was no N_2 bubbling or stirring during this process. The Pt electrodes were weighed before and after the electrodeposition to evaluate the exact electrodeposition yield. The results of electrodeposition as a function of time, pH and applied current are illustrated in Figs 3.5, 3.6 and 3.7, respectively.

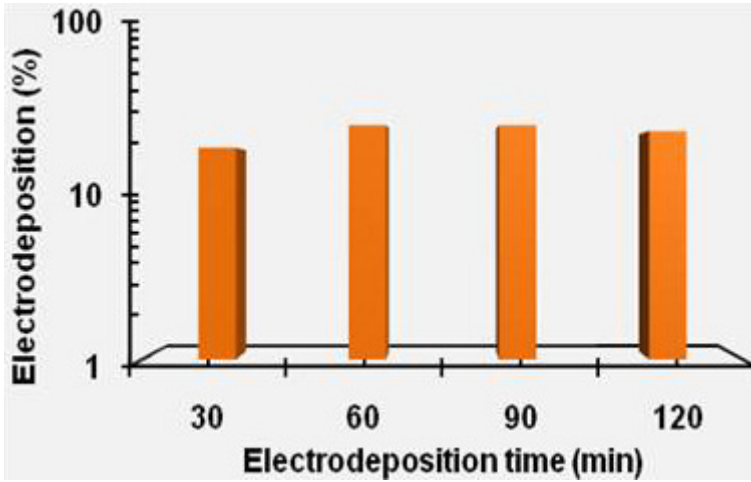


FIG. 3.5. Electrodeposition of yttrium as a function of electrodeposition time.

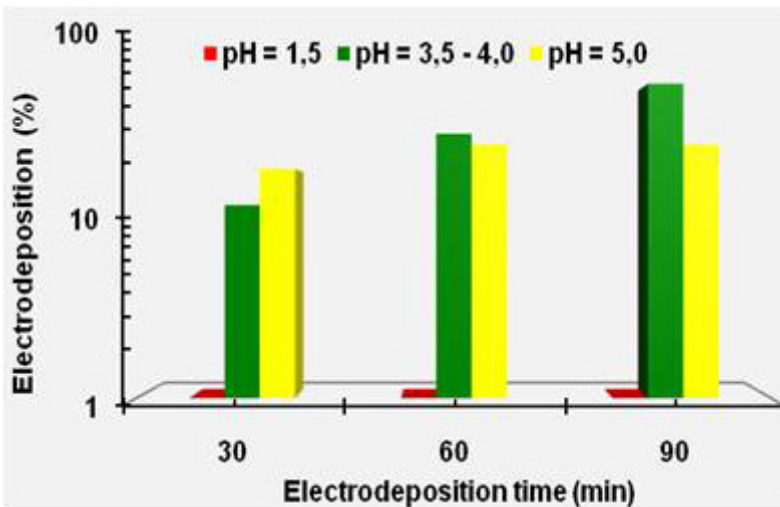


FIG. 3.6. Electrodeposition of yttrium as a function of electrodeposition time and different values of pH.

The best results were achieved at an electrodeposition time between 60 and 90 min, a pH between 3.5 and 4.0, a current I of 60 mA and a mean voltage of 5 V. The overall electrodeposition yield was ~60% for yttrium.

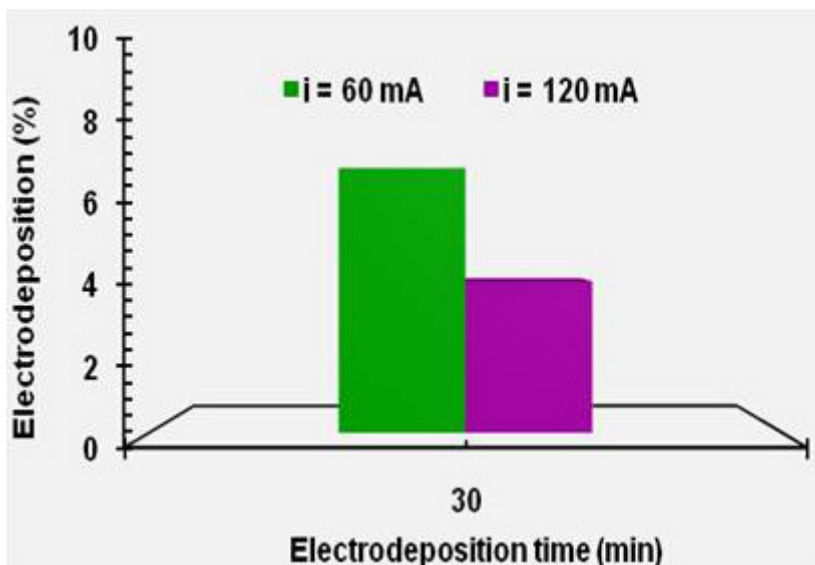


FIG. 3.7 Electrodeposition of yttrium as a function of applied current.

The effect of bubbling N_2 gas during the electrodeposition process in the solution was studied. From Table 3.1, it is evident that N_2 bubbling is mandatory during the electrodeposition process, independent of the quantity of Y_2O_3 in the solution, as it releases gases produced during electrolysis and keeps the solution in a dynamic form. The table also indicates that use of lower concentrations of Y_2O_3 in the solution gives better electrodeposition of yttrium.

TABLE 3.1. EFFECT OF N_2 BUBBLING DURING ELECTRODEPOSITION OF ^{90}Y

Electrolysis	Mass of yttrium oxide (g)	Amount of yttrium electroplated (%)
With N_2	0.20	11
	0.05	27
Without N_2	0.20	8
	0.05	6

The results of the experiments of recovery of yttrium from the electrode are shown in Table 3.2. The recovery yields were better with a clean solution of 1M HNO₃, even for shorter times, compared to the yield with 0.001M HNO₃.

The experiments of electrodeposition of strontium showed that in all conditions studied, there was no significant electrodeposition of strontium.

TABLE 3.2. RECOVERY YIELDS FOR YTTRIUM IN CLEAN SOLUTION WITH DIFFERENT CONCENTRATIONS OF HNO₃

HNO ₃ (0.001M)	
Recovery time (min)	Recovery yield (%)
15	83
30	79
HNO ₃ (1.0M)	
Recovery time (min)	Recovery yield (%)
5	97
10	97

3.1.2.2. Electrolysis with radiotracer materials

The electrolysis process was performed with a mixture of irradiated Sr(NO₃)₂ and irradiated Y₂O₃. These materials were irradiated at nuclear reactor IEA-R1m, producing ⁸⁸Y (γ emitter, half-life $T_{1/2} = 106.64$ d) and ⁸⁵Sr (γ emitter, $T_{1/2} = 64$ d).

The solutions were analysed using γ spectroscopy before and after electrodeposition, to evaluate the electrodeposition yield, using the HPGe detector. The recovery stage was performed in 10 min, and the recovery yield was evaluated by measuring the solutions before and after the process in the HPGe detector. At the end of the experiment, the electrodes were washed with 3M HNO₃ and acetone.

The experiment was performed with a mixture of ⁸⁵Sr and ⁸⁸Y, under ideal conditions of electrodeposition: $I = 60$ mA, initial pH3.5–4.0 with final pH2.5 in each electrolysis, bubbling N₂ gas, low concentration of yttrium oxide in the solution and recovery with 1M HNO₃ (pH = 2.5) (see Fig. 3.8). It can be observed that in the first 30 min of electrolysis, there was no yttrium electrodeposition,

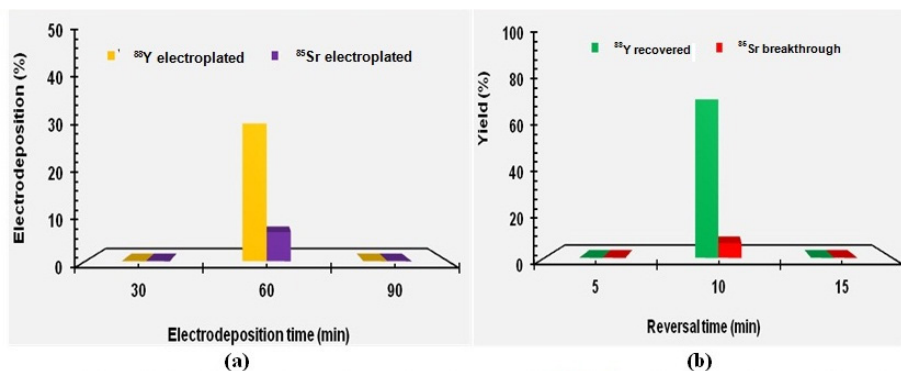


FIG. 3.8. (a) Percentage of electrodeposition of ($^{85}\text{Sr} + ^{88}\text{Y}$) as a function of electrodeposition time. (b) Percentage of ^{88}Y recovery, after electrodeposition and current reversal, as a function of time.

but after 60 min, yttrium was obtained with an electrodeposition yield of 30% (see Fig. 3.8(a)) and recovery of 70%, with <10% of ^{85}Sr being electroplated together with ^{88}Y (see Fig. 3.8(b)). There was no significant electrodeposition when electrolysis was done for 90 min. Thus, ideal conditions for electrodeposition and recovery of yttrium were established with low contamination with strontium.

3.1.2.3. Electrolysis with $^{90}\text{Sr}/^{90}\text{Y}$

Table 3.3 shows the results obtained for electrolysis using the pair $^{90}\text{Sr}/^{90}\text{Y}$ with a 1 mol/L HNO_3 solution at pH5.0. The conditions for the process were potential difference $\text{ddp} = 3.5 \text{ V}$, $I = 60 \text{ mA}$, with N_2 gas and stirring. For the reversal process, a new solution of 1 mol/L HNO_3 at pH4.0 was used. The parameters were $\text{ddp} = 3.0 \text{ V}$ and $I = 60 \text{ mA}$.

According to Table 3.3, 32% of ^{90}Y was electroplated, and after 5 min of reversion, there was a recovery of ~82% of ^{90}Y . The global yield was 26%, less than obtained in the literature [3.1, 3.2]. An experiment was performed using the electrolysis conditions described in the literature [3.1, 3.2], and no deposition of ^{90}Y was observed. It can be concluded that the apparatus utilized was not the correct one, but experience was gained in carrying out this type of process.

TABLE 3.3. RESULTS FOR $^{90}\text{Sr}/^{90}\text{Y}$ ELECTROCHEMICAL GENERATOR

Electrolysis (separation)	Volume (mL)	Activity (MBq)	Amount of Y-90 electroplated (%)
Solution I ^a (before process)	30	431.79	0
Solution I ^a (after 30 min)	30	330.78	23
Solution I ^a (after +30 min)	30	223.11	32
Electrolysis (reversal)	Volume (mL)	Activity (MBq)	Y-90 recovery (%)
Solution II ^b (after 5 min)	29.77	83.25	82
Solution II ^b (after +5 min)	28.95	30.93	29

^a Solution I: 1 mol/L HNO₃ solution, pH5.0.

^b Solution II: 1 mol/L HNO₃ solution, pH4.0.

3.1.3. Strontium-90/yttrium-90 generators via colloid formation

The basis was to form colloids of yttrium in hydroxide medium and then dissolve colloidal particles with HCl. The initial experiments involved the use of different filter materials and a solution of $^{85}\text{SrCl}_2$ dissolved in H₂O with 1 mol/L HCl. The separation efficiency was evaluated using γ spectrometry, and the results are shown in Fig. 3.9.

According to Fig. 3.9, the best results were obtained using a Millipore filter and porous plate column, where ^{85}Sr is not retained when washed with a 1 mol/L NH₄OH solution.

Figure 3.10 shows the study performed to evaluate the behaviour of the selected filter materials with the use of irradiated Y₂O₃ (after dissolution in a 2 mol/L HNO₃ solution by heating).

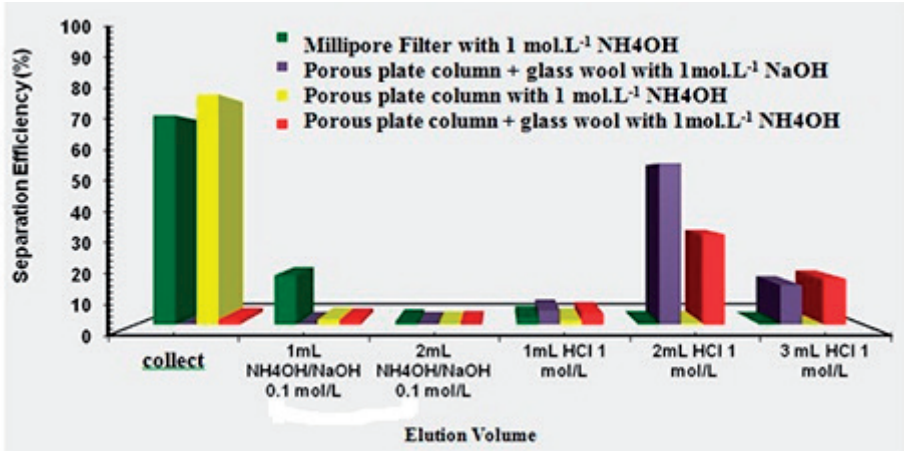


FIG. 3.9. Comparative study with different filter materials used for ^{85}Sr colloid.

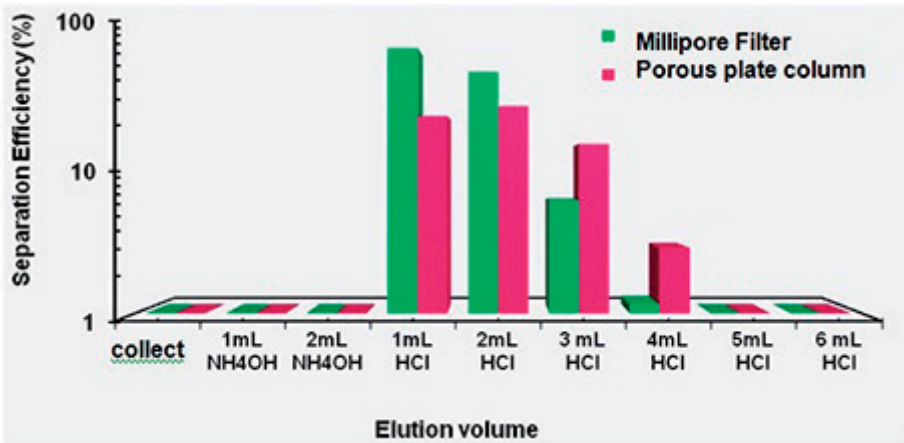


FIG. 3.10. Evaluation of filter materials used for washing Y_2O_3 with a 1 mol/L NH_4OH solution followed by aqueous HCl.

According to Fig. 3.10, the Millipore filter was more efficient in releasing yttrium. The next steps involved the use of the pair $^{90}\text{Sr}/^{90}\text{Y}$. The elution curve in Fig. 3.11 shows an experiment performed with 222 MBq of $^{90}\text{Sr}/^{90}\text{Y}$ wherein the solution was neutralized with NH_4OH solution, passed through the Millipore filter that was previously washed with NH_4OH solution and the elutions carried out with HCl solution. A good separation between both the radionuclides was achieved, but with a low recovery yield of ^{90}Y .

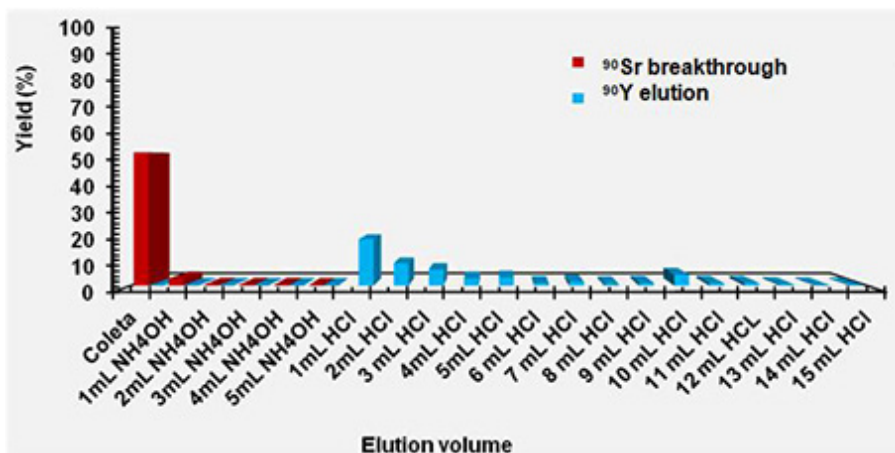


FIG. 3.11. Elution yield of a $^{90}\text{Sr}/^{90}\text{Y}$ colloid generator using a Millipore filter and 1 mol/L NH_4OH and 2 mol/L HCl .

3.1.4. Quality control

3.1.4.1. ICP OES

A method for the determination of strontium was developed using the ICP OES methodology wherein the equipment used was Varian Vista — MPX, Varian Inc., United States of America. Calibration curves were carried out in decreasing concentrations of strontium certified solutions: 0.2–1 ppm, 0.02–0.1 ppm and 0.002–0.01 ppm. The linear regression analysis of the curves showed good results, and values of quantification limits (QLs) and DLs were calculated. The values found were $\text{QL} = 0.23$ ppb and $\text{DL} = 0.057$ ppb. Thus, it is possible to detect the mass of strontium equivalent to a concentration of $0.03 \mu\text{Ci}$ of ^{90}Sr , calculated solely by the decay of ^{90}Sr . Table 3.4 shows the radionuclidic purity of the two generator technologies developed: cation exchange and colloid formation using ICP OES.

It can be observed that the cation exchange generators showed lower ^{90}Sr breakthrough than the colloid generator.

3.1.4.2. Extraction paper chromatography

EPC was carried out for all the generators developed where Whatman 3MM was used as the stationary phase and 0.9% NaCl as the mobile phase. The complexes oxime (8-hydroxyquinoline) and 2-ethylhexyl-phosphoric acid mono-2-ethylhexyl ester (PC88A) were evaluated for the separation of the

two species of strontium and yttrium. Analysis was performed using a liquid scintillation counter (LSC). Figure 3.12 shows the EPC of $^{90}\text{YCl}_3$ solution using both complexes.

TABLE 3.4. STRONTIUM-90 BREAKTHROUGH OBTAINED USING ICP OES

Generator	Elution	Intensity (counts/s)	Sr-90 breakthrough (%)
G ₁ cation exchange	(8.63 ± 0.52) mL 0.03 mol/L EDTA	(3.9 ± 0.5) × 10 ³	<0.001
G ₂ cation exchange	(5.44 ± 0.60) mL 0.03 mol/L EDTA	(4.3 ± 0.8) × 10 ³	<0.001
Colloid formation	(1.14 ± 0.13) mL HCl 1 mol/L	(37.3 ± 7.6) × 10 ³	19 ± 4

Note: Mean ± standard deviation ($n = 11$ and $n = 10$ for G1 and G2 cation generators and $n = 2$ for colloid generator).

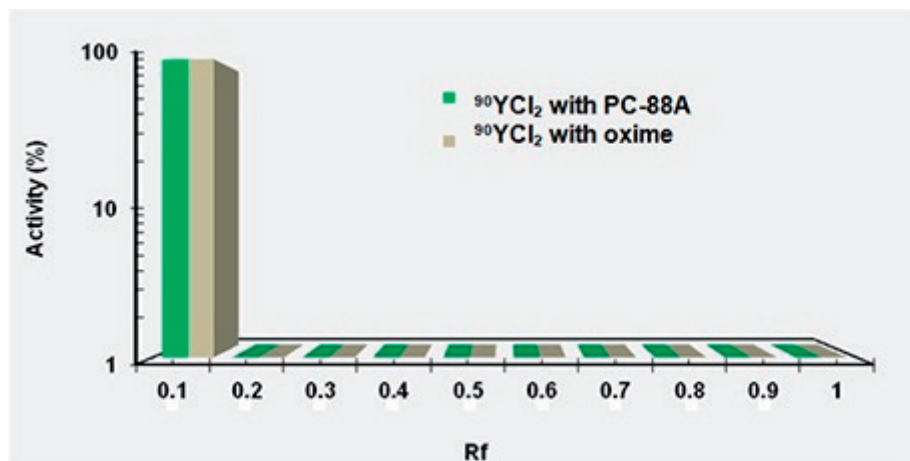


FIG. 3.12. EPC for $^{90}\text{YCl}_3$.

According to Fig. 3.12, there is a good complexation with both complexes. For the $^{90}\text{Sr}/^{90}\text{Y}$ generators, particularly in the case of the cation exchange generator, where the study was performed to evaluate the presence of EDTA after destruction. The results are shown in Fig. 3.13.

According to Fig. 3.14, PC88A shows a better separation than oxime for ^{90}Y , but does not differentiate between free ^{90}Y and its complex with EDTA. Figure 3.14 shows the global results for EPC performed for the three generator technologies developed.

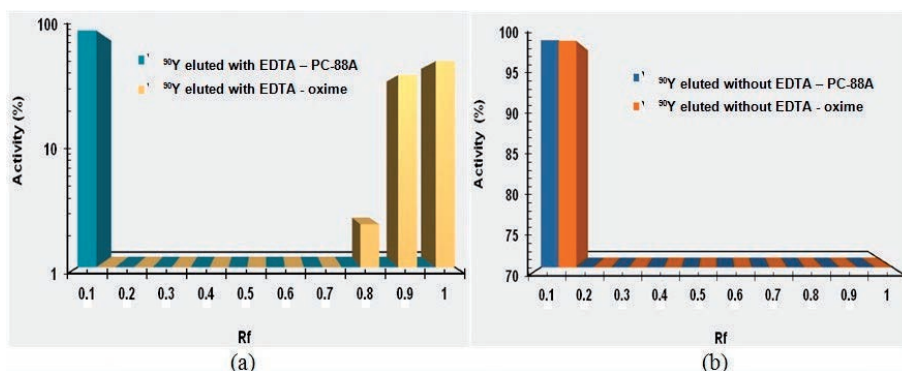


FIG. 3.13. EPC performed in cation exchange generators to evaluate EDTA destruction.

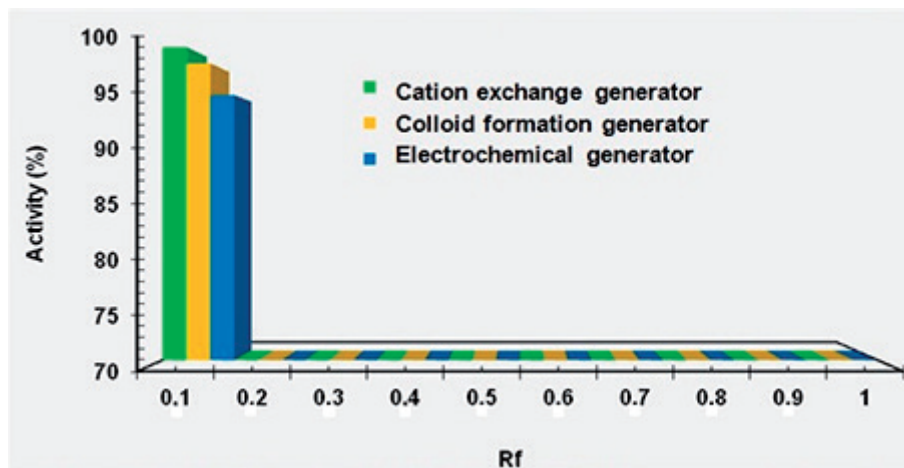


FIG. 3.14. EPC using PC88A for the three $^{90}\text{Sr}/^{90}\text{Y}$ generators developed.

3.1.4.3. Liquid scintillation counting

A new LSC, a Hydrex 300SL model, was acquired, and operation started in March 2010. This equipment has three photomultiplier tubes aligned at 120° to each other. These three photomultiplier tubes enable triple to double coincidence ratio counting, allowing a direct way of obtaining counting efficiency and activity results. Figure 3.15 shows the spectra obtained from $^{90}\text{YCl}_3$ and $^{90}\text{Sr}/^{90}\text{Y}$ eluted from all generators developed.

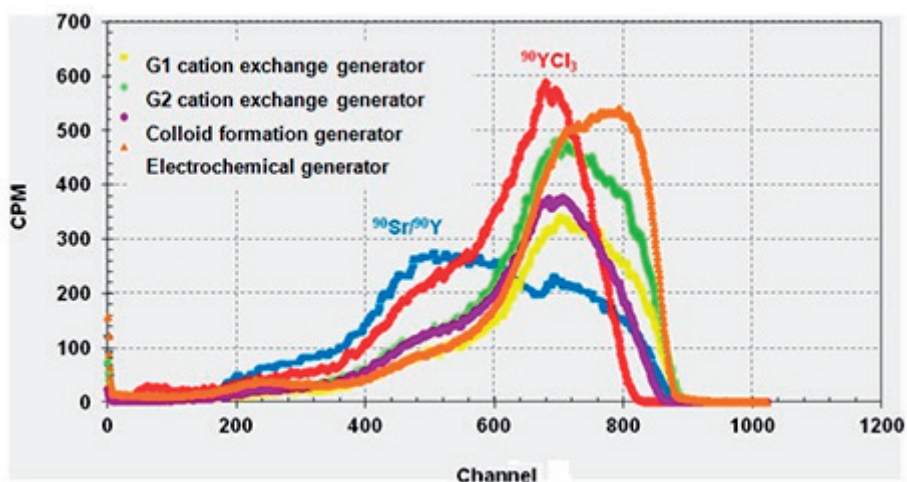


FIG. 3.15. The β spectra of $^{90}\text{YCl}_3$ and $^{90}\text{Sr}/^{90}\text{Y}$ samples and the generators developed.

3.2. MOLECULES LABELLED WITH ^{188}Re

3.2.1. Anti-CD20

3.2.1.1. Reduction of anti-CD20

Rituximab (10 mg, MabThera/Roche) was reduced by reaction with 2-mercaptoethanol (5 μL , 2-ME/Sigma) at room temperature for 30 min, and the resulting solution was passed through a PD-10 column (Sephadex G-25, Pharmacia) using phosphate buffered saline (PBS), pH7.4, purged with nitrogen as the mobile phase, and fractions of 1 mL were collected. The concentration of the reduced antibody was determined by absorbance at 280 nm on an ultraviolet (UV) visible spectrophotometer (Hitachi Instruments U-2010). The number of resulting free sulphydryl groups ($-\text{SH}$) was assayed with Ellman's

reagent (Sigma). The mean recovery of the reduced antibody was $98.5\% \pm 2.6\%$ (mean \pm standard deviation (SD), $n = 4$) and the number of $-SH$ groups generated per molecule of antibody was 5.0 ± 1.0 (mean \pm SD, $n = 4$).

3.2.1.2. Radiochemical quality control of ^{188}Re rituximab

The labelling efficiency was evaluated using instant thin layer chromatography (ITLC). Both 0.9% NaCl and acetone were used as mobile phases to separate free perrhenate ($^{188}\text{ReO}_4^-$). Rhenium-188 tartrate and $^{188}\text{ReO}_4^-$ moved with the solvent front ($R_f = 1$) when 0.9% NaCl was used as the mobile phase, while radiocolloid ($^{188}\text{ReO}_2$) and ^{188}Re rituximab remained at the origin ($R_f = 0$). When acetone was used as the mobile phase, ^{188}Re rituximab, ^{188}Re tartrate and $^{188}\text{ReO}_2$ stayed at the origin, while $^{188}\text{ReO}_4^-$ moved to the solvent front. ITLC silica gel (SG) strips impregnated with HSA (5%) were used as the stationary phase and ethanol:ammonia:water (2:1:5 vol.%) was used as the mobile phase. In this chromatographic system, $^{188}\text{ReO}_2$ remained at the origin, while ^{188}Re rituximab, ^{188}Re tartrate and $^{188}\text{ReO}_4^-$ moved towards the solvent front.

3.2.1.3. Labelling of anti-CD20 and optimization of radiolabelling

The labelling studies were first performed using a liquid formulation of rituximab, based on the literature [3.4], that contained 1 mg of rituximab, 82.8 mg of sodium tartrate, 1.67 mg of SnCl_2 and 0.25 mg of gentisic acid. Perrhenate eluted from the $^{188}\text{W}/^{188}\text{Re}$ generator in 0.9% NaCl was added (~ 642.5 MBq). The solution was incubated for 1 h at room temperature at pH5.5. The labelling yield was $67.0\% \pm 0.2\%$. Because of this low labelling yield, a series of parameters was varied to identify a best formulation that could attain a high labelling yield, including antibody mass (0.25, 0.5, 1.0 and 2.5 mg), reducing agent mass (0.25, 0.5, 1.0, 1.67, 3.0, 5.0 and 7.0 mg), tartrate mass (20.7, 41.4, 82.8, 165.6 and 331.2 mg), reaction time (15, 30, 60 and 120 min), ^{188}Re volume (1 and 2 mL) and activity (3463.2 MBq). The stability for the optimized formulation was studied at different temperatures (room temperature, cold temperature of 5°C and dry ice) and at different times (4, 6 and 24 h). Figures 3.16–3.19 show the results of the effects seen on the labelling efficiency of ^{188}Re rituximab due to the variations made in the reducing agent mass, antibody mass, tartrate mass and reaction time. A volume of 1 mL of ^{188}Re seemed to be superior to the volume of 2 mL, with higher labelling yields and lower impurities. When rituximab was labelled with a high activity of ^{188}Re , the impurity levels of $^{188}\text{ReO}_2$ and $^{188}\text{ReO}_4^-$ were $>25\%$, indicating that further studies are necessary to improve the labelling efficiency.

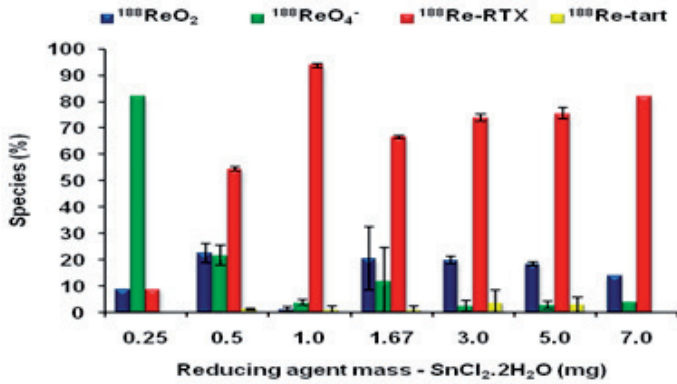


FIG. 3.16. Variation of RCP (%) of ¹⁸⁸Re rituximab with amount of reducing agent.

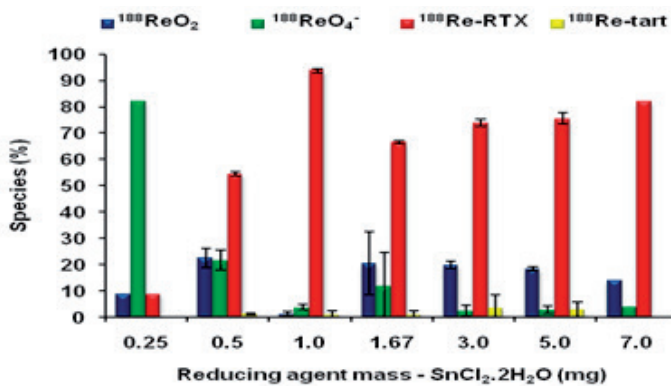


FIG. 3.17. Variation of RCP (%) of ¹⁸⁸Re rituximab with amount of antibody.

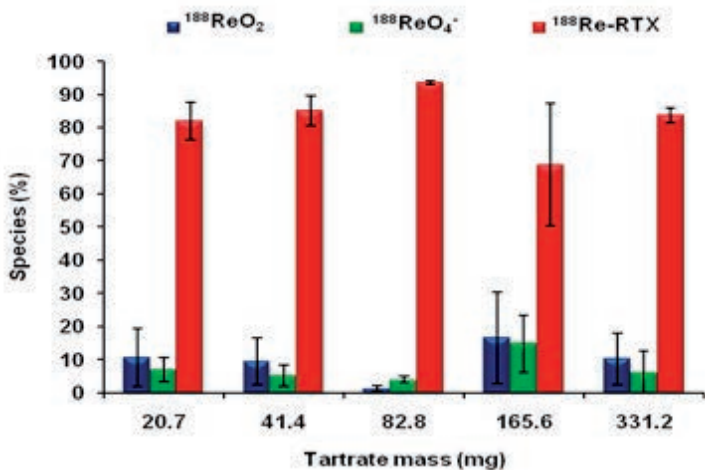


FIG. 3.18. Variation of RCP (%) of ¹⁸⁸Re rituximab with amount of tartrate salt.

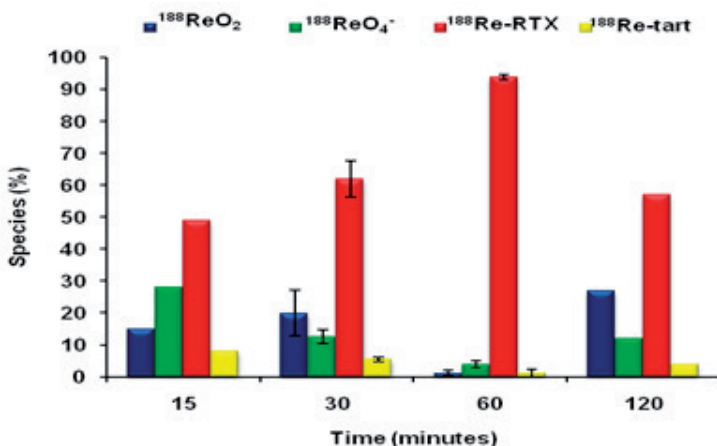


FIG. 3.19. Variation of RCP (%) of ¹⁸⁸Re rituximab with reaction time.

The stability at room temperature, cold temperature (5°C) and dry ice and at different times (4, 6 and 24 h) was studied for optimized formulation (1.0 mg rituximab, 82.8 mg tartrate, 1 mg SnCl₂·2H₂O, 0.25 mg gentisic acid, 1 mL ¹⁸⁸ReO₄⁻, 1 h of reaction), as shown in Fig. 3.20.

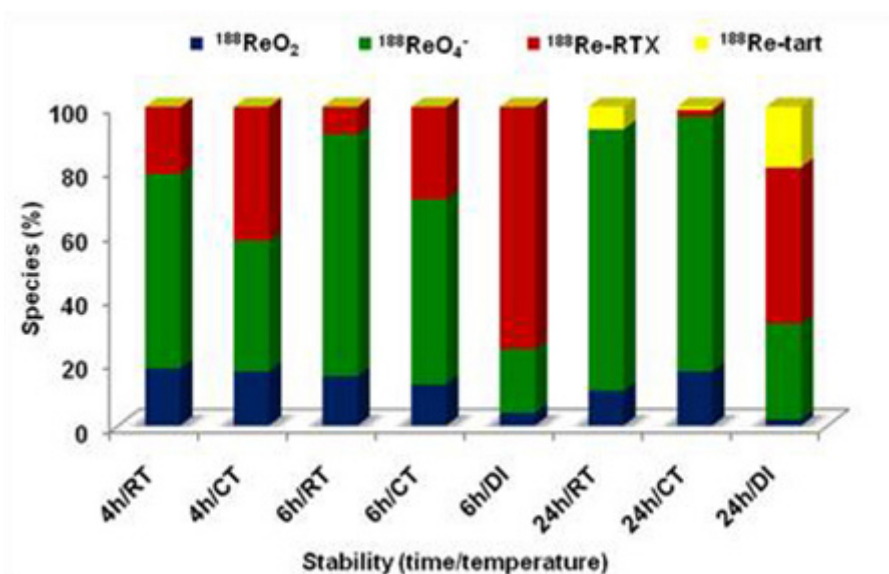


FIG. 3.20. Variation of RCP (%) of ^{188}Re rituximab (best formulation) at different times and different temperatures. CT: cold temperature (5°C); DI: dry ice; RT: room temperature.

A different approach was employed for labelling anti-CD20 antibody using the $^{99\text{m}}\text{Tc}$ and ^{188}Re tricarbonyl technique. This project was developed at the Paul Scherrer Institute (Switzerland), in cooperation with R. Schibli. The study was successful and the results (not described here) have been published [3.5].

3.2.2. DMSA(V)

3.2.2.1. Preparation of ^{188}Re -DMSA(V)

The RCP was evaluated using TLC on SG strips to determine the labelling efficiency and impurity formation. TLC SG strips ($1.5\text{ cm} \times 12\text{ cm}$) were developed in two different solvent systems. Acetone was used to separate $^{188}\text{ReO}_4^-$ ($R_f = 1$) from ^{188}Re DMSA(V) and $^{188}\text{ReO}_2$ ($R_f = 0$), and 5% glycine was used to separate $^{188}\text{ReO}_2$ ($R_f = 0$) from ^{188}Re DMSA(V) and $^{188}\text{ReO}_4^-$ ($R_f = 1$).

Method I: Initially, ^{188}Re DMSA(V) was prepared using a commercial kit of DMSA(III) for labelling with $^{99\text{m}}\text{Tc}$ (IPEN-CNEN/SP). The kit contained 1.0 mg of DMSA, 0.44 mg of $\text{SnCl}_2 \cdot 2\text{H}_2\text{O}$, 0.70 mg of ascorbic acid and 50 mg of inositol. The labelling was performed using 1 mL of $^{188}\text{ReO}_4^-$ (185 MBq), and the reaction time was 30 min at high temperature (100°C). The variables studied were reaction temperature (100°C and room temperature), reaction time

(20 and 30 min) and volume of $^{188}\text{ReO}_4^-$ (1.0 and 2.0 mL). Figures 3.21, 3.22 and 3.23 show the results of the effect of the variation of reaction temperature, time and volume on the labelling efficiency of ^{188}Re DMSA(V) prepared using a commercial kit of $^{99\text{m}}\text{Tc}$ DMSA(III). The best labelling yield (>98%) was achieved when 1 mL $^{188}\text{ReO}_4^-$ was used for 30 min of reaction while heating at 100°C [3.6].

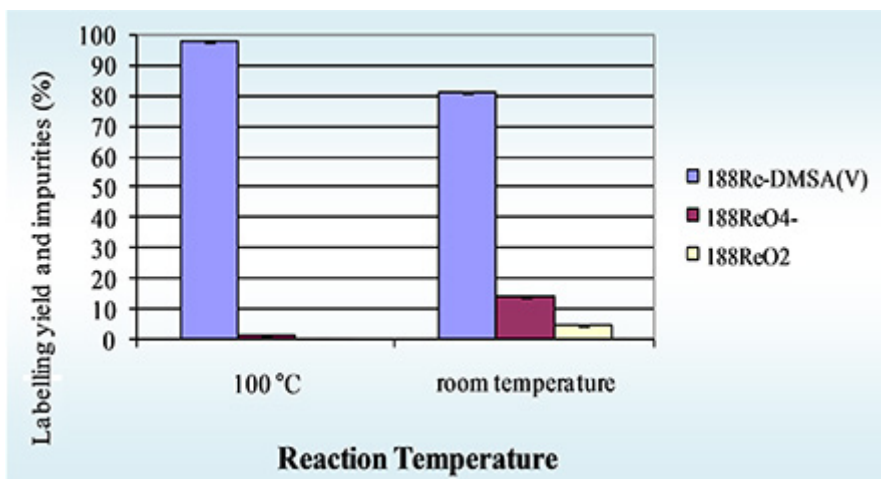


FIG. 3.21. Variation of labelling yield with reaction temperature.

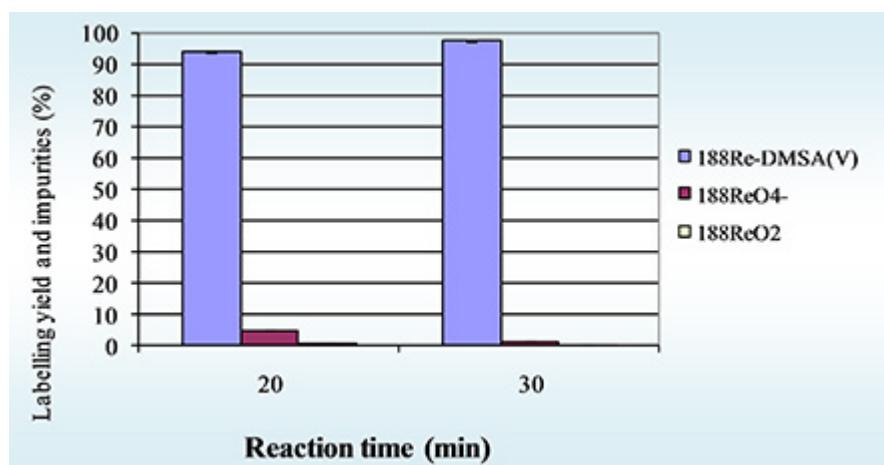


FIG. 3.22. Variation of labelling yield with reaction time.

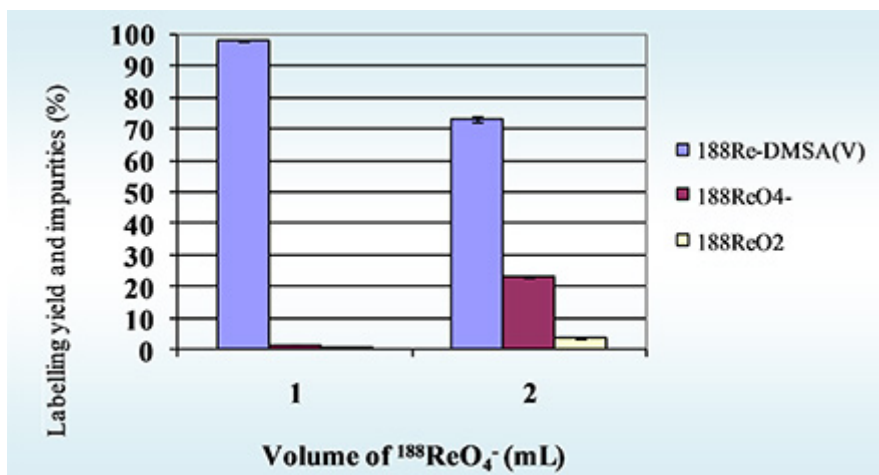


FIG. 3.23. Variation of labelling yield with volume of $^{188}\text{ReO}_4^-$.

Method II: The second method was carried out in a vial containing 2.5 mg of DMSA, 0.2 mg of $\text{SnCl}_2 \cdot 2\text{H}_2\text{O}$ and 10.5 mg of sodium oxalate, in a total volume of ~ 1 mL. The pH was adjusted to ~ 1.5 with 37% HCl. The labelling was done with 1 mL of $^{188}\text{ReO}_4^-$ (185 MBq) and the reaction time was 40 min at room temperature. The variables studied were pH (1.5, 2.5, 3.5 and 5), amount of reducing agent at pH 3.5 (0.2, 0.5 and 1.0 mg) and labelling stability (0, 2, 4 and 24 h). Figure 3.24 shows the results of the effect of pH variation, Fig. 3.25 shows the effect of the variation of the reducing agent at pH 3.5 and Fig. 3.26 shows the labelling stability. The advantage of this method is that it does not require high temperatures to achieve good labelling yields owing to the use of oxalate. This latter compound binds ^{188}Re in a more appropriate geometry, thus promoting a more efficient reduction of $^{188}\text{ReO}_4^-$ in comparison to method I [3.7–3.9].

3.2.3. Bisphosphonates

The objective of this work was the optimization of the labelling of sodium MDP, EDTMP and clodronate with ^{188}Re .

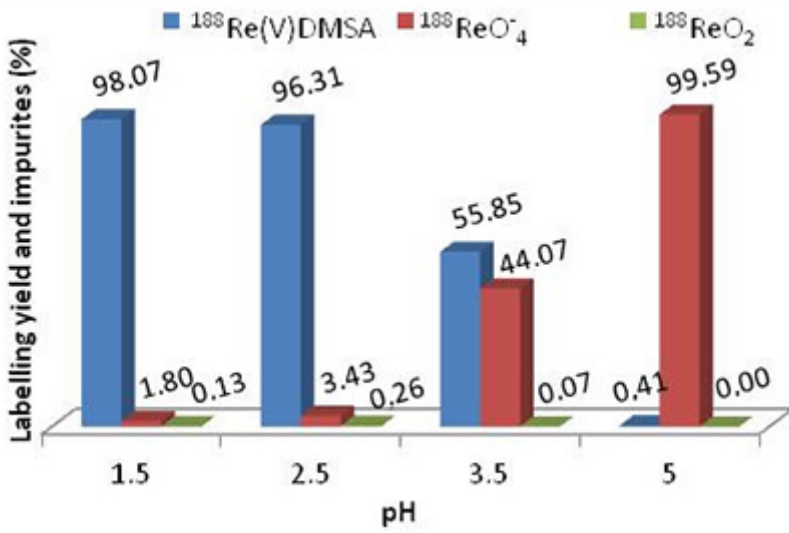


FIG. 3.24. Variation of labelling yield with pH.

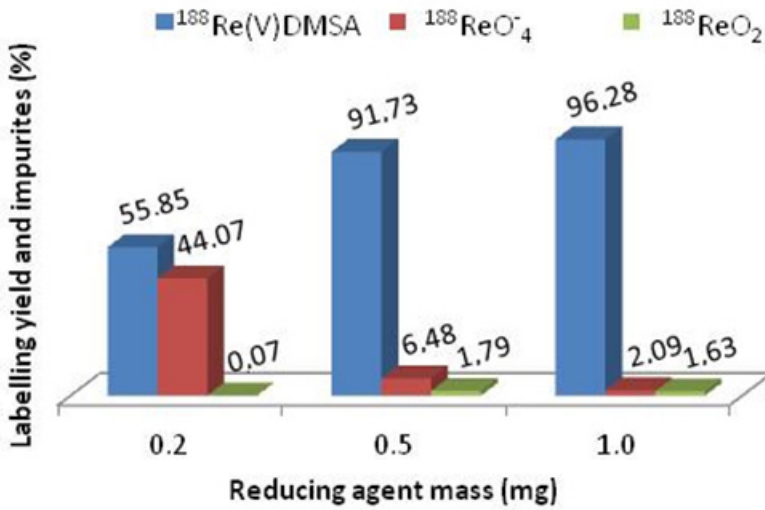


FIG. 3.25. Variation of labelling yield with amount of reducing agent at pH 3.5.

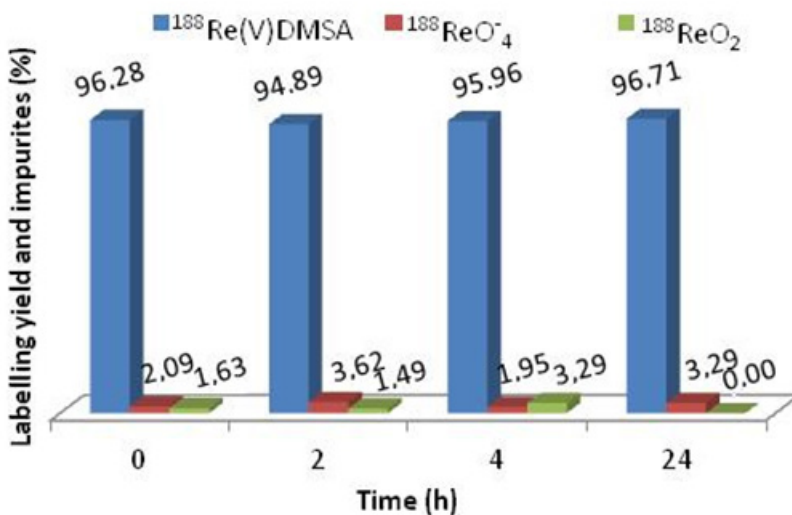


FIG. 3.26. Stability of $^{188}\text{Re(V) DMSA}$ at pH3.5 and room temperature.

3.2.3.1. Methods

Rhenium-188 was obtained by eluting a $^{188}\text{W}/^{188}\text{Re}$ generator obtained from POLATOM. Ascorbic acid and SnCl_2 were used as reducing agents for the labelling of MDP, EDTMP and clodronate. The variables studied for MDP and EDTMP labelling were amount of ligand (3, 6 and 10 mg), SnCl_2 (5, 7, 10 and 11 mg) and ascorbic acid (1, 3, 5 and 6 mg), reaction time (15, 60, 120 and 360 min) and pH (1, 2, 3 and 5). The variables studied for clodronate labelling were reaction time (30, 60 and 90 min) and temperature (room temperature, 50°C and 100°C). The radiochemical quality control, which also measures the efficiency of labelling, was evaluated by Whatman 3MM paper chromatography using acetone and 0.9% NaCl as solvents.

3.2.3.2. Results

The ideal formulations for each phosphonate labelling were:

- MDP: 10 mg of MDP, 5 mg of SnCl_2 , 3 mg of ascorbic acid, 30 min reaction time, room temperature and pH1, to attain a labelling yield of 98%;
- EDTMP: 50 mg of EDTMP, 8 mg of SnCl_2 , 30 mg of ascorbic acid, 60 min reaction time, room temperature and pH2, to achieve a labelling yield of 83%;

- (c) Clodronate: 20 mg of clodronate, 3 mg of SnCl_2 , 2 mg of ascorbic acid, 60 min reaction time, temperature of 100°C and pH1, to achieve a labelling yield of 85%.

An excellent labelling yield of 98% was achieved for ^{188}Re MDP. However, the best labelling yield so far obtained for ^{188}Re EDTMP was 83%, which is not satisfactory. Further experiments are required to improve the product formation. A few experiments have been performed for labelling clodronate with ^{188}Re , but they did not give a satisfactory yield.

3.2.4. Routine production of ^{90}Y hydroxyapatite

IPEN produced colloids for radiation synovectomy, and the main product was ^{90}Y HA. The labelling yield was 80% with RCP $>98\%$, the radioactive concentration was 450–550 MBq/mL and the mean particle size was 15 μm .

Figure 3.27 shows a comparison of the images upon administration of ^{90}Y citrate (imported) and ^{90}Y HA (homemade) into patients.

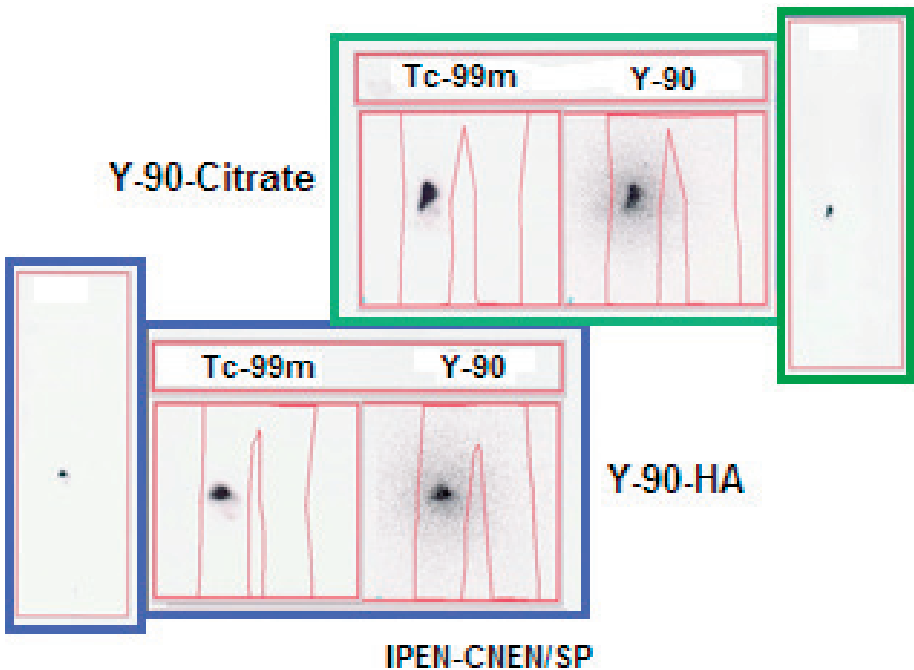


FIG. 3.27. Application of ^{90}Y citrate and ^{90}Y HA in patients.

Future experiments will involve the use of homemade HA and ^{90}Y produced from homemade generators for evaluation of their quality.

ACKNOWLEDGEMENT

The authors of this chapter wish to thank the IAEA, IPEN, the Foundation for Research Support of the State of São Paulo and the National Council for Scientific and Technological Development (Brazil) for support.

REFERENCES TO CHAPTER 3

- [3.1] BARRIO, G., OSSO, J.A., Development of ^{90}Sr - ^{90}Y generators using the cation exchange technique at IPEN-CNEN-SP, Q. J. Nucl. Med. Mol. Imaging **54** (2010) 73.
- [3.2] BARRIO, G., OSSO, J.A., “Radionuclide impurities in $^{90}\text{Sr}/^{90}\text{Y}$ generators: Experience at IPEN/CNEN-SP”, Proc. Int. Symp. Technetium and Other Radiometals in Chemistry and Medicine, Bressanone, SGEEditoriali, Padova, Vol. 1 (2010) 469.
- [3.3] BARRIO, G., Desenvolvimento de Tecnologias de Preparo de Geradores de $^{90}\text{Sr}/^{90}\text{Y}$ na Diretoria de Radiofarmácia do IPEN/CNEN-SP, Masters Thesis, São Paulo, Brazil (2010).
- [3.4] DIAS, C.R., et al., “Comparative stability studies of antibody anti-CD20 labeled with ^{188}Re by direct method and tricarbonyl core”, Proc. Int. Symp. Technetium and Other Radiometals in Chemistry and Medicine, Bressanone, SGEEditoriali, Padova, Vol. 1 (2010) 413.
- [3.5] DIAS, C.R., et al., Radiolabeling of rituximab with ^{188}Re and $^{99\text{m}}\text{Tc}$ using the tricarbonyl technology, Nucl. Med. Biol. **38** (2011) 19.
- [3.6] BRAMBILLA, T. P., OSSO, J.A., Studies of labelling procedures for the preparation of ^{188}Re -DMSA(V), Q. J. Nucl. Med. Mol. Imaging, **54** (2010) 69–70.
- [3.7] DE PAULA BRAMBILLA, T., Desenvolvimento de Método para Preparação do Kit de DMSA Pentavalente para Marcação com $^{99\text{m}}\text{Tc}$, Masters Thesis, São Paulo, Brazil (2009).
- [3.8] DE BARROS RODRIGUES DIAS, C.A., Estudos da Química dos Complexos Nitrido-metal na Marcação de Biomoléculas com Tc-99m e Re-188”, PhD Thesis, São Paulo, Brazil (2010).
- [3.9] BOLZATI, C., et al., An alternative approach to the preparation of ^{188}Re radiopharmaceuticals from generator-produced $[\text{}^{188}\text{ReO}_4]^-$: Efficient synthesis of ^{188}Re (V)-meso-2,3-dimercaptosuccinic acid, Nucl. Med. Biol. **27** (2000) 309.

Chapter 4

EVALUATION OF THE $^{90}\text{Sr}/^{90}\text{Y}$ ELECTROCHEMICAL GENERATOR KAMADHENU AND USE OF ITS ^{90}Y ELUATE FOR LABELLING MAbS

A. ALBERTI
Isotopes Centre,
Havana, Cuba

J. COMOR
ELEX Commerce,
Belgrade, Serbia

A. CRUZ
Isotopes Centre,
Havana, Cuba

R. LEYVA
Isotopes Centre,
Havana, Cuba

I. HERNÁNDEZ
Isotopes Centre,
Havana, Cuba

A. PERERA
Clinical Research Centre,
Havana, Cuba

Abstract

During the second period of this CRP, Cuba received a prototype of an electrochemical generator, named Kamadhenu¹, for performance evaluation. Under the supervision of J. Comor, an evaluation process was carried out related to elution parameters, such as composition of electrolyte, applied current, time of electrolysis, number of washing and purification steps, among others. As an innovation to the process, carrier strontium was used to reduce ^{90}Sr in the

¹ Kamadhenu, in Hindu mythology kama-dhenu, ‘wish-cow’, was a miraculous cow of plenty who could give her owner whatever he desired.

final solution to <1 ppm, as demonstrated by EPC. Results obtained with almost 100 elutions showed that the generator is reliable, and ^{90}Y can be obtained with the necessary characteristics for biomolecule labelling. DOTA and DTPA conjugation of anti-CD20 MAb (rituximab) were carried out and labelling was performed with ^{90}Y from the Kamadhenu generator. Experimental conditions were standardized using different molar ratios of chelating agent and antibody to obtain a suitable conjugated antibody. Subsequently, the binding properties of the conjugated antibody were assessed using flow cytometry. Binding properties of ^{90}Y DTPA rituximab were also assessed using conventional and Lindmo methods. The results demonstrated that ^{90}Y obtained from the Kamadhenu generator was of good quality.

4.1. INTRODUCTION

Yttrium-90 is widely used for radiolabelling different molecules for the treatment of various pathologies such as cancer, bone pain and rheumatoid arthritis. This radioisotope can be made conveniently available from a radionuclide generator [4.1–4.3]. One of the principal achievements of the CRP in previous years was the development of a $^{90}\text{Sr}/^{90}\text{Y}$ generator based on different separation methods: extraction, ion exchange and electrochemical. Cuba received a prototype electrochemical generator, and, under the supervision of expert J. Comor, started the installation, set up and evaluation of the Kamadhenu generator. The main concern in the production of ^{90}Y was related to ^{90}Sr content as an impurity, which localizes in the skeleton, and, owing to its long half-life (28.9 years), has a very low maximum permissible body burden of 74 kBq (2 μCi). Other parameters related to generator performance were also studied.

Rituxan is a chimeric antibody that recognizes the CD20 receptor in human B cells. It is useful in the treatment of NHL and autoimmune diseases such as systemic lupus erythematosus and rheumatoid arthritis. CD20 is a non-glycosylated protein present on the surface of B cells during its ontogeny development, but is not in blood circulating cells [4.4]. Increased expression of CD20 is found in pathogenic B cells such as lymphomas. Hence, it is an attractive target for therapy [4.5], and its potential has been characterized by various in vitro and in vivo investigations [4.6–4.9].

4.2. MATERIALS AND METHODS

4.2.1. Evaluation of Kamadhenu

The first prototype of this generator, model KA01, was installed at the Isotope Center of Havana, Cuba, for set up and evaluation.

Kamadhenu consists of five main components:

- (a) A fluid processing electrochemistry module;
- (b) A ^{90}Sr stock reservoir;
- (c) An industrial standard control unit;
- (d) A programmable power supply for electrolysis;
- (e) A computer based user interface.

To evaluate the generator, different parameters were adjusted during the initial set up of Kamadhenu so that ^{90}Y was produced with very low levels of ^{90}Sr contamination. The parameters studied included current to be applied, time of electrolysis process, composition of electrolyte, addition (or not) of strontium carrier, number of purification and washing steps, among others.

In all cases, ^{90}Sr was obtained as $^{90}\text{Sr}(\text{NO}_3)_2$ in 2M HNO_3 , and different dilutions were made according to the purpose of the experiments. The final composition of the stock solution, after some experiments, was defined as 0.01M HNO_3 containing 70 mg $\text{Sr}(\text{NO}_3)_2/\text{dm}^3$ and 625 mg $\text{NH}_4\text{NO}_3/\text{dm}^3$ with a pH in the range 2.5–3.0 and containing the available ^{90}Sr activity. The maximum activity transferred to the electrochemical cell was 50 mCi.

The electrochemical separations were all made at a constant current mode of operation. To optimize the current to be applied for selective deposition of ^{90}Y , the effect of applied current on deposition was studied by measuring the percentage deposition of ^{90}Y as a function of current when electrochemical deposition was performed at pH 2.5–3.0.

The use of $\text{Sr}(\text{NO}_3)_2$ as a carrier in the electrolyte was considered to investigate its influence on the ^{90}Sr content in the final ^{90}Y solution.

The ^{90}Sr contamination in ^{90}Y eluted from the generator was determined with the EPC method [4.10] using the chelating agent 2-ethylhexyl, 2-ethylhexyl phosphonic acid (KSM-17) and measuring the chromatograms by liquid scintillation.

4.2.2. Radiolabelling of monoclonal antibodies with ^{90}Y from electrochemical generator Kamadhenu

*4.2.2.1. MAb*s

A chimeric MAb, rituximab (rituxan, Roche), was used. A modified antibody, T1hT [4.8] was used as the isotype control.

4.2.2.2. Cell line and culture

Ramos cell line (CRL-1596, ATCC) was used for binding experiments in Roswell Park Memorial Institute (RPMI) 1640 (Gibco) media supplemented with penicillin (100 units/mL), streptomycin (100 µg/mL) and foetal calf serum (10%). Cells were incubated at 37°C in 5% CO₂.

4.2.2.3. DOTA conjugation

Rituximab (15 mg/mL) was incubated overnight at room temperature with NHS DOTA in 0.1M PBS, pH8.5, at different molar ratios (1:160, 1:80 and 1:40). Then, a purification step using exclusion chromatography in a Sephadex column (PD-10, Pharmacia) was performed.

4.2.2.4. DTPA conjugation

Rituximab (10 mg/mL) was incubated overnight with CHX-A DTPA (N-[(R)-2-amino-3-(p-isothiocyanato-phenyl) propyl]-trans-(S,S)-cyclohexane-1,2-diamine-N,N,N',N'',N'''-pentaacetic acid) in NaHCO₃ buffer 0.1M, pH8.5 at room temperature and at different molar ratios (1:30, 1:20, 1:10 and 1:5). Then, purification by exclusion chromatography in a Sephadex column (PD-10, Pharmacia) was performed.

Conjugated antibodies were concentrated by spin concentration, and 10 mg fractions of conjugated antibody were stored in 1 mL Eppendorf tubes at 4°C until use.

4.2.2.5. Binding experiments of conjugated antibodies to Ramos cells

Approximately 2×10^5 Ramos cells were incubated with 10 µg/mL of conjugated antibody for 30 min. Cells were washed with physiological saline and centrifuged at 2000 rev./min for 2 min. After the second incubation step with a rabbit antihuman IgG (Fcγ) coupled to fluorescein isothiocyanate (FITC; Dako) in ice for 30 min, flow cytometry analysis was performed (FACScan, Becton Dickinson).

4.2.2.6. Yttrium-90 radiolabelling and quality control of conjugated rituxan

In the case of DOTA conjugated rituximab, radiolabelling was carried out at 42°C, in acetate buffer 0.1M, pH5.2, for 45 min.

In the case of DTPA conjugated rituximab, radiolabelling was carried out at room temperature, in acetate buffer 0.25M, pH5.5, for 15 min.

Quality control of radiolabelling was performed using paper chromatography (Whatman 3MM, NH₄Ac 0.1M, pH5.5–6.0, EDTA 50mM) and ITLC strips (methanol (MeOH):NH₃ (10%) ratio of 1:1).

4.2.2.7. Cell binding assay of ⁹⁰Y DTPA rituximab

For binding experiments, cells were centrifuged and washed in isotonic PBS/bovine serum albumin, pH7.4, and resuspended in the same buffer at different cell concentrations (2.4, 1.2, 0.6, 0.3, 0.15 and 0.075 × 10⁶ cell/mL). The conjugate DTPA rituximab obtained at a 20:1 molar ratio was used for cell binding experiments after labelling. In duplicates, 10 μL of diluted radiolabelled antibody (5000 counts/min) was added to 1 mL of each cell dilution. Cell binding was processed with variable antigen concentrations according to previously described procedures [4.11, 4.12].

4.3. RESULTS

4.3.1. Evaluation of Kamadhenu

The final design and installation of the generator in a hot cell is depicted in Fig. 4.1 and the technical scheme is shown in Fig. 4.2.



FIG. 4.1. Strontium-90/yttrium-90 electrochemical generator assembly.

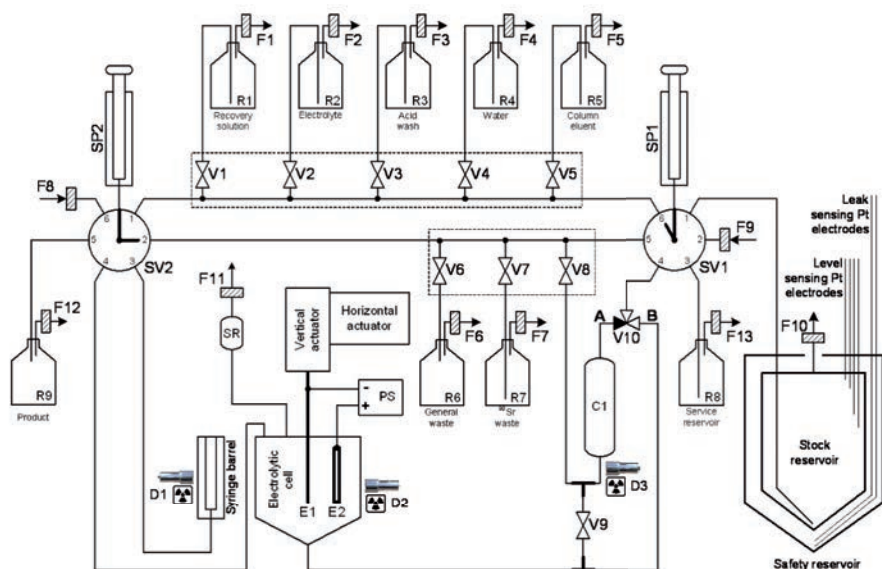


FIG. 4.2. Technical scheme of Kamadhenu. C1: liquid chromatographic column; D1–D3: radioactivity detectors; E1: straight platinum wire electrode; E2: spiral platinum wire (Winkler) electrode; F1–F13: filters; PS: programmable constant current/constant voltage power supply; R1–R9: reservoirs; SP1 and SP2: syringe pumps; SR: aerosol trapping safety reservoir; SV1 and SV2: six port selection valves; V1–V10: solenoid operated valves.

The electrochemical separations in all cases were made at a current constant mode of operation; however, the generator was designed to perform electrolysis also under constant voltage mode. The effects of applied current on ^{90}Y deposition at pH2.5–3.0 are summarized in Table 4.1 and the rate of deposition of ^{90}Y is shown in Fig. 4.3.

From these results, the current to be applied for carrying out the electrochemical deposition of ^{90}Y from the stock solution was selected. The percentage of ^{90}Y deposited was observed to increase by increasing the current value and it reached a maximum at $I = 0.8$ A. Further increasing the current caused a very high resistance of the electrolyte and consequently a high voltage, which ultimately can increase the possibility of codeposition of ^{90}Sr .

We evaluated the use of $\text{Sr}(\text{NO}_3)_2$ as a carrier in the electrolyte with the purpose of reducing the active strontium contamination in the final ^{90}Y solution. Figure 4.4 and Table 4.2 show the findings related to the use of strontium as the carrier and its influence on the rate of deposition of ^{90}Y .

The electrochemical deposition of ^{90}Y was very fast when the strontium carrier was not added. Approximately 99% of ^{90}Y deposition yield was achieved in 20 min. Table 4.2 shows that the ^{90}Sr contamination in ^{90}Y was more than the acceptable limit (20 μCi of ^{90}Sr in 1.0 Ci of ^{90}Y).

TABLE 4.1. EFFECTS OF APPLIED CURRENT ON ELECTRODEPOSITION OF ^{90}Y

Sample	Applied current (A)	Deposition of ^{90}Y (%) (90 min)
1	0.15	77
2	0.30	84
3	0.50	90
4	0.80	>97

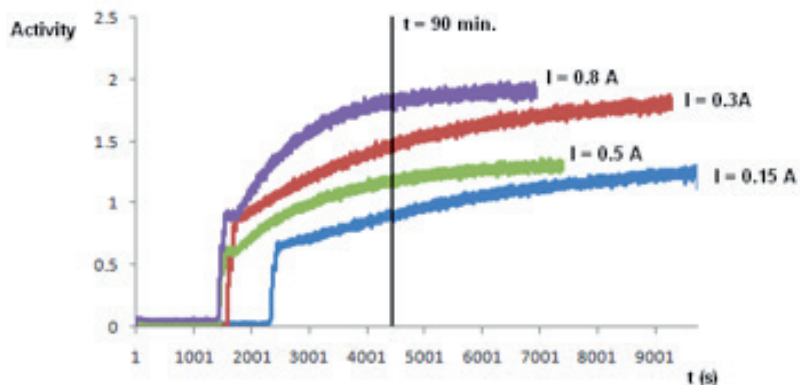


FIG. 4.3. Electrodeposition of ^{90}Y as a function of applied current.

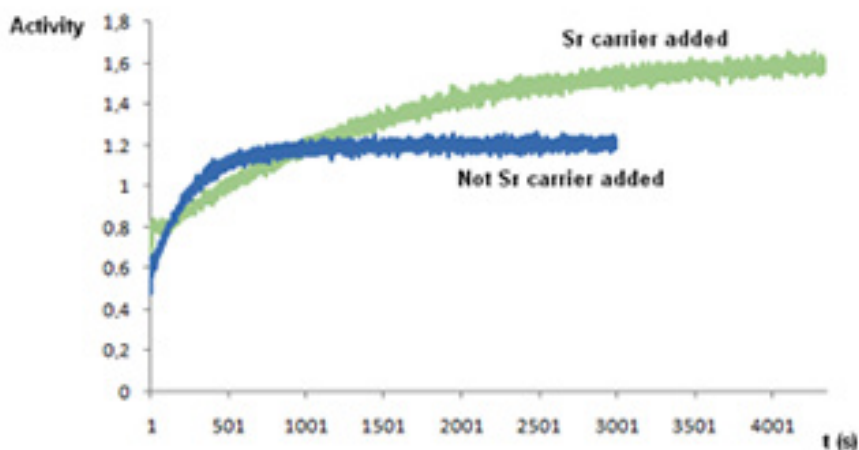


FIG. 4.4. Influence of $\text{Sr}(\text{NO}_3)_2$ carrier on ^{90}Y electrodeposition.

TABLE 4.2. STRONTIUM-90 CONTENTS IN THE RECOVERED ^{90}Y SOLUTIONS

Sample	Sr carrier	Sr-90 (ppm)
1	None added	13 ± 5
2	Added	$<1^a$

Note: Mean \pm SD; $n = 5$.

^a DL for liquid scintillation determination of ^{90}Sr under experimental conditions.

These experiments related to the strontium carrier helped to establish the best composition for the electrolyte: 0.01M HNO_3 containing $70 \text{ mg/dm}^3 \text{ Sr}(\text{NO}_3)_2$ and $625 \text{ mg/dm}^3 \text{ NH}_4\text{NO}_3$ with pH values in the range 2.5–3.0 (pH was adjusted by dropwise addition of concentrated ammonia solution).

The electrochemical separation process involved two electrolysis cycles. The first cycle was for separation and the second cycle for purification of ^{90}Y . This was not enough to achieve the desired radionuclide purity of ^{90}Y . The separation factor between yttrium and strontium was not sufficiently high, even after two purification cycles. Typically, three refining electrolysis cycles were needed and the duration of the milking process was ~ 6 h. A typical curve of the process is shown in Fig. 4.5.

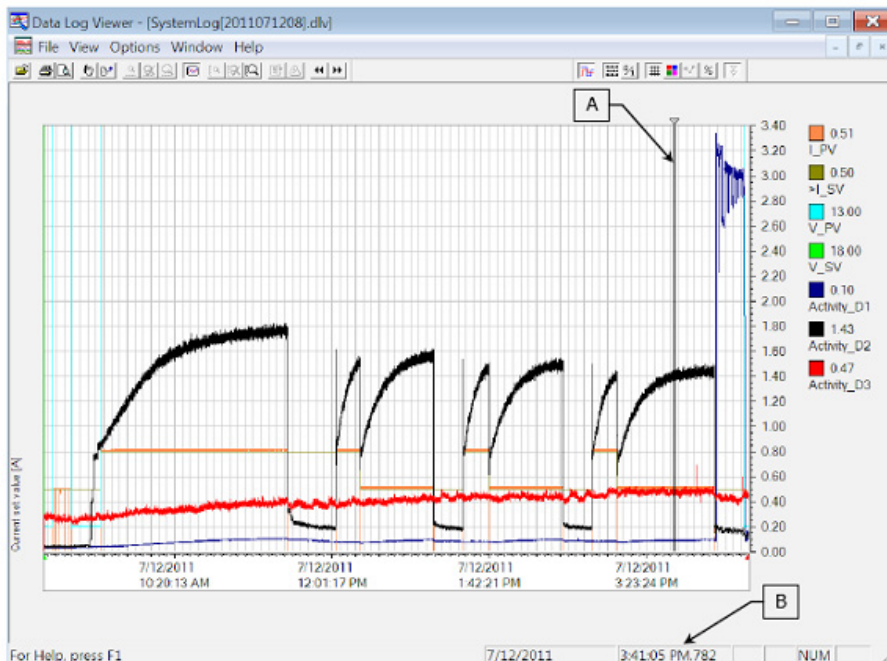


FIG. 4.5. Typical pattern of the whole separation process.

4.3.2. Performance of Kamadhenu

Each time, the generator provided a product in 0.05M HCl containing $^{90}\text{YCl}_3$ of radiochemical grade with <20 ppm of ^{90}Sr (typically <1 ppm). Approximately 90% of the initial activity was always recovered from the electrode and transferred into the product vial (see Table 4.3).

After standardization of the separation process, the amount of ^{90}Sr in the final product was kept below the acceptable limit in all separations. Furthermore, most of the results showed that it was well below the DL determined, in these conditions, using the EPC method (1 ppm).

Setting up all operating parameters for the electrochemical separation process allowed the following definitions of the consumption of raw materials (solvents) for every milking process:

- Recovery solution (HCl, 0.05M): 5.17 mL;
- Electrolyte (HNO_3 , 0.01M): 144.00 mL;
- Acid wash (HNO_3 , 1M): 92.90 mL;
- Water: 323.70 mL.

TABLE 4.3. ELECTROLYTIC YIELD OF ^{90}Y

Batch No.	Sr-90 (MBq (mCi))	Expected Y-90 (MBq (mCi))	Y-90 recovered (MBq (mCi))	Y-90 (%)
1	555 (15)	555 (15)	516 (13.9)	93.0
2	555 (15)	515 (13.9)	464 (12.5)	89.9
3	555 (15)	555 (15)	504 (13.6)	90.8
4	925 (25)	925 (25)	830 (22.4)	89.7
5	925 (25)	892 (24.1)	818 (22.1)	91.7
6	1110 (30)	1110 (30)	1030 (27.8)	92.8
7	1110 (30)	1091 (29.5)	973 (26.3)	89.2
8	1850 (50)	1850 (50)	1692 (45.7)	91.4
9	1850 (50)	1850 (50)	1661 (44.9)	89.8

The amount of waste generated after every milking was:

- General waste: 200.05 mL;
- Strontium containing waste: 365.00 mL (the strontium content in this waste was not significant and was of the order of a few microcuries).

The minimum volume of $^{90}\text{YCl}_3$ in the product vial that could be obtained was 0.36 mL. For washing and decontamination steps:

- Acid wash: 1.0M HNO_3 ;
- Solvent: water for injection.

4.3.3. Recovery of ^{90}Sr from waste

Although loss of strontium during the regular operation of the module was not high and because ^{90}Sr is not very expensive, software (SCADA) was incorporated for recovering ^{90}Sr from the radioactive waste. Figure 4.6 presents the elution profile of ^{90}Sr recovery from waste after passing it through two different columns prepared with strong cation exchange Dowex 50 resin

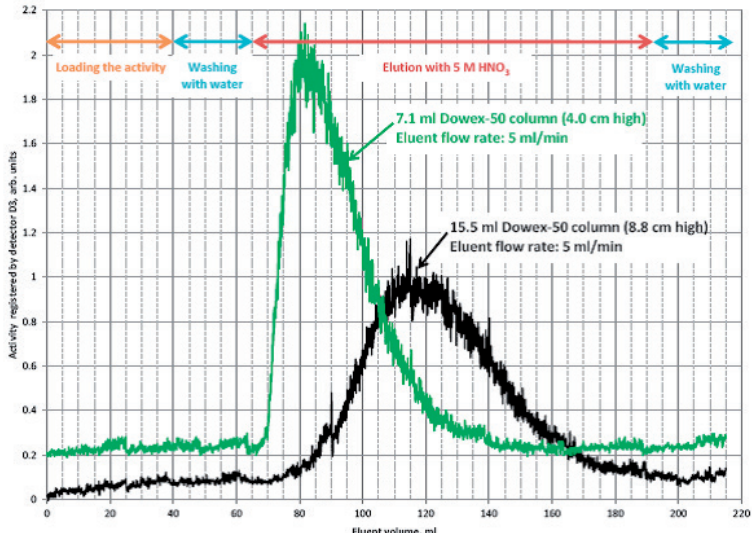


FIG. 4.6. Elution profile from the chromatographic column during ^{90}Sr recovery from simulated waste.

(7.1 mL, 4 cm high and 15.5 mL, 8.8 cm high). The ^{90}Sr depleted solution (15 mCi) was transferred to the column that was washed with water and the elution was performed using 5M HNO₃.

From this result, the 7.1 mL Dowex 50 column (4 cm high) was chosen for installation in the generator, whereby the amount of liquid waste could be reduced by a factor of 30. Any liquid waste generated by the normal operation of the module, which might contain reasonable quantities of ^{90}Sr , was collected in a specific reservoir. The process was organized in such a way that the acid used for washing the electrochemical cell (1M HNO₃) as well as all water washes were directed into this reservoir. In this way, the acid was constantly diluted to such an extent that the waste could be directly pumped through a strong cation exchanger resin to collect all ^{90}Sr . During one milking process, ~100 mL of acidic waste and ~265 mL of water in the ^{90}Sr waste reservoir could be collected, whereby the acid concentration of the waste would be 0.27M. Hence, strontium could be maintained in the liquid phase (the pH is low enough to prevent hydrolysis and to minimize strontium adsorption on the glassware) and can strongly bind on common strong cation exchangers.

4.3.4. Radiolabelling of monoclonal antibodies with ^{90}Y from electrochemical generator Kamadhenu

Binding capacity was evaluated at different antibody:DOTA molar ratios. As shown in Fig. 4.7, binding of the conjugated antibody decreased with respect to rituxan when the molar ratio increased, which is more evident at 80:1 and 160:1 molar ratios.

As shown in Fig. 4.8, recognition of DTPA conjugated rituxan by CD20 in Ramos cells yields very similar results at all evaluated molar ratios.

FITC conjugated antibody is Fc γ specific. Hence, a binding decrement could be because of poor CD20 recognition or Fc fragment damage. Nonetheless, both factors are very important to determine in vivo behaviour of radiolabelled antibodies.

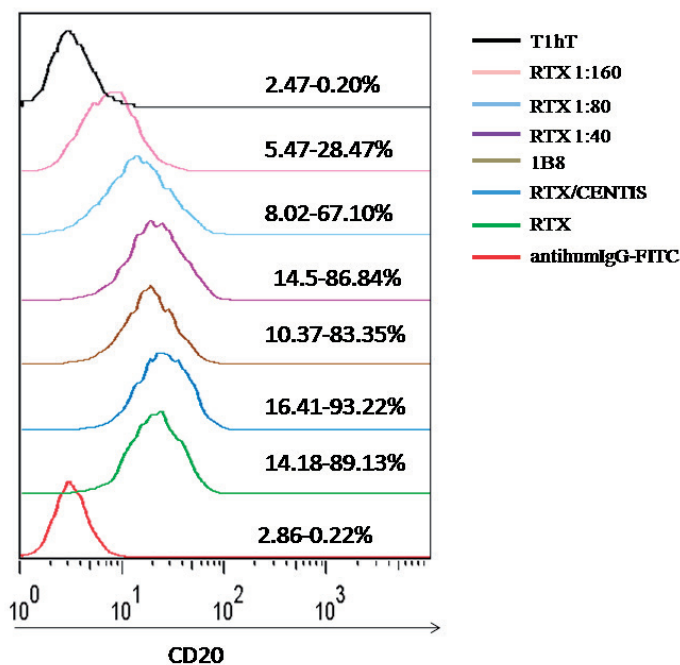


FIG. 4.7. CD20 recognition in Ramos cells of DOTA conjugated rituxan (numbers represent fluorescence intensity and percentage of CD20 expressing cells).

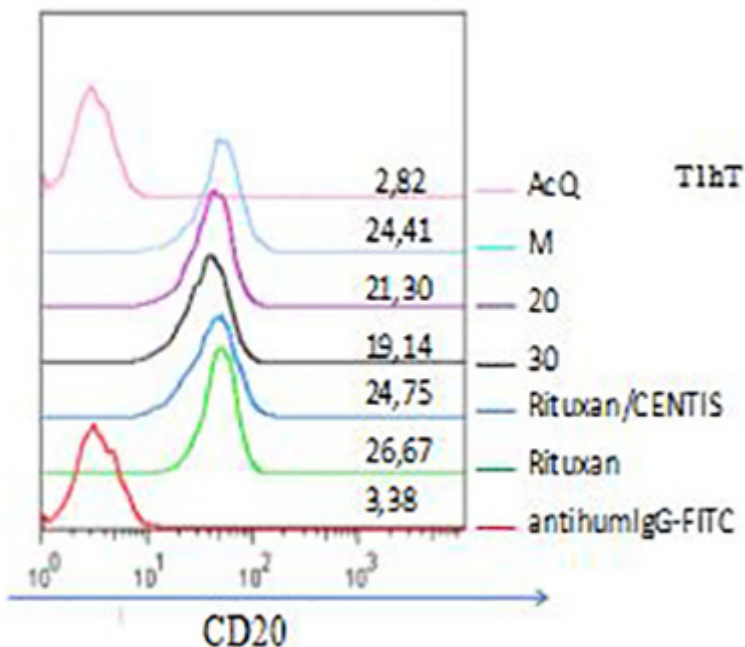


FIG. 4.8. CD20 recognition in Ramos cells of DTPA conjugated rituxan (numbers represent fluorescence intensity).

4.3.4.1. Yttrium-90 radiolabelling and quality control of conjugated rituxan

The RCP of the DTPA conjugated antibody was initially superior to the RCP obtained with the DOTA conjugated antibody, as shown in Table 4.4.

TABLE 4.4. RCP OF RADIOLABELLED ANTIBODIES

DOTA antibody		DTPA antibody	
Molar ratio	RCP (%)	Molar ratio	RCP (%)
160:1	97–99	30:1	96–98
80:1	90–95	20:1	96–98
40:1	~80	10:1	96–98
		5:1	10–12

4.3.4.2. Cell binding assay of ^{90}Y DTPA rituximab

Conventional and Lindmo [4.11] plots are depicted in Fig. 4.9. A value of the immunoreactive fraction of 0.96, which is an excellent result, was estimated using both procedures [4.12]. Hence, it may be concluded that the conjugation procedures did not affect the binding capacity of rituximab.

4.4. CONCLUSION

- After the evaluation and optimization of all parameters for production of $^{90}\text{YCl}_3$ with the required quality, Kamadhenu can now be operated either in fully automated or in manual mode of operation.
- The automated mode of operation provides a comfortable, reproducible and good manufacturing practice compliant means of operation.
- Rituximab conjugated with DOTA and DTPA shows good binding with Ramos cells in vitro, DOTA rituximab at 40:1 molar ratio and DTPA rituximab at 20:1 molar ratio show good binding affinity as demonstrated by flow cytometry.
- Yttrium-90 labelled DOTA rituximab and DTPA rituximab were obtained with >90% RCP.
- Yttrium-90 labelled DTPA rituximab showed good receptor recognition in Ramos cells, as demonstrated by binding experiments.
- Electrochemical generator Kamadhenu provides ^{90}Y of good quality for biomolecule radiolabelling.

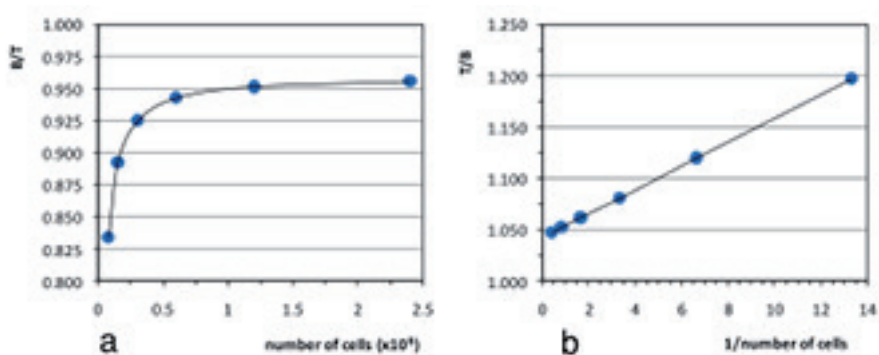


FIG. 4.9. Results of binding experiments: (a) conventional plot and (b) Lindmo plot.

4.5. RECOMMENDATIONS AND FUTURE WORK

- Increase the ^{90}Sr activity to 1 Ci in the reservoir;
- Evaluate the ^{90}Sr losses at these levels of activities;
- Continue cell binding experiments of radiolabelled rituximab to compare results with both chelating agents;
- Perform biodistribution and pharmacokinetic experiments in mice tumour models to determine in vitro/in vivo correlations.

REFERENCES TO CHAPTER 4

- [4.1] ELEX COMMERCE, Kamadhenu, Electrochemical $^{90}\text{Sr}/^{90}\text{Y}$ Generator, Model KA01, Operating Manual, Elex Commerce (2013), www.elexcomm.com/kamadhenu-eng.html
- [4.2] CHAKRAVARTY, R., et al., Development of an electrochemical ^{90}Sr - ^{90}Y generator for separation of ^{90}Y suitable for targeted therapy, *Nucl. Med. Biol.* **35** (2008) 245.
- [4.3] LUKIC, D., et al., High efficiency production and purification of ^{86}Y based on electrochemical separation, *Appl. Radiat. Isotopes* **67** (2009) 523.
- [4.4] CARTRON, G., WAITER, H., GOLAY, J., CELIGNY-SOLAL, P., From the bench to the bedside: Ways to improve rituximab efficacy, *Blood* **104** (2004) 2635.
- [4.5] HWANG, W.Y., FOOTE, J., Immunogenicity of engineered antibodies, *Methods* **36** (2005) 3.
- [4.6] DI GAETANO, N., et al., Complement activation determines the therapeutic activity of rituximab in vivo, *J. Immunol.* **171** (2003) 1581.
- [4.7] REFF, M.E., et al., Depletion of B cells in vivo by a chimeric mouse human monoclonal antibody to CD20, *Blood* **83** (1994) 435.
- [4.8] ROQUE-NAVARRO, L., et al., Humanization of predicted T-cell epitopes reduces the immunogenicity of chimeric antibodies: New evidence supporting a simple method, *Hybrid Hybridomics* **22** (2003) 245.
- [4.9] VAN DER KOLK, L.E., GRILLO-LOPEZ, A.J., BAARS, J.W., Complement activation plays a key role in the side-effects of rituximab treatment, *Br. J. Haematol.* **115** (2001) 807.
- [4.10] PANDEY, U., et al., A novel extraction paper chromatography (EPC) technique for the radionuclidic purity evaluation of ^{90}Y for clinical use, *Anal. Chem.* **80** (2008) 801.
- [4.11] LINDMO, T., BOVEN, E., CUTTITTA, F., Determination of the IF of radiolabeled monoclonal antibodies by linear extrapolation to binding at infinite antigen excess, *J. Immunol. Methods* **72** (1984) 77.
- [4.12] KONISHI, S., et al., Determination of immunoreactive fraction of radiolabeled monoclonal antibodies: What is an appropriate method? *Cancer Biother. Radiopharm.* **19** (2004) 706.

Chapter 5

PRECLINICAL EVALUATION OF ⁹⁰Y LABELLED RITUXIMAB AND ERIC-1: TWO ANTIBODIES FOR TUMOUR THERAPY

K. SCHOMÄCKER, T. FISCHER
Department of Nuclear Medicine,
University of Cologne,
Cologne, Germany

Abstract

The project described in this chapter focuses on harnessing the great potential of radionuclide therapy, using various vehicles to transport radionuclides into tumour tissues. The main aim of the project was to make specific vehicle molecules whose tumour affinity and suitability for radioactive coupling have been proven through laboratory trials on animals and cell cultures at the Department of Nuclear Medicine, University of Cologne, Germany, and to label them with ⁹⁰Y. The vectors to transport radionuclides into tumour tissue for treatment were antibodies against lymphomas and neuroblastomas.

Tumour pretargeting has shown clear advantages over the direct application of labelled antibodies with regard to tumour to background ratios. The pretargeting strategy would be first evaluated on cell cultures and the results then transferred to *in vivo* experiments on tumour bearing mice. Briefly, the first component of a three step pretargeting strategy would consist of the biotinylated antibody. This would include the protocol for determination of the number of biotin molecules per antibody. Using this technique, a stock of biotinylated antibody in lyophilized form can be built up, ready for further experiments. In the second step, commercially available avidin streptavidin would be used. The third and final step is the binding of radiolabelled (¹⁸⁸Re, ⁹⁰Y) biotin to the tumour cells through the avidin antibody bridge, after administration of a clearing agent.

Initial evaluations of the potential radiopharmaceuticals have been carried out by *in vitro* experiments on cell lines expressing the corresponding antigen. The work done so far for the three step pretargeting method can be summarized as follows:

- Yttrium-90 labelling of biotin DOTA;
- Coupling of biotinylated rituximab to CD20 positive Raji cells;
- Successful labelling of cells conjugated with a complex of biotinylated antibody and avidin with ⁹⁰Y DOTA biotin;
- First animal experiments with the pretargeting method: results are disappointing so far.

Furthermore, new results were achieved with ¹³¹I and ⁹⁰Y labelled ERIC1 antibodies directed against neural cell adhesion molecule (NCAM) positive neuroblastomas. The

radioiodine labelled anti-NCAM antibody ERIC1 seems to be a promising radiopharmaceutical for treatment of neuroblastoma. The optimal dose is 1–2 MBq/animal. This would correspond to ~600–1200 MBq in humans (for a child of 15 kg).

Initial experiments with ^{90}Y labelled ERIC1 have been very promising. These antibodies showed an unequivocal therapeutic effect, whereas ^{131}I MIBG had no influence on tumour growth, even when much higher radioactivity was injected per animal. Studies planned for the future include improved dose finding studies, fractionation of radiation dose realized by intravenous application of radiolabelled ERIC1, investigation of other radioimmunoconstructs directed against NCAM and investigation of other tumour types with NCAM on tumour cells and pretargeting.

5.1. EXPERIMENTS

5.1.1. Yttrium-90 or ^{111}In labelled rituximab

5.1.1.1. Introduction

The introduction of MAbs such as rituximab in recent years has brought about decisive progress in the treatment of aggressive and indolent NHL [5.1]. Since then, a number of antibodies have been developed for use in oncological disorders. Further improvement to the unmodified antibody has been its coupling to β emitters such as ^{131}I and ^{90}Y . The aim here was to establish the biodistribution of labelled chimeric antibody rituximab and to determine whether ^{111}In is a suitable surrogate for ^{90}Y .

5.1.1.2. Methods

The antibody against NHL can be acquired commercially. The labelling of rituximab to ^{90}Y first involves a non-radioactive modification of the antibody to allow chemical binding with ^{90}Y . This is achieved by the coupling of isothiocyanatobenzylDOTA (NCS-Bz-DOTA) to rituximab. The DOTA rituximab conjugate solution can subsequently be lyophilized to allow interim storage until labelling with the corresponding radionuclide.

The ^{111}In labelling for pretherapeutic dosimetry, the ^{90}Y labelling for therapeutic purposes and the quality control procedures were carried out under clean room conditions. Quality control of the radiopharmaceutical was carried out by size exclusion high performance liquid chromatography (HPLC). The final filtration and bottling were done under sterile conditions. The ready to use solutions should have an activity concentration of ~185 MBq (5 mCi) ^{111}In for dosimetry and ~740 MBq (20 mCi) ^{90}Y for therapeutic purposes, each in a volume of 3 mL.

Prior to the animal experiments, the affinity of the radioimmunoconjugates to CD20 positive Raji cells was measured in vitro. Labelling with ^{131}I or ^{111}In and ^{90}Y by DOTA was performed using standard methods. The various radioimmunoconjugates were injected intravenously into Burkitt lymphoma bearing severe combined immunodeficiency (SCID) mice. The biodistribution was measured at 24, 48, 72 and 96 h p.i. by taking samples of blood, urine, liver, kidney, spleen, gastrointestinal tract, femur, muscle, thyroid and tumour and measuring the radioactivity in a well counter. The results were recorded as percentages of the injected dose per gram organ weight.

5.1.1.3. Results

The dissociation constants obtained for radioimmunoconstruct binding to tumour cells were in the range 50–90nM. The tumour accumulation for ^{90}Y DOTA rituximab at 72 h p.i. was significantly higher (2.6-fold) than for ^{111}In DOTA rituximab (^{90}Y : 69.7%ID/g; ^{111}In : 25.4%ID/g, 96 h p.i.) (see Fig. 5.1). Yttrium-90 DOTA rituximab, in contrast to ^{111}In analogues, showed a markedly delayed blood clearance, a 2.5-fold higher accumulation in the spleen and a significantly higher accumulation in bone (threefold). The radiolabelled radioimmunoconstruct displayed markedly lower accumulation in both tissue and tumour (tenfold in tumour). The tumour to muscle ratios seemed to be promising, while tumour to blood ratios were very low. The tumour to background ratios of ^{90}Y and ^{111}In DOTA rituximab were not really comparable, but were higher in the case of the ^{90}Y labelled antibody (see Fig. 5.2).

5.1.1.4. Conclusion

Indium-111 is not a suitable substitute for ^{90}Y for measurement of the accumulation of antibodies in tumours. Yttrium-86 labelled analogues should be used for reliable pretherapeutic dose calculations for ^{90}Y radioimmunoconjugates. Yttrium-90 DOTA rituximab is a promising candidate for radioimmunotherapy. However, the tumour to background ratios are not good and need to be improved using pretargeting methods.

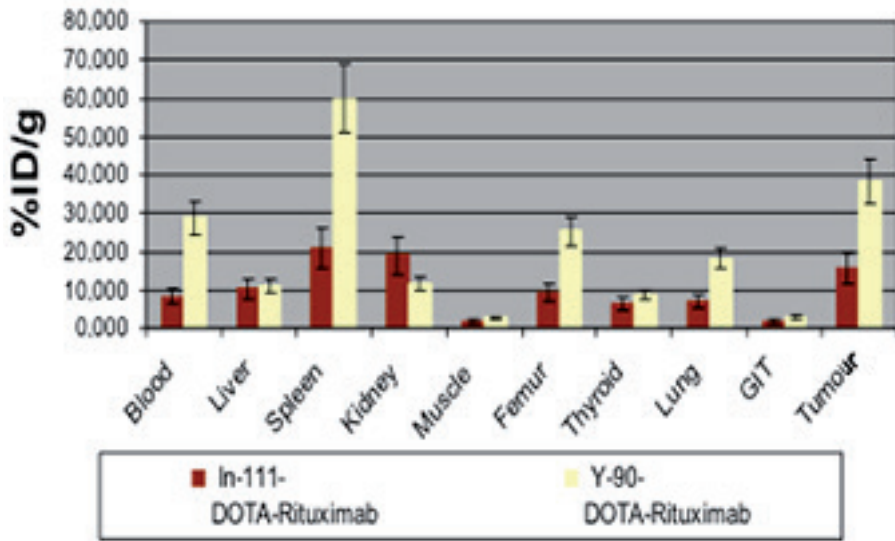


FIG. 5.1. Comparison of biodistribution of ^{111}In and ^{90}Y rituximab 72 h p.i.

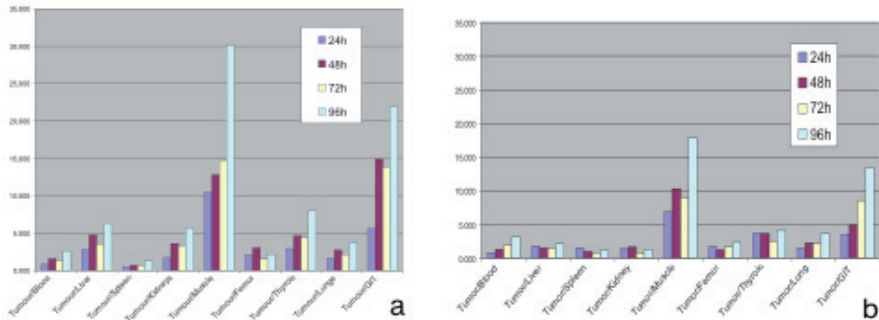


FIG. 5.2. Time course of tumour to background ratios: (a) ^{90}Y DOTA rituximab and (b) ^{111}In DOTA rituximab.

5.1.2. Pretargeting methods

Tumour pretargeting based on the avidin biotin system has shown clear advantages over the use of directly labelled antibodies in the treatment of solid tumours. A new potential application of ^{90}Y DOTA biotin radionuclide therapy has recently been proposed for breast cancer. The Italian group of Chinol et al.

have developed Intraoperative Avidination for Radionuclide Therapy (IART), which relies on the avidin biotin binding system [5.2]. In fact, the avidination of the anatomical area of the tumour with avidin, directly injected by the surgeon into and around the tumour bed, provides a target for ^{90}Y DOTA biotin injected intravenously 1 d later.

The major objective for cancer radioimmunotherapy is to enhance the effectiveness of the drug by concentrating it at the tumour site with fewer toxic side effects to normal organs. Tumour targeting was successful with long circulating radiolabelled MABs, but high radiation doses to normal organs, especially liver, blood and bone marrow, soon appeared as a significant problem. Thus, conventional radioimmunotherapy (radioactivity directly attached to the MAb) has achieved success in the treatment of leukaemias and lymphomas, in which the tumours are radiosensitive and the tumour cells are relatively accessible.

The pretargeting strategy would be first evaluated on cell cultures and those results transferred to *in vivo* experiments on tumour bearing mice.

Briefly, the first component of a three step pretargeting strategy consists of the biotinylation of the antibody. This includes determination of the number of biotin molecules per antibody. Using this technique, a stock of biotinylated antibody in lyophilized form can be prepared for further experiments. In the second step, commercially available avidin streptavidin is used. The third and final step is the binding of radiolabelled (^{188}Re , ^{90}Y) biotin to the tumour cells through the avidin antibody bridge after administration of a clearing agent (see Fig. 5.3).

Initial evaluations of the potential radiopharmaceuticals have been carried out by *in vitro* experiments on cell lines expressing the corresponding antigen. The results indicate that the strategies can now be applied in mice capable of developing the tumours foreseen for targeting. Permission for these experiments from the local authorities, as required by animal protection legislation in Germany, was received at the beginning of February 2010.

To prove the advantages of the proposed strategy, the biokinetic data resulting from the pretargeting approach will be compared with those after administration of directly labelled antibodies in the same animal model. The antibody against NHL can be acquired commercially.

The antibodies for direct use without a pretargeting strategy would be labelled with ^{90}Y after coupling isothiocyanatobenzyl DOTA to the antibodies. The DOTA antibody conjugate solution can be purified, lyophilized and stored under proper conditions until labelling with the corresponding radionuclide.

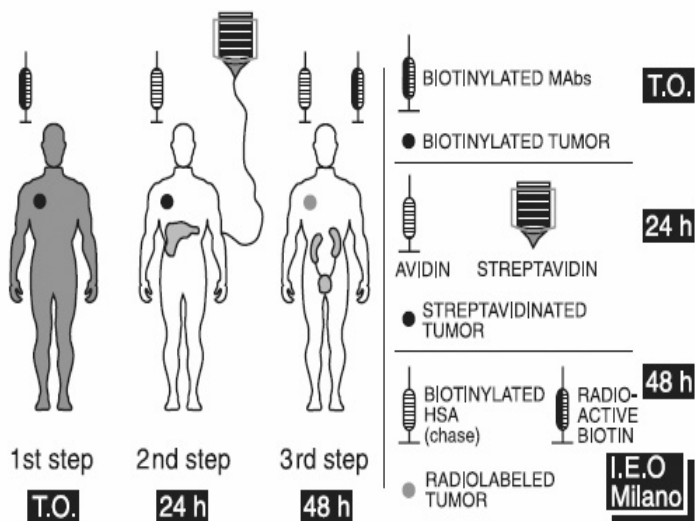


FIG. 5.3. Three step strategy. Biotinylated MAbs are injected intravenously and allowed to localize onto the target (first step). One day later, avidin and streptavidin are injected intravenously (second step). After 24 h, when unbound streptavidin and circulating avidin MAb complexes have been cleared from circulation, radiolabelled biotin is injected intravenously (third step) [5.2].

5.1.2.1. Biotinylation of antibodies

The protocol for biotinylation includes:

- Dialyse overnight an antibody solution in 0.1M sodium bicarbonate buffer, pH8.5, at 2–8°C;
- Prepare a solution of biotinyl aminocaproic acid N-hydroxysuccinimide ester in dimethyl sulphoxide (DMSO) at the same concentration as that of the antibody;
- Add a volume of 0.12 mL of the above biotinylation agent per millilitre of antibody (molar ratio of biotin:antibody is 10:1) under slow, continuous stirring for 2 h at room temperature;
- Dialyse against PBS (pH7.4) at 2–8°C (at least two changes of 5 L each);
- Filter through a 0.22 µm Millipore filter, determine the titre and then make aliquots;

- (f) Determine the biotinylation yield (number of biotins per molecule of antibody) using the 2-(4-hydroxyphenyl-azo)benzoic acid (HABA) method after enzymatic digestion of the antibody (see Section 5 of the Annex).

The binding behaviour of the biotinylated antibody was tested using fluorescence activated cell sorting analysis. This showed that the binding properties of the antibody did not deteriorate after biotinylation.

5.1.2.2. Labelling of biotin with ^{90}Y

The biotin DOTA, in saline solution, was labelled with ^{90}Y at a specific activity of 3.7 MBq/ μg . A concentration of 1M sodium acetate at pH5.0, at a volume equal to that of the radionuclide chloride solution, is used as the buffer. The biotin DOTA solution is added to the buffer and transferred into the radionuclide vial. The mixture is mixed and heated at 95°C for 30 min. The RCP of ^{90}Y DOTA biotin was tested by TLC using ITLC SG (Gelman Sciences). An aliquot of the radiolabelling solution mixed with 0.2 mL of an avidin DTPA solution (0.4mM avidin and 2.5mM DTPA, final pH6.0) served as a sample, and was kept at room temperature for 5 min. Five microlitres of the sample were spotted on the paper strip and isotonic saline solution was used as the eluent. Detection was carried out using a TLC scanner (Raytest, Rita Software) ($R_f = 0$ for labelled DOTA biotin, $R_f = 1$ for free radiometal). The RCP of ^{90}Y DOTA biotin was very high, with no free radiometal.

5.1.2.3. Three step pretargeting: Cell experiments

Two million Raji cells were suspended in 0.5 mL of medium. The antigen number was verified by binding studies to be 2×10^6 . Cells were incubated with 0.1 mg biotinylated rituximab (0.26 mL of PBS) for 30 min. After centrifugation, the cells were incubated with 0.06 mg avidin in 50 μL of PBS for 5 min, centrifuged and washed twice. Subsequently, the cells were incubated with 12 kBq ^{90}Y DOTA biotin (in 500 μL) for 30 min. After centrifugation and washing with PBS, the radioactivity in the cell pellets was measured to determine the binding of ^{90}Y biotin to the cells and compared with the standard. The assay was performed in triplicate and compared with cells incubated with non-biotinylated antibody, as shown in Table 5.1.

TABLE 5.1. THREE STEP PRETARGETING: RESULTS OF FIRST CELL EXPERIMENTS

Quantity	Sample 1 (counts/s)	Sample 2 (counts/s)	Sample 3 (counts/s)	Sample 4 ^b (counts/s)
Initial radioactivity	10 344	9897	10 004	9583
Cell bound activity ^a	8388	7944	7566	560

^a After background subtraction and washing.

^b Raji cells incubated with non-biotinylated rituximab.

5.1.2.4. Three step pretargeting: animal experiments

(a) Methods

Ten million Raji tumour cells were implanted in the hind leg of CB17 SCID mice (females, 4 weeks old), and tumours of 1 cm diameter appeared after 15 d. A mass of 0.2 mg (20 μ L doses) of biotinylated rituximab was injected into the tail vein of these mice. The following were administered via the tail vein: 0.1 mg of avidin (20 μ L) after 24 h, 0.2 mg of biotinylated HSA (20 μ L) after a further 4 h and, finally, 2 MBq ⁹⁰Y biotin DOTA (70 μ L) after a further 5 min.

(b) Preliminary results of animal experiments

The entire radioactivity was excreted in the urine, and there was no specific accumulation of radioactivity in tumour tissue. Further improvements are required, such as varying the experimental parameters (intervals between applications or amounts of substances applied).

5.1.3. Antineuroblastoma antibodies (¹¹¹In or ⁹⁰Y ERIC1)

5.1.3.1. Objectives

Neuroblastoma is the most frequent type of solid extracranial childhood tumour and also the most common neoplasm in the first year of life. The most frequent metastatic sites are bone, bone marrow and liver. Using a multidisciplinary therapeutic approach, based mainly on polychemotherapy, an overall five year survival rate of ~67% can be reached. Children with certain risk factors, such as amplification of the neural Myc gene, age at diagnosis >2 years

or relapsed disease, have a poorer prognosis. New diagnostic and treatment modalities are urgently required to offer these children a better chance of a cure.

Tumour targeting with ^{131}I MIBG is a well established method for tumour imaging and for treatment of relapsed disease. Iodine-131 MIBG therapy can achieve an objective tumour response rate of 35%, but its role is palliative. Unfortunately, side effects, including dose limiting thrombocytopenia, detract from the clinical usefulness and ~10% of all tumours investigated did not show any MIBG uptake and hence could not be treated.

A novel strategy of immunolocalization of human neuroblastoma was therefore developed to target the NCAM, which are overexpressed on neuroblastoma. In the present study, ^{131}I labelled anti-NCAM antibody ERIC1 was investigated in a human neuroblastoma xenograft SCID mouse model for the first time [5.3]. The main interest was focused on the potential of this radioimmunoconjugate for radioimmunotherapy. Biodistribution studies were carried out for dose calculations.

5.1.3.2. Results

Measurement of organ specific radioactivity showed low organ specific uptake (5.33%ID/g after 72 h), which decreased continuously over the 96 h investigation period, demonstrating clearance of radioactivity. In contrast, tumours accumulated radioactivity continuously up to a peak of 42.07%ID/g at the 96 h time point (31.07%ID/g at 72 h). This specific uptake could be blocked by application of unlabelled ERIC1 antibodies. Measurement of blood specific radioactivity revealed a characteristic clearance over the first 72 h. With 37 Gy, tumour specific radioactivity reached therapeutic doses after 96 h [5.2].

5.1.3.3. Conclusion

Preliminary experiments in Cologne [5.3] with a radioactive anti-NCAM antibody (^{131}I ERIC1), where high tumour doses were reached in neuroblastoma xenograft bearing SCID mice, will be used as a basis for further development of radioimmunotherapeutic methods of neuroblastoma treatment. The neuroblastoma antigen NCAM seems to be an ideal target antigen for this. Biokinetic studies with $^{90}\text{Y}/^{111}\text{In}$ DOTA ERIC1 are currently being carried out.

5.1.4. Therapeutic experiments with antibodies against neuroblastoma

5.1.4.1. Objectives

Our previous studies with anti-NCAM antibody ERIC1 labelled with ^{131}I showed high specific tumour uptake in neuroblastoma bearing mice. The aim of the present study is to investigate the therapeutic potential of the radioimmunoconstruct labelled with ^{131}I and ^{90}Y in animal trials. The therapeutic potential of NCAM radioimmunoconstruct would be compared with that of ^{131}I MIBG. Further experiments to test whether fractionated applications of radioimmunoconstructs have any advantage when comparable doses of radioactivity are applied need to be carried out.

5.1.4.2. Methods

SCID mice without T and B lymphocytes, but with an active natural killer cell system, were used as experimental animals. A total of 3×10^7 IMR5-75 cells were implanted subcutaneously. ERIC1 antibodies were labelled with ^{131}I using the chloramine T method and with ^{90}Y via DOTA conjugation. Activities administered were 0.5–20 MBq/animal.

Under similar criteria, a comparison was made between the therapeutic effect of the radiolabelled antibodies and that of ^{131}I MIBG (GE Healthcare). Fractionated applications have been performed solely with ^{131}I ERIC1. In addition, four times a day, every three days, a dose of 2 MBq or 0.5 MBq was administered, with an extra 1.5 MBq twice a day, every ten days. The therapeutic effect was assessed by measurement of the tumour volume. On studying the side effects of the radioimmunoconstruct, particular attention was given to blood tests, weight and survival of the treated animals in comparison to the two control groups. Each of two control groups comprised five tumour bearing animals: one group received no additional injections at all and the other group received non-radioactive cold antibodies.

5.1.4.3. Results

RCP of 75–85% was achieved on labelling the ERIC1 antibody with ^{90}Y . An activity of 1.45 MBq/animal of ^{90}Y DOTA ERIC1 caused a tumour remission, but with a mortality of 40% (see Fig. 5.4).

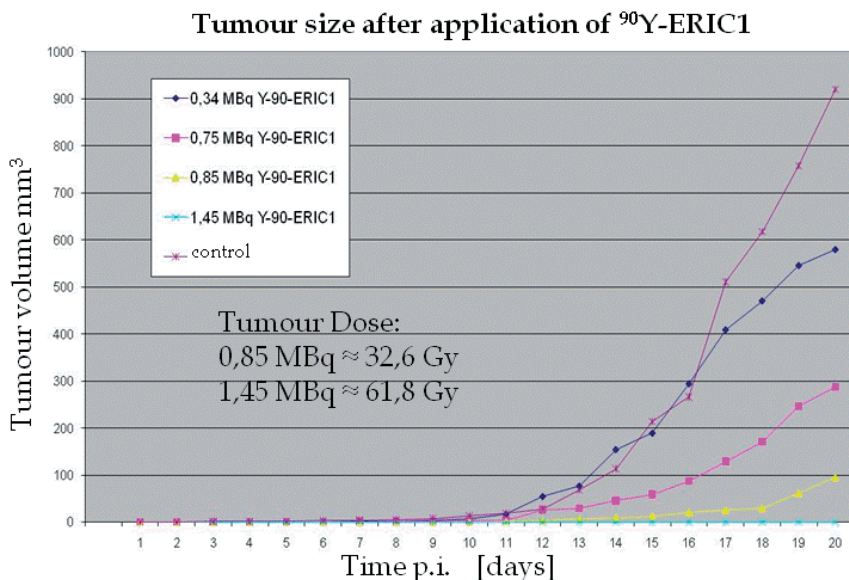


FIG. 5.4. Reduction of tumour volume in neuroblastoma bearing mice after application of ^{90}Y DOTA ERIC1 in different activities, in comparison with a control group.

Iodine-131 MIBG did not show a detectable influence on tumour growth when activities up to 10 MBq/animal were administered, while ^{131}I ERIC1, as in earlier studies [5.4], showed a therapeutic effect, even when markedly low doses of radioactivity were injected. In contrast, in the control group, where the cold ERIC1 antibody was injected, no reduction or slowing of tumour growth was observed in comparison to the controls. The influence of fractionation on the therapeutic effect could be studied previously only with ^{131}I ERIC1, wherein on application of single doses of 2 MBq of ^{131}I ERIC1 every three days, fast accumulation of activity of up to >4 MBq ^{131}I was seen in the animal. Thus, in this group, the therapeutic action was intensified, albeit with an increased lethality, with the animals dying 13–16 d p.i. free of tumours. An injected dose of 0.5 MBq ^{131}I was found to be effective, and, with this treatment, the animals did not show adverse side effects such as weight loss or increased lethality, but survived for more than six months. The future plan is to investigate whether fractionation has a favourable influence on the therapeutic outcome with ^{90}Y ERIC1, that is, if it reduces side effects, as ^{90}Y applied at activities of >1 MBq usually leads to massive weight loss and death in the animals treated.

5.1.4.4. Conclusion

The radioiodine labelled anti-NCAM antibody ERIC1 seems to be a promising radiopharmaceutical for treatment of neuroblastoma. The optimal dose is 1–2 MBq/animal, which would correspond to ~600–1200 MBq in humans (for a child of 15 kg). Initial experiments with ^{90}Y labelled ERIC1 have been very promising. These antibodies have shown an unequivocal therapeutic effect, whereas ^{131}I MIBG appears to have no influence on the tumour growth, even when higher radioactivity is administered per animal. Future studies will focus on:

- (a) Improved dose finding studies;
- (b) Fractionation of radiation dose realized by intravenous application of ^{90}Y labelled ERIC1;
- (c) Investigation of other radioimmunoconstructs against NCAM;
- (d) Investigation of other tumour types with NCAM on tumour cells (particularly, small cell lung carcinoma);
- (e) Pretargeting.

REFERENCES TO CHAPTER 5

- [5.1] SCHOMÄCKER, K., et al., Radioimmunotherapy with yttrium-90 ibritumomab tiuxetan. Clinical considerations, radiopharmacy, radiation protection, perspectives, *Nucl. Med.* **44** (2005) 166.
- [5.2] PAGANELLI, G., CHINOL, M., Radioimmunotherapy: Is avidin-biotin pretargeting the preferred choice among pretargeting methods? *Eur. J. Nucl. Med. Mol. Imaging* **30** (2003) 773.
- [5.3] OTTO, C., et al., Localization of ^{131}I -labelled monoclonal antibody ERIC1 in a subcutaneous xenograft model of neuroblastoma in SCID mice, *Nucl. Med. Commun.* **27(2)** (2006) 171.
- [5.4] GOLDENBERG, D.M., ROSSI, E.A., SHARKEY, R.M., McBRIDE, W.J., CHANG, C.H., Multifunctional antibodies by the dock-and-lock method for improved cancer imaging and therapy by pretargeting, *J. Nucl. Med.* **49** (2008) 158.

Chapter 6

DEVELOPMENT OF RADIOPHARMACEUTICALS BASED ON ^{188}Re AND ^{90}Y FOR RADIONUCLIDE THERAPY AT BARC

U. PANDEY, M. KAMESWARAN, S. SUBRAMANIAN, R. CHAKRAVARTY,
H.D. SARMA, G. SAMUEL, A. DASH, M. VENKATESH, M.R.A. PILLAI
Radiopharmaceuticals Division,
Bhabha Atomic Research Centre,
Trombay, Mumbai, India

Abstract

During the last decade, the group at Bhabha Atomic Research Centre (BARC), India, has focused attention on the development of ^{90}Y based radiopharmaceuticals for therapy. Because the $^{90}\text{Sr}/^{90}\text{Y}$ generator is the primary source of high specific activity ^{90}Y , local availability of the generator is crucial in the successful development of ^{90}Y radiopharmaceuticals. In this context, $^{90}\text{Sr}/^{90}\text{Y}$ generators based on SLM [6.1, 6.2] and electrochemical techniques [6.3] were designed and deployed at BARC for the elution of ^{90}Y to be used for preparation of ^{90}Y labelled products. This work formed a part of the IAEA CRP entitled Development of Generator Technologies for Therapeutic Radionuclides: ^{90}Y and ^{188}Re . In this chapter, work on the development of ^{90}Y labelled products for treatment of NHL and liver cancer is reported. In addition, validation of the EPC technique for determination of ^{90}Sr contamination in ^{90}Y eluates [6.4] and its comparison with the United States Pharmacopeia recommended method [6.5] is presented.

6.1. VALIDATION OF THE EPC TECHNIQUE FOR DETERMINATION OF ^{90}Sr CONTAMINATION IN ^{90}Y ELUTED FROM $^{90}\text{Sr}/^{90}\text{Y}$ GENERATOR SYSTEMS

6.1.1. Introduction

The preparation of ^{90}Y radiopharmaceuticals for receptor antigen targeting in the tumour requires ^{90}Y of high specific activity. Yttrium-90 from $^{90}\text{Sr}/^{90}\text{Y}$ generators is therefore used for preparation of such receptor specific radiopharmaceuticals. The use of generator produced ^{90}Y necessitates that the amount of ^{90}Sr in the ^{90}Y eluate is well below permissible limits (≤ 37 kBq ^{90}Sr in 37 GBq of ^{90}Y), as ^{90}Sr is highly radiotoxic. In this respect, a novel quality

control procedure for detection of ^{90}Sr in ^{90}Y eluted from $^{90}\text{Sr}/^{90}\text{Y}$ generator systems was developed at BARC based on the specific extraction of ^{90}Y by the chelating agent KSM-17 [6.4]. The developed method, called EPC, makes use of Whatman 3MM chromatography paper (12 cm \times 1 cm) impregnated with 10 μL of KSM-17 at a distance of 2 cm from one end, considered as the origin ($R_f = 0$). The spot is dried and 5 μL of ^{90}Y eluate (37 MBq/mL) from the generator is spotted over the dried spot of KSM-17. The paper is developed in saline, and, after drying, the activity at different regions of the paper is counted using an LSC by placing each segment in 10 mL of scintillation cocktail in a scintillation vial. In this system, ^{90}Y chelated to KSM-17 remains at the origin, while any trace ^{90}Sr migrates towards the solvent front.

To prove the validity of the EPC technique for ^{90}Sr estimation in $^{90}\text{YCl}_3$ solutions, it is essential to compare it with an already established and routinely used quality control technique for determination of ^{90}Sr in $^{90}\text{YCl}_3$ solutions used for radiolabelling. The United States Pharmacopeia monograph for ^{90}Y Ibritumomab tiuxetan injection describes a chromatography technique using Whatman cellulose phosphate paper for estimating the ^{90}Sr content in $^{90}\text{YCl}_3$ samples (herein called the reference method) [6.5]. The EPC technique was compared with the reference method to prove their equivalence in terms of the behaviour of ^{90}Sr and ^{90}Y in the system.

6.1.2. Comparison of EPC method with reference method

For carrying out the quality control procedure as per the reference method, a strontium/yttrium carrier solution containing 0.34 mg of yttrium chloride ($\text{YCl}_3 \cdot 6\text{H}_2\text{O}$) and 0.30 mg of strontium chloride ($\text{SrCl}_2 \cdot 6\text{H}_2\text{O}$) per millilitre of 0.1N HCl was prepared. Approximately 50 μL of this solution was applied at the origin of a 20 cm \times 2 cm cellulose phosphate chromatographic strip and allowed to dry. Five microlitres of the ^{90}Y chloride radiolabelling solution was applied at the origin, and the chromatogram was developed using 3N HCl acid as the developing solvent, until the solvent migrated to the 15 cm mark. It was then allowed to dry. The strip was then cut at the 8 cm mark and the solvent front placed in a liquid scintillation solvent and counted for presence of ^{90}Sr . The migration behaviour of $^{85/89}\text{Sr}(\text{NO}_3)_2$ and ^{90}Y acetate in EPC was compared to that in the reference method. Figure 6.1(a) shows the migration pattern of $^{85/89}\text{Sr}(\text{NO}_3)_2$ in the EPC method. It can be seen that Sr^{2+} ions migrate to the solvent front with $R_f = 0.9-1.0$. Figure 6.1(b) shows the migration pattern of $^{85/89}\text{Sr}(\text{NO}_3)_2$ using the reference method. Here too, Sr^{2+} ions migrate to the solvent front ($R_f = 0.9-1.0$). A $^{85/89}\text{Sr}$ tracer was used for these experiments instead of ^{90}Sr , as varying amounts of ^{90}Y will be present in ^{90}Sr , depending on factors such as the time elapsed after the previous elution, incomplete separation of ^{90}Y and decay of ^{90}Sr . In addition,

the $^{85/89}\text{Sr}$ tracer has γ emissions, which can be used for accurately estimating the activity content using a NaI(Tl) solid scintillation counter. Figure 6.2(a) depicts the chromatography pattern of $^{90}\text{Y}^{3+}$ ions using the EPC method. Owing to the affinity for KSM-17, $^{90}\text{Y}^{3+}$ ions are retained at the point of application ($R_f = 0$). A similar pattern is observed in the reference method also, wherein the $^{90}\text{Y}^{3+}$ ions are retained at $R_f = 0$ (see Fig. 6.2(b)). Figures 6.1 and 6.2 prove that Sr^{2+} ions and Y^{3+} ions follow similar migration patterns in the EPC and reference methods. This experiment confirms the suitability of the EPC method for estimation of ^{90}Sr contamination in ^{90}Y samples used for preparation of radiopharmaceuticals for therapy.

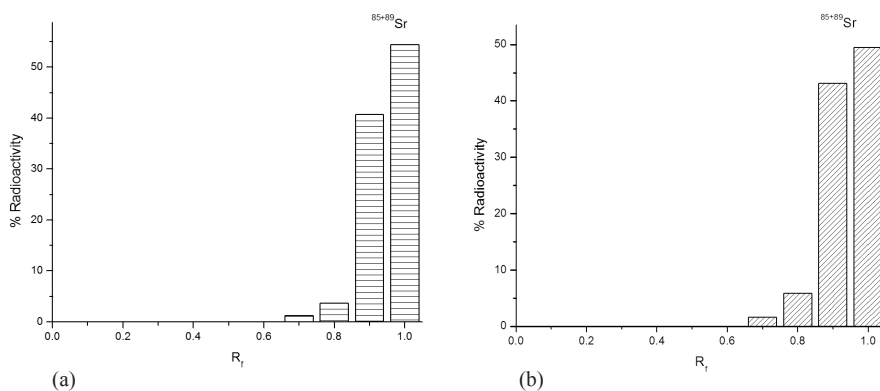


FIG. 6.1. Migration pattern of $^{85/89}\text{Sr}$ using (a) EPC and (b) the reference method.

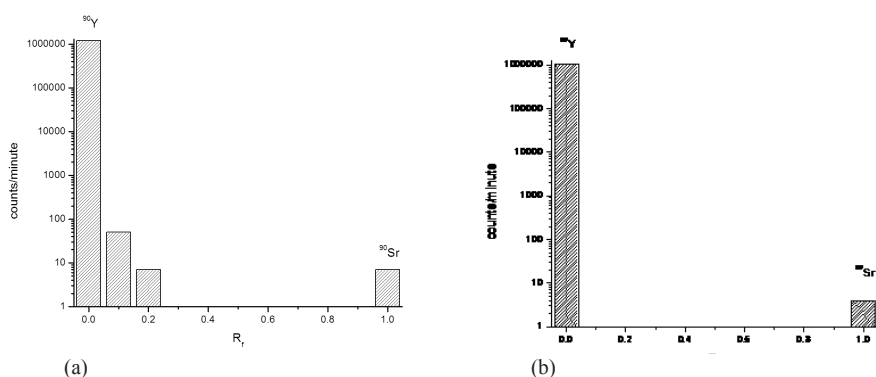


FIG. 6.2. (a) Migration pattern of ^{90}Y using (a) EPC and (b) the reference method.

6.1.3. Recovery of doped $^{85/89}\text{Sr}^{2+}$ determined by EPC

To confirm the efficiency of separation of ^{90}Sr from ^{90}Y using the EPC method, a doping experiment was carried out. Known counts of $^{85/89}\text{Sr}(\text{NO}_3)_2$ solution were doped in ^{90}Y solution. EPC was carried out with a mixture of 5 μL of $^{85/89}\text{Sr}(\text{NO}_3)_2$ and 5 μL of ^{90}Y acetate, as well as 5 μL of $^{85/89}\text{Sr}(\text{NO}_3)_2$ as control. The solvent front corresponding to $^{85/89}\text{Sr}$ counts was counted in a NaI(Tl) counter, and the counts corresponding to $^{85/89}\text{Sr}$ (in the solvent front) were compared to counts of $^{85/89}\text{Sr}(\text{NO}_3)_2$ to determine the efficiency of separation by the EPC system. Figure 6.3(a) shows the EPC pattern of $^{90}\text{Y} + ^{85/89}\text{Sr}$, while Fig. 6.3(b) is the EPC pattern of $^{85/89}\text{Sr}$ only. It was observed that almost all the $^{85/89}\text{Sr}$ activity could be recovered at the solvent front of the extraction chromatography paper.

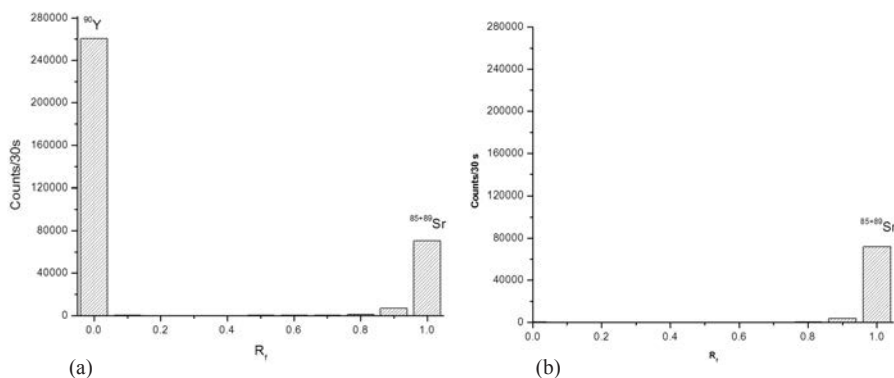


FIG. 6.3. EPC pattern of (a) $^{90}\text{Y} + ^{85/89}\text{Sr}$ and (b) $^{85/89}\text{Sr}$ only.

6.1.4. Analysis of long decayed ^{90}Y samples using the EPC technique

The $^{90}\text{YCl}_3$ or ^{90}Y acetate obtained from $^{90}\text{Sr}/^{90}\text{Y}$ generator systems were assigned batch numbers, and the samples were allowed to decay for more than two months from the date of elution from the generator. After two months, EPC was carried out for all samples. At the end of 60 days, ^{90}Y would have decayed by ~ 22.5 half-lives, by which time, it is expected that 99.99999% of the ^{90}Y has decayed and if any ^{90}Sr were present, it would still be present. At this juncture, the ^{90}Sr present would be in secular equilibrium with its in grown ^{90}Y , and the $^{90}\text{Sr}:$ ^{90}Y ratio would be equal to 1. The counts at the origin ($R_f = 0$) correspond

to ^{90}Y generated by any ^{90}Sr contamination, which would give an equal count at the solvent front ($R_f = 0.9-1.0$). The $^{90}\text{Sr}:$ ^{90}Y ratio in this case is expected to be nearly 1, if good separation is achieved using the EPC method. This procedure was carried out for several long decayed ^{90}Y samples to confirm the validity of the EPC procedure.

6.1.5. Analysis of serially diluted ^{90}Y samples

To determine the sensitivity of the EPC method at different count rates, ^{90}Y samples were diluted to different levels and EPC was carried out. Figure 6.4(a) shows the EPC pattern of a ^{90}Y sample (X) and Fig. 6.4(b) shows the EPC pattern of the same sample diluted 10-fold (X/10). It can be seen that the results from the EPC method confirm the dilution ratio, indicating its reliable separation efficiency.

6.1.6. Conclusion

The EPC technique was successfully validated by comparison with the United States Pharmacopeia recommended method [6.5]. The accuracy of the method was also established by recovering doped $^{85/89}\text{Sr}$ in the solvent front and by determination of $^{90}\text{Sr}:$ ^{90}Y ratios by EPC of long decayed ^{90}Y samples. The EPC method is a simple and user friendly method that can be used for real time estimation of ^{90}Sr content in ^{90}Y eluates from $^{90}\text{Sr}/^{90}\text{Y}$ generator systems.

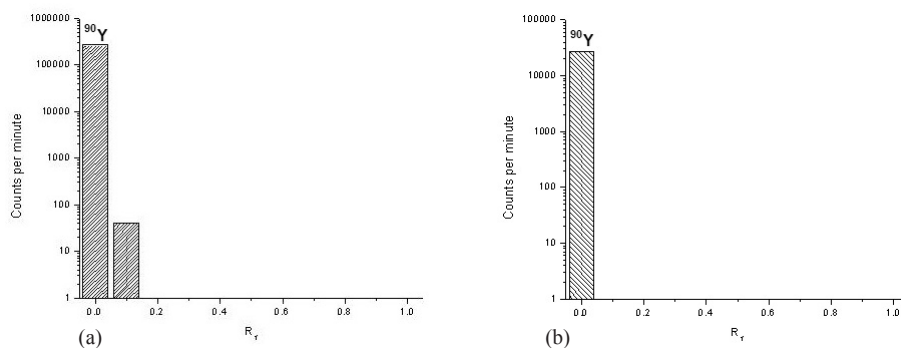


FIG. 6.4. EPC pattern of ^{90}Y acetate: (a) $X = 266,862$ counts/min and (b) $X/10 = 27,640$ counts/min.

6.2. PREPARATION AND BIOEVALUATION STUDIES OF ⁹⁰Y LABELLED RITUXIMAB AND TheraCIM ANTIBODIES

Targeted radionuclide therapy using β emitters such as ⁹⁰Y, ¹³¹I and ¹⁷⁷Lu has gained increased importance in nuclear medicine in recent times. The use of radiolabelled MABs for the targeted therapeutic approach has revolutionized the field of cancer treatment, especially in cases of lymphoma and breast cancer. This section briefly outlines the developmental efforts of the preparation of ⁹⁰Y labelled antibodies. Rituximab is a highly specific human chimeric MAB used in the therapy of NHL [6.6], primarily targeting the CD20 protein expressed on the surface of the B cells. TheraCIM is a recombinant humanized MAB designed to target and bind specifically to human epidermal growth factor receptor (EGFR) and blocks its activity. Excessive production of EGFR is observed in a variety of tumours and is associated with poor treatment response, disease progression and poor prognosis [6.7].

6.2.1. Preparation and characterization of ⁹⁰Y DOTA rituximab

6.2.1.1. Conjugation of rituximab with p-NCS-Bz-DOTA

The conjugation of rituximab with p-isothiocyanatobenzyl DOTA (p-NCS-Bz-DOTA) was carried out at different antibody:DOTA molar ratios (1:10, 1:25, 1:50 and 1:100). A 2 mL aliquot of rituximab (10 mg/mL) was concentrated to 1 mL using an Amicon Ultra centrifugal filtration device (cut-off at molecular weight (MW) = 10 000 Da) at 3000 rev./min for 30 min. The pH of the solution was adjusted to 9.0 with 0.2M bicarbonate buffer. Appropriate amounts of p-NCS-Bz-DOTA were added, and the reaction mixture was incubated at room temperature (25°C) for 1–2 h followed by overnight incubation at 4°C. A 100 μ L aliquot of the mixture was kept aside for the determination of the number of DOTA molecules bound to rituximab by radioassay. The reaction mixture was centrifuged in Amicon Ultra centrifugal filter devices to remove unreacted p-NCS-Bz-DOTA. The process was repeated two or three times until all the free p-NCS-Bz-DOTA was removed. The presence of free-DOTA was monitored using TLC in CH₃OH:NH₃ (99:1), in which unconjugated p-NCS-Bz-DOTA migrates to the solvent front, while the DOTA rituximab conjugate remains at the point of spotting. The conjugate was dissolved in 0.05M phosphate buffer (pH7.4) and stored at 4°C.

6.2.1.2. Determination of the number of DOTA molecules bound to rituximab

The number of chelator (p-NCS-Bz-DOTA) molecules bound to rituximab was determined by two methods: radioassay using cold $^{89}\text{YCl}_3 \cdot 6\text{H}_2\text{O}$ spiked with a trace of ^{90}Y acetate and spectroscopic assay using the Cu(II) arsenazo(III) complex [6.8].

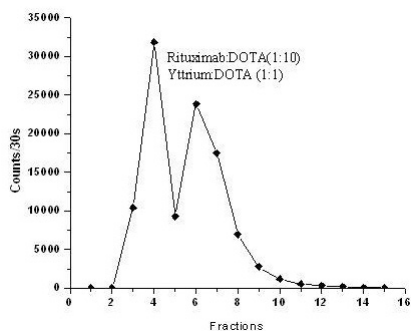
(a) Radioassay

Aliquots approximating to 100 μg of rituximab of each of the reaction mixtures corresponding to different antibody:DOTA molar ratios (1:10, 1:25, 1:50 and 1:100) were taken. Approximately 200 μCi of ^{90}Y acetate was added, together with cold $^{89}\text{YCl}_3$ in the ratio of 1:1 (yttrium:DOTA). The reaction was carried out at 40°C for 2 h, and the reaction mixture was purified using a PD-10 column. Fractions of 1 mL were collected using 0.05M phosphate buffer (pH7.4) and the radioactivity associated with each fraction was measured. The elution patterns are as shown in Fig. 6.5. The percentage of radioactivity associated with rituximab in comparison with the total radioactivity gave an indication of the numbers of DOTA molecules bound to the antibody, which were estimated to be ~5, 12, 20 and 36 for rituximab:DOTA conjugated at 1:10, 1:25, 1:50 and 1:100 ratios, respectively.

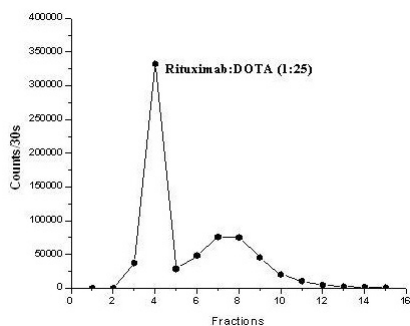
The reaction mixture of a 1:10 ratio of DOTA rituximab was spiked with cold $^{89}\text{YCl}_3$ corresponding to 0.5:1, 1:1 and 2:1 yttrium:DOTA ratios to confirm the number of DOTA bound to rituximab. Radiolabelling was carried out as described in Section 6.2.1.4 and purification was carried out using a PD-10 column. The elution patterns (see Fig. 6.6) show ~67.9%, 49% and 56.1% for 0.5:1, 1:1 and 2:1 yttrium:DOTA ratios, respectively. These patterns indicated that approximately five molecules of DOTA were bound to the antibody.

(b) Spectroscopic assay using Cu(II) arsenazo(III) assay

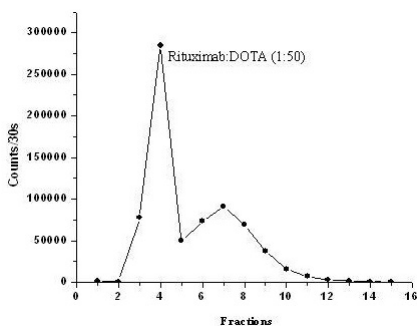
The number of DOTA molecules bound to rituximab was also determined using the Cu(II) arsenazo(III) assay, as reported by Brady et al. [6.8]. A stock solution referred to as copper reagent composed of 25 μM of Cu(II) and 100 μM of arsenazo(III) in 0.15M NH_4OAc (OAc = acetate anion), pH7.0, was prepared. Serial dilutions of this reagent were made to ensure that this reagent obeyed Beer Lambert's law by determining the absorbance at 652 nm. A spectrum of the copper reagent was taken and absorbance at 652 nm was recorded. The experiment indicated that for 1 mL of the copper arsenazo (III) reagent, absorbance (A) was 0.079. Using Beer's law, the molar extinction coefficient ϵ was calculated to be $3160 \text{ L} \cdot \text{cm}^{-1} \cdot \text{mol}^{-1}$.



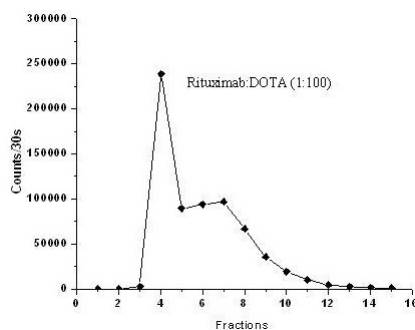
(a)



(b)

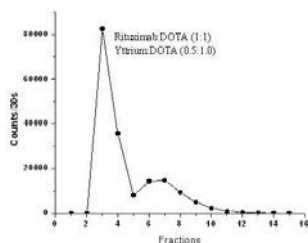


(c)

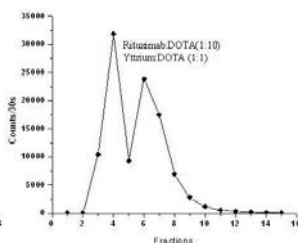


(d)

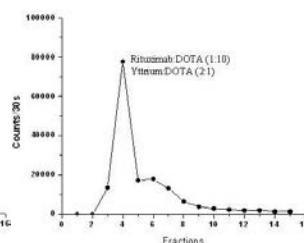
FIG. 6.5. PD-10 column elution patterns of reaction mixture of $^{89/90}\text{Y}$ DOTA rituximab in antibody:DOTA ratios of (a) 1:10, (b) 1:25, (c) 1:50 and (d) 1:100 (Y:DOTA of 1:1 ratio).



(a)



(b)



(c)

FIG. 6.6. PD-10 column elution patterns of $^{89/90}\text{Y}$ DOTA rituximab (1:10) reaction mixture at (a) 0.5:1 yttrium:DOTA, (b) 1:1 yttrium:DOTA and (c) 2:1 yttrium:DOTA ratios.

To determine the absorbance of the purified rituximab DOTA conjugates, 100 μL of the copper reagent was replaced with 100 μL of the rituximab DOTA conjugate, and the absorbance was determined at 280 and 652 nm at regular intervals of 5 min up to 30 min, until the readings stabilized. It was observed

that while the absorbance at 280 nm increased, indicating the presence of the antibody conjugate, the absorbance at 652 nm dropped in response to Cu(II) exchange from the arsenazo (III) complex to form the copper DOTA antibody conjugate, as indicated in Table 6.1.

TABLE 6.1. ABSORBANCE OF COPPER REAGENT AT 280 AND 652 nm

Description	Absorbance at 280 nm	Absorbance at 652 nm
1 mL Cu reagent	0.156	0.079
900 μ L Cu reagent + 100 μ L rituximab DOTA conjugate	0.238	0.072
800 μ L Cu reagent + 200 μ L rituximab DOTA conjugate	0.319	0.064

The concentration of DOTA in the rituximab DOTA conjugate was determined based on the change in absorbance at 652 nm, the dilution factor and the extinction coefficient. The concentrations of the antibody and the antibody conjugate were independently determined using Lowry's method as well as by measuring the absorbance at 280 nm. By comparing the concentrations of the DOTA antibody conjugate and the antibody, the number of DOTA molecules bound to the antibody could be determined. The experiment showed that the antibody conjugate with a molar ratio of 1:10 had approximately seven molecules of DOTA bound to one molecule of antibody.

*6.2.1.3. Determination of the integrity of the DOTA rituximab conjugate:
SDS PAGE*

To determine the integrity of the DOTA rituximab conjugate stored at 4°C for long periods of time, sodium dodecyl sulphate polyacrylamide gel electrophoresis (SDS PAGE) under reducing and non-reducing conditions was carried out. Rituximab and rituximab DOTA (1:5) at different dilutions were subjected to SDS PAGE in a 12.5% homogenous gel. After electrophoresis, the gel was stained with coomassie brilliant blue. Molecular weight standards were simultaneously run in the same gel for comparison. On destaining, it was observed that both rituximab and the rituximab DOTA conjugate, under non-reducing conditions, showed comparable distinct bands at 150–160 kDa, while the same samples under reducing conditions showed two distinct bands at ~50 kDa (heavy chains of antibody) and at ~25 kDa (light chains of antibody),

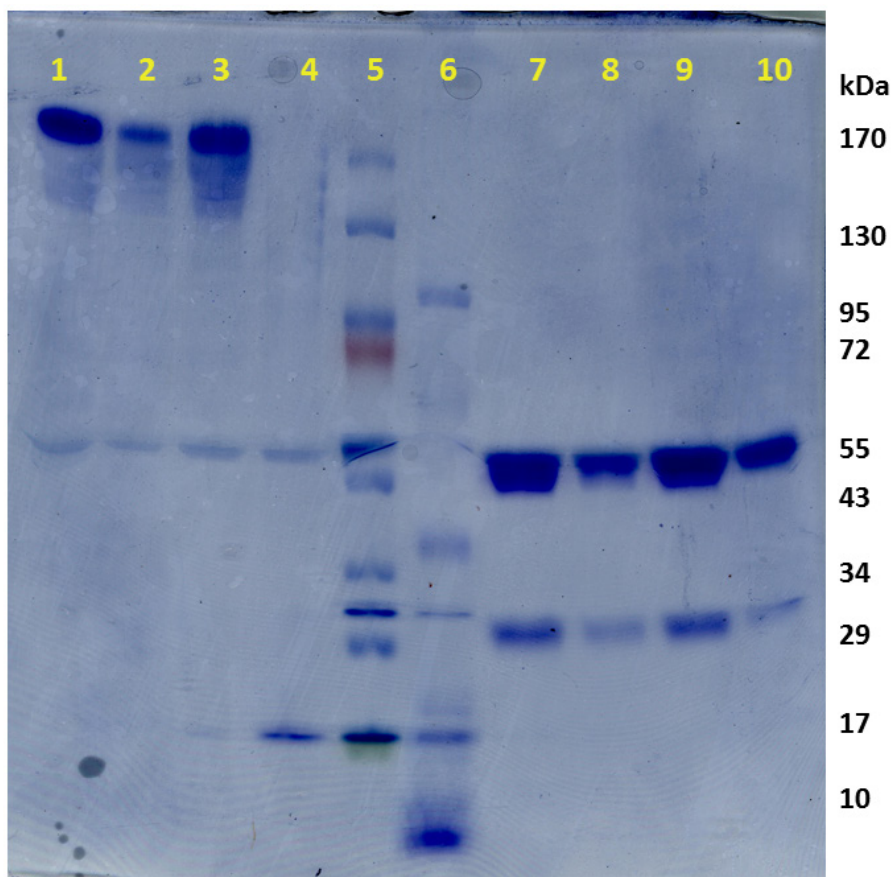


FIG. 6.7. SDS PAGE pattern of rituximab and rituximab DOTA under non-reducing (lanes 1–4) and reducing conditions (lanes 7–10). Lanes 1 and 7: rituximab antibody (50 μ g); lanes 2 and 8: rituximab antibody (25 μ g); lanes 3 and 9: rituximab DOTA (50 μ g); lanes 4 and 10: rituximab DOTA (25 μ g); lanes 5 and 6: molecular weight standards.

as shown in Fig. 6.7. This experiment indicated that no major change occurred to the antibody on conjugation with approximately five molecules of DOTA when stored at 4°C.

6.2.1.4. Radiolabelling of the DOTA rituximab conjugate with ^{90}Y

One milligram of the DOTA rituximab conjugate was taken in 200 μ L of ammonium acetate buffer (pH5.5). An activity of 74–111 MBq (2–3 mCi) of ^{90}Y acetate was added to the conjugate. Yttrium-90 acetate was eluted from the

electrochemical generator developed in house [6.3]. The reaction was carried out at ~pH6 for 2 h at 40°C. Yttrium-90 DOTA rituximab was characterized using HPLC carried out on a TSK G3000SWxL gel column, along with a SWxL guard column, using 0.05M PO_4^{3-} buffer, pH6.8, as the mobile phase (see Fig. 6.8). The radiolabelling yield was ~70%. In the standardized HPLC system, ^{90}Y DOTA rituximab had a retention time of 15 min, while free $^{90}\text{Y}^{3+}$ had a retention time of 22 min.

The ^{90}Y DOTA rituximab reaction mixture was purified by passing through a PD-10 column and eluted with 0.05M phosphate buffer (pH7.4). The elution pattern obtained is shown in Fig. 6.9. Figure 6.10 shows the HPLC pattern of

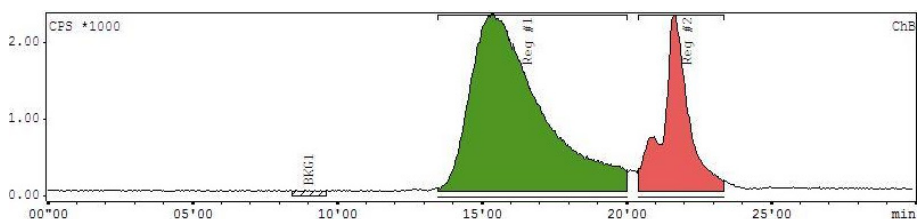


FIG. 6.8. HPLC pattern of ^{90}Y DOTA rituximab reaction mixture.

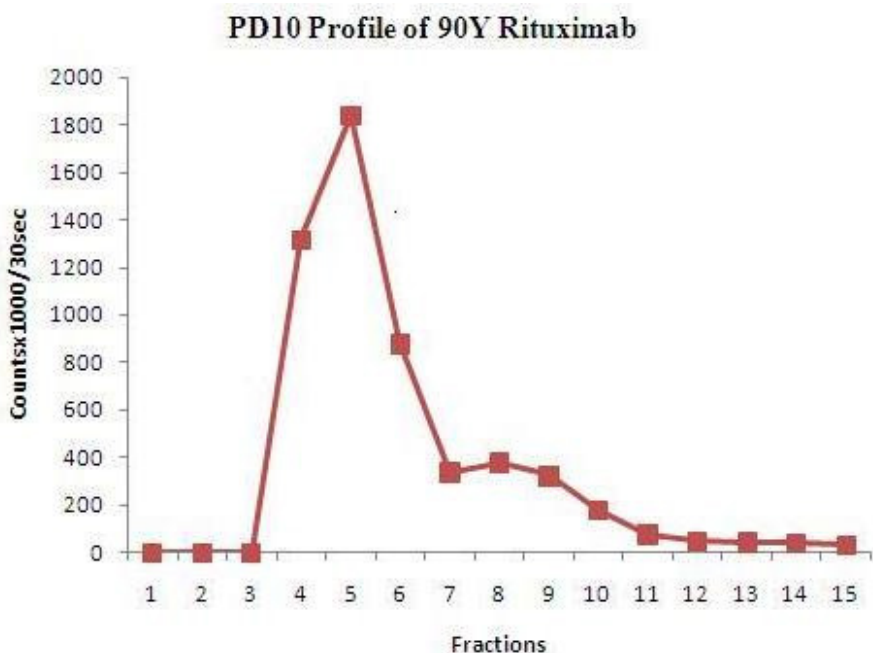


FIG. 6.9. Elution profile of ^{90}Y rituximab DOTA on PD-10 column.

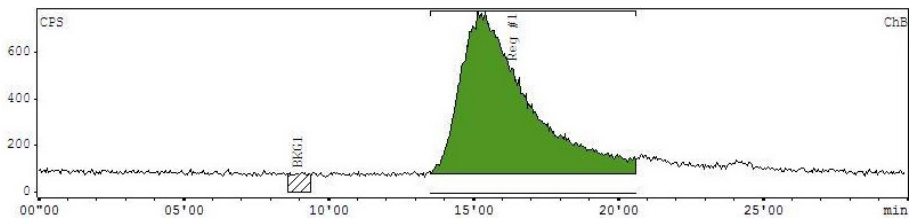


FIG. 6.10. HPLC pattern of pure ^{90}Y DOTA rituximab.

pure ^{90}Y DOTA rituximab. The radiolabelled antibody could be obtained in >98% purity after PD-10 purification. The pure conjugate had a retention time of 15 min in the HPLC system. The stability of the radioconjugate stored at 4°C and room temperature (25°C) was studied using HPLC. The RCP values determined after 24 and 48 h are presented in Figs 6.11 and 6.12.

6.2.1.5. Biological evaluation of ^{90}Y DOTA rituximab

(a) In vitro cell binding studies

Raji cells (Burkitt lymphoma), which express CD20 antigen on their surface, were used for in vitro binding studies of ^{90}Y DOTA rituximab conjugate [6.9]. Cells were grown to confluence in RPMI medium containing 10% foetal calf serum. After harvesting, 1×10^6 cells in exponential growth

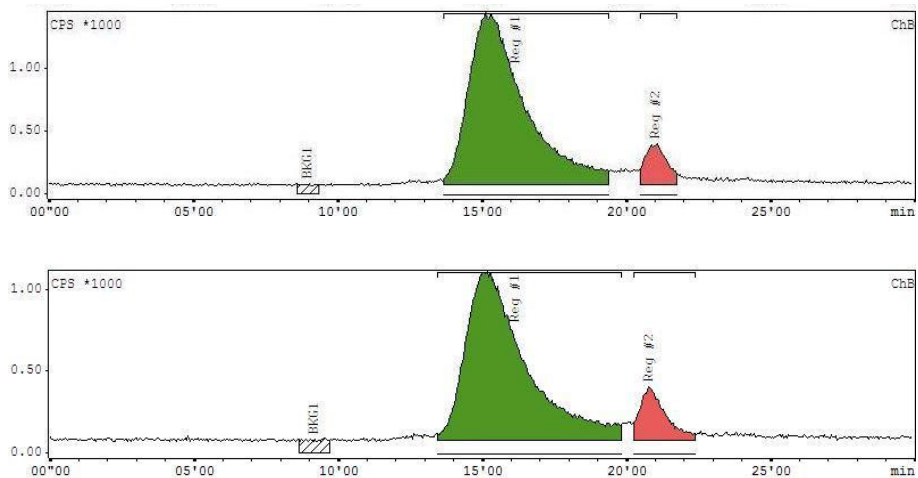


FIG. 6.11. Stability of the radioconjugate after 24 and 48 h at 4°C.

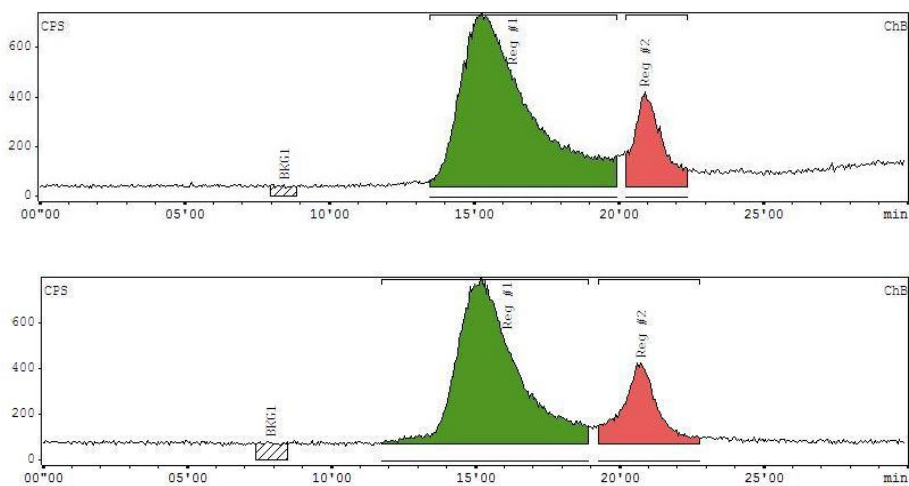


FIG. 6.12. Stability of the radioconjugate after 24 and 48 h at room temperature.

(i.e. 1×10^7 cells/mL) were incubated with ^{90}Y DOTA rituximab (5:1 ratio) for 2 h at 37°C . After incubation, the cells were washed with 1 mL of 0.05M phosphate buffer (pH7.4) and centrifuged at 2000 rev./min for 20 min at room temperature. The supernatant was aspirated and the pellet was measured for radioactivity. Inhibition studies were carried out to confirm specificity of binding by incubation of the same number of cells with 10, 50 and 100 μg of cold antibody under similar experimental conditions. Non-specific binding studies were carried out using U937 cell lines that do not express CD20 antigen on its surface. The results are presented in Fig. 6.13.

(b) Equilibrium binding studies

Specific binding [6.10] was measured at six different concentrations of ^{90}Y DOTA rituximab ranging from 0.17nM to 33.3nM to determine the equilibrium dissociation constant (K_d) by Scatchard analysis using GraphPad Prism 5 software. Two million Raji cells in 0.4 mL RPMI medium were incubated with ^{90}Y DOTA rituximab (0.17–33.3nM) for 2 h in a shaker at 37°C . The cells were washed twice with 0.05M phosphate buffer containing 1% bovine serum albumin, the cells were centrifuged and the supernatant was separated from the cell pellet. Both the cell pellet and supernatant were counted. Non-specific binding was measured by saturating the receptors with 25 μg of unlabelled rituximab. Specific binding was determined by subtracting the non-specific binding from the total bound counts at each concentration of the radioimmunoconjugate. A plot of the percentage specific binding on the y axis versus the concentration of the

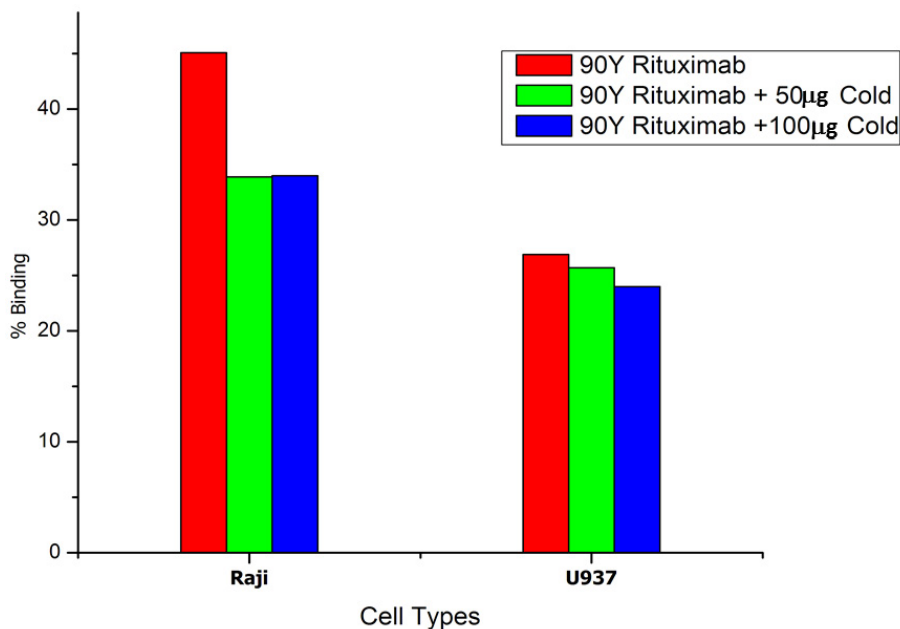


FIG. 6.13. Cell binding studies with ^{90}Y DOTA rituximab.

radioimmunoconjugate on the x axis was constructed. The concentration at 50% binding is equivalent to the K_d , which was determined directly from the x axis. The data were analysed by a Scatchard plot using GraphPad Prism 5 software. The K_d for ^{90}Y DOTA rituximab was determined to be 3.38nM, as shown in Fig. 6.14.

(c) Biodistribution studies in normal Swiss mice

Biodistribution studies were carried out in normal Swiss mice at 3, 24 and 48 h p.i. using ~ 370 kBq of ^{90}Y DOTA rituximab. The mice weighing 20–25 g were administered with ~ 370 kBq of ^{90}Y DOTA rituximab in 0.1 mL via the lateral tail vein. Animals were divided into three groups of four each, for each time interval studied, viz. 3, 24 and 48 h. The animals were sacrificed, blood was collected and organs dissected and weighed. The radioactivity in each organ/tissue was measured in a flat geometry NaI(Tl) counter. Percentage doses per organ were calculated for all the major organs and blood, and are as presented in Fig. 6.15.

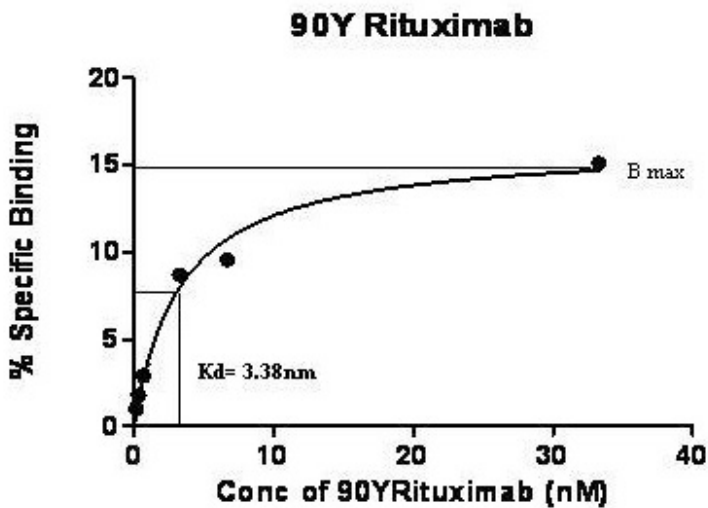


FIG. 6.14. K_d of ⁹⁰Y DOTA rituximab.

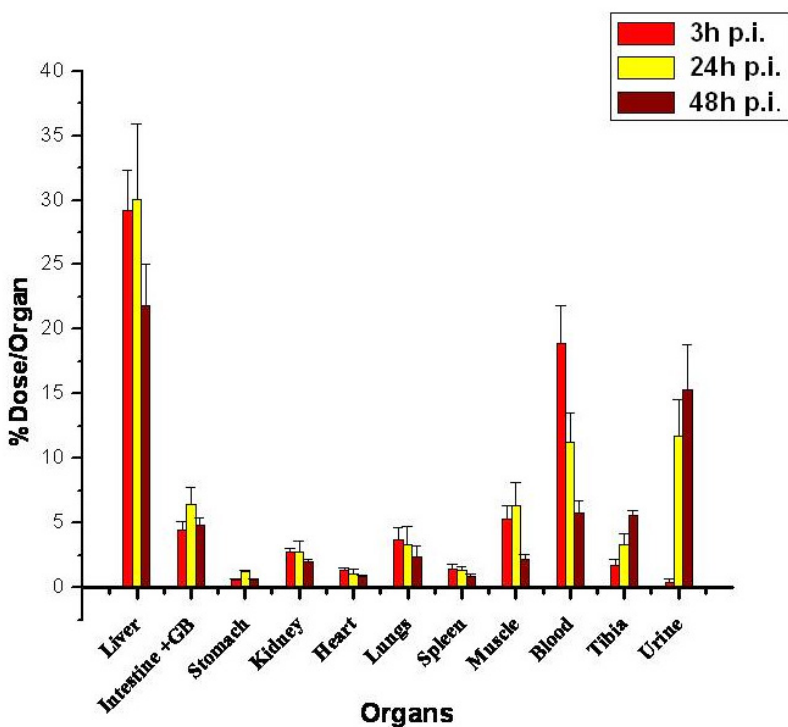


FIG. 6.15. Biodistribution pattern of ⁹⁰Y DOTA rituximab in normal Swiss mice.

6.2.1.6. Conclusion

The procedure for the conjugation of DOTA to rituximab was standardized. The number of DOTA molecules linked to rituximab was determined using carrier added studies as well as by using copper arsenazo assay. It could be determined that approximately six to seven DOTA molecules are attached to rituximab when conjugation of DOTA to the antibody is carried out in a 10:1 ratio. The integrity of the conjugate was determined by SDS PAGE and found to be stable. Approximately 70% radiolabelling yield could be obtained using 2–3 mCi of ^{90}Y acetate. The product exhibited RCP >99% after purification and was stable when studied up to 48 h at room temperature. In vitro cell binding studies showed specific binding to the CD20 antigen in Raji cells. In vivo biodistribution studies in Swiss mice showed normal distribution. Further in vivo studies in animal models of NHL are planned.

6.2.2. Preparation and characterization of ^{90}Y DOTA TheraCIM

6.2.2.1. Conjugation of TheraCIM with p-NCS-Bz-DOTA

The conjugation of TheraCIM with DOTA NCS was carried out at a 1:10 molar ratio of antibody:DOTA. Four millilitres of TheraCIM (5 mg/mL) was concentrated to a final volume of 1 mL using an Amicon Ultra centrifugal filtration device (cut-off at MW = 10 000 Da) at 3000 rev./min for 30 min. The pH of the solution was adjusted to 9.0 with a bicarbonate buffer. Approximately 1 mg of p-NCS-Bz-DOTA was added, and the reaction mixture was incubated at room temperature for 1–2 h followed by overnight incubation at 4°C. An aliquot was retained for radioassay. Unconjugated p-NCS-Bz-DOTA was separated from the mixture by centrifugation in Amicon Ultra centrifugal filter devices. The process was repeated until all the free p-NCS-Bz-DOTA was removed. The presence of free DOTA was monitored using TLC in $\text{CH}_3\text{OH}:\text{NH}_3$ (99:1), in which unconjugated p-NCS-Bz-DOTA moves to the solvent front, while the DOTA TheraCIM conjugate remains at the point of spotting. The conjugate was dissolved in 0.05M phosphate buffer (pH7.4) and stored at 4°C.

6.2.2.2. Determination of number of DOTA molecules bound to TheraCIM

The number of DOTA molecules bound to the antibody molecule was determined by radioassay using $^{89}\text{YCl}_3$.

(a) Radioassay

Three tubes, each containing ~1 mg of the antibody DOTA conjugate reaction mixture (molar ratio of 1:10), were taken. To this, a trace amount of ^{90}Y (~200 μCi) in NH_4OAc (pH5.5) was added. Each of these tubes was spiked with various amounts of $^{89}\text{YCl}_3$ in the ratios 0.5:1, 1:1 and 2:1 (Y:DOTA). The reaction was carried out at 40°C for 2 h and passed through a PD-10 column using a 0.05M phosphate buffer (pH7.4). Fractions were collected and counted. The elution patterns are as shown in Fig. 6.16. The number of DOTA molecules bound to the antibody was estimated as described in Section 6.3.1.2. The elution patterns showed that approximately six molecules of DOTA were bound to one antibody molecule.

6.2.2.3. Radiolabelling of DOTA TheraCIM conjugate with ^{90}Y

One milligram of the DOTA TheraCIM conjugate was taken together with 200 μL of ammonium acetate buffer (pH5.5). An activity of 74–111 MBq (2–3 mCi) of ^{90}Y acetate was added to the conjugate. The pH of the final reaction mixture was in the range 5–6. The reaction was carried out at 40°C for 2 h. The ^{90}Y DOTA TheraCIM reaction mixture was purified by passing through a PD-10 column and eluting with 0.05M phosphate buffer (pH7.4). The radiolabelling yield was found to be ~70–75%, and the elution pattern obtained is shown in Fig. 6.17.

6.2.2.4. Conclusion

DOTA could be conjugated to TheraCIM in a 6:1 ratio. Radiolabelling of the DOTA TheraCIM conjugate with ^{90}Y acetate was standardized. It is planned to carry out further in vitro and in vivo bioevaluation studies in the near future.

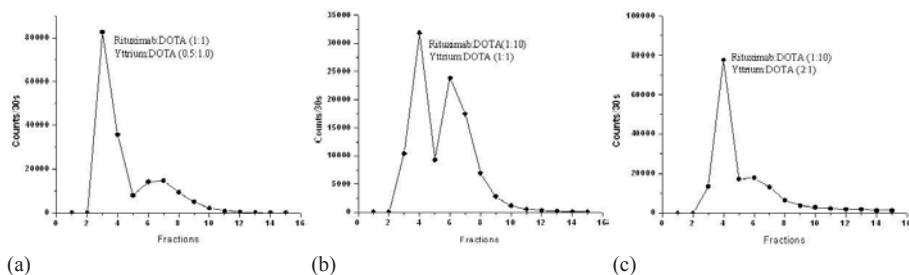


FIG. 6.16. PD-10 column elution patterns of $^{89/90}\text{Y}$ DOTA TheraCIM (1:10) reaction mixture at: (a) 0.5:1, (b) 1:1 and (c) 2:1 $^{89/90}\text{Y}$:DOTA ratios.

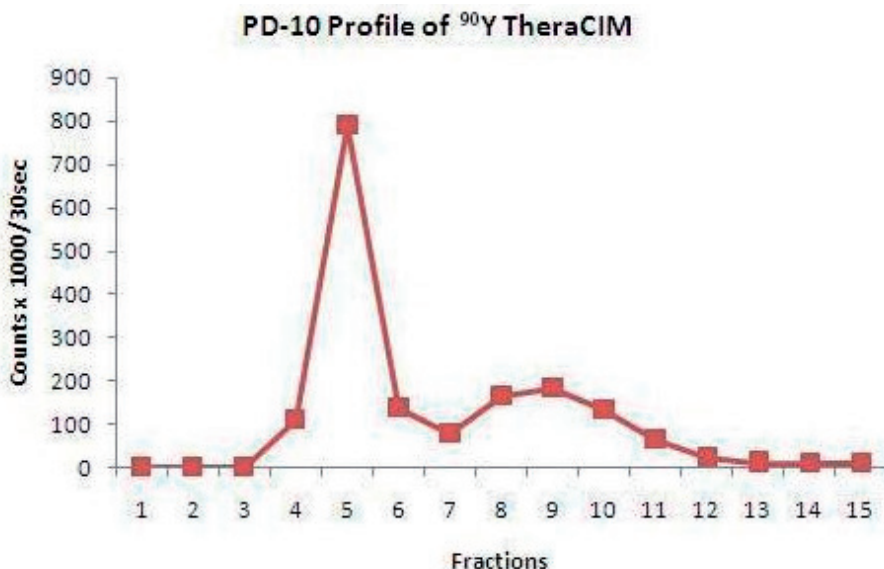


FIG. 6.17. Elution profile of ^{90}Y DOTA TheraCIM through PD-10 column.

6.3. YTTRIUM-90 RADIOPHARMACEUTICALS FOR LIVER CANCER

In recent years, research towards the treatment of hepatocellular carcinoma (HCC) has focused on the application of radiolabelled complexes containing therapeutically relevant β emitting radioisotopes directly injected into the hepatic artery, which are subsequently localized in the liver [6.11]. There are two approaches to the above mentioned radioembolization. In one approach, the radioactivity is incorporated into a strongly lipophilic preparation that permeates through the hepatocellular tissue and is retained there long enough for the therapeutic effect. In the other approach, the therapeutic isotope is incorporated into non-biodegradable or very slowly degrading particulates that are several micrometres in diameter, which get localized in the capillaries [6.12]. In the scope of the work under this CRP, preliminary biological evaluation of ^{90}Y labelled oxine in lipiodol as a lipophilic carrier of ^{90}Y into the liver tissue was carried out [6.13]. Biological assessment of the ^{90}Y oxine complex was carried out using in vitro and in vivo methodologies. Subsequently, ^{90}Y labelled Bio-Rex 70 resin microparticles have been prepared as a particulate delivery vehicle for ^{90}Y into the liver capillaries, from where it may be envisaged to deliver the therapeutic β emissions.

6.3.1. Preparation and in vitro and in vivo assessment of ^{90}Y oxine

Yttrium-90 oxine was prepared as per the procedure reported by Flieger et al. [6.9]. In brief, 5 mg of 8-hydroxyquinoline (oxine) was dissolved in ethanol and reacted with $\sim 74\text{--}111$ MBq of ^{90}Y chloride at 50°C for 30 min. The radiolabelling yield was determined by extraction in chloroform, and was found to be $>90\%$. For in vitro assessment, the Hep G2 human liver carcinoma cell line was employed. This was procured from the accredited cell line repository National Centre for Cell Science (India). The cells were cultured in minimal essential medium with 10% foetal bovine serum as a growth supplement. They were maintained at 37°C in a 5% CO_2 atmosphere. The viability of cells was estimated using a haemocytometer count with trypan blue differential stain. Cell viability $>95\%$ was the criterion applied when using cells for in vitro assays.

6.3.1.1. In vitro assessment

(a) MTT cell viability assay

The viability of Hep G2 cells on exposure to ^{90}Y oxine was studied using thiazolyl blue tetrazolium bromide (MTT) assay. Here, the ability of viable cells to metabolize MTT to give formazan is used to quantitatively assess cellular viability. Briefly, cells were plated in 96 well plates at a density of 10^4 cells/well. Cells were exposed to differing concentrations of ^{90}Y oxine (dissolved in ethanol). The total incubation volume was maintained at $200\ \mu\text{L}$ and the final ethanol concentration was $<0.5\%$. The cells were exposed to the labelled complex for 24 h. MTT was freshly dissolved in PBS at a concentration of $5\ \text{mg/mL}$. After the 24 h incubation, $20\ \mu\text{L}$ of this MTT solution was added to each well and mixed gently. This was incubated for 4 h, after which the supernatant was aspirated completely and the wells rinsed with PBS. Then, $200\ \mu\text{L}$ of DMSO was added to dissolve the formazan metabolite formed inside the viable cells. This reaction was kept in the dark for 30–45 min and was read on an enzyme linked immunosorbent assay (ELISA) reader (560 nm, background corrected at 670 nm). In the MTT assay, $>50\%$ loss in cell viability was observed at exposure to a minimum activity of $4.6\ \text{MBq}$ of ^{90}Y oxine/ 10^4 cells for 24 h. Further in vitro work was performed at this concentration.

(b) Lactate dehydrogenase release assay

The integrity of the cell membrane was assayed using an assay of cytoplasmic lactate dehydrogenase (LDH) released into the medium from the cells. Here, LDH reduces nicotinamide adenine dinucleotide to its protonated

form NADH, which, in turn, causes the stoichiometric conversion of a tetrazolium dye, leading to the formation of a coloured product. In the assay protocol followed, Hep G2 cells were exposed to the labelled preparation (4.6 MBq of ^{90}Y oxine/ 10^4 cells) for ~ 3 h (controls used cold oxine). The assay for released LDH was performed using an LDH based cytotoxicity assay kit. It was observed that the cells exposed to ^{90}Y oxine showed significant release of cytoplasmic LDH compared to the controls, indicating loss of cell membrane integrity as a consequence of absorbed dose in the given period, as shown in Fig. 6.18.

(c) Polymerase chain reaction based marker assay

Polymerase chain reaction (PCR) assay was performed to assess the expression of various markers associated with apoptotic cell death. The assay was performed on cells exposed for three hours to the optimized value of ^{90}Y oxine. The RNA of the cells was isolated using a column purification kit and transcribed to cDNA using reverse transcriptase enzyme reaction. The cDNA amplification was performed using PCR and the expression of the marker genes was assessed by electrophoresis of amplified DNA. It was observed that the RNA expression of proapoptotic marker *bax* was up-regulated on exposure to ^{90}Y oxine in vitro compared to the controls.

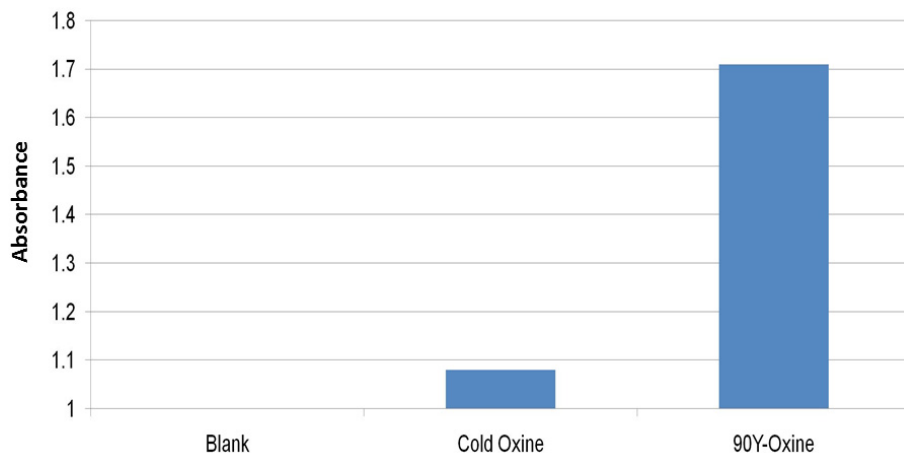


FIG. 6.18. LDH release by Hep G2 cells.

(d) Caspase 3 assay

Assay was performed to assess the involvement of apoptosis marker protein caspase 3 in the cell death process. Using a colorimetric assay kit, the activity of caspase 3 was assayed in Hep G2 cultures exposed to the radiolabelled complex. However, no appreciable difference could be observed between the sample and the unexposed controls. As no protease inhibitor was used in the assay, it is possible that degradation of caspase 3 in the sample may have occurred, which needs to be investigated further.

6.3.1.2. In vivo assessment

In vivo assessment was performed in Wistar rats. A liver cancer model was raised in the animals by chemical carcinogenesis using diethylnitrosamine. After the induction period, the animals were taken for in vivo experiments. Approximately 37 MBq (1 mCi) of ^{90}Y oxine in lipiodol (100 μL) was administered into the liver via the intrahepatic artery. The in vivo distribution patterns of the radiolabelled complex at 24 and 96 h are given in Fig. 6.19. The in vivo patterns show significant disadvantages to potential application as a liver cancer radiopharmaceutical. Even at 24 h, only ~50% of the injected activity is retained in the liver, which reduces to <15% at 96 h. More importantly, a significant proportion of the leached activity appears to localize in the skeletal tissue, where it can give unnecessary dose burdens to non-target tissue.

Histologic sections of the treated liver tissue from control and HCC induced animals are shown in Fig. 6.20. It is seen from these sections that the tumour induced tissue shows a greater degree of damage than the control tissue, indicating that the treatment has a therapeutic effect on HCC, but the problem of leakage and non-target dose burden significantly hinders the prospect of using oxine as a delivery vehicle for ^{90}Y based therapy of cancer in the liver.

6.3.2. Preparation of ^{90}Y labelled Bio-Rex 70 microparticles for use in liver cancer

Yttrium-90 acetate (74–111 MBq) was mixed with 0.5M ammonium acetate solution to make a volume of 2 mL (pH adjusted to ~5.0–5.5 using 0.1M HCl), to which the carrier yttrium equivalent to 50 mCi was added. To the above mixture was added 20 mg of Bio-Rex 70 microparticles. Radiolabelling was carried out at room temperature for 60 min with intermittent mixing. After the incubation period, the radiolabelled particles were separated by centrifugation at 2000 g. The total activity and the activity associated with the supernatant were counted to estimate the radiolabelling yield, which was found to be ~99.2%. The particles

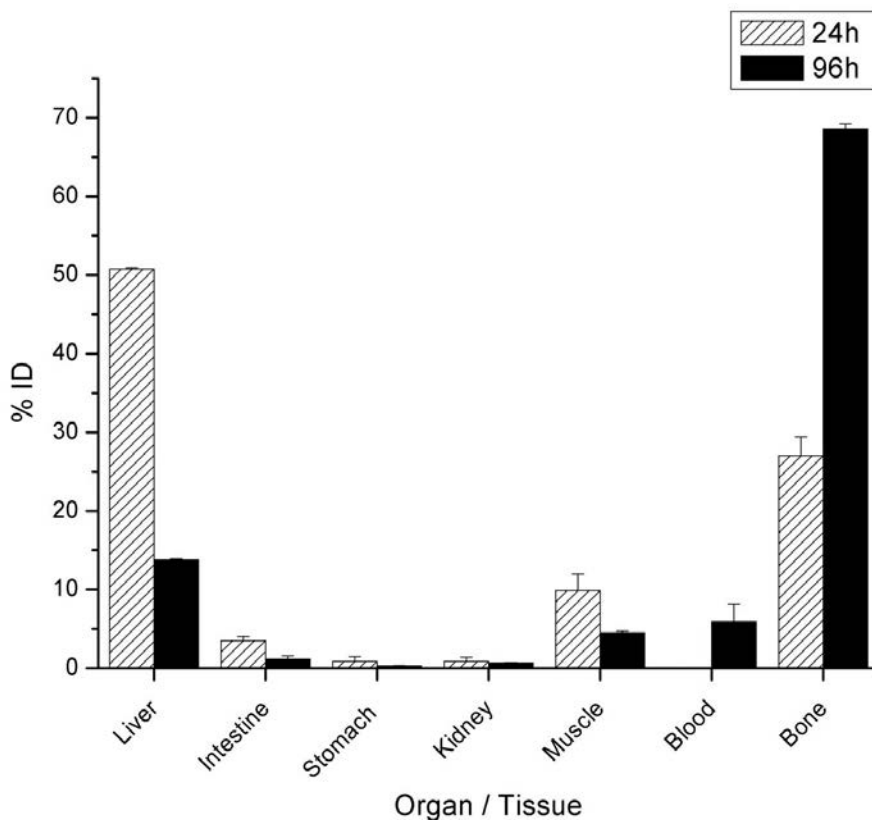


FIG. 6.19. In vivo distribution patterns of the radiolabelled complex at 24 and 96 h.

were washed twice with 0.5M ammonium acetate solution. Then, 2 mL of saline was added and kept at room temperature. At different intervals (1, 4 and 7 d), the suspension was centrifuged at 2000 g, and the particles and supernatant were separated and counted to estimate the leaching of ^{90}Y from the particles. Table 6.2 shows the stability profile of ^{90}Y labelled Bio-Rex 70 particles. It can be seen that ^{90}Y labelled Bio-Rex 70 microparticles are very stable with very little leaching of radioactivity from the preparation, even after seven days at room temperature. Further in vivo studies in animal models are planned.

6.3.3. Conclusion

In vitro and in vivo evaluation of ^{90}Y oxine for use in therapy of HCC has been carried out. Although the in vitro studies gave promising results, it was observed that the complex exhibited significant in vivo dissociation, resulting

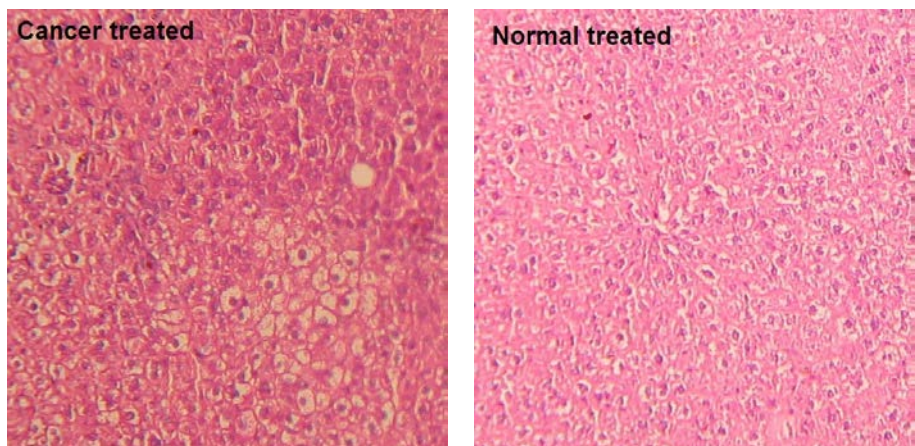


FIG. 6.20. Histologic sections of the treated liver tissue from control and HCC induced animals.

TABLE 6.2. IN VITRO STABILITY OF ^{90}Y LABELLED BIO-REX 70 MICROPARTICLES

Sample. no.	Time (d)	Leaching (%)
1	1	0.81 ± 0.01
2	4	0.31 ± 0.02
3	7	0.17 ± 0.01

in accumulation of ^{90}Y activity in the bone. Yttrium-90 labelling of Bio-Rex 70 microparticles was carried out to have a stable radiolabelled product that would not leach out of the liver owing to its particle size. In the studies, Bio-Rex 70 microparticles could be radiolabelled with >99% yield under the optimized conditions, and the particles exhibited excellent in vitro stability for up to seven days at room temperature. It is further planned to carry out in vivo bioevaluation studies in animal models of HCC.

ACKNOWLEDGEMENTS

The authors of this chapter express their sincere thanks to the IAEA for the opportunity to participate in this CRP. The authors are grateful to the Center of Molecular Immunology (CIM) (A. Casaco and the CIM Management), Cuba, for providing TheraCIM for the studies. The authors are grateful to P.S. Dhami and team, Fuel Reprocessing Division, BARC, for help in providing ^{90}Y from the SLM generator.

REFERENCES TO CHAPTER 6

- [6.1] DHAMI, P.S., et al., Studies on the development of a two stage supported liquid membrane system for the separation of carrier-free ^{90}Y using KSM-17 and CMPO as carriers, *Sep. Sci. Technol.* **42** (2007) 1107.
- [6.2] VENKATESH, M., et al., Complexation studies with ^{90}Y from a novel ^{90}Sr - ^{90}Y generator, *Radiochimica Acta* **89** (2001) 413.
- [6.3] CHAKRAVARTY, R., et al., Development of an electrochemical ^{90}Sr - ^{90}Y generator for separation of ^{90}Y suitable for targeted therapy, *Nucl. Med. Biol.* **35** (2008) 245.
- [6.4] PANDEY, U., et al., A novel extraction paper chromatography (EPC) technique for the radionuclidic purity evaluation of ^{90}Y for clinical use, *Anal. Chem.* **80** (2008) 801.
- [6.5] United States Pharmacopeia Monograph: Yttrium Y 90 Ibritumomab Tiuxetan Injection (2010),
www.pharmacopeia.cn/v29240/usp29nf24s0_m89430.html
- [6.6] PLOSKER, G.L., FIGGITT, D.P., Rituximab: A review of its use in non-Hodgkin's lymphoma and chronic lymphocytic leukaemia, *Drugs* **63** (2003) 803.
- [6.7] NICHOLSON, R.I., GEE, J.M., HARPER, M.E., EGFR and cancer prognosis, *Eur. J. Cancer* **37** Suppl. 4 (2001) S9.
- [6.8] BRADY, E.D., CHONG, H., MILENIC, D.E., BRECHBIEL, M.W., Development of a spectroscopic assay for bifunctional ligand-protein conjugates based on copper, *Nucl. Med. Biol.* **31** (2004) 795.
- [6.9] FLIEGER, D., RENOTH, S., BEIER, I., SAUERBRUCH, T., SCHMIDT-WOLF, I., Mechanism of cytotoxicity induced by chimeric mouse human monoclonal antibody IDECC2B8 in CD20-expressing lymphoma cell lines, *Cell Immunol.* **204** (2000) 55.
- [6.10] MELHUS, K.B., et al., Evaluation of the binding of radiolabeled rituximab to CD20 positive lymphoma cells: An in vitro feasibility study concerning low-dose-rate radioimmunotherapy with the α emitter ^{227}Th , *Cancer Biother. Radiopharm.* **22** (2007) 469.
- [6.11] SUNDARAM, F.X., Radionuclide therapy of hepatocellular carcinoma, *Biomed. Imaging Interv. J.* **2** (2006) e40.

- [6.12] SANGRO, B., et al., Treatment of hepatocellular carcinoma by radioembolization using ^{90}Y microspheres, *Dig. Dis.* **27** (2009) 164.
- [6.13] YU, J., HAFELI, U.O., SANDS, M., DONG, Y., ^{90}Y -oxine-ethiodol, a potential radiopharmaceutical for the treatment of liver cancer, *Appl. Radiat. Isotopes* **58** (2003) 567.

Chapter 7

DEVELOPMENT OF THERAPEUTIC RADIOPHARMACEUTICALS BASED ON ^{90}Y BIOTIN

L. GARABOLDI, M. CHINOL
Division of Nuclear Medicine,
European Institute of Oncology,
Milan, Italy

Abstract

The preparation of a biotin derivative labelled with ^{90}Y to be employed as a breast cancer therapeutic radiopharmaceutical in the application of the new IART approach is described in this chapter. The effects of pH on the labelling yield and in vitro affinity for avidin of the resulting radiolabelled conjugate are evaluated. Radiolabelling was performed using a manual and an automated procedure, and radiation exposure was measured for each operational condition. Microbiological tests were conducted on each final batch after decay of activity. Results obtained from a first clinical study are also described.

7.1. INTRODUCTION

The major objective of cancer radioimmunotherapy is to enhance the effectiveness of the radionuclide by concentrating it at the tumour site, which also has the benefit of producing fewer toxic side effects in normal organs. However, radioimmunotherapy is limited by a poor tumour to non-tumour ratio [7.1, 7.2]. For this reason, tumour targeting with long circulating radiolabelled MABs has achieved success, primarily in the treatment of leukaemias and lymphomas, in which the tumours are radiosensitive and the cancer cells are relatively accessible [7.3]. In an attempt to improve the therapeutic efficacy of radiolabelled MABs, various studies have examined the concept of tumour pretargeting [7.4, 7.5].

Based on previous clinical experience in locoregional treatment of peritoneal carcinomatosis and recurrent high grade glioma using the avidin biotin pretargeting technique, a potential application of ^{90}Y labelled biotin radionuclide therapy in breast cancer was foreseen [7.6, 7.7]. The avidin biotin system is widely used for in vitro applications, in immunohistochemistry, ELISA and molecular biology. Avidins are a family of proteins functionally defined by their ability to bind biotin with high affinity and specificity; no physiological compound other

than biotin is recognized and bound with any strength by avidins. They are small oligomeric proteins, made up of four identical subunits, each bearing a single binding site for biotin. Each mole of avidin can therefore bind up to four moles of biotin, and their binding affinity is very high. The dissociation constant of the avidin biotin complex is of the order of 10^{-15} M. For practical purposes, the binding of biotin to avidin can be regarded as an irreversible process [7.8].

Biotin (cis-hexahydro-2-oxo-1-H-thieno-[3,4]-imidazole-4-valeric acid) is a 244 Da molecule commonly known as vitamin H involved in the metabolism of amino acids and carbohydrates in organisms. In the preparation of biotin labelled with ^{90}Y , biotin is derivatized with an appropriate spacer carrying a specific chelating agent for the radiometal. A significant improvement in stability for ^{90}Y was achieved by using DOTA instead of DTPA [7.9]. However, any new biotin derivative could not be used for in vivo applications unless stable to the enzymatic cleavage by biotinidase. A novel stable biotin derivative conjugated to DOTA (named r-BHD), which is devoid of the amide target site for the biotinidase, has been developed [7.10] (see Fig. 7.1).

The novelty of this conjugate was that the amide carboxylic group was reduced to a methylene one, thus generating the N-aminohexyl biotinamido derivative in which the amide is transformed into a secondary amine without affecting the length of the biotin side arm involved in avidin streptavidin binding. Preliminary in vitro experiments (pH, specific activity and avidin binding) indicated the potential of this new conjugate [7.11]. Application of ^{90}Y r-BHD to a new radionuclide targeting technique (IART) has been initiated [7.12, 7.13]. The principle is that native avidin is directly injected into and around the tumour bed immediately after tumour removal. The inflammation owing to surgery results in

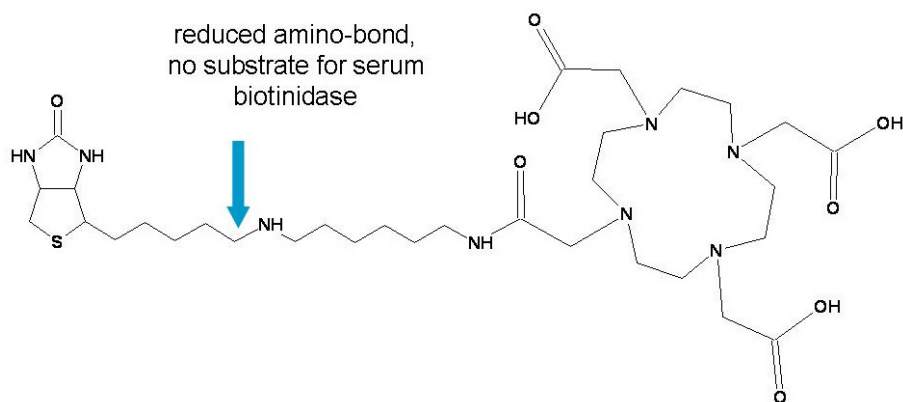


FIG. 7.1. Deoxy biotinyl hexamethylenediamine DOTA.

the residual breast tissue becoming a cation exchange material so that avidin is held in that tissue for several days. Yttrium-90 r-BHD administered intravenously ~1 d later homes in on the avidin held in the breast tissue to deliver a radiation dose to the tissue. To allow further clinical studies with this technique, it would be necessary that the ^{90}Y r-BHD be prepared in a pharmaceutically controlled environment or, alternatively, be prepared by means of an automatic module that may be considered a closed system, thus requiring less strict environmental constraints. Therefore, a study was done on the labelling of r-BHD with ^{90}Y in an automatic module of synthesis (PharmTracer) and a disposable sterile single use kit employed in the department for the labelling of peptides with ^{177}Lu and ^{90}Y .

7.2. MATERIALS AND METHODS

7.2.1. Reagents

Yttrium-90 chloride ($^{90}\text{YCl}_3$) in 0.05M HCl was purchased from PerkinElmer. The r-BHD was provided by Sigma Tau S.p.A. and dissolved in saline at a concentration of 2 mg/mL. Pure hen egg avidin was provided by Tecnogen S.p.A. Sodium acetate anhydrous DTPA, HABA, D-biotin (vitamin H) and non-radioactive $^{89}\text{YCl}_3$ at the highest analytical grade available were purchased from Sigma-Aldrich. Pharmaceutical grade ascorbic acid was purchased from Carlo Erba. Unless otherwise stated, all solutions were prepared using ultrapure water (18 M Ω ·cm resistivity).

7.2.2. Synthesis of r-BHD

Details of the synthetic pathway and chemical characterization of 10-[2-[6-[5-[3,4-(3aS,4S,6aR)-hexahydro-2-oxo-1H-thieno[3,4]imidazol-4-yl]-1-pentylamino]-1-hexylamino]-2-oxoethyl][1,4,7,10-tetraazacyclododecane-1,4,7,10-tetraacetic acid] DOTA have been described elsewhere [7.10].

7.2.3. Effect of pH on radiolabelling

To determine the optimal pH for the labelling of r-BHD with ^{90}Y , the experiments were performed at a pH ranging between 3.6 and 5.6 using 2.0M sodium acetate buffer. Because of the high buffering capacity, the final pH of the reaction mixtures was equal to that of the 2.0M sodium acetate buffer used, as confirmed by electronic pH meter measurements (Hanna Instruments). All experiments were carried out in triplicate.

7.2.4. Avidin r-BHD binding studies

Binding studies were performed using the spectrophotometric method known as HABA assay, based on the use of 4-hydroxazobenzene-2-carboxylic acid [7.14]. The method was aimed at determining the binding stoichiometry of r-BHD, compared with natural biotin (vitamin H), towards avidin at a 1:4 avidin:r-BHD molar ratio, which is the saturation ratio for avidin:biotin. HABA absorbs light at 350 nm and shifts to 500 nm on interaction with the biotin binding site in avidin ($K_d = 10^{-6}M$) [7.15]. In the experiments, the HABA avidin complex was obtained by adding avidin (10.4 mg in 40 mL of 0.05M sodium phosphate buffer, pH6.0) in 1 mL of filtered HABA (24.2 mg in 10 mL of 0.01N NaOH). The HABA assay was initially validated for biotin testing the 1:4 avidin:biotin molar ratio. Because of the higher affinity constant of the avidin biotin complex ($K_d = 10^{-15}M$), the addition of increasing biotin molar amounts displaced the dye HABA from the binding sites of avidin, causing a change in colour, which was measured by the decrease in optical density at 500 nm (OD500) up to a plateau (100% displacement). OD500 was assayed using a UV visible spectrophotometer (Ultrospec 3000, Pharmacia Biotech). In the HABA assay, the compound was tested by adding to the HABA avidin complex an increasing amount of r-BHD (1:1, 1:2, 1:4, 1:6, 1:8, 1:12 and 1:16 avidin:r-BHD molar ratios) to achieve 100% displacement of the dye HABA from the complex. Subsequently, r-BHD avidin affinity at a 1:4 molar ratio was determined at 37°C by comparing OD500 (1:4) with the saturation OD500 value. To evaluate changes in affinity after labelling, this colorimetric method was also applied on r-BHD labelled with a molar excess of non-radioactive metal ($^{89}YCl_3$), adopting the reaction conditions of the general radiolabelling procedure. Non-specific HABA displacement was tested in the absence of r-BHD using $^{89}YCl_3$ only.

7.2.5. Radiolabelling general procedure

The radiolabelling general procedure has been optimized using r-BHD dissolved in saline at a specific activity of 3.7 MBq/ μ g.

7.2.5.1. Manual procedure

Radiolabelling was performed with ^{90}Y , using r-BHD in saline (2 mg/mL) at a specific activity of 2.6 MBq/nmol. Sodium acetate (1.0M, pH5.0), with a volume equal to that of the radionuclide chloride solution, was used as a buffer. The r-BHD solution was added to the buffer and transferred to the radionuclide supplier vial. The mixture was then mixed and heated at 95°C for 30 min.

7.2.5.2. Automatic procedure

The labelling of r-BHD with ^{90}Y was studied and performed in an automatic module of synthesis (Modular Lab PharmTracer, Eckert & Ziegler) and a disposable sterile single use kit. Before starting the synthesis, it is important to verify the integrity of the cassette to avoid leakage of activity inside the hot cell. The synthesis consists of the following steps:

- (a) The laptop computer is turned on and all the connections and valves in the module are checked.
- (b) The sterile cassette is installed and the integrity is verified by running the specific program.
- (c) Following the checklist, different vials are connected to the appropriated valves.
- (d) First, the saline vial (~60 mL), then the ethanol 50% vial (20 mL) and finally the ascorbic acid (1.5 mL) and the solution of DOTA biotin in the reaction vial (reactor) are used to obtain a specific activity of 0.1 Ci/mg.
- (e) The activity contained in the ^{90}Y vial is measured in a precalibrated calibrator dose.
- (f) The ventilation needle is inserted in the ^{90}Y vial and then a second long needle is placed touching the bottom of the vial.
- (g) Yttrium-90 activity is transferred into the reactor containing r-BHD and then the ^{90}Y vial is washed with the ascorbic acid solution, which is also added into the reactor.
- (h) The automatic PharmTracer program is started to remotely achieve all the labelling steps.
- (i) The reactor is heated at 95°C for 30 min continuous monitoring of the temperature and activity.
- (j) The reaction mixture is then transferred onto a C18 cartridge for purification to eliminate the unbound ^{90}Y .
- (k) Yttrium-90 DOTA biotin is eluted with a solution of 50% ethanol in water.
- (l) The purified radiopharmaceutical is transferred to the dispensing vial passing through a sterilizing $0.22\ \mu\text{m}$ filter and diluted with saline.

The module is capable of performing, at the end of the synthesis, a test to check the filter integrity by applying gas pressure and comparing with a closed system, as recommended by the rules of good manufacturing practice to ensure the sterility of the final product.

The RCP was assessed using ITLC SG (Gelman Sciences). An aliquot of the radiolabelled solution was mixed with a molar excess of avidin and DTPA, then spotted in triplicate. Quantitation of ^{90}Y r-BHD ($R_f = 0$) and the free amount

of ^{90}Y complexed to DTPA ($R_f = 1$) was carried out using a high performance storage phosphor screen (Cyclone, Packard BioScience).

7.2.6. Microbiological tests

For every batch, an aliquot of the product was stored for decay. After complete decay (>3 months), the sample was tested for sterility and pyrogens. Sterility was assayed by plating the sample over Petri dishes with growth medium, and the samples were incubated in a thermostatic oven at 35°C for 14 d. After incubation, samples were analysed for any growth and, in case of positive results, the number of colony forming units was determined.

For pyrogens, a control limulus amoebocyte lysate (LAL) test based on the kinetic chromogenic method was used. The LAL test was performed using an Endosafe-PTS spectrophotometer (Charles River Laboratories International Inc.). Four samples of volume 25 μL were put in a disposable capillary cassette containing LAL reagent and an internal standard. The cassette was incubated in the PTS system and the time of colour formation measured. Time was internally correlated to the endotoxin amount and the final amount was displayed on the system. The reference value for parenterals was considered to be 17.5 EU/mL (EU = endotoxin units).

7.2.7. IART protocol

After tumour resection, the surgeon injected directly into the tumour bed, 100 mg of avidin diluted in 20–30 mL of saline. At a mean of 18 ± 3 h after avidin administration, 20 mg of biotinylated HSA (chase) was administered intravenously over 5 min to mop up any circulating avidin before administration of the radiolabelled biotin. Ten minutes later, 3.7 GBq of ^{90}Y r-BHD (specific activity of 4 GBq/mg) was delivered intravenously over 30 min using a dedicated disposable system.

7.3. RESULTS

7.3.1. Effect of pH on radiolabelling

The synthesis of r-BHD was performed according to the procedure described by Sabatino et al. [7.10]. The purity of the isolated compound was checked by reverse phase (RP) HPLC and carbon, hydrogen and nitrogen (CHN) elemental analysis. The experiments, aimed at evaluating the effect of pH on RCP values, were performed with a sodium acetate buffer up to pH5.6. The results in Fig. 7.2

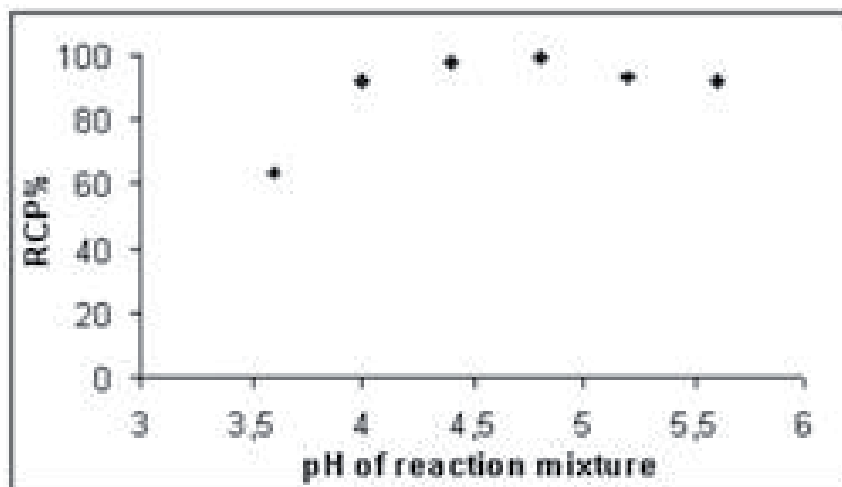


FIG. 7.2. RCP values of ^{90}Y r-BHD depending on the pH.

show that the highest RCP values (nearly 99%) were obtained in the pH range 4.4–4.8. At pH values outside of this range, RCP dropped. In particular, at a pH <4.0 or >5.2, RCP was <93%. Taking into account these results, the optimal pH (4.4–4.8) was adopted in the general procedure using a diluted buffer such as 1.0M sodium acetate (pH5.0).

7.3.2. Avidin binding studies

As expected, using the HABA assay, vitamin H showed 100% binding to avidin at the 1:4 avidin: vitamin H molar ratio. At the same molar ratio, r-BHD resulted in a binding efficiency to avidin of $85\% \pm 1\%$ (mean \pm SD, $n = 5$) (see Table 7.1). This last result was also obtained when r-BHD was labelled with non-radioactive $^{89}\text{YCl}_3$, confirming no changes in affinity after r-BHD labelling. Moreover, a blank experiment ($n = 5$) using only $^{89}\text{YCl}_3$ showed no influence on the displacement of HABA from the binding sites of avidin.

7.3.3. Radiolabelling: General procedure

RCP values of >99% were routinely achieved with both radiolabelling methods; nevertheless, the automatic module synthesis introduced a further purification step of the final product, thus guaranteeing radiopharmaceutical safety.

TABLE 7.1. AVIDIN BINDING STUDIES BY HABA ASSAY AT 1:4 AVIDIN:COMPOUND MOLAR RATIO

Compound	Binding towards avidin (%)
Vitamin H	100 ± 0.3
r-BHD	85 ± 1
Y-89 r-BHD	85 ± 1

7.3.4. Microbiological tests

Results of sterility tests showed a continuous level of bacterial absence in all samples. Pyrogen contamination was always kept well below 17.5 EU/mL (see Fig. 7.3). Moreover, after each automatic synthesis, a pressure hold test was performed by the module to confirm the sterilizing filter integrity.

7.3.5. IART protocol

The women administered with 100 mg of avidin and 3.7 GBq of ⁹⁰Y r-BHD received a mean absorbed dose to the breast of 19.5 ± 4.0 Gy in the area of highest uptake with a corresponding best estimated dose of 21.2 ± 4.3 Gy. The uptake of injected radioactivity by the operated breast reached a maximum of ~12% of the total injected dose with a mean value of ~8%.

7.4. DISCUSSION

The feasibility of targeting radiolabelled biotin derivatives to avidin conjugated MAbs previously localized on tumours was first demonstrated nearly 20 years ago. Preclinical and clinical studies have shown that tumour targeting via a multistep avidin biotin system presents advantages compared with directly radiolabelled MAbs. The three step pretargeting approach has been successfully applied in patients, with encouraging results in the therapy of malignant tumours such as glioma [7.6, 7.7] and oropharyngeal carcinoma [7.15], where high doses of radiolabelled biotin could be systemically administered without appreciable bone marrow toxicity.


```

***** ENDOSAFE Test Record *****
          V7.12A 7/30/2008
DateTime: ..... 21-12-09 @ 11:24:17
Device: ..... 2578
OperatorID: ..... VS
Cartridge: ..... Endotoxin
Temperature: Start: 37.0C End: 37.0C
Method: ..... KX-122
Cartridge Lot#: ..... 9177136
Cartridge Cal Code: ..... 514134184671
Range: ..... 5-0.05
Range Time: ..... Sec: 141-741
Onset Times: ..... >741 298 >741 268
Slope: -0.360 Intercept: +2.401
Dilution: .....100
Sample Lot: ..... 090326
          Sample ID: ..... 90Y-Biotin
Sample Rxn Time CV: ..... 0.0% Pass
Spike Value: ..... 0.673 EU/mL
Spike Rxn Time CV: ..... 7.5% Pass
Spike Recovery: ..... 102% Pass
Test Suitability: ..... Pass
Sample Value: ..... <0.100 EU/mL

```

FIG. 7.3. Pyrogen test shows results below 17.5 EU/mL.

A wide variety of radiometal chelated biotin derivatives have been developed for application to pretargeting aimed at the radiotherapy of cancer. Wilbur et al. reported novel studies focused on improving the in vivo behaviours of radiohalogenated biotin derivatives for delivering ^{211}At in cancer pretargeting protocols [7.16]. Because biotin derivatives are subject to in vivo degradation by biotinidase, for optimal in vivo tumour targeting, it is essential to design conjugates that are resistant to the enzymatic action while retaining a high binding affinity towards avidin. First generation radiolabelled biotin conjugates had an amide bond between the carboxylic group of biotin and the amino group of the spacer carrying the chelating moiety, thus they were easily hydrolysable by biotinidase. Avoiding enzyme degradation was then attempted by introducing steric hindrance at the level of the amide bond (second generation). In this respect, Wilbur et al. found that a carboxylate or hydroxymethylene group adjacent to the biotinamide bond blocked the serum biotinamide hydrolysis, while the slow dissociation rate of the biotin derivative from avidin was retained [7.17]. Foulon et al. impaired

recognition by biotinidase with a new class (third generation) of radioiodinated biotin conjugate, in which the amide bond between the valeryl chain of biotin and the prosthetic group was reversed (i.e. the NH–CO bond) [7.18]. A novel stable biotin derivative conjugated to DOTA, which was devoid of the amide target site for the biotinidase, has been reported by Sabatino et al. [7.10]. The novelty of this conjugate was that the amide carboxylic group was reduced to a methylene one, thus generating the N-aminohexyl biotinamido derivative (r-BHD) in which the amide is transformed into a secondary amine without affecting the length of the biotin side arm involved in avidin. The DOTA ligand, in this compound, was directly linked to the amino group of the reduced biotin hexamethylenediamine derivative through one of the four N-acetic side arms. Moreover, the synthetic flexibility of r-BHD allows the synthesis of a variety of new biotin derivatives, for example, with two DOTA chelators conjugated to the side chain of biotin, with the purpose of increasing the efficacy of targeted radionuclide therapy by delivering a higher radiation dose to the tumour. The goal of the studies conducted within the framework of the CRP was to optimize the radiometal chelation, RCP and stability of the label linked to this new biotin conjugate to support its use in pretargeting therapy trials.

To establish the optimal specific activity, the parameters influencing reaction kinetics and RCP were investigated. As the pH of the reaction mixture has a dramatic impact on the rate of radiometal chelation and the solubility of Y^{3+} decreases with increasing pH owing to formation of hydroxides, the first purpose of the study was to determine the influence of pH on RCP. For this reason, test labellings were performed using a 2.0M sodium acetate buffer to maintain the pH of the radiomixture at known values in the range 3.6–5.6. The best RCP (>99%) was obtained at ~pH4.5. This result matches with data reported by Breeman et al. in the radiolabelling of DOTA peptides [7.19]. Subsequently, general radiolabelling procedures were carried out at this optimal pH using a 1.0M sodium acetate pH5.0 buffer to avoid any possible influence of the buffer in the radiometal complexation. Moreover, to complete the radioisotope chelation without generating radiolytic or thermal decomposition, incubation was performed for 30 min at 95°C. Although the resistance to biotinidase action is an essential parameter towards the clinical application of a new biotin conjugate, it is imperative that these modifications do not affect the binding to avidin. The binding affinities of ^{90}Y r-BHD towards avidin were obtained using a HABA assay. HABA is commonly used to determine the degree of biotinylation of different molecules through its displacement by biotin. In the present study, the avidin r-BHD binding was evaluated after validation of the method with vitamin H and testing the aspecific HABA displacement. As expected, the binding of vitamin H at 1:4 avidin:vitamin H molar ratio was 100%. The binding studies of the new compound showed that 85% of r-BHD was bound

to avidin at the 1:4 avidin:r-BHD molar ratio. A blank HABA assay using only $^{89}\text{YCl}_3$ showed no influence in the displacement of HABA from the binding sites of avidin. The new ^{90}Y r-BHD compound was tested in a pilot study according to the pretargeting IART protocol. The trial showed a lack of haematological, major kidney and local toxicity of the treatment, and provided partial irradiation therapy immediately after surgery, thus allowing reduction of the duration of a standard course of whole breast external beam radiation therapy.

Although these encouraging data may justify randomized trials in a large patient population, the microbiological safety of the locally labelled ^{90}Y r-BHD may hamper its wider use. Therefore, the labelling conditions in an automatic module of synthesis (PharmTracer) fitted with a disposable sterile single use kit were tested [7.20]. The remotely controlled steps of purification through a C18 cartridge to eliminate the unbound ^{90}Y and the final filtration through a sterilizing 0.22 μm filter allowed a safe injectable product to be obtained. In addition, the module is capable of performing, at the end of the synthesis, a test to check the filter integrity by applying gas pressure and comparing with a closed system, as recommended by good manufacturing practice rules to ensure the sterility of the final product. A secondary objective related to the use of the automated module was to evaluate whether its use decreased the finger radiation dose of the operator [7.21]. Preliminary measurements showed that finger radiation exposure decreased twofold using this automatic remote system compared to the previously used manual procedure, namely from 12 $\mu\text{Sv/GBq}$ to 5.4 $\mu\text{Sv/GBq}$ (see Fig. 7.4).

7.5. CONCLUSION

In the time frame of this CRP, a new biotin DOTA derivative was developed, and labelling conditions with the therapeutic radionuclide ^{90}Y were optimized. Implementation of an automatic module for the synthesis of the radiopharmaceutical ^{90}Y DOTA biotin with a high RCP and sterility may represent a step forward in the spread of the IART approach in clinical trials.

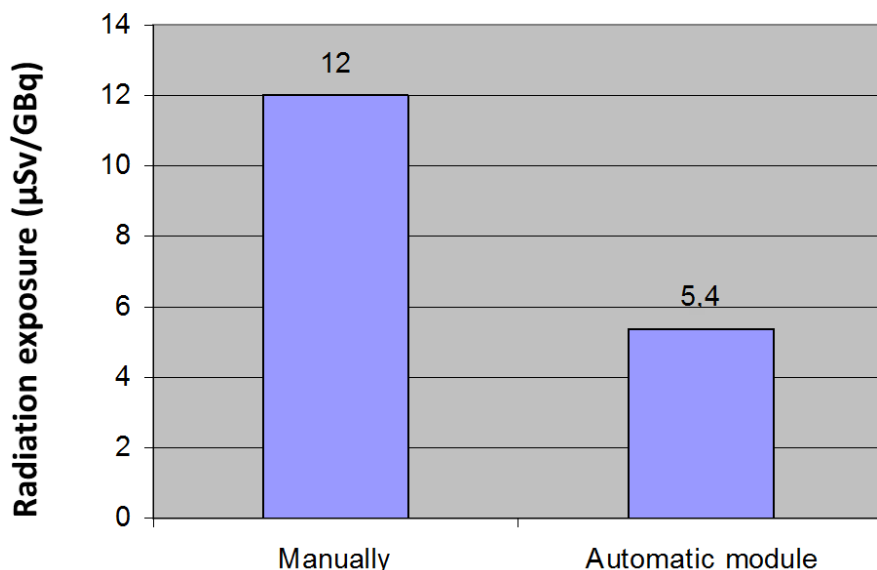


FIG. 7.4. Finger radiation exposure comparison between the automatic remote system and the previously used manual procedure.

REFERENCES TO CHAPTER 7

- [7.1] GOODWIN, D.A., Pharmacokinetics and antibodies, *J. Nucl. Med.* **28** (1987) 1358.
- [7.2] VAUGHAN, A.T.M., ANDERSON, P., DYKES, P.W., CHAPMAN, C.E., BRADWELL, A.R., Limitations to the killing of tumors using radiolabeled antibodies, *Br. J. Radiol.* **60** (1987) 567.
- [7.3] FORERO, A., et al., Phase 1 trial of a novel anti-CD20 fusion protein in pretargeted radioimmunotherapy for B-cell non-Hodgkin lymphoma, *Blood* **104** (2004) 227.
- [7.4] GOODWIN, D.A., MEARES, C.F., Advances in pretargeting biotechnology, *Biotechnol. Adv.* **19** (2001) 435.
- [7.5] PAPI, S., et al., "Pretargeted radioimmunotherapy in cancer: An overview", *Methods of Cancer Diagnosis, Therapy and Prognosis*, Springer (HAYAT, M.A., Ed.), Vol. 7, Ch. 7, New York (2010) 81–98.
- [7.6] PAGANELLI, G., et al., Antibody-guided three-step therapy for high grade glioma with yttrium-90 biotin, *Eur. J. Nucl. Med.* **26** (1999) 348.
- [7.7] GRANA, C., et al., Pretargeted adjuvant radioimmuno therapy with yttrium-90-biotin in malignant glioma patients: A pilot study, *Br. J. Cancer* **86** (2002) 207.
- [7.8] SAVAGE, M.D., et al., *Avidin-Biotin Chemistry: A Handbook*, Pierce Chemical Company, Rockford (1992).

- [7.9] SU, F.M., GUSTAVSON, L.M., AXWORTHY, D.B., et al., Characterization of a new Y-90 labeled DOTA-biotin for pretargeting, *J. Nucl. Med.* **36** Suppl. 5 (1995) 154P.
- [7.10] SABATINO, G., et al., A new biotin derivative-DOTA conjugate as a candidate for pretargeted diagnosis and therapy of tumors, *J. Med. Chem.* **46** (2003) 3170.
- [7.11] URBANO, N., et al., Evaluation of a new biotin-DOTA conjugate for pretargeted antibody-guided radioimmunotherapy (PAGRIT), *Eur. J. Nucl. Med. Mol. Imaging* **34** (2007) 68.
- [7.12] PAGANELLI, G., et al., IART: Intraoperative avidination for radionuclide treatment. A new way of partial breast irradiation, *Breast* **16** (2007) 17.
- [7.13] PAGANELLI, G., et al., Intraoperative avidination for radionuclide treatment as a radiotherapy boost in breast cancer: Results of a phase II study with (90)Y-labeled biotin, *Eur. J. Nucl. Med. Mol. Imaging* **37**(2) (2010) 203.
- [7.14] LIYNAH, O., BAYER, E.A., WILCHEK, M., SUSSMAN, J.L., The structure of the complex between avidin and the dye, 2-(4'-hydroxyazo-benzene) benzoic acid (HABA), *FEBS Lett.* **328** (1993) 165.
- [7.15] PAGANELLI, G., et al., Combined treatment of advanced oropharyngeal cancer with external radiotherapy and three-step radioimmunotherapy, *Eur. J. Nucl. Med.* **25** (1998) 1336.
- [7.16] WILBUR, D.S., HAMLIN, D.K., CHYAN, et al., Biotin reagents in antibody pretargeting. 6. Synthesis and in vivo evaluation of astatinated and radioiodinated aryl- and nido-carboranyl-biotin derivatives, *Bioconjug. Chem.* **15** (2004) 601.
- [7.17] WILBUR, D.S., HAMLIN, D.K., CHYAN, M.K., KEGLEY, B.B., PATHARE, P.M., Biotin reagents for antibody pretargeting. 5. Additional studies of biotin conjugate design to provide biotinidase stability, *Bioconjug. Chem.* **12** (2001) 616.
- [7.18] FOULON, C.F., ALSTON, K.L., ZALUTSKY, M.R., Synthesis and preliminary biological evaluation of (3-Iodobenzoyl) norbiotamide and ((5-Iodo-3-pyridinyl) carbonyl) norbiotamide: Two radioiodinated biotin conjugates with improved stability, *Bioconjug. Chem.* **8** (1997)179.
- [7.19] BREEMAN, W., DE JONG, M., VISSER, T.J., ERION, J.L., KRENNING, E.P., Optimizing conditions for radiolabeling of DOTA-peptides with ⁹⁰Y, ¹¹¹In and ¹⁷⁷Lu at high specific activities, *Eur. J. Nucl. Med.* **30** (2003) 917.
- [7.20] PETRIK, M., et al., Radiolabelling of peptides for PET, SPECT and therapeutic applications using a fully automated disposable cassette system, *Nucl. Med. Commun.* **32** (2011) 887.
- [7.21] CREMONESI, M., et al., Dosimetry in radionuclide therapies with ⁹⁰Y-conjugates: The IEO experience, *Q. J. Nucl. Med.* **44** (2000) 325.

CHAPTER 8

LABELLING OF BIOTIN WITH ^{188}Re

M. PASQUALI
Laboratory of Nuclear Medicine,
Department of Radiological Sciences,
University of Ferrara,
Ferrara, Italy

E. JANEVIK
Faculty of Medical Sciences,
University 'Goce Delcev',
Stip, Republic of Macedonia

L. UCCELLI
Laboratory of Nuclear Medicine,
Department of Radiological Sciences,
University of Ferrara,
Ferrara, Italy

A. BOSCHI
Laboratory of Nuclear Medicine,
Department of Radiological Sciences,
University of Ferrara,
Ferrara, Italy

A. DUATTI
Laboratory of Nuclear Medicine,
Department of Radiological Sciences,
University of Ferrara,
Ferrara, Italy

Abstract

Different chemical strategies have been employed for labelling biotin using ^{188}Re with the aim to develop a sterile and pyrogen free kit formulation that is suitable for clinical use. A number of biotin conjugated ^{188}Re complexes were prepared and evaluated to determine their affinity for avidin. The most difficult challenge was to devise an efficient reaction pathway that was able to obtain the final radiocompounds in a high radiochemical yield. This work describes the molecular design and the chemical strategy that were followed to obtain reliable preparation of the new radiopharmaceuticals starting from generator produced [$^{188}\text{ReO}_4$] $^-$.

8.1. INTRODUCTION

In past years, the pretargeting approach based on avidin biotin interaction has been extensively used to overcome problems associated with the use of radiolabelled antibodies for diagnostic and therapeutic purposes [8.1, 8.2]. The common approach exploits the extremely high affinity of biotin for avidin [8.3–8.5], which is one of the strongest receptors for biological interactions, and the relative simplicity of labelling biotin with a variety of radionuclides without affecting its biological characteristics. Although there are a few different versions of avidin biotin technology applied to antibodies, essentially the procedure always involves the first administration of an avidin antibody conjugate, and, subsequently, the administration of radiolabelled biotin for *in vivo* recognition of the antibody after its localization on the target tissue.

Recently, a new application of the avidin biotin system has been proposed as an adjuvant of the surgical treatment of breast cancer [8.6–8.8]. This method, dubbed IART, was designed to eliminate every residue of cancerous tissue after surgical removal of the primary lesion. Except for avidin and biotin, it does not require the use of any specific antibodies or other biomolecules. Briefly, it consists of first covering the surgical bed with avidin by means of *in situ* injections of small portions of an avidin solution and then delayed intravenous administration of radiolabelled biotin. The same authors have already demonstrated the selective uptake of radiolabelled biotin at the surgical site using a new DOTA biotin derivative labelled with both ^{111}In and ^{90}Y [8.7, 8.8]. The nuclear properties of ^{90}Y (β decay with $E_{\beta_{\text{max}}} = 2.2$ MeV, half-life = 64.1 h) make it particularly suitable for IART to achieve a long range penetration of the β particle and a significant crossfire effect for complete ablation of the remaining malignant tissue.

A major drawback of ^{90}Y is the absence of any photon emission that could be conveniently exploited for imaging the biodistribution of the radiolabelled biotin. Rhenium-188 is an attractive alternative to ^{90}Y because it decays through β emission with almost the same energy ($E_{\beta_{\text{max}}} = 2.1$ MeV, half-life = 17 h), but with an associated 155 keV γ emission that is well suited for imaging purposes. The scope of the present work was to develop a novel ^{188}Re labelled biotin conjugate with properties suitable for its use as an alternative to ^{90}Y DOTA biotin for the IART approach. Obviously, this is not the first study attempting to prepare ^{188}Re biotin derivatives, and various publications on this subject have appeared previously in the scientific literature [8.9–8.12]. However, none of these works reported convincing evidence that the chemical procedures employed were able to afford a stable ^{188}Re biotin conjugate in high radiochemical yield (>98%). This result is of utmost importance to avoid unnecessary and dangerous radiation burden to the patient caused by radioactivity not associated with the required chemical form. Most importantly, because ^{188}Re is supplied through the

$^{188}\text{W}/^{188}\text{Re}$ transportable generator system analogous to the $^{99}\text{Mo}/^{99\text{m}}\text{Tc}$ generator, availability of a freeze-dried kit formulation adequate for hospital use would be highly convenient, particularly for the routine application of the IART approach. However, no example of this type has been reported so far for the preparation of ^{188}Re biotin derivatives. In the following sections, all steps involved in the development of a useful ^{188}Re biotinylated derivative will be described, including the molecular design, the chemistry employed for the high yield preparation and the development of a freeze-dried kit formulation.

8.2. DESIGN OF ^{188}Re BIOTIN COMPLEXES

A fundamental prerequisite for developing a therapeutic agent with some potential clinical utility is to afford a final metallic conjugate showing high chemical inertness and stability under physiological conditions. The design of a robust ^{188}Re conjugate can be achieved through a careful selection of the most stable rhenium cores. A rhenium atom tightly bound to some characteristic ligand forms these functional groups that usually are strongly resistant to hydrolysis by water molecules. The rhenium(V) nitride, $[\text{Re}\equiv\text{N}]^{2+}$ and the rhenium(I) tricarbonyl, $[\text{Re}(\text{CO})]^{3+}$ cores are among the most stable chemical fragments.

In this study, the $[\text{Re}\equiv\text{N}]^{2+}$ core has been selected as a basic functional motif for the preparation of biotinylated ^{188}Re derivatives [8.13, 8.14]. Obviously, the intrinsic stability of this core has to be complemented by the concomitant coordination of a suitable set of ancillary ligands completing the coordination sphere. The essential features of the selected molecular arrangement for these complexes are schematically illustrated in Fig. 8.1(a).

This class of compounds is composed of an apical $^{188}\text{Re}\equiv\text{N}$ group surrounded by a tridentate dianionic ligand (XYW) and a monodentate tertiary phosphine ligand (PR_3) spanning the four coordination positions on the basal plane of a distorted square pyramidal geometry (thus, the acronym of 3 + 1 complexes). Ligands possessing the 2,2'-diamrcapto diethylamine (SNS) $\{[\text{S}(\text{CH}_2)_3\text{NH}(\text{CH}_2)_3\text{S}]^{-2}\}$ set of coordinating atoms provide a convenient source of XYZ type ligands. In Fig. 8.1(b), the crystal structure of a Re(V) nitride complex incorporating the simple SNS ligand and triphenylphosphine is reported. The SNS type tridentate chelating system utilized here was obtained by tethering two cysteine residues (cys-cys), as shown in Fig. 8.2(a), whereas the monodentate phosphines were (triscyanoethyl)phosphine (PCN) and 1,3,5-triaza-7-phosphaadamantane (PTA) (see Fig. 8.2(b)).

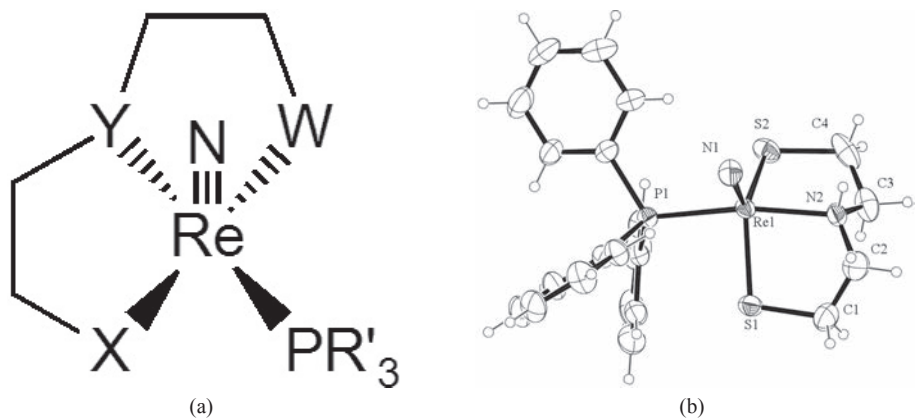


FIG. 8.1. (a) Schematic illustration of the structure of 3 + 1 rhenium(V) nitride complexes and (b) crystal structure of the complex $[Re(N)(SNS)(PPh_3)]$ (PPh_3 = triphenylphosphine; SNS = 2,2'-diethylmercapto diethylamine).

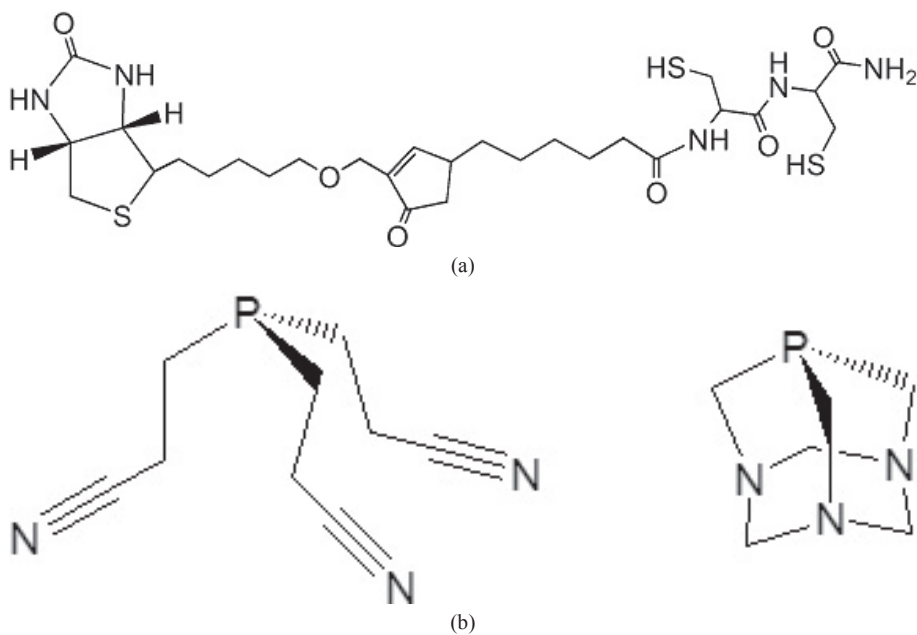


FIG. 8.2. (a) The cys-cys chelating system for the Re(V) nitride core and (b) the monophosphines PCN and PTA utilized in this study.

The tridentate cys–cys ligand was also employed as a scaffold for assembling the final bifunctional ligand incorporating the biotin bioactive group. The various reaction pathways employed for this synthesis are pictured in Fig. 8.3.

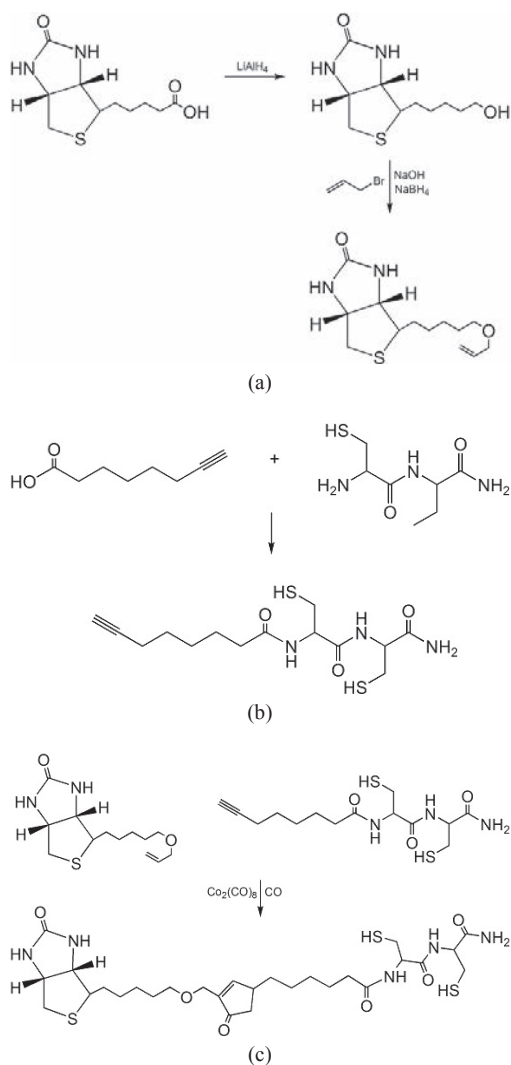


FIG. 8.3. Reaction diagram for the synthesis of the bifunctional ligand cys–cys biotin: (a) synthesis of allyl biotin, (b) synthesis of cys–cys alkyne and (c) Pauson–Khand cycloaddition to form the final cys–cys biotin.

Preliminary synthesis of the biotin allyl (see Fig. 8.3(a)) and cys–cys alkyne (see Fig. 8.3(b)) derivatives was needed to allow the final cys–cys biotinylated bifunctional ligand to be assembled through a Pauson–Khand cycloaddition reaction (see Fig. 8.3(c)) [8.15]. Although the final yield of preparation was <6%, the formation of the heterocyclic moiety imparted a strong stability to the resulting ligand cys–cys biotin towards degradation by the enzyme biotidinas that is ubiquitously present in body fluids and tissues [8.16].

8.3. DEVELOPMENT OF A KIT FORMULATION FOR BIOTINYLATED ^{188}Re COMPLEXES

The reactions required for the high yield preparation of $^{99\text{m}}\text{Tc}$ radiopharmaceuticals comprising a $[\text{}^{99\text{m}}\text{Tc}\equiv\text{N}]^{2+}$ group were discovered more than a decade ago [8.13]. As a result, a freeze-dried kit formulation was easily developed according to the general reaction scheme [8.13] given in Eq. (8.1):



where N^{3-} stands for a suitable reagent capable of donating nitrogen atoms to form the Tc(V) nitride core. Usually, succinic dihydrazide (SDH = $[\text{H}_2\text{NNHC}(=\text{O})\text{CH}_2]_2$) is employed as a convenient source of N^{3-} groups.

Although it is sometimes claimed that the chemical similarities between technetium and rhenium may allow for the transfer of the methods employed for $^{99\text{m}}\text{Tc}$ radiopharmaceuticals to the preparation of the corresponding ^{188}Re radiopharmaceuticals, this statement does not surely hold for the reaction given in Eq. (8.1). In fact, when $[\text{}^{99\text{m}}\text{TcO}_4]^-$ is replaced by $[\text{}^{188}\text{ReO}_4]^-$ in Eq. (8.1), no reaction occurs to a significant extent, under the same experimental conditions. The addition of some adjuvant reagent was found to be necessary for igniting the initial reduction of $[\text{}^{188}\text{ReO}_4]^-$, which is always required to allow formation of the final product. It was discovered that the sodium salt of the simplest dicarboxylic acid was one example of this kind of reagent. Accordingly, the simple inclusion of sodium oxalate in Eq. (8.1) dramatically changed the course of the reaction, and a high yield formation of the $[\text{}^{188}\text{Re}\equiv\text{N}]^{2+}$ core was finally observed. The chemical mechanism behind this phenomenon has previously been described [8.13, 8.17].

Another key ingredient to be specified in Eq. (8.1) was the chemical form of the nitride nitrogen donor. Again, it was found that SDH, which was successfully employed with ^{99m}Tc , did not give satisfactory results with ^{188}Re , with the final radiochemical yield always being $<80\%$. Conversely, another N^{3-} donor, S-methyl, N-methyl dithiocarbamate [DTC = $\text{H}_2\text{NN}(\text{CH}_3)\text{-C}(=\text{S})\text{SCH}_3$] proved to be much stronger as a source of nitride groups and, hence, the $[\text{}^{188}\text{Re}\equiv\text{N}]^{2+}$ core was obtained in a very high yield ($>95\%$) using this reagent. However, an important drawback of this compound is that it also exhibits good coordinating properties towards this metallic core, and it is able to form stable bis-substituted Re(V) nitride complexes. Although this behaviour nicely accounts for the observed powerful capacity of DTC to stabilize the $^{188}\text{Re}\equiv\text{N}$ bond, for the purpose of obtaining the final biotinylated complex, this was surely a disadvantage owing to the difficulty of replacing coordinated DTC with the *cys-cys* biotin ligand. To overcome this problem, a possible strategy focused on the attempt at weakening the bonding affinity of DTC for the $^{188}\text{Re}\equiv\text{N}$ group, by appending a sterically encumbering group to either its amino [8.18] or thiol sulphur terminal atoms [8.19]. The resulting DTC derivatives are shown in Fig. 8.4.

The compound shown in Fig. 8.4(a) (polyethyleneglycol (PEG) DTC) was prepared by tethering a polyethylene glycol chain to the terminal amino group of DTC, whereas the compound illustrated in Fig. 8.4(b) (DMG DTC = dimaleimido thioglucose) was obtained by reaction of DTC with 2,3-dibromomaleimide and 1- β -thioglucose. Using the new reagents PEG DTC and DMG DTC, two freeze-dried kit formulations for preparing the $[\text{}^{188}\text{Re}\equiv\text{N}]^{2+}$ core were developed with the following compositions: (i) SnCl_2 (0.1 mg), PEG DTC (10 mg), sodium oxalate (25 mg) and glacial acetic acid (0.15 mL) and (ii) SnCl_2 (0.1 mg), DMG DTC (5 mg), sodium oxalate (25 mg) and glacial acetic acid (0.15 mL). To complete the kit formulation for preparing the ^{188}Re biotin conjugate, the ligands *cys-cys* biotin and the appropriate monophosphine (PTA or PCN) were lyophilized in a second vial. This mixture was reconstituted with saline and added to the vial containing the $[\text{}^{188}\text{Re}\equiv\text{N}]^{2+}$ intermediate to afford the final complex $[\text{}^{188}\text{Re}(\text{N})(\text{cys-cys biotin})(\text{PR}_3)]$ ($\text{PR}_3 = \text{PTA, PCN}$).

The structure of this conjugate complex is reported in Fig. 8.5. As expected, the complex comprises a tridentate *cys-cys* biotin bound to the $[\text{}^{188}\text{Re}\equiv\text{N}]^{2+}$ core through the two sulphur atoms and the amino group of the *cys-cys* motif, and a monodentate phosphine ligand occupying the residual position on the basal plane of a square pyramidal geometry.

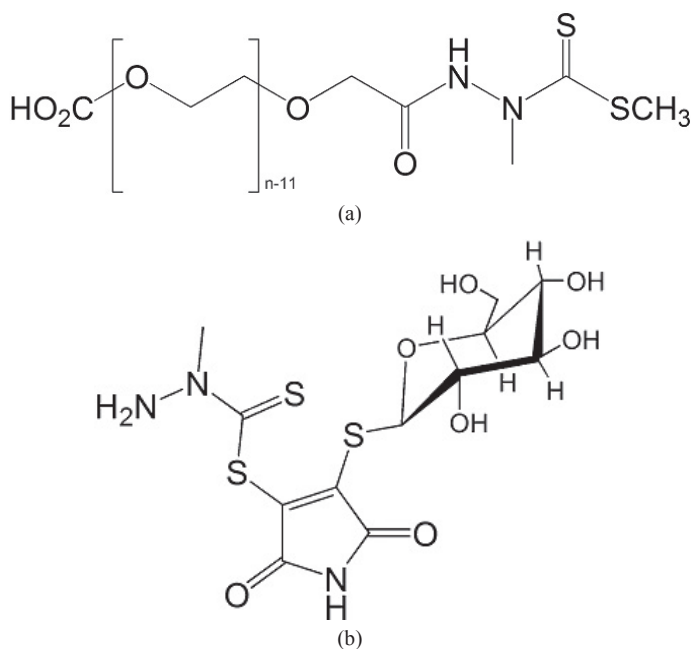


FIG. 8.4. (a) PEGylated and (b) thiol protected derivatives of DTC.

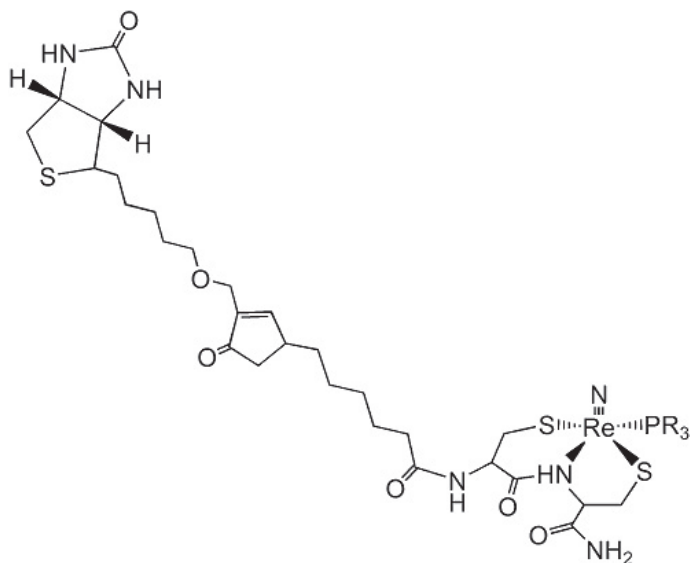


FIG. 8.5. Structure of the conjugated complex $[^{188}\text{Re}(\text{N})(\text{cys-cys biotin})(\text{PR}_3)]$.

8.4. BIOLOGICAL EVALUATION

In vitro binding studies were carried out to evaluate the affinity of both the free ligand, *cys-cys* biotin, and the biotinylated ^{188}Re complexes for avidin. Analysis of the fraction of activity bound to avidin was obtained using TLC and HPLC. It was found that when the avidin:biotin ratio was 1:4, the affinity of both radioactive complexes was ~99.8%.

Biodistribution studies have been carried out in rats, and the results are shown in Tables 8.1 and 8.2 for PTA and PCN derivatives, respectively. The complexes are both hydrophilic, with the main elimination route being through the kidneys. The PTA containing complex appears to have a higher hydrophilic character than the analogous PCN derivative, presumably because of the more pronounced water solubility of the monophosphine PTA.

A rat model was developed to mimic the in vivo condition after surgical removal of the tumour lesion followed by in situ pretreatment with avidin. Injection of the biotinylated ^{188}Re complex was performed 12 h after surgery. The distribution of activity was monitored using a small animal scanner and by collecting the γ emission from the ^{188}Re nuclide. Planar images collected at 1 h p.i. (see Fig. 8.6) clearly show high accumulation of activity at the surgical site determined by the interaction of the biotinylated ^{188}Re complex with locally deposited avidin.

TABLE 8.1. BIODISTRIBUTION IN RATS OF [$^{188}\text{Re}(\text{N})$ (CYS-CYS BIOTIN) (PTA)] COMPLEX

Organ	Biodistribution for three rats (%ID/g) (mean \pm SD)				
	2 min	10 min	30 min	60 min	120 min
Blood	0.16 \pm 0.10	0.06 \pm 0.00	0.03 \pm 0.00	0.02 \pm 0.01	0.01 \pm 0.00
Heart	0.57 \pm 0.02	0.58 \pm 0.09	0.37 \pm 0.05	0.20 \pm 0.10	0.23 \pm 0.19
Lungs	0.53 \pm 0.10	0.12 \pm 0.05	0.08 \pm 0.00	0.05 \pm 0.04	0.02 \pm 0.00
Liver	1.46 \pm 0.16	1.23 \pm 0.50	0.60 \pm 0.10	0.43 \pm 0.03	0.24 \pm 0.04
Kidneys	10.57 \pm 0.89	17.51 \pm 3.08	2.64 \pm 0.04	1.30 \pm 0.06	0.03 \pm 0.02
Intestine	1.25 \pm 0.30	1.34 \pm 0.89	1.43 \pm 0.23	0.94 \pm 0.09	0.08 \pm 0.04
Muscle	0.21 \pm 0.00	0.18 \pm 0.01	0.08 \pm 0.04	0.07 \pm 0.01	0.03 \pm 0.01

TABLE 8.2. BIODISTRIBUTION IN RATS OF [$^{188}\text{Re}(\text{N})$ (CYS-CYS BIOTIN) (PCN)] COMPLEX

Organ	Biodistribution for three rats (%ID/g) (mean \pm SD)				
	2 min	10 min	30 min	60 min	120 min
Blood	0.20 \pm 0.10	0.15 \pm 0.00	0.10 \pm 0.01	0.07 \pm 0.00	0.05 \pm 0.00
Heart	0.61 \pm 0.16	0.57 \pm 0.09	0.05 \pm 0.01	0.05 \pm 0.02	0.01 \pm 0.00
Lungs	0.09 \pm 0.07	0.04 \pm 0.02	0.07 \pm 0.01	0.03 \pm 0.01	0.01 \pm 0.00
Liver	2.88 \pm 0.06	1.75 \pm 0.14	0.77 \pm 0.08	0.52 \pm 0.02	0.17 \pm 0.04
Kidneys	9.38 \pm 0.52	11.56 \pm 1.93	2.35 \pm 1.00	1.13 \pm 0.12	0.14 \pm 0.03
Intestine	1.19 \pm 0.60	4.96 \pm 1.64	3.20 \pm 1.28	1.45 \pm 0.87	0.72 \pm 0.11
Muscle	0.16 \pm 0.09	0.09 \pm 0.01	0.07 \pm 0.05	0.04 \pm 0.03	0.07 \pm 0.02

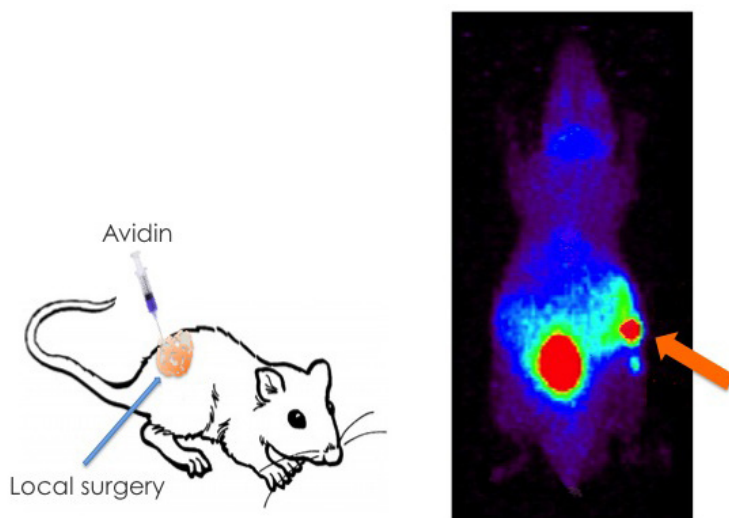


FIG. 8.6. Planar images of the distribution of the ^{188}Re biotinylated complex (with PTA as the ancillary ligand) in a female rat surgically treated with avidin.

8.5. EXPERIMENTS

8.5.1. Labelling

The preparation of the ^{188}Re biotin conjugates was carried out using a two vial (A and B) freeze-dried kit formulation. Vial A contained 100.0 μg of SnCl_2 , 25.0 mg of sodium oxalate and 10.0 mg of DTC PEG (or 5.0 mg of DMG DTC). Vial B contained 500.0 μg of cys–cys biotin and 2.0 mg of the appropriate monophosphine (PCN or PTA). Vial A was first reconstituted with 0.1 mL of glacial acetic acid and 1.0 mL of generator eluted $[\text{}^{188}\text{ReO}_4]^-$ (activity ranging from 500 MBq to 3 GBq), and gently heated at 50°C for 5 min to dissolve the reagents. Vial B was reconstituted with 1.0 mL of physiological solution, and the resulting solution was then transferred with a syringe to vial A (caution: the volume of the reaction solution must be ≤ 3.0 mL). The reaction vial was heated at 100°C for 15 min.

8.5.2. Chromatography

The RCP was assessed using HPLC performed with a column, Zorbax 300SB-C18, 300Anst., 5 μm (4.6 mm \times 250 mm) with a guard column, and a mobile phase composed of a mixture of A = 0.1% trifluoroacetic acid (TFA) in water and B = 0.1% TFA in CH_3CN . The following gradient was applied at a flow rate of 1 mL/min: 0–25 min, B = 0–100%; 25–30 min, B = 100%; 30–35 min, B = 100–0%. A representative HPLC chromatogram for the (3 + 1) ^{188}Re complex is shown in Fig. 8.7 ($R_f(\text{PCN}) = 8.9$ min; $R_f = 7.4$ min).

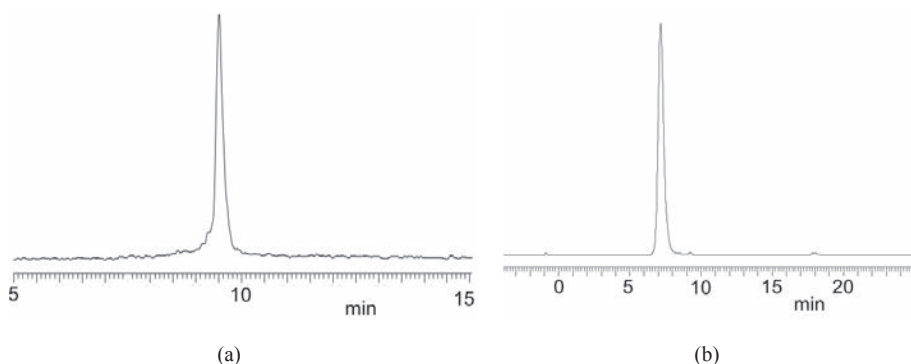


FIG. 8.7. HPLC of the 3 + 1 biotinylated rhenium nitride complexes with (a) PCN or (b) PTA as ancillary ligands.

A specific binding to avidin was evaluated as follows. A biotin solution (10 μL , 10mM) in phosphate buffer (0.1M, pH7.4) was added to a propylene test tube containing phosphate buffer (70 μL , 0.1M, pH7.4) and an aliquot of a water solution of avidin (0.0, 1.0, 10.0 and 50.0 $\mu\text{g}/10.0 \mu\text{L}$). The mixture was vortexed and then incubated at 37°C for 1 h. A constant activity (10–15 $\mu\text{Ci}/10 \mu\text{L}$) of the appropriate ^{188}Re compound was mixed, and the resulting solution was incubated at 37°C for 24 h. At 1 and 24 h, aliquots (3 μL) of the reaction mixture were withdrawn and analysed using ITLC SG. The plates were eluted with a mixture of saline and isopropyl alcohol (1:1). The radiolabelled biotin avidin complex remained at the origin, whereas the free biotinylated compounds migrated to the solvent front.

An alternative method employed was HPLC for evaluating the fraction of the activity bound to avidin using the following experimental conditions. Column: Zorbax 300SB-C18; mobile phase: A = B, phosphate buffer, 0.4M, pH7.4; flow rate: 1.0 mL/min; isocratic. The R_f of both free ^{188}Re complexes was 18.5 min and the R_f of the avidin bound ^{188}Re complexes (measured at the avidin:biotin ratio of 1:4) was 12.0 min.

8.5.3. Biological studies

Animal experiments were performed according to the animal welfare regulations of the Italian authorities. The protocols for these studies were approved by the Animal Care and Use Committee of the University of Ferrara (Italy). Female, Sprague Dawley rats, weighing 200–250 g, were not fed for 12 h before experiments and were then anaesthetized with intramuscular injection of a mixture of ketamine (80 mg/kg) and xilazine (19 mg/kg). The appropriate ^{188}Re complex (100 μL , 500–580 kBq) was administered through the jugular vein. The animals ($n = 3$) were sacrificed by cervical dislocation at 2, 10, 30, 60 and 120 min p.i. Blood was withdrawn from the heart through a syringe immediately after sacrifice and counted for radioactivity. Organs were excised, rinsed with saline, weighed and the radioactivity was determined using a NaI well counter. The percentages of injected dose per gram for each organ and blood were calculated.

To mimic the situation occurring in vivo after surgical removal of the primary tumour lesion, the following animal model was developed. The upper muscle of the right thigh in the left paw of an anaesthetized female Sprague Dawley rat was surgically exposed and a small portion of this tissue surgically removed. Avidin solution was then administered and distributed around the surgical bed with an insulin syringe. The wound was stitched surgically and the animal left to recover from anaesthesia overnight. After 12 h, the animal was again anaesthetized and injected with the appropriate ^{188}Re complex (100 μL ,

700 kBq) through the jugular vein. Planar images were collected 1 h after administration with a YAP(S) PET small animal scanner.

ACKNOWLEDGEMENTS

The authors of this chapter are grateful to M. Chinol, S. Papi and G. Paganelli for helpful discussions.

REFERENCES TO CHAPTER 8

- [8.1] BOERMAN, O.C., VAN SCHAIJK, F.G., OYEN, W.J., CORSTENS, F.H., Pretargeted radioimmunotherapy of cancer: Progress step by step, *J. Nucl. Med.* **44** (2003) 400.
- [8.2] LIU, S., EDWARDS, D.S., Fundamentals of receptor-based diagnostic metallo radiopharmaceuticals, *Top. Curr. Chem.* **222** (2002) 259.
- [8.3] LESCH, H.P., KAIKKONEN, M.U., PIKKARAINEN, J.T., YLÄ-HERTTUALA, S., Avidin-biotin technology in targeted therapy, *Expert Opin. Drug Deliv.* **7** (2010) 551.
- [8.4] McMAHON, R.J., Biotin in metabolism and molecular biology, *Annu. Rev. Nutr.* **22** (2002) 221.
- [8.5] DE SANTIS, R., et al., OXavidin for tissue targeting biotinylated therapeutics, *J. Biomed. Biotechnol.* **2009** (2009) 921434.
- [8.6] PAGANELLI, G., et al., Intraoperative avidination for radionuclide treatment as a radiotherapy boost in breast cancer: Results of a phase II study with ⁹⁰Y-labeled biotin, *Eur. J. Nucl. Med. Mol. Imaging* **37** (2010) 203.
- [8.7] PAGANELLI, G., et al., Intraoperative avidination for radionuclide therapy: A prospective new development to accelerate radiotherapy in breast cancer, *Clin. Cancer Res.* **15** (2007) 5646s.
- [8.8] URBANO, N., et al., Evaluation of a new biotin-DOTA conjugate for pretargeted antibody-guided radioimmunotherapy (PAGRIT), *Eur. J. Nucl. Med. Mol. Imaging* **34** (2007) 68.
- [8.9] JAMES, S., et al., Extension of the single amino acid chelate concept (SAAC) to bifunctional biotin analogues for complexation of the M(CO)₃+I core (M = Tc and Re): Syntheses, characterization, biotinidase stability, and avidin binding, *Bioconjug. Chem.* **17** (2006) 579.
- [8.10] RUDOLF, B., et al., Metallo-carbonyl conjugates of biotin and biocytin, *J. Organomet. Chem.* **668** (2003) 95.
- [8.11] KAM-WING LO, K., HUI, W.-K., CHUN-MING, N.G.D., Novel rhenium(I) polypyridine biotin complexes that show luminescence enhancement and lifetime elongation upon binding to avidin, *J. Am. Chem. Soc.* **124** (2002) 9344.
- [8.12] KAM-WING LO, K., HUI, W.-K., Design of rhenium(I) polypyridine biotin complexes as a new class of luminescent probes for avidin, *Inorg. Chem.* **44** (2005) 1992.

- [8.13] BOSCHI, A., DUATTI, A., UCCELLI, L., Development of technetium-99m and rhenium-188 radiopharmaceuticals containing a terminal metal–nitrido multiple bond for diagnosis and therapy, *Top. Curr. Chem.* **252** (2005) 85.
- [8.14] BOSCHI, A., BOLZATI, C., UCCELLI, L., DUATTI, A., High-yield synthesis of the terminal ^{188}Re triple bond N multiple bond from generator-produced $[\text{}^{188}\text{ReO}_4]^-$, *Nucl. Med. Biol.* **30** (2003) 381.
- [8.15] CHUNG, Y.K., Transition metal alkyne complexes: The Pauson–Khand reaction, *Coord. Chem. Rev.* **188** (1999) 297.
- [8.16] HYMES, J., FLEISCHHAUER, K., WOLF, B., Biotinidase in serum and tissues, *Methods Enzymol.* **279** (1997) 422.
- [8.17] BOLZATI, C., et al., An alternative approach to the preparation of ^{188}Re radiopharmaceuticals from generator-produced $[\text{}^{188}\text{ReO}_4]^-$: Efficient synthesis of ^{188}Re (V)-meso-2,3-dimercaptosuccinic acid, *Nucl. Med. Biol.* **27** (2000) 309.
- [8.18] BOSCHI, A., MASSI, A., UCCELLI, L., PASQUALI, M., DUATTI, A., PEGylated N-methyl-S-methyl dithiocarbamate as a new reagent for the high-yield preparation of nitrido Tc-99m and Re-188 radiopharmaceuticals, *Nucl. Med. Biol.* **37** (2010) 927.
- [8.19] SMITH, M., CADDICK, S., BAKER, J., Thiol protecting group, United States patent No. WO 2011/018612 A2 (2011).

Chapter 9

DEVELOPMENT OF RADIOPHARMACEUTICALS BASED ON ^{188}Re AND ^{90}Y FOR RADIONUCLIDE THERAPY IN POLAND

D. PAWLAK, T. DZIEL, A. MUKLANOWICZ, J.L. PARUS,
P. GARNUSZEK, W. MIKOLAJCZAK, M. MAURIN,
J. PIJAROWSKA, A. JARON, U. KARZMARCZYK,
E. LASZUK, A. KORSAK, E. JAKUBOWSKA,
E. BYSZEWSKA-SZPOCINSKA, R. MIKOŁAJCZAK
Radioisotope Centre,
Institute of Atomic Energy,
POLATOM,
Swierk-Otwock, Poland

Abstract

The main areas of work during this CRP were the development of a method for determination of ^{90}Sr contamination in ^{90}Y solutions, biotinylation of antibodies, radiolabelling of antibodies via chelating agents, studies on radiolabelling of ^{188}Re DMSA and investigation of chromatographic methods for evaluation of RCP of ^{188}Re DMSA(V) and ^{188}Re and ^{90}Y radiolabelling of particulates such as HSA microspheres and colloids.

9.1. DETERMINATION OF ^{90}Sr CONTAMINATION IN ^{90}Y ELUATE USING SOLID PHASE EXTRACTION ON A DGA COLUMN

Reliable methods for assessment of ^{90}Sr contamination in ^{90}Y used for medical application are needed [9.1, 9.2]. For the determination of trace levels of ^{90}Sr present in extracted ^{90}Y , a set of two extraction chromatography columns connected in series was used [9.3, 9.4]. The first column is filled with strontium resin and the second column with DGA resin (N,N,N',N'-tetra-n-octyldiglycolamide), which is a selective extractant system [9.5]. Strontium-90 is retained on the first column and ^{90}Y on the second column. Strontium-90 is eluted with water from the first column and measured using an LSC. The eventual remaining amount of ^{90}Sr appears in a liquid leaving the DGA column. The use of the DGA column itself seems also to be sufficient for ^{90}Sr determination at the DL of $10^{-5}\%$. The aim was to develop an analytical procedure for rapid determination of ^{90}Sr activity in

^{90}Y solution obtained from a $^{90}\text{Sr}/^{90}\text{Y}$ generator after ^{90}Sr separation using DGA resin.

9.1.1. Preparation of the DGA column

DGA resin was soaked in 5M HNO_3 (100 mg of resin in 1 mL of acid) for a minimum of 24 h. Suspended resin was agitated at 800 rev./min for at least 1 h using a magnetic stirrer. Agitation was repeated for 10 min before column preparation. A volume of 1 mL of DGA suspension was introduced into a 1 mL polypropylene column with a fritted polypropylene disc at the bottom. The column bed was covered with another fritted disc. The resin bed must be free from air bubbles and must always be covered with the acid solution.

9.1.2. Recovery of strontium from the DGA column using ^{85}Sr as a tracer

Experiments were performed to determine the strontium recovery from the DGA column using ^{85}Sr as a tracer. To 8 mL of 5M HNO_3 , 125 mg of strontium (500 μL of the 250 mg strontium/mL stock solution) and 25 μL of ^{85}Sr solution were added. The volume of solution was made to 10 mL by adding 5M HNO_3 . A volume of 1 mL of this solution was taken for measurement of ^{85}Sr activity using γ spectrometry. Two similar solutions were prepared by adding 114.8 and 120.7 kBq of ^{85}Sr . These solutions were loaded into two different columns using a peristaltic pump with a flow rate of 1 mL/min. The void volume of the set-up was 1.5 mL. Each column was rinsed in turn with 6 mL of 5M HNO_3 , 8 mL of 0.1M HNO_3 and 10 mL of 0.1M HCl . Fractions of 2 mL were collected, and ^{85}Sr activity in the fractions was measured using γ spectrometry. The mean value of ^{85}Sr recovery was 99.86% (SD = 0.135%).

9.1.3. Separation of ^{90}Sr from ^{90}Y on the DGA column

Separation of ^{90}Sr from ^{90}Y was done on the DGA column containing 100 mg of resin. A solution of $^{90}\text{YCl}_3$, from lots 34/11, 35/11 and 36/11 with radioactivities from 200 to 270 MBq on the separation date, was used for purification.

For the experiment, to ~ 250 MBq of $^{90}\text{YCl}_3$ solution, 125 mg of strontium (500 μL of the 250 mg strontium/mL stock solution) was added and, subsequently, 5M HNO_3 was added to get a final volume of 21 mL for A1–A4 samples or 6 mL for A5–A7 samples. For samples A1–A4, after transferring 21 mL of ^{90}Y solution, the column was rinsed with 6 mL of 0.1M HNO_3 and ^{90}Y was later eluted from the column with 0.1M HCl . For samples A5–A7, after transferring 6 mL of ^{90}Y solution, the column was rinsed with 4 mL of 5M HNO_3 followed by 6 mL of 0.1M HNO_3 and then ^{90}Y was eluted with 0.1M HCl . The flow rate was 1 mL/min

and 2 mL fractions were collected. To determine the activity of ^{90}Y loaded onto the column, 1 mL of $^{90}\text{YCl}_3$ solution prepared for transferring onto the column was measured (ionization chamber, Capintec CRC-15 beta). The radioactivity in each of the fractions was measured using three methods:

- Well type scintillation counter, with a 10 s measurement time;
- Ionization chamber Capintec CRC-15 beta, with ^{90}Y only;
- Beta radiation in a liquid scintillator, Wallac 1411 instrument Ultima Gold scintillator.

For samples A1–A2, to 10 mL of the scintillator, 1 mL of the fraction was added; this was not appropriate because after mixing the scintillator with the sample, the mixture looked opaque and two phases appeared after a few hours. It was obvious that the 5M HNO_3 was in very high concentration. It was then experimentally determined that the maximum acceptable volume of 5M HNO_3 was 0.15 mL. Therefore, for samples A3–A7, the volume of samples added to the scintillator was 0.1 mL.

9.1.4. Validation of the ^{90}Sr determination procedure using the standard ^{90}Sr addition method

To validate the ^{90}Sr recovery from the ^{90}Y solution, the standard method was used. Activities of 50, 100 and 250 Bq of ^{90}Sr were added to the same solution of ^{90}Y (lot 39/11). Six aliquots were prepared for each amount added. The diluted ^{90}Y solution containing 7.7 GBq/g was used. To 4 mL of strontium solution (31.25 mg Sr/mL in 5M HNO_3), 0.030 mL of ^{90}Y solution (230 ± 5 MBq) and weighed aliquots of ^{90}Sr standard corresponding to ~50, 100 and 250 Bq were added.

The prepared aliquots were loaded onto DGA columns containing 100 mg of DGA resin, which were rinsed in turn with 4 mL of 5M HNO_3 , 2 mL of 5M HNO_3 and 2 mL of 0.1M HNO_3 . The flow rate was maintained at 1 mL/min. Three fractions were collected:

- (a) A fraction of 8 mL volume, a loaded sample and 4 mL of 5M HNO_3 column rinsing (fraction 1);
- (b) A fraction of 2 mL volume of 5M HNO_3 column rinsing (fraction 2);
- (c) A fraction of 2 mL volume of 0.1M HNO_3 column rinsing (fraction 3).

From each fraction, a ~1 g aliquot was taken by weight into 20 mL LSC vials. Volumes of 1.5 mL deionized water and 10 mL of Ultima Gold AB liquid scintillator were added into each vial. Measurements were carried out using a Wallac 1411 spectrometer. The spectra of these three fractions are shown in Fig. 9.1.

Fraction 1 contained the total ^{90}Sr activity with a few counts of ^{90}Y owing to the decay of ^{90}Sr during collection of the ^{90}Sr fraction and measurement. Fractions 2 and 3 did not contain any activity. The spectra showed only background counts.

The relationship between the added and measured ^{90}Sr activity is shown in Fig. 9.2. The intersection point of the straight line with the ordinate axis determines the ^{90}Sr activity in ^{90}Y used for validation. The determination limit of ^{90}Sr in 230 MBq of ^{90}Y was equal to $3.5 \times 10^{-6}\%$ for a measurement time of 200 s. This limit can be lowered to $1 \times 10^{-6}\%$ for a 3600 s measurement time.

9.2. COMPARISON OF METHODS FOR CHROMATOGRAPHIC SEPARATION OF DMSA COMPLEXES WITH $^{99\text{m}}\text{Tc}$ AND ^{188}Re IN (III) AND (V) OXIDATION STATES; IMPLICATIONS OF PRODUCT DEVELOPMENT (IN COLLABORATION WITH VINČA INSTITUTE OF NUCLEAR SCIENCES, BELGRADE, SERBIA)

The reliable method for determination of RCP is key to the success of further radiopharmaceutical development. This is especially relevant when more than one type of radiometal ligand complex can be formed during labelling. In the case of DMSA complexes with $^{99\text{m}}\text{Tc}$ or ^{188}Re , depending on the pH, the metal can occur at +3 or +5 oxidation states [9.6]. Although, the European Pharmacopoeia monograph [9.7] describes RCP tests for $^{99\text{m}}\text{Tc(III)}$ DMSA based on ITLC SG chromatography, this method is not specific for distinct forms of complex and allows only determination of free $^{99\text{m}}\text{Tc}$ pertechnetate. Both $^{99\text{m}}\text{Tc(III)}$ DMSA and $^{99\text{m}}\text{Tc(V)}$ DMSA are retained at the origin similar to colloidal residues of $^{99\text{m}}\text{Tc}$. The method proposed by Westera et al. [9.8] utilizing SG coated plates and BuOH:H₂O:acetic acid (3:3:2) allows separation of $^{99\text{m}}\text{Tc(III)}$ DMSA from $^{99\text{m}}\text{Tc(V)}$ DMSA complexes in a separation process lasting 2 h, but still does not allow determination of technetium tin colloid (BuOH = butanol).

The goal of this work was to evaluate possibilities for optimization of chromatographic systems leading to a one step analytical method for determination of the RCP of DMSA complexes with $^{99\text{m}}\text{Tc}$ or ^{188}Re .

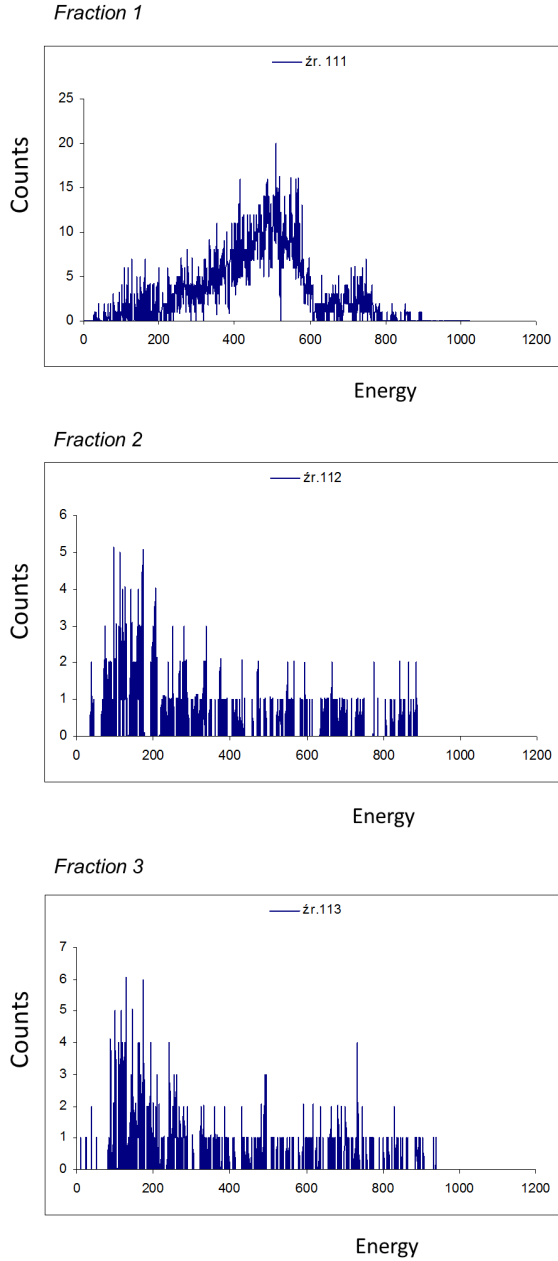


FIG. 9.1. Spectra of three collected fractions from the DGA column; 50 Bq of ^{90}Sr added to 230 MBq of ^{90}Y ; measurement time of 200 s.

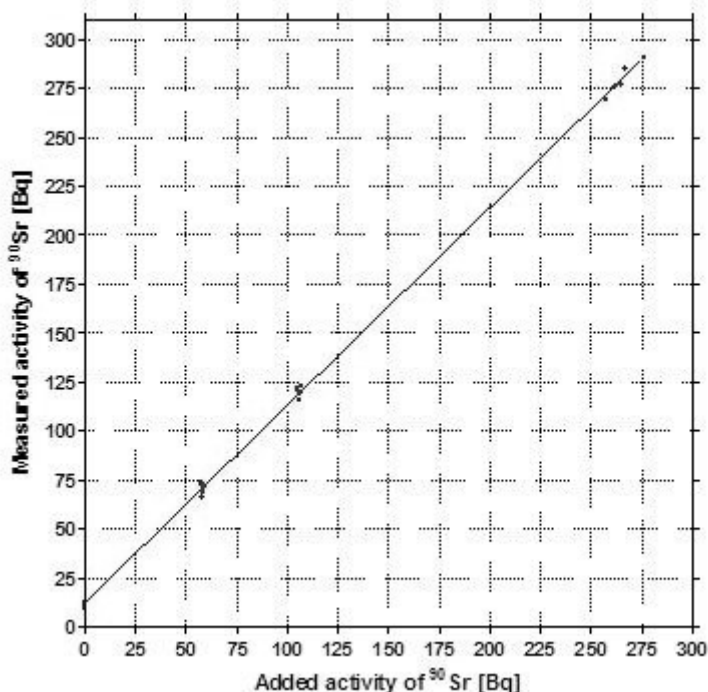


FIG. 9.2. Relationship between ^{90}Sr activity measured after separation from ^{90}Y chloride solution and added to this solution before separation on the DGA column.

9.2.1. Materials and methods

Technetium-99m(III) DMSA was obtained from DMSA kits (POLATOM) following manufacturer instructions for $^{99\text{m}}\text{Tc}$ labelling. For preparation of $^{99\text{m}}\text{Tc}$ DMSA(V) complexes, an additional 0.18 mL of 7% NaHCO_3 was added to the kit vial prior to $^{99\text{m}}\text{Tc}$ to obtain $\sim\text{pH}8$ [9.9]. For preparation of ^{188}Re DMSA(V), either the direct labelling method in alkaline solution was used [9.10] or a preformed complex of ^{188}Re EDTA was added to DMSA at $\text{pH}7.4$ [9.11]. For both methods, dry kit formulations were prepared. RCP was evaluated using an HPLC column PLRP-S (Polimer Laboratories) and a gradient of 0.1% TFA in water and 0.1% TFA in acetonitrile (ACN). TLC was carried on SG60 coated plates, ITLC SG plates and RP18 plates developed in $\text{PrOH}:\text{H}_2\text{O}:\text{CH}_3\text{COOH}$ and $\text{BuOH}:\text{H}_2\text{O}:\text{CH}_3\text{COOH}$ systems ($\text{PrOH} = \text{propanol}$) (see Table 9.1).

TABLE 9.1. SUMMARY OF CHROMATOGRAPHIC SYSTEMS UTILIZED FOR DETERMINATION OF RCP OF ^{99m}Tc COMPLEXES WITH DMSA

Compound	ITLC SG: methylethylketone RCP (%) / R_f	SG60 BuOH:H ₂ O:CH ₃ COOH (3:3:2) RCP (%) / R_f	SG60 PrOH:H ₂ O:CH ₃ COOH (4:3:1) RCP (%) / R_f
Re-188 perrhenate	0.9–1.0	0.8–0.9	0.8–0.9
Re-188(V) DMSA direct labelling	Not determined	100/0.6	100/0.6
Re-188(V) DMSA with exchange from Re-188 EDTA	Not determined	5.85 ± 0.75/0.0 36.2 ± 3.4/0.4 44.7 ± 1.8/0.6 13.2 ± 0.85/0.9	16.8 ± 0.55/0.0 27.7 ± 3.2/0.5 37.7 ± 0.3/0.6 17.8 ± 3.25/0.9
Tc-99m(V) DMSA	100/0.9–1.0	25.2 ± 4.3/0.0 74.8 ± 4.3/0.6	27.1 ± 0.5/0.0 72.9 ± 0.5/0.6
Tc-99m(III) DMSA	100/0.9–1.0	90.9 ± 4.3/0.0–0.4 8.9 ± 0.1/0.6	86.6 ± 1.0/0.0–0.4 ± 1.0/0.6

9.2.2. Conclusion

Using the SG plates and replacing BuOH with PrOH by varying the proportion of H₂O and acetic acid in the developing solution, it was observed that the formed complexes of $^{99m}\text{Tc}/^{188}\text{Re(III)}$ DMSA and $^{99m}\text{Tc}/^{188}\text{Re(V)}$ DMSA could be well separated from each other and from the impurities in the form of free pertechnetate and colloidal $^{99m}\text{Tc}/^{188}\text{Re}$. The results of TLC separation correlated well with the HPLC results. Furthermore, the method of indirect preparation of $^{188}\text{Re(V)}$ DMSA by exchange from ^{188}Re EDTA results in a mixture of $^{188}\text{Re(III)}$ and $^{188}\text{Re(V)}$ complexes.

9.3. RHENIUM-188 RADIOLABELLING OF DPA ALE (IN COLLABORATION WITH DIVISION OF IMAGING SCIENCES, KING'S COLLEGE LONDON, UK)

The aim of this project was to label DPA ale with ^{188}Re using the tricarbonyl approach. This report presents the efforts made to radiolabel DPA ale

with ^{188}Re obtained from the $^{188}\text{W}/^{188}\text{Re}$ generator according to a methodology described elsewhere in this publication (see Chapter 13).

9.3.1. Radiolabelling using an Iso-Link kit

In the first step of the study, analytical conditions for monitoring the tricarbonyl intermediate were evaluated using an Iso-Link kit and the $^{99\text{m}}\text{Tc}$ eluate. The Iso-Link kit was labelled with $^{99\text{m}}\text{Tc}$ according to manufacturer instructions. The $^{99\text{m}}\text{Tc}$ tricarbonyl complex was obtained with >95% yield, which confirms the quality of the kits, as shown in the HPLC pattern (see Fig. 9.3).

A similar approach to label the Iso-Link kit with ^{188}Re did not result in a radioactive carbonyl complex (see Fig. 9.4). Only the signal corresponding to free ^{188}Re perrhenate was present in the HPLC radiochromatogram. Increasing the time of incubation to 1 h did not show any change in the radiolabelling yield.

Because the results in preparation of ^{188}Re tricarbonyl moiety using the commercial Iso-Link kit were not satisfactory, the procedure was modified slightly by addition of 6 mg of $\text{BH}_3\cdot\text{NH}_3$ to the kit followed by 400 μL of acidified (with 7 μL of 85% H_3PO_4) ^{188}Re eluate (radioactivity ~ 1 GBq). The mixture was then incubated for 20 min at 60°C . The radiolabelling yield was determined using TLC SG60 in 99% MeOH:1% HCl. The yield of $^{188}\text{Re}(\text{CO})_3$ was $\sim 65\%$, as shown in Fig. 9.5.

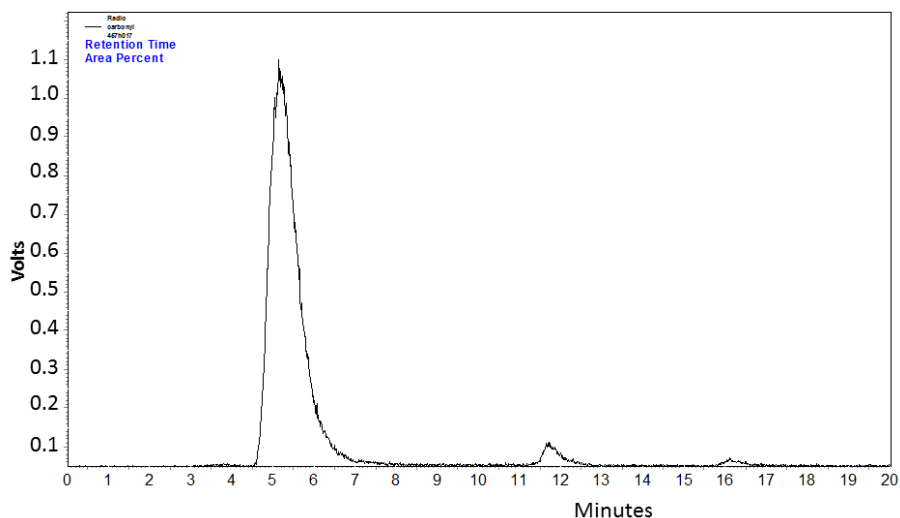


FIG. 9.3. HPLC radiochromatogram of $^{99\text{m}}\text{Tc}$ tricarbonyl moiety obtained using Iso-Link kit (Nucleosil C18; mobile phase: (a) triethylammonium phosphate (TEAP) and (b) MeOH); gradient according to the Iso-Link leaflet, flow rate = 0.7 mL/min.

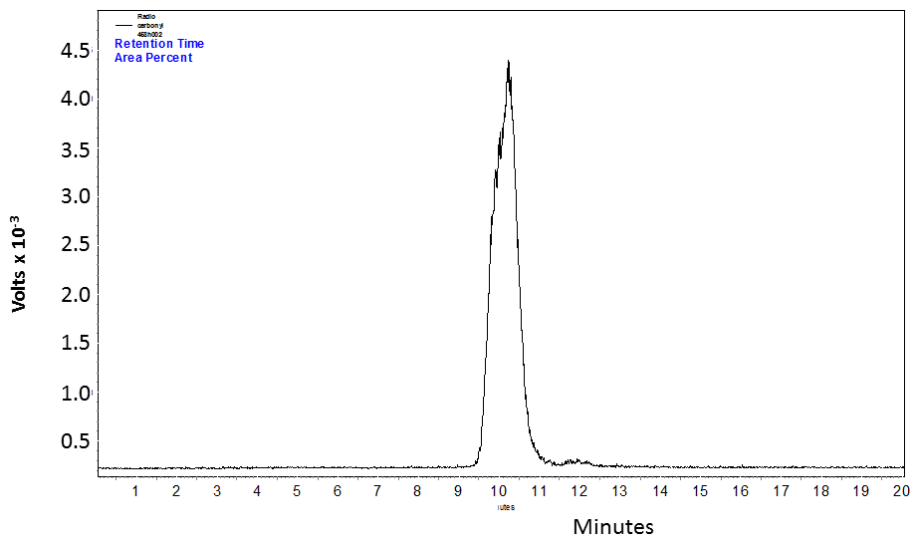


FIG. 9.4. HPLC radiochromatogram of ^{188}Re labelled Iso-Link after additional heating (HPLC conditions).

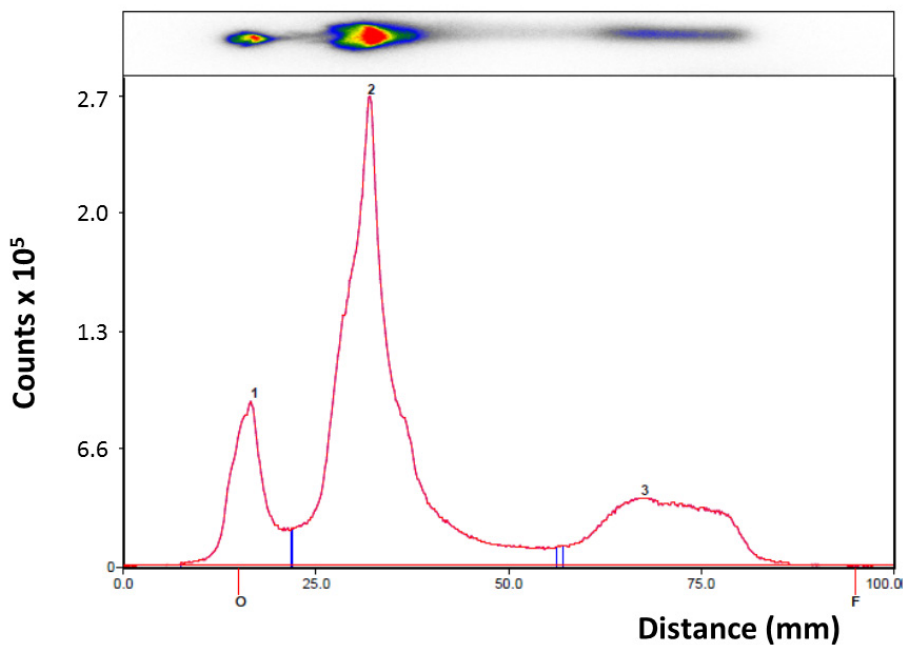


FIG. 9.5. Radiochromatogram of $^{188}\text{Re}(\text{CO})_3$ reaction mixture after 2 h incubation.

9.3.2. Labelling of DPA ale

DPA ale was labelled with the prepared ^{188}Re tricarbonyl intermediate by addition of 100 μL $\text{Re}(\text{CO})_3$ to 100 μL of DPA ale (0.1 mg/mL) buffered with 100 μL of 0.1M phosphate buffer, pH6.7. The mixture was incubated for 30 min at 75°C. TLC radiochromatography (SG60 plates developed in 99% MeOH:1% HCl) did not indicate formation of the radiolabelled compound (6.8% colloidal residue plus possibly radiolabelled phosphonate, 7.9% $\text{Re}(\text{CO})_3$ and 83% of the free ^{188}Re perrhenate), as shown in Fig. 9.6.

9.3.3. Homemade kit for tricarbonyl preparation

The precursor for the labelling was prepared according to the following procedure. In each of the six penicillin vials, 5 mg of $\text{BH}_3\cdot\text{NH}_3$ was added, sealed with a rubber stopper and capped. The contents of the vials were exposed to a stream of CO for 20 min. The flow of CO was stopped in such a way that ensured the gas pressure in the vials was ~ 20 MPa. To one of the prepared vials, 0.5 mL of $^{188}\text{ReO}_4$ acidified with 7 μL of 85% H_3PO_4 with radioactivity ~ 1 GBq was added.

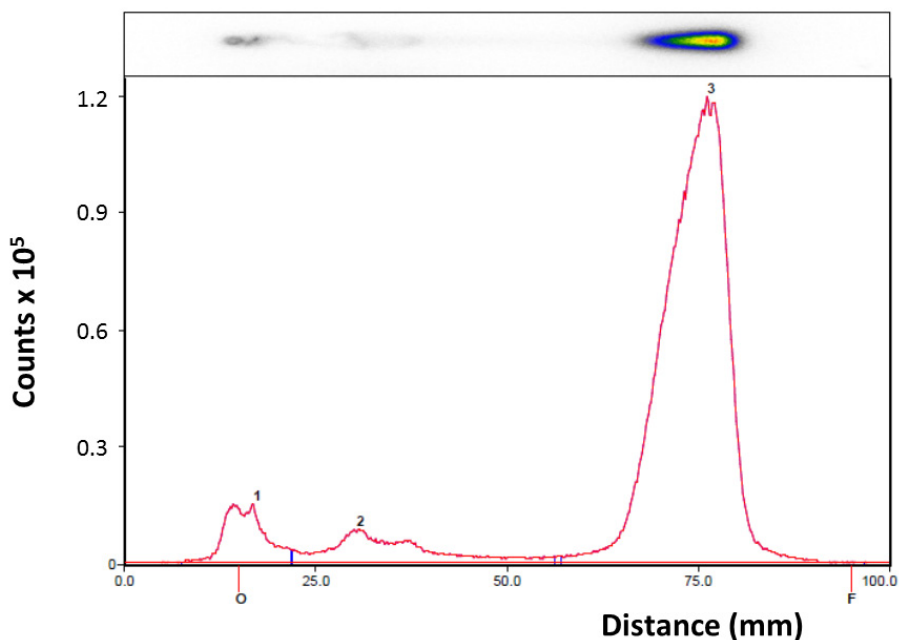


FIG. 9.6. TLC radiochromatogram of DPA ale + $\text{Re}(\text{CO})_3$ (SG60 plates developed in 99% MeOH:1% HCl).

This was incubated for 20 min at 60°C. The radiolabelling yield was verified using TLC. The results (before purification) are shown in Fig. 9.7 with 71% of $^{188}\text{Re}(\text{CO})_3$, 20% of ^{188}Re colloids and 9% of ^{188}Re perrhenate.

The carbonyl complex obtained was purified by filtration using a 0.22 μm membrane to remove colloidal residue, and the results of the purified complex are shown in Fig. 9.8.

The radiolabelling of DPA ale was carried as follows: to 50 μL of DPA ale (0.1 mg/mL), 100 μL 0.1M of phosphate buffer (pH6.7) and 100 μL of $^{188}\text{Re}(\text{CO})_3$ were added. The mixture was incubated for 15 min at 60°C. The progress of the reaction was followed using TLC (see Fig. 9.9). According to De Rosales et al. (see Chapter 13), the R_f value for radiolabelled DPA ale is 0.1. To distinguish between the obtained phosphonate and ^{188}Re colloid, the sample was filtrated using a 0.22 μm membrane before the TLC analysis (see Fig. 9.10).

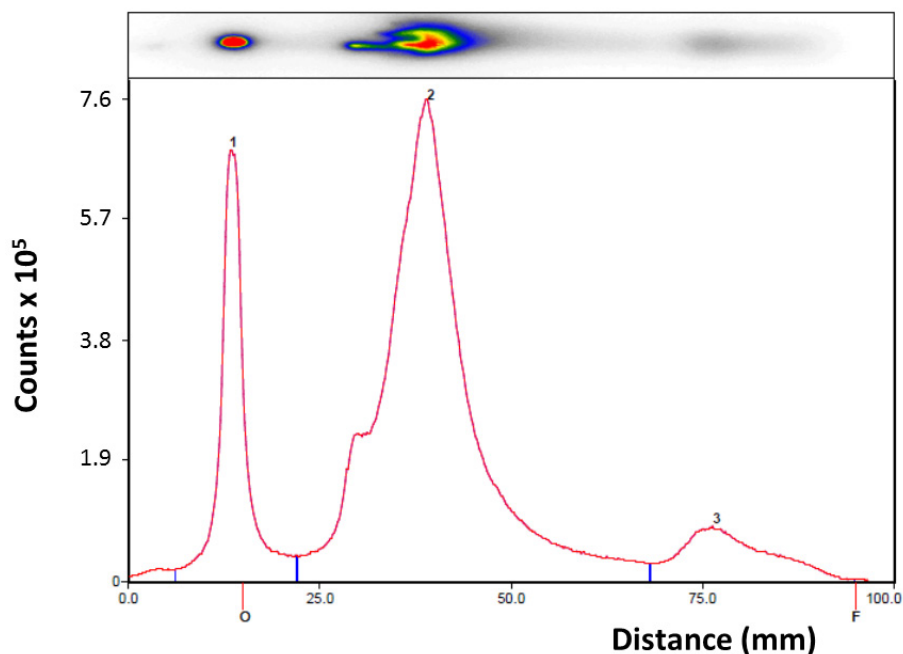


FIG. 9.7. TLC radiochromatogram of $^{188}\text{Re}(\text{CO})_3$ prepared from the home tricarbonyl kit (SG60, 99% MeOH:1% HCl).

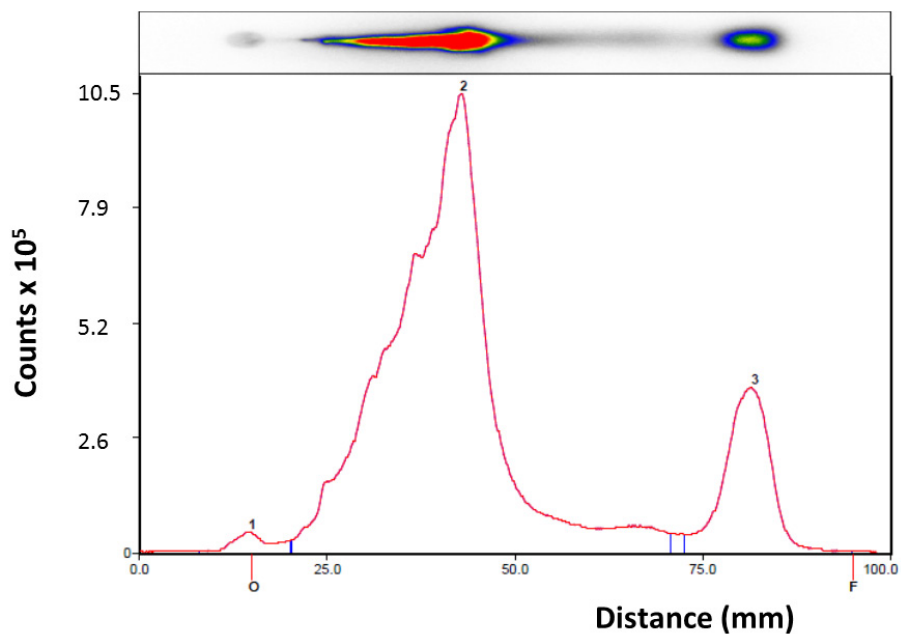


FIG. 9.8. TLC radiochromatogram of $^{188}\text{Re}(\text{CO})_3$ after filtration (SG60, 99% MeOH:1% HCl).

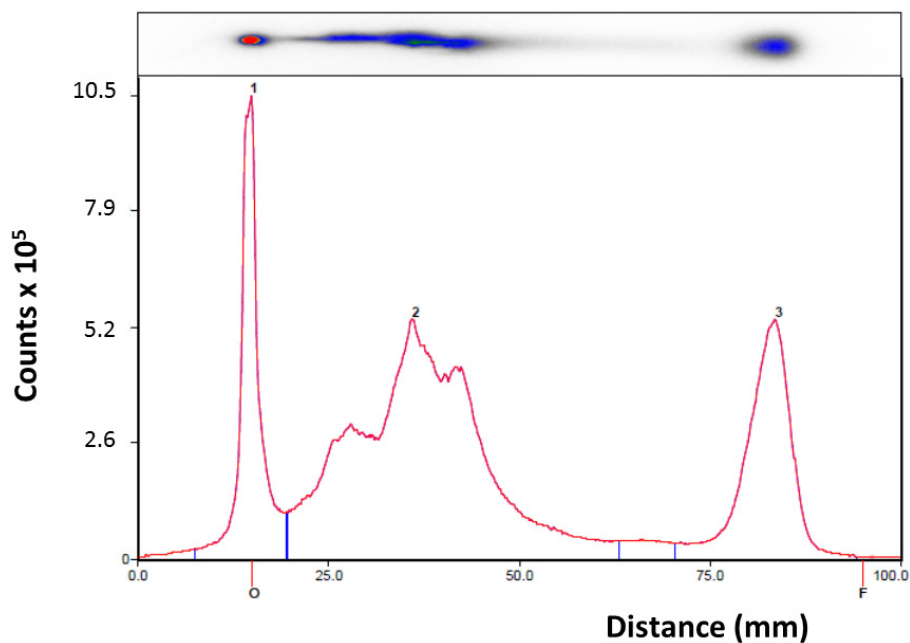


FIG. 9.9. TLC radiochromatogram of DPA ale + $\text{Re}(\text{CO})_3$ (SG60, 99% MeOH:1% HCl).

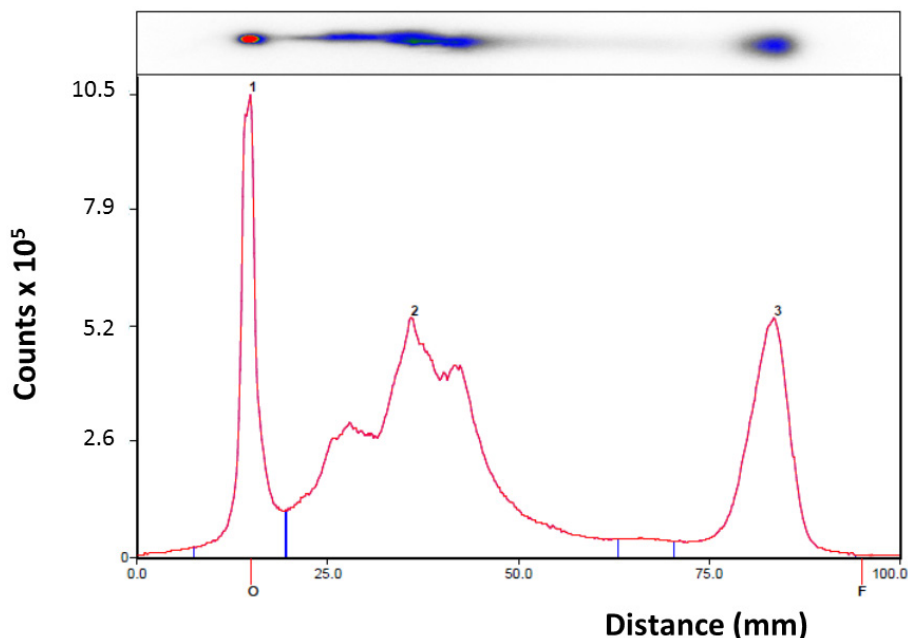


FIG. 9.10. TLC radiochromatogram of DPA ale + $\text{Re}(\text{CO})_3$ after filtration (SG60, 99% MeOH:1%HCl).

From these experiments, the formation of radiolabelled DPA ale was not confirmed.

9.3.4. Electrophoresis of $^{99\text{m}}\text{Tc}$ and ^{188}Re tricarbonyls

Because of insufficient labelling via the ^{188}Re tricarbonyl method, electrophoresis on Whatman No. 1 paper strips was carried out to establish the electrical charge of the prepared tricarbonyls (see Fig. 9.11). It was observed on the radioelectrophoregram that the ^{188}Re tricarbonyl complexes that were supposed to be prepared by the method described in Section 9.3.3., migrated towards the anode (negatively charged complex) contrary to the $^{99\text{m}}\text{Tc}$ carbonyl complexes (Iso-Link), which migrated towards the cathode. On this basis, it was assumed that the negative charge of the ^{188}Re complex could be the reason for the lack of radiolabelling of DPA ale.

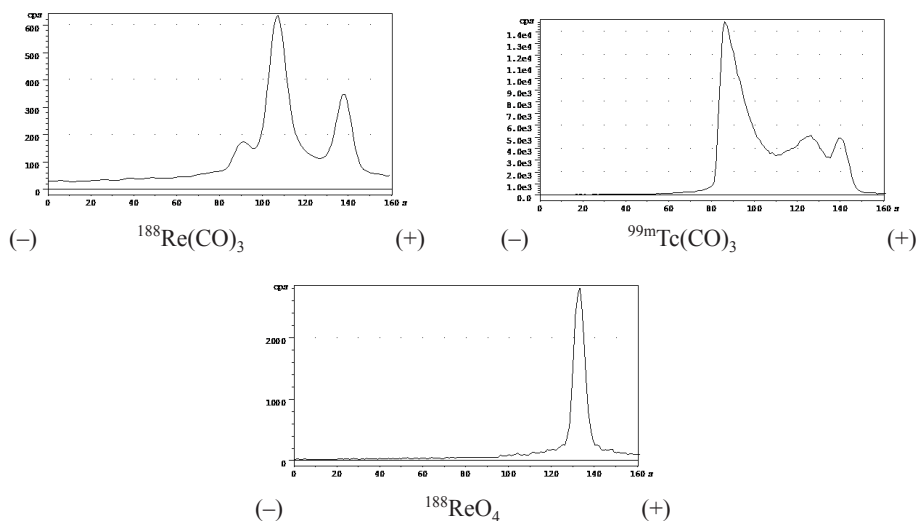


FIG. 9.11. Electrophoretic separation of obtained ^{188}Re complexes (electrophoresis parameters: Whatman No. 1; 0.05M NaClO_4 ; 500 V, 30 min, application 5 μL).

9.4. DEVELOPMENT OF A METHOD FOR PREPARATION OF HUMAN SERUM ALBUMIN MICROSPHERES FOR LABELLING WITH ^{188}Re AND ^{90}Y

The purpose of this study was to develop a method for the preparation of human albumin microspheres, with reproducible grain size and reproducible physical and biological parameters, that can be labelled with a variety of radionuclides. Albumin microspheres are spherical microaggregates of denaturated and coagulated HSA. They have been widely used in clinical nuclear medicine as carriers for radioactive diagnostics and therapeutic molecules since 1969 [9.12, 9.13]. Since then, albumin microspheres have been considered as useful radiopharmaceutical carriers because of their spherical shape, non-toxicity, non-immunogenicity and fast biodegradation after administration [9.14, 9.15].

Albumin microspheres of size $\sim 10\text{--}50\ \mu\text{m}$ in diameter and labelled with $^{99\text{m}}\text{Tc}$ have found an application in lung perfusion scintigraphy. Technetium-99m microspheres introduced into the bloodstream by intravenous injection are trapped first in the capillary system. More than 95% of the injected radioactivity is extracted by the pulmonary capillaries and arterioles in a single passage and distributed in the lungs according to regional pulmonary arterial blood flow.

Capillary sizes may vary from organ to organ, and a fraction of the blood may pass through arteriovenous shunts. Under these conditions, ^{99m}Tc microspheres bypass the pulmonary circulation when injected for lung perfusion scintigraphy. The scintigraphy image obtained after application of the radiopharmaceutical is fast and precise, showing disturbances in blood circulation.

It is expected that albumin microspheres labelled with ^{90}Y , ^{177}Lu or ^{188}Re could become convenient carriers for the radionuclides useful in nuclear medicine as a tool in therapy of HCC and liver metastases [9.16, 9.17]. In a procedure called radioembolization, the radiolabelled particles are directly applied into the tumour via catheterization of the artery that supplies the tumour. Owing to their size, particles are trapped in the capillary bed of the tumour and can locally deliver radiotoxic effects. Yttrium-90 glass microspheres, where ^{90}Y is an integral constituent of the glass matrix, and ^{90}Y resin microspheres have shown promising results in the therapy of HCC [9.18].

Microspheres labelled with ^{99m}Tc are described in many Pharmacopoeia monographs. However, for the microspheres labelled with other radionuclides, monographs are not available. Therefore, as a reference level for the current study, the requirements for ^{99m}Tc microspheres were referred to. As stated in European Pharmacopoeia monograph 01/2005:0570 [9.16]:

- (a) The RCP of the radioactive product should be >95%.
- (b) The microspheres should be spherical regular particles with diameters in the range 10–50 μm .
- (c) The number of microspheres in 1 mL of the injection solution should be 100 000–250 000 particles.
- (d) The biodistribution (concentration of radioactivity should be >80% in lungs and <5% in liver and spleen).
- (e) The radiopharmaceutical kit should be sterile and endotoxin free.
- (f) The microspheres should be biodegradable and excreted at definite (repeatable) times.

9.4.1. Preparation of human serum albumin microspheres

In general, the preparation of albumin microspheres consists of dispersion of HSA solution in a suitable medium and stabilization of spherical particles by heat. In the present study, microspheres were prepared by emulsification using a heat stabilization technique described previously [9.12, 9.13] with minor modifications. The processing parameters of homogenization (speed and time), oil phase (volume, concentration of emulsifier and denaturing agent), water phase (volume and HSA concentration) and heat denaturation of protein (temperature and time) were selected experimentally. In the optimized method,

the HSA solution containing sodium dodecyl sulphate (SDS) was added to liquid paraffin containing SDS and Tween 80, and the mixture was stirred using a mechanical stirrer to obtain a water oil emulsion. This emulsion was then heated to allow the formation and solidification of microspheres and left at room temperature. Supernatant oil was removed by decantation and microspheres were washed with diethyl ether. The particles were dried in a vacuum and later sieved.

Ten batches of microspheres with diameters ranging from 10 to 32 μm were prepared using the above described method. Particle size analysis was performed by optical microscopy using a light microscope equipped with an ocular micrometer and a light camera (see Fig. 9.12). The microspheres were sized and photographed in normal saline containing Tween 80 to prevent aggregation. The particles in each prepared batch were measured using a calibrated ocular micrometer .

The contribution of microsphere particles in the selected size ranges (in percentages) was determined for three batches by weight analysis (see Table 9.2).

The production yield of albumin microspheres for the desired size range 10–32 μm was 84% and the mean size of particles was estimated to be $\sim 15 \mu\text{m}$. Optical micrographs showed very regular spherical forms with quite smooth surfaces and a slight scatter of size in the range 10–32 μm .

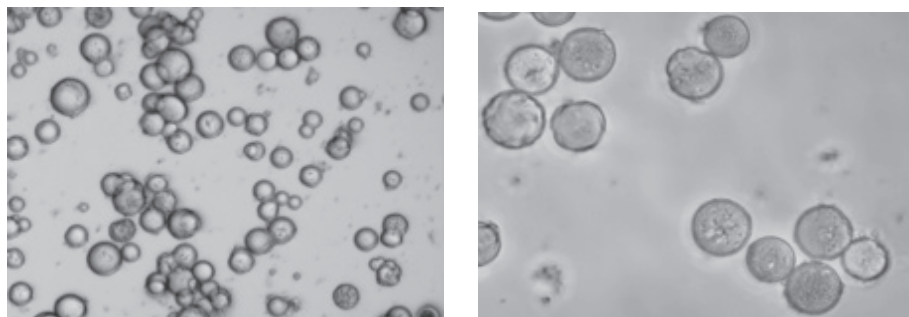


FIG. 9.12. Optical micrographs of HSA microspheres in a mean size range of 10–32 μm taken at two different magnifications: (left) $\times 200$ and (right) $\times 400$.

TABLE 9.2. PARTICLE SIZE RANGES OF ALBUMIN MICROSPHERES

Batch No.	Frequency (%) of albumin microspheres in the size range				
	<10 μm	10–32 μm	32–50 μm	50–100 μm	>100 μm
1	0.9	86.9	7.2	2.3	2.7
2	0.4	84.1	11.8	2.2	1.5
3	0.3	81.8	13.9	2.1	1.9
Mean	0.5	84.3	11.0	2.2	2.0

For the labelling of microspheres with $^{99\text{m}}\text{Tc}$, it was necessary to reduce the valency of technetium. $\text{SnCl}_2 \cdot 2\text{H}_2\text{O}$ was used as the reducing agent and the method of tin(II) coating was developed based upon published procedures [9.19]. The dried microspheres, stored in an argon atmosphere, were suspended in 0.044M $\text{SnCl}_2 \cdot 2\text{H}_2\text{O}$ solution in 0.2N HCl, shaken and heated at 80°C for 2 h. After cooling, the particles were filtered, washed with 0.2M HCl and ethanol and dried under vacuum. For $^{99\text{m}}\text{Tc}$ labelling, microspheres (2.5 mg) with Tween 80 were suspended in 1 mL of 0.9% saline solution, and ~ 175 MBq of $^{99\text{m}}\text{Tc}$ sodium pertechnetate, eluted from a $^{99}\text{Mo}/^{99\text{m}}\text{Tc}$ generator, was added. The vial was incubated at room temperature for 30 min with shaking. Microspheres of $^{99\text{m}}\text{Tc}$ were separated from the non-bound pertechnetate by filtration. The labelling yield determined as a relationship of the measured radioactivity remaining in the membrane filter to the total radioactivity was $>99.6\%$ (see Table 9.3).

9.4.2. Serum stability testing and biodistribution study of $^{99\text{m}}\text{Tc}$ albumin microspheres

In vitro stability of $^{99\text{m}}\text{Tc}$ microsphere complexes was determined after incubation in human serum for 4 h at 37°C . Figure 9.13 presents the results of the in vitro stability study. Technetium-99m microspheres showed high in vitro stability in human plasma with only $<5\%$ loss of radioactivity after 4 h. The biodistribution was studied after intravenous injection in the tail vein of rats. In accordance with the European Pharmacopoeia monograph [9.16] for $^{99\text{m}}\text{Tc}$ HSA microspheres, the animals were sacrificed after 15 min, selected organs (lungs, liver and spleen) were isolated and the radioactivity counted. Organ concentration of radioactivity was calculated as the percentage of total radioactivity injected (%ID). Table 9.4 presents results of a biodistribution study of three batches of $^{99\text{m}}\text{Tc}$ microspheres.

TABLE 9.3. RESULTS OF ^{99m}Tc LABELLING OF TIN(II) COATED ALBUMIN MICROSPHERES

Batch No.	Radioactivity (MBq)		Radiolabelling yield (%)
	Filter	Filtrate	
18/10	149.0	0.4	99.7
19/10	148.0	0.6	99.6
18/10 Sn2	185.8	0.8	99.6
19/10 Sn2	190.6	0.8	99.6
19/10 Sn4	130.0	0.0	100.0
19/10 Sn4U	126.5	0.3	99.8
18/10 Sn4	118.5	0.5	99.6
18/10 Sn4/1	176.2	0.1	99.9
18/10 Sn4/1U	172.3	0.1	99.9

Stability in Human Plasma

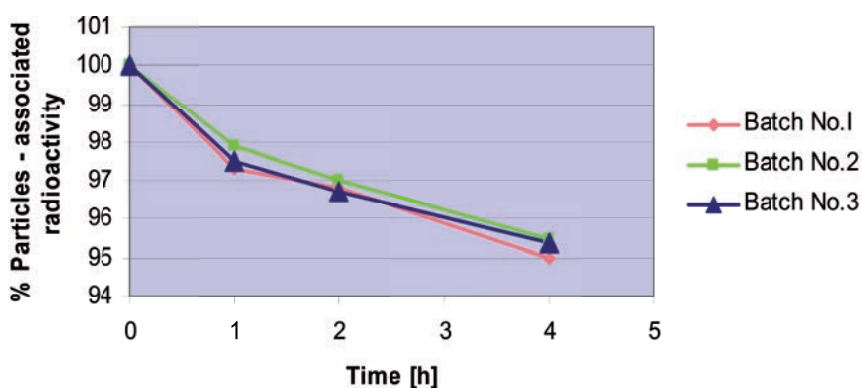


FIG. 9.13. In vitro stability of ^{99m}Tc microspheres.

TABLE 9.4. BIODISTRIBUTION OF ^{99m}Tc MICROSPHERES ACCORDING TO THE EUROPEAN PHARMACOPOEIA MONOGRAPH [9.16]

Biodistribution of Tc-99m microspheres (%ID/g)			
Organ	Batch No. 1	Batch No. 2	Batch No. 3
Lungs	87.4 ± 0.8	86.1 ± 1.0	91.1 ± 5.5
Liver and spleen	2.6 ± 0.1	3.3 ± 0.2	2.7 ± 0.0

9.4.3. Rhenium-188 labelling of albumin microspheres

Radioactive microspheres labelled with ^{188}Re were prepared using the procedure described previously by Wunderlich et al. [9.20, 9.21]. Tin(II) coated microspheres (10–20 mg) with Tween 80 were suspended in water for injection. A solution of tin chloride (50 μmol) in gentisic acid (60 μmol) and ~ 800 MBq of ^{188}Re sodium perrhenate eluted from a $^{188}\text{W}/^{188}\text{Re}$ generator (POLATOM) were added to the vial. The mixture was heated to 95°C and incubated for 30 min with shaking. Subsequently, a solution of potassium sodium tartrate (150 μmol) was added to the vial and shaken again. The preparation was ready for injection without any additional steps. To evaluate the labelling yields, the radioactive products were separated by filtration. Two batches of HSA microspheres were labelled with ^{188}Re according to this procedure, and the mean radiolabelling yield was $99.3\% \pm 0.4\%$ (see Table 9.5).

TABLE 9.5. RESULTS OF ^{188}Re LABELLING OF TIN(II) COATED ALBUMIN MICROSPHERES

Batch and amount of microspheres	Filtrate activity (MBq)	Filter activity (MBq)	Radiolabelling yield (%)
MA Sn ₂ (V) 10 mg	2.6	775.0	99.7
MA Sn ₂ (V) 15 mg	8.2	735.1	98.9
MA Sn ₂ (V) 20 mg	6.0	740.0	99.2
MA Sn ₂ (I) 10 mg	3.4	765.8	99.6

9.4.4. Yttrium-90 and ^{177}Lu labelling of albumin microspheres

The labelling of albumin microspheres with ^{90}Y and ^{177}Lu was carried out according to the following procedure. Microspheres (5 mg, 32–50 μm diameter) were suspended in solution (0.9% saline or ascorbic buffer, pH4.5) and incubated with ~ 50 mCi of ^{90}Y and ^{177}Lu at 90°C for 30 min, then filtered through a 0.2 μm filter and washed twice with 1 mL of the initial solution. The radioactivity of the filtrate and that retained on the filter was measured. The radiolabelling yield (see Table 9.6) was calculated as a ratio of radioactivity retained on the filter to the total radioactivity of the sample (filtrate + filter).

9.4.5. Biodistribution study of ^{177}Lu microspheres

The biodistribution of ^{177}Lu microspheres was studied after intravenous administration in the tail vein of rats. In this experiment, rats were sacrificed at different time intervals (15 min, 4, 24, 72 and 168 h), selected organs were isolated and the radioactivity was counted. Lungs were considered as the target organ. Radioactivity in the organs was calculated as the percentage of the total radioactivity injected. Table 9.7 represents results of the biodistribution study with ^{177}Lu albumin microspheres.

TABLE 9.6. RESULTS OF ^{90}Y AND ^{177}Lu LABELLING OF ALBUMIN MICROSPHERES

Batch	Radiolabelling yield of Y-90 microspheres (%)		Radiolabelling yield of Lu-177 microspheres (%)	
	0.9% saline	Ascorbic buffer	0.9% saline	Ascorbic buffer
1	98.80 \pm 4.90	99.20 \pm 4.90	98.00 \pm 4.90	98.40 \pm 4.90
2	98.00 \pm 4.90	98.30 \pm 4.90	95.10 \pm 4.80	98.00 \pm 4.90
3	92.70 \pm 4.10	97.80 \pm 4.90	99.50 \pm 4.95	99.20 \pm 4.95
4	96.00 \pm 4.80	98.00 \pm 4.90	93.20 \pm 4.90	98.90 \pm 4.90

TABLE 9.7. BIODISTRIBUTION (%ID/g) (mean \pm SD) OF ^{177}Lu ALBUMIN MICROSPHERES

Organ	Time after administration				
	15 min	4 h	24 h	72 h	168 h
Lungs	91.98 \pm 0.86	75.15 \pm 0.93	37.99 \pm 4.59	13.27 \pm 5.79	6.36 \pm 1.49
Spleen	0.04 \pm 0.02	0.14 \pm 0.05	0.51 \pm 0.16	1.05 \pm 0.23	1.14 \pm 0.10
Liver	1.14 \pm 0.19	2.91 \pm 0.52	11.27 \pm 3.50	16.72 \pm 5.14	18.05 \pm 0.14
Bone	0.06 \pm 0.01	0.67 \pm 0.07	1.93 \pm 0.14	2.77 \pm 0.28	2.75 \pm 0.14
Urine	0.35 \pm 0.25	2.90 \pm 0.50	7.04 \pm 0.71	13.83 \pm 3.27	18.28 \pm 0.89

9.4.6. Serum stability testing and biodistribution study of ^{177}Lu albumin microspheres

To estimate the in vitro stability of the radiolabelled complexes, samples of ^{90}Y and ^{177}Lu albumin microspheres were incubated with human plasma for 48 h at 37°C using methods based upon published procedures [9.22]. Microspheres were labelled in an ascorbic buffer, centrifuged, washed with buffer and again centrifuged. The radiolabelling yield was measured. Fresh human serum was added and the vial shaken at 37°C. Aliquots of the suspension after centrifugation were taken after 1, 24 and 48 h, and particle associated radioactivity was calculated. The same volume of serum was added to the vial and incubation continued. Figure 9.14 presents results of the in vitro stability of ^{90}Y and ^{177}Lu albumin microspheres.

9.4.7. Conclusion

The technology for tin(II) coated albumin microspheres preparation at a 5 g scale was established. The production yield of microspheres in the size range 10–32 μm was 84%. Optical micrographs showed microspheres as very regular spherical forms with smooth surfaces. The labelling yields determined as a relationship of measured radioactivity remaining after filtration on the membrane filter to the total radioactivity was >99% for $^{99\text{m}}\text{Tc}$ and ^{188}Re , >97% for ^{90}Y and >98% for ^{177}Lu microspheres. Labelled microspheres showed high in vitro stability in human plasma with only 4–5% loss of radioactivity for ^{90}Y and

Stability in Human Plasma

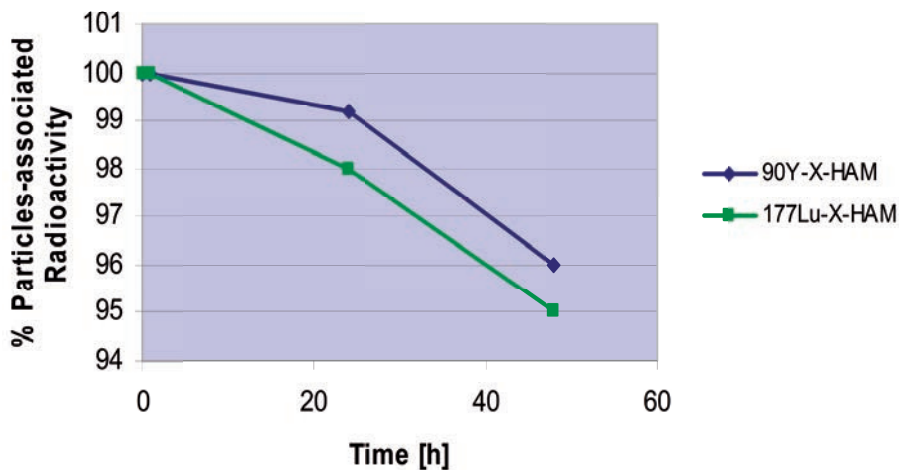


FIG. 9.14. *In vitro* stability of ^{90}Y and ^{177}Lu albumin microspheres.

^{177}Lu microspheres at 48 h and <5% loss of radioactivity for $^{99\text{m}}\text{Tc}$ microspheres at 4 h. The biodistribution at 15 min after administration showed >80% activity in lungs and <5% in liver and spleen for $^{99\text{m}}\text{Tc}$ microspheres, and >90% activity in lungs for ^{177}Lu microspheres. However, the growing radioactivity in liver and bone at 4 and 24 h p.i. indicated a fast dissociation of ^{177}Lu from the complex. Further studies are essential to confirm the *in vivo* stability of microspheres with ^{177}Lu and ^{90}Y .

9.5. COLLOIDS FOR RADIOSYNOVECTOMY

The project was carried out in collaboration with the Department of Radiochemistry of Colloids, Maria Curie-Skłodowska University (Poland) under the supervision of W. Janusz. Extensive experiments were carried out on the syntheses of yttrium citrate, erbium citrate and rhenium heptasulphide. The products obtained were analysed using various methods: X ray diffraction (XRD) to determine the crystal structure of the compound; CHN analysis to determine the elemental composition; and infrared (IR) spectroscopy to identify the main species and grain size distribution using a Zetasizer Nano instrument (Malvern Instruments Ltd).

9.5.1. Yttrium citrate

Precipitation of yttrium citrate from yttrium nitrate solution led to formation of material containing significant amounts of nitrogen, probably as basic yttrium nitrate. The content of yttrium citrate determined from CHN and XRD analyses was low.

Synthesis based on reaction of yttrium chloride with sodium citrate at room temperature led to formation of a precipitate, which was very soluble to such an extent that it was impossible to wash it with water. Synthesis based on the reaction of yttrium chloride at elevated temperature led to formation of an insoluble precipitate with a composition and structure close to yttrium citrate.

Based on the number of attempts made, the ideal way to obtain yttrium citrate was the synthesis in which hydroxide was precipitated from the yttrium chloride or nitrate solution with ammonia. After washing out the chloride ions, the hydroxide was reacted with citric acid at high temperatures. The content of carbon and hydrogen was close to the theoretical values of yttrium citrate \times H₂O, and the XRD analysis confirmed the structure of yttrium citrate. The particle diameter was in the range 0.4–10 μ m.

9.5.2. Erbium citrate

Based on the 20 different syntheses of erbium citrate carried out, it is recommended to use the following reagents: erbium oxide, concentrated HCl, ammonium citrate or citric acid and water. Erbium oxide was first dissolved in hot concentrated HCl solution, evaporated to dryness and then dissolved in water to give a solution of pH4–5. To this mixture, a solution of ammonium citrate or citric acid in a molar ratio 1:1 was added and then heated at 160°C for 72 h with continuous mixing. The composition of the product differed from stoichiometric values. In the modified synthesis, erbium hydroxide was precipitated and after careful purification by washing, it was dissolved in citric acid solution and autoclaved for 120 h at 120°C with continuous mixing. Elemental analysis showed the carbon and hydrogen content corresponding to erbium citrate \times H₂O. XRD analysis confirmed the presence of erbium citrate and some unidentified small peaks (probably, erbium dicitrate). The grain size was in the range 0.2–20 μ m. More pure product was obtained when 0.1M NaOH was used for precipitation of erbium hydroxide.

9.5.3. Procedure for yttrium and erbium colloid preparation

All solutions should be filtered through a 0.2 μ m filter prior to use, and the procedure is then as follows:

- (a) Place 1.12 mL of 0.2M yttrium or erbium nitrate solution in a vial.
- (b) Add 75 μL of 1M sodium citrate and mix.
- (c) Add 10 mL of saline.
- (d) Add ~ 4 mL of 0.1M NaOH in 100 μL portions, adjust the pH to 7 and wait for 1 min to obtain a proper value of pH before measurement.
- (e) Transfer the vial contents to a 10 mL penicillin vial and incubate at 100°C for 1 h.
- (f) Transfer the contents of the penicillin vial to a 50 mL Falcon vial, add 40 mL of saline and centrifuge at 1500 rev./min for 10 min.
- (g) Remove the supernatant, add 10 mL of saline, mix and take 1 mL for grain size measurement.
- (h) Sterilize the colloid in the autoclave at 121°C for 25 min.
- (i) Take a 1 mL sample for grain size analysis.

The grain size distribution of colloids obtained according to the described procedure [9.23] is shown in Fig. 9.15. Measurements were carried out using a Zetasizer instrument (Zetasizer Nano ZS 3600 manufactured by Malvern Instruments Ltd). The graphs show the mean values from five syntheses. The mean size of yttrium citrate particles was ~ 1500 nm in the range 800–2000 nm.

The mean synthesis yield of yttrium citrate was equal to $87.2\% \pm 6.6\%$ (see Table 9.8).

The mean size of erbium citrate particles is 2000 nm in the range 800–6000 nm, as shown in Fig. 9.16. Sterilization narrows the size range.

9.5.4. Rhenium sulphide

It was experimentally confirmed that the method of synthesis described by Jungfeng et al. [9.24] gave the best product. The ratio of $\text{Na}_2\text{S}_2\text{O}_3:\text{KReO}_4$ concentration was 70:1, with a heating time of 30 min. The grain size was in the range 2–40 μm , with a mean value of 9 μm . The product was amorphous with some content of sulphur. A number of methods were used for characterization of the product, e.g. XRD, X ray fluorescence, atomic force microscopy, scanning electron microscopy, absorption and desorption of N_2 and Raman spectroscopy, and it was found that the particles are porous. The product was non-stoichiometric and contained water and sulphur. A method for determination of free sulphur is necessary. The ratio of reagents used by various authors differs, and the characterization of the final product is generally not given.

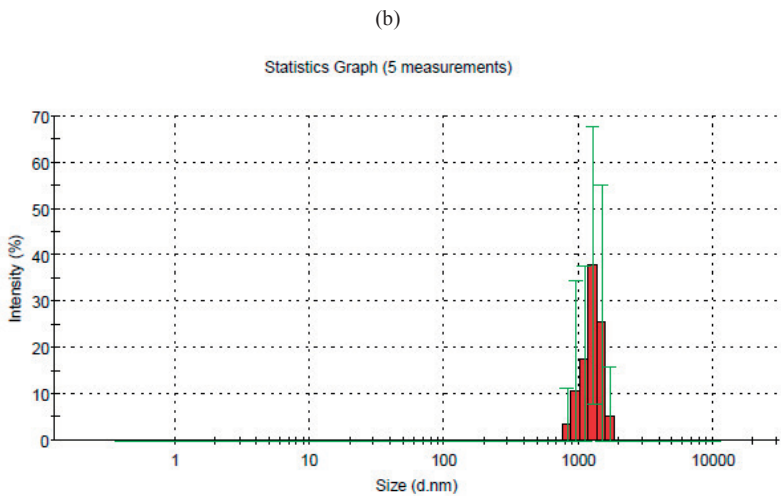
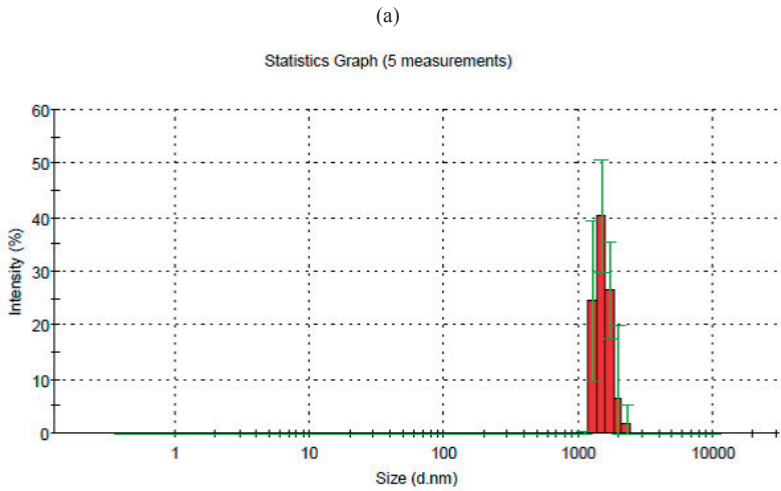


FIG. 9.15. Grain size distribution of yttrium citrate colloids: (a) before centrifugation and (b) after centrifugation.

TABLE 9.8. YTTRIUM-90 CITRATE COLLOID YIELD

Sample No.	Y-90 activity 10 s count	Background 10 s count	Y-90 activity of supernatant 10 s count	Radioactivity in supernatant (%)
1	127 047	212	20 232	15.94
2	66 471	90	2877	4.33
3	31 679	76	5940	18.77
4	23 105	79	4122	17.87
5	1808	76	124.8	7.05

Preparation of colloidal rhenium sulphide was carried out according to Venkatesan et al. [9.25]:

- (a) Put 1 mg of $KReO_4$ in a vial.
- (b) Add 200 mg of $Na_2S_2O_3$.
- (c) Pour 5 mL of H_2O and mix.
- (d) Add 15 mL of 1M HCl to this mixture.
- (e) Heat the vial for 7–10 min at $80^\circ C$ and mix using a magnetic stirrer until the solution becomes black.
- (f) Cool to $4^\circ C$ with cold water.
- (g) Centrifugate for 10 min at 1500 rev./min and remove the supernatant, add the same volume of saline and repeat centrifugation and all operations as above.
- (h) Measure the grain size using the Zetasizer meter.
- (i) Irradiate the mixture with ultrasound for 5 min at 200 W to crush the agglomerates and repeat the measurement of grain size.

The grain size distribution of rhenium heptasulphide colloids is shown in Fig. 9.17. Irradiation of colloids with ultrasound improved the particle distribution. The size ranged from 350 to 3000 nm. The Zetasizer instrument measures the particle size distribution using the Brownian motion phenomenon. The measurement based on non-invasive backscattering lowers the limit of size detection to 0.6 nm. The measured diameter of the colloid particle is a so-called hydrodynamic diameter. This value represents the particle itself and particles of water attracted by this particle having an electric charge. Dialysis of the colloidal

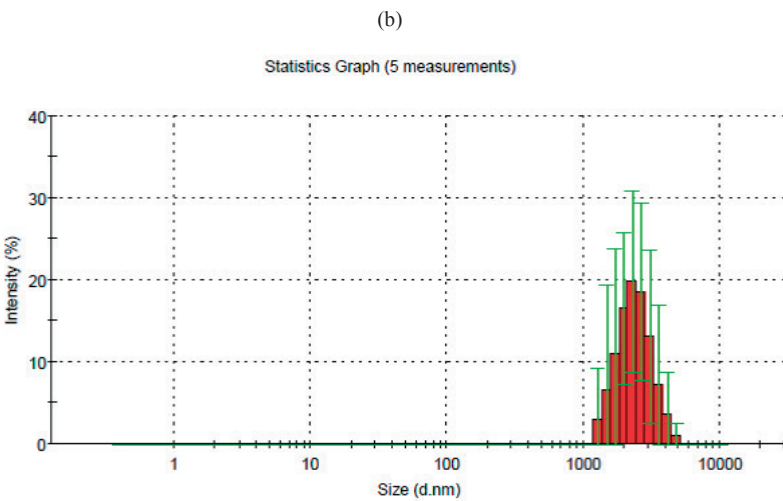
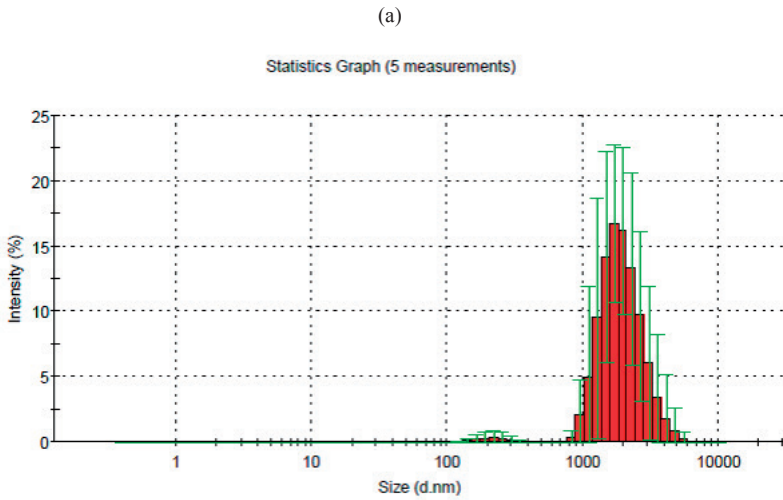


FIG. 9.16. Grain size distribution of erbium citrate: (a) after centrifugation but before sterilization and (b) after sterilization.

suspension resulted in a significant decrease in the measured diameters of the particles. This requires further study, including the measurement of particle diameters using an electron microscope.

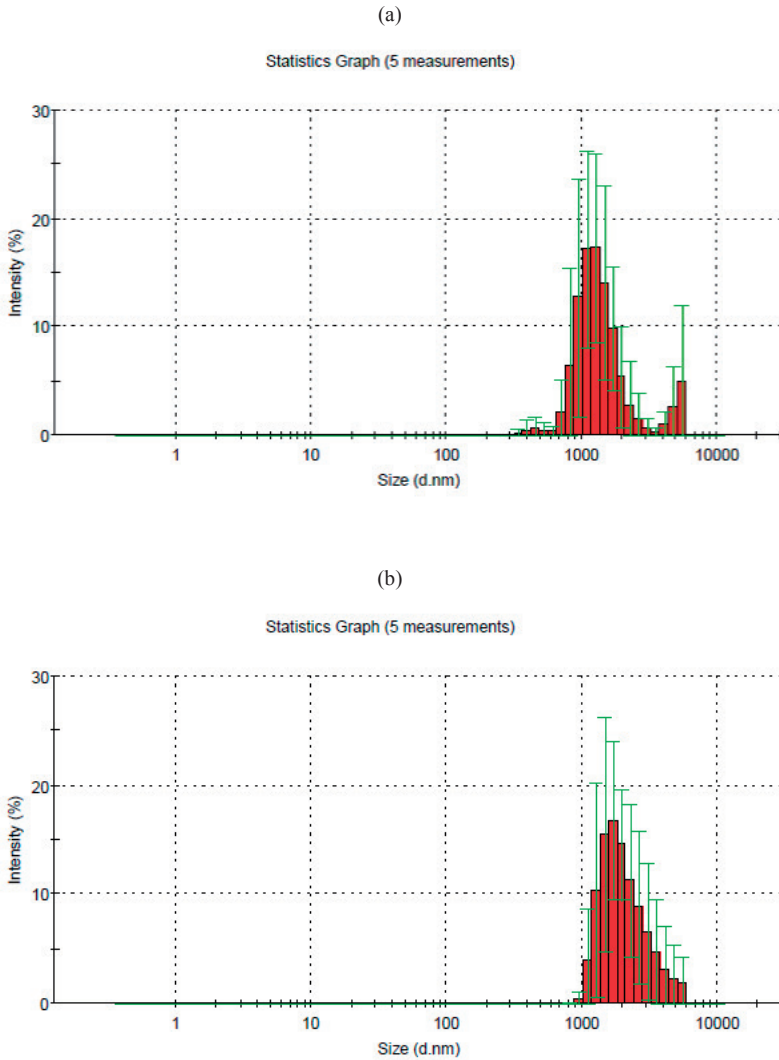


FIG. 9.17. Grain size distribution of rhenium heptasulphide colloids: (a) before ultrasound irradiation and (b) after ultrasound irradiation.

The usefulness of yttrium citrate colloid for radiation synovectomy was evaluated by measuring the ^{90}Y organ distribution in rats after ^{90}Y citrate colloid injection into the knee joint. After 1 h, 98.5% of ^{90}Y administered radioactivity was localized in a joint, as given in Table 9.9. After 24 and 96 h of administration

of ^{90}Y citrate, the amount of radioactivity in the joint was almost constant and close to 83% of the initial administered value, as observed in Table 9.10.

TABLE 9.9. BIODISTRIBUTION AFTER ADMINISTRATION OF ^{90}Y CITRATE COLLOID 1 h AFTER ADMINISTRATION TO THE JOINT IN COMPARISON WITH BIODISTRIBUTION OF ^{90}Y CHLORIDE INJECTION IN THE SAME WAY

Organ	Y-90 chloride ($n = 3$) 1 h p.i.		Y-90 citrate colloid ($n = 3$) 1 h p.i.	
	%ID \pm SD	%ID/g \pm SD	%ID \pm SD	%ID/g \pm SD
Blood		0.41 \pm 0.04		0.01 \pm 0.01
Liver	4.29 \pm 1.62	0.64 \pm 0.36	0.03 \pm 0.01	0.00 \pm 0.00
Kidneys	6.34 \pm 0.64	4.16 \pm 0.54	0.01 \pm 0.01	0.01 \pm 0.01
Spleen	0.21 \pm 0.00	0.39 \pm 0.01	0.00 \pm 0.01	0.01 \pm 0.01
Intestine	2.30 \pm 0.02	0.14 \pm 0.02	0.01 \pm 0.00	0.00 \pm 0.00
Stomach	0.57 \pm 0.07	0.37 \pm 0.09	0.01 \pm 0.01	0.01 \pm 0.00
Tibia	2.96 \pm 0.97	5.56 \pm 1.76	0.00 \pm 0.00	0.01 \pm 0.01
Muscle		0.22 \pm 0.11		0.01 \pm 0.01
Knee joint	39.98 \pm 3.66		98.48 \pm 0.46	
Urine and bladder	7.62 \pm 0.87		0.08 \pm 0.01	
Carcass	33.34 \pm 0.87		1.33 \pm 0.49	

TABLE 9.10. BIODISTRIBUTION AFTER ADMINISTRATION OF ^{90}Y CITRATE COLLOID 24 AND 96 h AFTER ADMINISTRATION TO THE JOINT

Organ	Y-90 citrate colloid ($n = 3$) 24 h p.i.		Y-90 citrate colloid ($n = 3$) 96 h p.i.	
	%ID \pm SD	%ID/g \pm SD	%ID \pm SD	%ID/g \pm SD
Blood		0.01 \pm 0.01		0.02 \pm 0.01
Liver	0.15 \pm 0.10	0.02 \pm 0.02	0.08 \pm 0.03	0.01 \pm 0.15
Kidneys	0.01 \pm 0.01	0.01 \pm 0.01	0.02 \pm 0.03	0.01 \pm 0.01
Spleen	0.02 \pm 0.02	0.05 \pm 0.05	0.04 \pm 0.02	0.13 \pm 0.02
Intestine	0.88 \pm 1.48	0.00 \pm 0.00	0.08 \pm 0.04	0.00 \pm 0.88
Stomach	0.02 \pm 0.03	0.00 \pm 0.00	0.01 \pm 0.02	0.01 \pm 0.02
Tibia	0.30 \pm 0.27	0.55 \pm 0.51	0.02 \pm 0.02	0.05 \pm 0.30
Muscle		0.01 \pm 0.01		0.31 \pm 0.37
Knee joint	82.64 \pm 7.03		83.28 \pm 19.23	
Urine and bladder	1.34 \pm 1.09		1.05 \pm 0.01	
Carcass	14.61 \pm 6.29		15.15 \pm 19.33	

9.6. BIOTINYLATION OF MONOCLONAL ANTIBODIES AND RADIOLABELLING OF BIOTIN AS A TARGET AND EFFECTOR AGENT FOR PRETARGETING STRATEGY IN RADIOIMMUNOTHERAPY OF CANCER

Radioimmunotherapy aims at using MAbs to deliver radionuclides for therapy of cancer. In conventional (direct) radioimmunotherapy, a radioisotope is coupled to a MAb to form a tumour specific target agent [9.26]. However, the blood clearance of the antibodies is slow and tumour to non-tumour ratios of radioactivity in this system are rather low. To increase the target to background ratio, the concept of pretargeting has been proposed. The strategy is based on the

separate administration of the MAb and radiolabel [9.26, 9.27]. Owing to the fact that avidin binds to biotin selectively with extremely high affinity ($K_d = 10^{-15}$), the avidin biotin system was first applied for pretargeting. In the most complex three step avidin biotin system, the antibodies were coupled with biotin, which was used as the primary targeting agent (step 1), this was followed by bridging with avidin (cleaning agent, step 2) and then administration of biotin conjugated effector with radionuclide (step 3).

Within the IAEA CRP Development of Therapeutic Radiopharmaceuticals based on ^{188}Re and ^{90}Y for Radionuclide Therapy, the antibody biotinylation was investigated using MAb rituximab (Roche) and sulpho NHS biotin (Pierce Biotechnology) as the biotinylating agent. Sulpho NHS biotin effectively reacts at pH7–9 with primary amino groups of proteins forming stable amide bonds (see Fig. 9.18). The MAb at concentration 2 mg/mL in PBS was reacted with a 20-fold molar excess of sulpho NHS biotin solution. After 1 h incubation at room temperature, unreacted and hydrolysed biotinylation reagent was removed by dialysis with PBS. The effect of MAb biotinylation was evaluated by adding an aliquot of biotinylated antibody to the mixture of HABA and avidin. The spectrophotometric method of biotin determination is based on the decrease of HABA avidin complex absorbance when HABA is replaced by biotin. The number of biotin molecules conjugated to MAbs using the HABA avidin method was 3.9.

Among the radionuclides for radioimmunotherapy, ^{90}Y is of particular interest owing to its superior properties including pure β emission ($E_{\beta \text{ max}} = 2.2 \text{ MeV}$) and 64.1 h half-life. Bifunctional macrocyclic chelating agents such as DOTA analogues can be complexed by metal ions with high stability [9.28].

Investigation of biotin labelling with ^{90}Y was performed using the conjugate of biotin with DOTA as DOTA biotin sarcosine (Macrocyclics) (see Fig. 9.19).

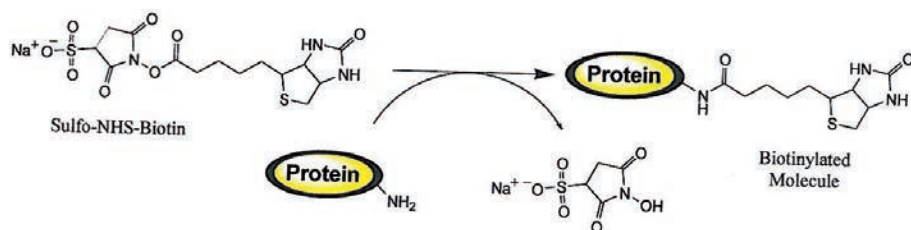


FIG. 9.18. Biotinylation of proteins using sulpho NHS biotin.

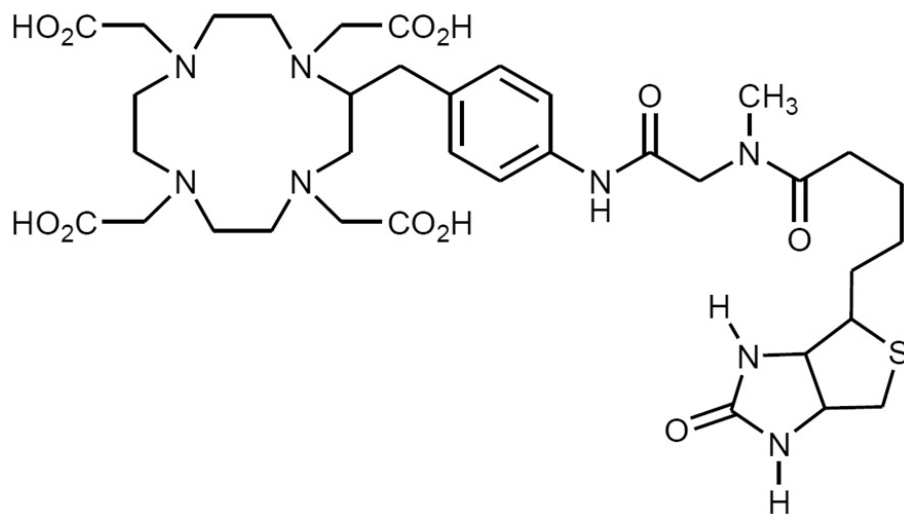


FIG. 9.19. Structure of DOTA biotin sarcosine (DOTA biotin).

DOTA biotin was labelled with ^{90}Y at pH5.5 at 95°C for 30 min. RCP of the ^{90}Y DOTA biotin was investigated after addition of avidin (for binding of labelled biotin) and DTPA (for binding of free ^{90}Y) to the reaction mixture. The specific activity of the resulting radiocompound was 34 MBq/nmol, and the RCP of ^{90}Y DOTA biotin was 99% using TLC analysis and 89% using HPLC analysis (see Fig. 9.20).

In vitro studies with ^{90}Y DOTA biotin in human serum were stable for 3 h at 37°C . Further investigations of the clinical application of the pretargeting approach to radioimmunotherapy are in progress.

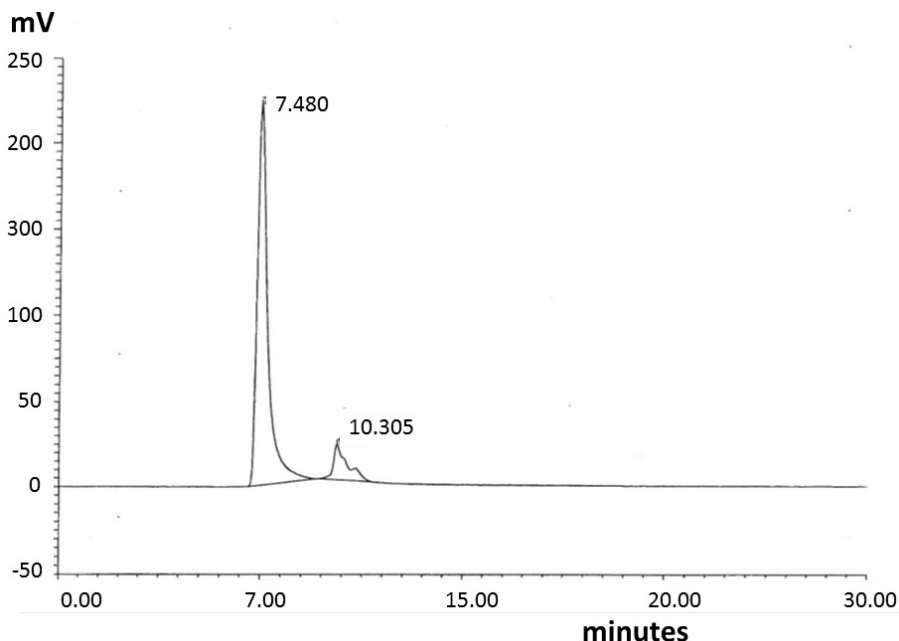


FIG. 9.20. HPLC radiochromatogram of ^{90}Y DOTA biotin avidin and ^{90}Y DTPA.

REFERENCES TO CHAPTER 9

- [9.1] DU, J., CHINOL, M., SAVONEN, A., HILTUNEN, J., Simple and safe production of yttrium-90 from a new type of $^{90}\text{Sr}/^{90}\text{Y}$ generator, *Radiochim. Acta* **93** (2005) 111.
- [9.2] BONARDI, M.L., MARTANO, L., GROPPI, F., CHINOL, M., Rapid determination of ^{90}Sr impurities in freshly "generator eluted" ^{90}Y for radiopharmaceutical preparation, *Appl. Radiat. Isot.* **67** (2009) 1874.
- [9.3] DIETZ, M.L., HORWITZ, E.P., Improved chemistry for the production of yttrium-90 for medical applications, *Appl. Radiat. Isot.* **43** (1992) 1093.
- [9.4] HORWITZ, E.P., McALISTER, D.R., BOND, A.H., BARRANS, R.E., WILLIAMSON, J.M., A process for the separation of ^{177}Lu from neutron irradiated ^{176}Yb targets, *Appl. Radiat. Isot.* **63** (2005) 23.
- [9.5] HORWITZ, E.P., McALISTER, D.R., BOND, A.H., BARRANS, R.E., Jr., Novel extraction of chromatographic resins based on tetraalkyldiglycolamides: Characterization and potential applications, *Solvent Extr. Exch.* **23** (2005) 319.
- [9.6] BLOWER, P.J., et al., Pentavalent rhenium-188 dimercaptosuccinic acid for targeted radiotherapy: Synthesis and preliminary animal and human studies, *Eur. J. Nucl. Med.* **25** (1998) 613.
- [9.7] Monograph 0643: Technetium ($^{99\text{m}}\text{Tc}$) succimer injection, *European Pharmacopoeia*, 5th edn (2005) 865.

- [9.8] WESTERA, G., GADZE, A., HORST, W., A convenient method for the preparation of $^{99m}\text{Tc(V)}$ dimercaptosuccinic acid ($^{99m}\text{Tc(V)}$ -DMSA), *Int. J. Appl. Radiat. Isot.* **36** (1985) 311.
- [9.9] WASHBURN, L.C., BINIAKIEWICZ, D.S., MAXON, H.R., Reliable preparation of $^{99m}\text{Tc(V)}$ DMSA by a simple modified method using a commercial kit for $^{99m}\text{Tc(III)}$ DMSA, *Nucl. Med. Biol.* **22** (1995) 689.
- [9.10] KOTHARI, K., et al., Preparation of [^{186}Re]Re-DMSA and its bio-distribution studies, *Appl. Radiat. Isot.* **51** (1999) 43.
- [9.11] SEIFERT, S., PIETZSCH, H.J., The $^{188}\text{Re(III)}$ -EDTA complex — a multipurpose starting material for the preparation of relevant ^{188}Re complexes under mild conditions, *Appl. Radiat. Isot.* **64** (2006) 223.
- [9.12] RHODES, B.A., ZÖLLE, I., BUCHANAN, J.W., WAGNER, H.N., Radioactive albumin microspheres for studies of the pulmonary circulation, *Radiology* **92** (1969) 1453.
- [9.13] ZOLLE, I., RHODES, B.A., WAGNER, H.N., Jr., Preparation of metabolizable radioactive human serum albumin microspheres for studies of the circulation, *Int. J. Appl. Rad. Isot.* **21** (1970) 155.
- [9.14] EVANS, R.L., United States patent no. 663.687 (16.05.1972).
- [9.15] NIJSEN, J.F.W., et al., Advances in nuclear oncology: Microspheres for internal radionuclide therapy of liver tumours, *Curr. Med. Chem.* **9** (2002) 73.
- [9.16] European Pharmacopoeia, 7th Edition, Monograph 0570: Technetium (^{99m}Tc) Human Albumin Microspheres Injection (2011).
- [9.17] SALEM, R., THURSTON, K.G., Radioembolization with ^{90}Y trium microspheres: A state-of-the-art brachytherapy treatment for primary and secondary liver malignancies: Part 1: Technical and methodologic considerations, *J. Vasc. Interv. Radiol.* **17** (2006) 1251.
- [9.18] SALEM, R., et al., Treatment of unresectable hepatocellular carcinoma with use of ^{90}Y microspheres (TheraSphere): Safety, tumor response and survival, *J. Vasc. Interv. Radiol.* **16** (2005) 1627.
- [9.19] RHODES, B.A., STERN, H.S., BUCHANAN, J.A., ZOLLE, I., WAGNER, H.N., Lung scanning with ^{99m}Tc -microspheres, *Radiology* **99** (1971) 613.
- [9.20] WUNDERLICH, G., et al., Preparation and biodistribution of rhenium-188 labelled albumin microspheres B 20: A promising new agent for radiotherapy, *Appl. Radiat. Isot.* **52** (2000) 63.
- [9.21] WUNDERLICH, G., DREWS, A., KOTZERKE, J., A kit for labeling of [^{188}Re] human serum albumin microspheres for therapeutic use in nuclear medicine, *Appl. Radiat. Isot.* **62** (2005) 915.
- [9.22] SCHILLER, E., et al., Yttrium-86-labelled human serum albumin microspheres: Relation of surface structure with in vivo stability, *Nucl. Med. Biol.* **35** (2) (2008) 227.
- [9.23] AUNGURARAT, A., DANGPRASERT, M., PHUMKEM, S., Yttrium-90 labelled compound for radiation synovectomy, *Proceedings of the Conference on Nuclear Science and Technology*, 16–17 August 2007, Bangkok, Thailand, p. 10.

- [9.24] JUNGFENG, Y., et al., [¹⁸⁸Re]Rhenium sulfide suspension: A potential radiopharmaceutical for tumor treatment following intra-tumor injection, *Nucl. Med. Biol.* **26** (1999) 573.
- [9.25] VENKATESAN, P.P., SHORTKROFF, S., ZALUTSKY, M.R., SLEDGE, C.B., Rhenium heptasulfide: A potential carrier system for radiation synovectomy, *Nucl. Med. Biol.* **17** (1990) 357.
- [9.26] PAGANELLI, G., et al., Pilot therapy trial of CEA positive tumors using a three step pretargeting approach, *Tumor Target.* **3** (1998) 96.
- [9.27] PAGANELLI, G., CHINOL, M., Radioimmunotherapy: Is avidin–biotin pretargeting the preferred choice among pretargeting methods? *Eur. J. Nucl. Med. Mol. Imaging* **30** (2003) 773.
- [9.28] GOODWIN, D.A., MEARES, C.F., OSEN, M., Biological properties of biotin-chelate conjugates for pretargeted diagnosis and therapy with the avidin/biotin system, *J. Nucl. Med.* **39** (1998) 1813.

Chapter 10

DEVELOPMENT, PREPARATION AND QUALITY ASSURANCE OF RADIOPHARMACEUTICALS BASED ON ^{188}Re AND ^{90}Y FOR RADIONUCLIDE THERAPY: IN HOUSE PRODUCTION OF RADIOISOTOPES AT VINČA INSTITUTE OF NUCLEAR SCIENCES

D. DJOKIĆ, N.S. NIKOLIĆ, D.L. JANKOVIĆ,
S.D. VRANJEŠ-DJURIĆ, D.Ž. PETROVIĆ

Laboratory for Radioisotopes,
Vinča Institute of Nuclear Sciences,
University of Belgrade,
Belgrade, Serbia

Abstract

The objective of the project described in this chapter was the development of different radiolabelled compounds with ^{188}Re and ^{90}Y and optimization of labelling procedures. Four different groups of compounds were evaluated as follows: different polyphosphonates (HEDP, MDP and (2-hydroxy-3,4-dioxopentyl) phosphate (DPD)) and DMSA; HA particles; colloids like antimony trisulphide and tin colloid for radiosynovectomy and/or HCC; and biodegradable microspheres of HSA for HCC. During the project, the work was focused on the development of a $^{90}\text{Sr}/^{90}\text{Y}$ electrochemical generator, quality control methods for radionuclidic purity of ^{90}Y , use of ^{90}Y for radiometallation of a DOTA conjugated somatostatin analogue, [DOTA, Tyr3] octreotate, and preparation of ^{90}Y DOTATATE for peptide receptor radionuclide therapy (PRRT). In vitro and in vivo evaluation of the labelled molecules and collection of data of promising radiotracers for clinical trials were also carried out.

10.1. INTRODUCTION

In recent years, the use of compounds labelled with radionuclides for therapeutic treatment in the medical field has grown considerably [10.1–10.3]. Radiopharmaceuticals are increasingly used for cancer therapy, pain palliation because of bone metastasis and for the treatment of rheumatoid arthritis. Targeted radionuclide therapy involves the specific deposition of β emitting radionuclides in malignant tumours via labelled ligands that specifically bind to tumour cells, and it has been found effective in treatment for pain palliation. Several classes of chelating ligands are being evaluated for therapy, and simple effective methods

are available. Therapeutic radiopharmaceuticals, based on radionuclides decaying by the emission of β particles, are preferred in most of these applications.

The radioisotopes ^{186}Re and ^{188}Re have favourable properties for therapy [10.4]. They decay through the emission of high energy β particles and the emission of γ photons (^{186}Re : $T_{1/2} = 90$ h, $E_{\beta} = 1.1$ MeV, $E_{\gamma} = 137$ keV (~10%); ^{188}Re : $T_{1/2} = 16.7$ h, $E_{\beta} = 2.1$ MeV, $E_{\gamma} = 155$ keV (~15%)), which allows evaluation of the in vivo biodistribution of Re radiopharmaceuticals using a gamma camera. While ^{186}Re is a reactor produced radioisotope, ^{188}Re can be obtained from a $^{188}\text{W}/^{188}\text{Re}$ radionuclide generator system. The chemistry of rhenium resembles that of technetium. Rhenium-188 is a very attractive radioisotope for systematic radiotherapy, with some key advantages, especially because it can be obtained from a transportable $^{188}\text{W}/^{188}\text{Re}$ generator.

Currently, the radioisotope ^{90}Y is widely used for therapy. It can be obtained from the decay of ^{90}Sr , which is, in turn, a high yield fission product. Yttrium-90 is a pure high energy β particle emitter, with $E_{\beta\text{max}} = 2.2$ MeV and $T_{1/2} = 64.1$ h. Furthermore, the path length of its β particles ($r_{95} = 5.9$ mm) in tissues is a major advantage in the treatment of solid tumours. In fact, higher particle energies and longer penetration ranges in tissues could be of crucial help in the treatment of large tumours.

10.2. RHENIUM-188 LABELLED BONE SEEKING AND TUMOUR SPECIFIC AGENTS FOR RADIONUCLIDE THERAPY

10.2.1. Preparation of ^{186}Re HEDP

10.2.1.1. Materials and methods

Rhenium-186 was prepared by irradiation of 1–4 mg of metallic rhenium target (3.6 mg of natural rhenium irradiated for 1 d at a neutron flux of 5×10^{13} neutrons \cdot cm $^{-2}$ \cdot s $^{-1}$) in the nuclear reactor at the National Centre for Scientific Research ‘Demokritos’ (Greece). The irradiated target, with an activity of 62 mCi, was dissolved in 0.5–2 mL of hydrogen peroxide acid for 2 h and subsequently evaporated to dryness. The residue was dissolved in water for injection. The RCP of $^{186}\text{ReO}_4^-$ (ITLC SG methylethylketone) was >99%.

A solution of $^{186}\text{ReO}_4^-$ (2.2 mL containing 0.5–2 mCi of ^{186}Re in 0.052–0.150 mg of metallic rhenium) was then transferred to a vial containing HEDP. Three different samples of ^{186}Re HEDP, labelled as A, B and C, were prepared with 52, 113 and 150 μg of metallic rhenium, respectively. For this purpose, the standard kit prepared at Demokritos was modified, wherein the pH of HEDP solutions was adjusted to 2.0–2.5 (labelling was performed at

acidic pH) and the vial heated for 30 min in boiling water. On cooling, sodium acetate buffer, pH8.7, was added, and the solution was filtered and dispensed into sterile vials using a 0.22 µm sterile filter.

The RCP of ^{186}Re HEDP was determined using ITLC SG and Whatman 3MM strips as the stationary phase and two solvent systems as the mobile phase (methylethylketone and aqueous etidronate solution), whereby both free perrhenate and reduced hydrolysed rhenium could be identified.

For biodistribution studies, after dilution, 0.3 mL of ^{186}Re HEDP was administered to Wistar rats. A first group of animals was sacrificed at 1 h p.i. and another at 24 h p.i. The organs of interest were dissected and the radioactivity measured using a γ counter.

10.2.1.2. Results

Table 10.1 reports results of RCP tests. The compound ^{186}Re HEDP showed high RCP ($\geq 95\%$ at 30 min and $\geq 98\%$ at 24 h after labelling).

The ^{186}Re HEDP (vial C) was diluted with saline (dilutions 1:5 and 1:10, respectively) for biodistribution and stability studies. These results have shown that ^{186}Re HEDP has a high stability with only 2.04% of residual $^{186}\text{ReO}_4^-$ and 1.02% of residual $^{186}\text{ReO}_2$.

Biodistribution studies were performed with a diluted vial C at 1 and 24 h p.i., and the results are presented in Fig. 10.1 and Table 10.2 for the skeleton and total urine in terms of the percentage of injected dose per organ (%ID/organ).

10.2.1.3. Conclusion

The compound ^{186}Re HEDP was prepared at Vinča Institute of Nuclear Sciences at a high yield and high RCP, and showed high uptake in bones and low uptake in other tissues, with a fast urinary clearance. Hence, this method is convenient to use for the preparation of the radiopharmaceutical for clinical use.

TABLE 10.1. RCP OF ^{186}Re HEDP (%) 30 MIN AFTER LABELLING

Compound	Vial A (52 µg Re_{metal})	Vial B (113 µg Re_{metal})	Vial C (150 µg Re_{metal})
Re-186 HEDP	96.7	96.0	99.26
Re-186(O_4) ⁻	3.0	3.7	0.38
Re-186(O_2)	0.3	0.3	0.36

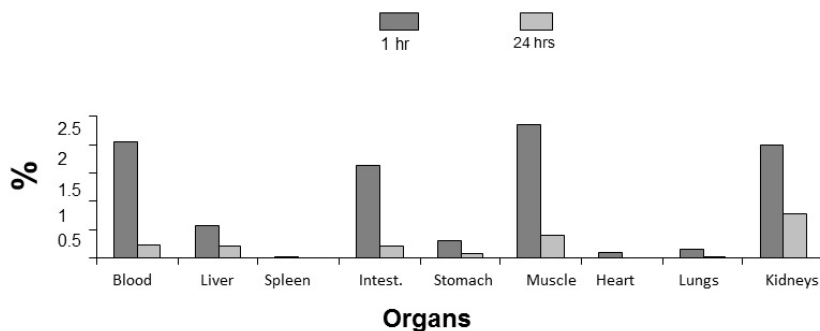


FIG. 10.1. Biodistribution results of ¹⁸⁶Re HEDP in healthy rats (%ID/organ).

TABLE 10.2. BIODISTRIBUTION RESULTS OF ¹⁸⁶Re HEDP IN HEALTHY RATS (%ID/ORGAN)

Organ	Time (h p.i.)	
	1	24
Bone	27.98	20.88
Urine	60.88	75.17

10.2.2. Preparation of ¹⁸⁸Re(V) DMSA

DMSA labelled with pentavalent oxotechnetium, ^{99m}Tc(V) DMSA, is a high specificity tumour seeking agent that is used for the detection of medullary thyroid carcinoma, soft tissue tumours and metastatic bone lesions. The rhenium analogues are ¹⁸⁶Re(V) DMSA and ¹⁸⁸Re(V) DMSA, which are β emitters. Initial biodistribution studies of ¹⁸⁸Re(V) DMSA have shown that its general pharmacokinetic properties are similar to those of ^{99m}Tc DMSA(V), and hence this agent could be used for targeted radiotherapy of the same tumours, i.e. medullary thyroid carcinoma, bone metastases, soft tissue, and head and neck tumours. In the therapy of medullary thyroid carcinoma, ¹⁸⁸Re(V) DMSA could be an excellent alternative, especially for specific types of tumours that do not show ¹³¹I uptake.

10.2.2.1. *Materials and methods*

(a) Preparation of $^{188}\text{Re(V)}$ DMSA

Rhenium-188, as sodium perrhenate, was obtained by elution from a $^{188}\text{W}/^{188}\text{Re}$ generator (Radioisotope Centre, Institute of Atomic Energy, POLATOM) with saline. The eluate was concentrated to 1 mL by passing 10 mL of eluate serially through an AG 50WX-12 resin (Bio-Rad) in a sample preparation column and a Sep-Pak cartridge (Water-Accell Plus QMA Cartridges). The radioactivity trapped on the latter column was eluted with the required volume (1 mL) of physiological solution and sterilized by filtration. Radionuclidic purity was >99.9%, with a volume activity of >1.85 GBq/cm³ (50 mCi/cm³). For preparation of the kit, meso-DMSA, stannous chloride and ascorbic acid were obtained from Sigma. The DMSA kit was prepared in a lyophilized form under aseptic conditions, in cooperation with the Radioisotope Centre.

Rhenium-188(V) DMSA was prepared using a two vial kit formulation as described in the following:

- Vial No. 1: 22 mg of DMSA was dissolved in 11 mL of 0.05M carbonate buffer (pH9.0). The solution was purged with nitrogen for at least 1 min and then filtered through a membrane filter (0.22 μm , Millipore). A 1 mL aliquot of the filtrate was withdrawn and lyophilized.
- Vial No. 2: 44 mg of SnCl_2 was dissolved in 22 mL of 1M HCl and purged with nitrogen for 1 min. The solution was filtered through a membrane filter (0.22 μm) and divided into 2 mL aliquots.

Labelling of the DMSA kit with perrhenate was done by adding and mixing 11 mL eluate of $^{188}\text{ReO}_4^-$ solution (800–950 MBq) to vial No. 1. To this, 1 mL of solution from vial No. 2 was added and mixed. Labelling was done by heating the solution for 30 min at 95°C. After cooling, the solution was filtered through a 0.22 μm filter into an evacuated vial to remove any particulates and also to effect terminal sterilization. This solution could be used for animal or human studies within 30 min after turning off heating. The pH of the final solution was in the range 1.0–1.5, which was adjusted to 7.5–8.0 with carbonate buffer before use in animal or human studies. The effects of various parameters, such as concentration, pH, temperature, reaction time, volume and labelling yield, were evaluated.

(b) Quality control of $^{188}\text{Re(V)}$ DMSA

(i) RCP:

- TLC was performed using SG strips (TLC, Kieselgel 60 F₂₅₄, Merck) with different systems: (i) N-butanol:acetic acid:water (3:2:3), (ii) N-propanol:acetic acid:water (4:1:1), (iii) N-propanol:acetic acid (3:1) and (iv) N-propanol:acetic acid:water (4:1:3). The ITLC chromatograms were analysed by cutting the strips into segments of 1 cm and, then measuring the radioactivity in a well type NaI(Tl) γ counter (Wallac Comp Gamma Counter LKB).
- The labelled samples were analysed using RP HPLC (column Hamilton PRP-1, 250 mm, with a gradient elution system comprising 0.1% trifluoroacetic acid in water (solvent A) and 0.1% trifluoroacetic acid in ACN (solvent B)). The flow rate was adjusted to 2 mL/min and the gradient was as follows: 0–1 min, 0% B; 1–8 min, 0–50% B; 8–15 min, 50% B; 15–19 min, 50–0% B; 19–24 min, 0% B. The eluate was continuously analysed serially using UV–visible absorbance and γ ray detection.

(ii) In vitro stability:

- In vitro stability of $^{188}\text{Re(V)}$ DMSA was determined under optimal conditions for 4 h at room temperature using TLC and HPLC.

In vivo studies:

- Biodistribution studies of $^{188}\text{Re(V)}$ DMSA were performed in male Wistar rats. A volume of 0.2 mL (21.5 MBq) was injected through the tail vein and rats were sacrificed at 1 h p.i. Five rats were used for each preparation. The tissues and organs were excised, rinsed with saline, weighed and counted. Distribution of the activity in different organs was calculated as the percentage of injected dose per gram, as well as the percentage of injected dose per organ.

(iii) Human studies with $^{188}\text{Re(V)}$ DMSA:

- Therapeutic administration was carried out according to the protocol developed by V. Papantoniou from the Nuclear Medicine Department of Alexandra University Hospital (Greece). Before administration of $^{188}\text{Re(V)}$ DMSA, two patients were subjected to whole body scintigraphy and scintimammography for localization of primary and metastatic lesions.

Using a semiquantitative method, the tumour to background ratio was calculated and the retention index determined.

10.2.2.2. Results and discussion

The production of $^{188}\text{Re(V)}$ DMSA was performed using a simple freeze-dried kit formulation that could be easily labelled with ^{188}Re . The kit contained higher amounts of DMSA and SnCl_2 compared to the kit for the preparation of $^{99\text{m}}\text{Tc(III)}$ DMSA, which is a radiopharmaceutical used for kidney imaging.

Quality control by TLC SG using N-propanol:water:acetic acid (4:3:1) as the solvent was found to be more effective than using these solvents without water. Hydrolysed ^{188}Re (if present) was expected to remain at the origin ($R_f = 0$), while $^{188}\text{ReO}_4^-$ moved towards the solvent front and the R_f value of the final complex was ~ 0.6 . TLC SG and gave much better separation patterns of radiochemical species than ITLC SG.

The $^{188}\text{Re(V)}$ meso-DMSA complex was obtained with $>99\%$ radiochemical yield at an optimum pH in the range 1.0–1.5. The yield decreased by increasing the pH beyond 1.5. The complex was stable for 4 h at room temperature without any detectable decomposition. Table 10.3 presents biodistribution results in rats.

TABLE 10.3. BIODISTRIBUTION OF $^{188}\text{Re(V)}$ DMSA IN WISTAR RATS (1 h p.i., $n = 5$, MEAN BODY MASS = 192 ± 9 g)

Organ	Biodistribution (%ID/organ)
Blood ^a	0.34 ± 0.04
Liver	1.3 ± 0.1
Stomach	0.3 ± 0.1
Lung	0.5 ± 0.2
Kidney	2.1 ± 0.2
Femur (thigh bone)	0.9 ± 0.1
Urine	46.0 ± 2.4
Rest body	32.3 ± 2.7

^a %ID/g.

A case study was conducted in a 30 year old female patient diagnosed with medullary thyroid carcinoma. Whole body SPECT and targeted scintigraphy were performed by M. Matović, Department of Nuclear Medicine, Clinical Center Kragujevac (Serbia). Scintigraphic images were collected after administration of the somatostatin radiolabelled analogue ^{99m}Tc tektrotyd and of $^{188}\text{Re(V)}$ DMSA, as shown in Fig. 10.2. By semiquantitative methods, it was found that there were several larger zones of intensive accumulation and pathological accumulation of ^{99m}Tc tektrotyd in retrosternal or mediastinum, which fitted well with the earlier surveys of areas visualized using SPECT/computed tomography (CT) with $^{99m}\text{Tc(V)}$ DMSA and $^{188}\text{Re(V)}$ DMSA. The described changes corresponded to areas with underlying disease. The intensity of accumulation of the somatostatin analogue was consistent with lesions corresponding to grades II–III, thus indicating a relatively high expression of somatostatin receptors.

Scintigraphic imaging of the whole body as well as target scintigraphy were carried out 1.5, 3 and 12 h after administration of 3.20 GBq $^{188}\text{Re(V)}$ DMSA (see Fig. 10.3).

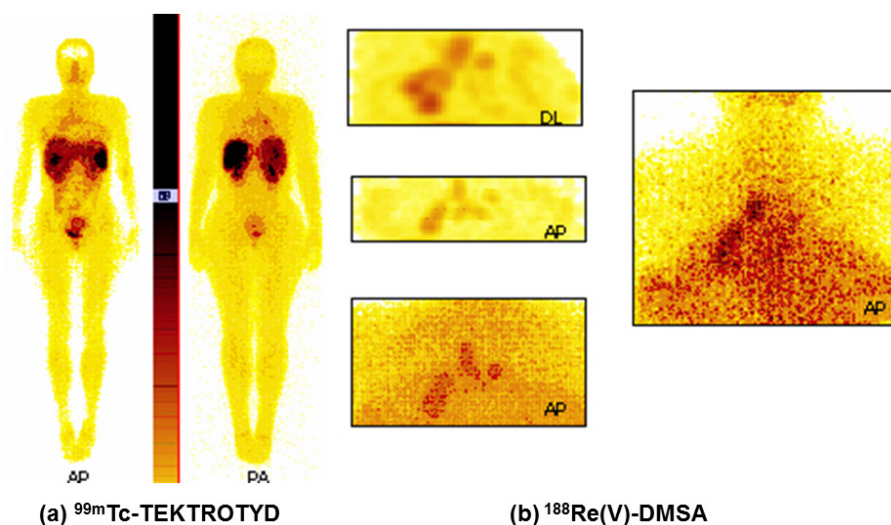
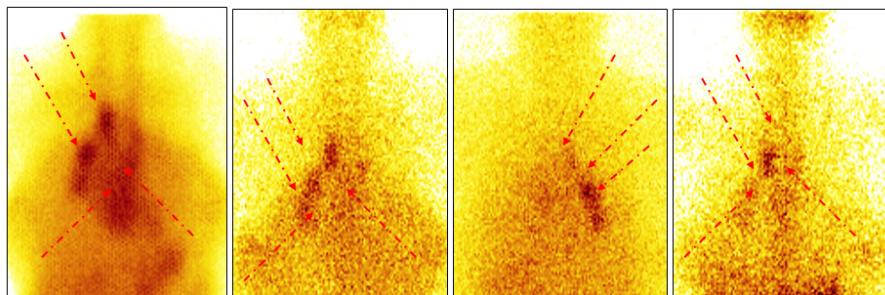


FIG. 10.2. Whole body, SPECT and target scintigraphy: (a) ^{99m}Tc tektrotyd and (b) $^{188}\text{Re(V)}$ DMSA.



AP after 1.5 h p.i. AP after 3 h p.i. PA after 3 h p.i. AP after 12 h p.i.

FIG. 10.3. Whole body, SPECT and target scintigraphy with $^{188}\text{Re}(\text{V})$ DMSA. AP: anteroposterior view, PA: posteroanterior view.

After evaluation of the results, it could be concluded that the visualization of a few hot spots with increased uptake of $^{188}\text{Re}(\text{V})$ DMSA in the mediastinum was in accordance with PET/CT results.

10.2.2.3. Conclusion

The kit formulation provides a convenient method for preparation of $^{188}\text{Re}(\text{V})$ DMSA for clinical use. This method is easily applicable in nuclear medicine laboratories. Because significant uptake of $^{188}\text{Re}(\text{V})$ DMSA is observed in tumours and in metastases, this agent should show good potential as a therapeutic agent.

10.3. YTTRIUM-90 LABELLED BONE SEEKING AND TUMOUR SPECIFIC AGENTS FOR RADIONUCLIDE THERAPY

10.3.1. Preparation of ^{90}Y complexes with HEDP, MDP and DPD

The objective of these studies was to investigate the possibility of ^{90}Y complexation with the polyphosphonate ligands MDP, HEDP and DPD. The labelling of polyphosphonate ligands was carried out using varying experimental parameters such as ligand concentration, pH, reaction time and reaction temperature. Analysis of the complexes included determination of RCP (ITLC, paper chromatography and HPLC), in vitro stability studies of ^{90}Y complexes and biodistribution studies in healthy male Wistar rats [10.5].

10.3.1.1. Materials and methods

A direct labelling method was optimized by varying HEDP, MDP and DPD concentration, pH of the labelling mixture, reaction temperature and reaction time. The stock solution of polyphosphonate ligands was prepared by dissolving the desired ligand (concentration 0.01–10 mg/mL) in double distilled water. Then, the appropriate amount of ^{90}Y chloride solution (~ 370 MBq per vial) was added. The pH values of the resulting reaction mixtures were adjusted to 6.5–7.5. The total reaction volume in each vial was kept at 3 mL. Ascorbic acid (10 mg) was used as the radiolytic stabilizer in all samples. The steps followed were:

- *RCP studies*: ITLC SG, mobile phase, 0.9% NaCl or CH_3OH ($R_f = 0.9$ – 1.0 for free $^{90}\text{Y}^{3+}$ and $R_f = 0.0$ – 0.2 for the ^{90}Y complex).
- *Serum stability studies*: Stability of ^{90}Y HEDP, ^{90}Y MDP and ^{90}Y DPD in human serum was assessed by measuring the release of ^{90}Y from the complex at 37°C over a period of 10 d.
- *Organ distribution studies*: Experiments were done as a distribution per organ of animals (healthy male Wistar rats). Major tissues of the body were removed and assayed for radioactivity. The radioactivity was measured using a NaI(Tl) detector and percentages of injected dose in the tissues were calculated. The results were expressed as percentages of injected activity per organ or gram of tissue for blood, muscle and bone.

10.3.1.2. Results and discussion

The RCP for all ^{90}Y complexes was $>95\%$. The serum stability results showed that the complex was quite stable up to 10 d. There was no significant dissociation of activity from the complex, i.e. $<2.0\%$ of ^{90}Y was released from the complex after 10 d.

The results for organ distribution studies of ^{90}Y complexes are shown in Table 10.4.

The organ distribution study of ^{90}Y HEDP has shown that complexes were largely localized in the skeleton. Similar satisfactory results of ^{90}Y MDP organ distribution in healthy test animals were obtained 24 h after intravenous application with high skeletal uptake and significant activity in the liver and spleen. However, more favourable organ distribution results were obtained for ^{90}Y DPD where the uptake in bone was 11–13%ID/g after 24 h. With a high skeletal uptake and low soft tissue uptake and rapid blood clearance, ^{90}Y DPD complex seems to be an excellent candidate for tumour therapy, as well as for bone palliation.

TABLE 10.4. ORGAN DISTRIBUTION STUDIES OF ^{90}Y MDP, ^{90}Y HEDP AND ^{90}Y DPD (%ID/ORGAN OR %ID/g \pm SD)

Y-90 complexes	Y-90 MDP (pH7.0)	Y-90 HEDP (pH6.5)	Y-90 DPD (pH7.5)
Organ	1 h 24 h p.i.	1 h 24 h p.i.	1 h 24 h p.i.
Blood*	0.206 \pm 0.065 0.057 \pm 0.031	0.469 \pm 0.039 0.038 \pm 0.006	0.251 \pm 0.037 0.115 \pm 0.014
Heart	0.172 \pm 0.065 0.132 \pm 0.044	0.251 \pm 0.033 0.086 \pm 0.014	1.848 \pm 0.672 0.389 \pm 0.078
Lung	0.242 \pm 0.062 0.124 \pm 0.054	0.242 \pm 0.077 0.075 \pm 0.011	1.022 \pm 0.343 0.049 \pm 0.012
Liver	5.424 \pm 0.544 3.225 \pm 0.517	0.253 \pm 0.036 0.182 \pm 0.070	0.174 \pm 0.058 0.153 \pm 0.022
Spleen	1.072 \pm 0.360 1.424 \pm 0.765	0.139 \pm 0.049 0.128 \pm 0.054	1.680 \pm 0.734 0.105 \pm 0.055
Kidney	0.317 \pm 0.065 0.500 \pm 0.191	0.825 \pm 0.151 0.331 \pm 0.083	1.337 \pm 0.0425 0.581 \pm 0.187
Intestines	0.054 \pm 0.011 0.029 \pm 0.011	0.060 \pm 0.006 0.017 \pm 0.002	0.055 \pm 0.011 0.044 \pm 0.009
Stomach	0.417 \pm 0.205 0.199 \pm 0.071	0.204 \pm 0.007 0.114 \pm 0.061	0.253 \pm 0.068 0.161 \pm 0.043
Muscle*	0.170 \pm 0.011 0.144 \pm 0.014	0.227 \pm 0.060 0.111 \pm 0.020	0.092 \pm 0.015 0.024 \pm 0.008
Bone*	2.589 \pm 0.334 6.972 \pm 1.438	4.840 \pm 0.805 5.067 \pm 0.589	13.984 \pm 1.126 11.339 \pm 1.097

* %ID/g

10.3.1.3. Conclusion

The experimental results have shown that ^{90}Y complexes of the different polyphosphonate ligands MDP, DPD and HEDP have high RCP and favourable organ uptake. Hence, they may have potential for use in the palliative treatment of bone metastases. Because one of the objectives was to explore the potential of a therapeutic analogue of $^{99\text{m}}\text{Tc}$ complexes of polyphosphonate ligands MDP,

DPD and HEDP, the encouraging results using ^{90}Y MDP, ^{90}Y DPD and ^{90}Y HEDP gave the impetus to undertake the present study.

10.3.2. Preparation of ^{90}Y complexes of DMSA

The objective of the study was labelling of meso-DMSA with ^{90}Y , whereby a labelled complex for therapy of bone malignancies and for bone pain palliation could be prepared [10.6].

10.3.2.1. Materials and methods

The labelling with ^{90}Y was carried out using varying experimental parameters such as ligand concentration, pH, reaction time and temperature to maximize the labelling yield. The stock solutions of DMSA were prepared with double distilled water. The desired amounts of ligands (0.01–10 mg/mL) were placed in different vials. Then, ~ 370 MBq of ^{90}Y chloride was added to each vial. The pH of the resulting reaction mixtures was adjusted either to 3.0 or 8.0, and maintained at 8.0 using 0.1 mol/dm^3 phosphate buffer. The total reaction volume in each vial was kept at 3 mL. Ascorbic acid (10 mg) was used as the radiolytic stabilizer in all samples. Reagent concentrations and reaction time were optimized at the most suitable pH value.

Analysis of the complexes included RCP (ITLC, paper chromatography and HPLC), determination of pharmacokinetic parameters, serum stability and organ distribution studies in healthy male Wistar rats. Wistar rats weighing 100–120 g ($n = 3\text{--}5$ for each time point) were injected with 0.1 mL (18.5–37.0 MBq) of the labelled complex via the tail vein and then sacrificed at 2 and 24 h p.i.

UV absorption spectra of reference yttrium solutions (metal concentration of 0.50mM) with increasing concentrations of meso-DMSA were collected. A possible molecular structure of the complex ^{90}Y DMSA was proposed according to molecular modelling calculations. Molecular modelling studies were carried out using HyperChem software for Windows (release 6.03).

10.3.2.2. Results and discussion

HPLC radiochromatograms of the labelling mixture showed good separation of ^{90}Y DMSA from free ^{90}Y with retention time $R_t = 5.63$ and 6.55 min, respectively. The stability of the ^{90}Y DMSA complex was studied at various time points. After preparation, ^{90}Y DMSA (with and without ascorbic acid and at pH8.0) was incubated at room temperature for 24 h and the RCP was analysed. Yttrium-90 DMSA solutions, including ascorbic acid as the stabilizer, retained their initial RCP (95%) after 24 h incubation. The serum stability of ^{90}Y DMSA

was assessed by measuring the release of ^{90}Y from the complex at 37°C over a 10 d period. It was found that the complex with ascorbic acid was stable at different time points up to 10 d, with no significant dissociation of activity from the complex ($<5.0\%$ of ^{90}Y activity was released from this complex within 10 d).

The animals were sacrificed at 2 and 24 h p.i., and the results of biodistribution studies of ^{90}Y labelled DMSA at pH3.0 and pH8.0 are reported in Fig. 10.4.

10.3.2.3. Conclusion

RCP and organ distribution studies confirmed that ^{90}Y DMSA could be obtained with a high radiolabelling yield, a high RCP and a satisfactory organ distribution. Hence, ^{90}Y DMSA could be a potential radiopharmaceutical candidate for tumour therapy and for palliative treatment in bone metastases.

10.3.3. Yttrium-90 particulates

10.3.3.1. Preparation of ^{90}Y colloids for radiosynovectomy and HCC: ^{90}Y tin colloid

Radiocolloids, as diagnostic and therapeutic agents, play an important role in nuclear medicine. Radiocolloid properties such as particle size, shape, charge and stability are very significant parameters that determine organ distribution in

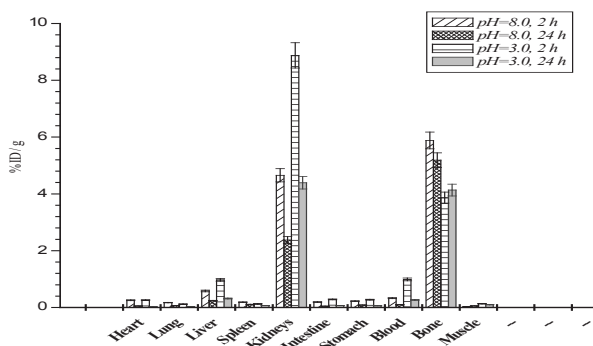


FIG. 10.4. Organ uptake study of ^{90}Y DMSA in healthy male Wistar rats ($n = 3-5\%$, ID/g or tissue).

vivo. In this study, tin colloid particles were labelled with ^{90}Y and characterized, taking into account their physicochemical properties and biological behaviour in rats. The suitability of ^{90}Y labelled tin colloid as a therapeutic radiopharmaceutical for radiosynovectomy and HCC was studied. The factors influencing the labelling yield and particle size distribution of ^{90}Y labelled tin colloid were explored [10.7, 10.8].

(a) Materials and methods

- *Preparation of ^{90}Y tin colloid*: One millilitre aliquots of nitrogen purged water for injection, containing 0.125 mg of tin(II) fluoride (SnF_2 , Cerac Micropure) and different amounts of sodium fluoride (NaF , Cerac Micropure) at $\sim\text{pH}5.5$, were dispensed into vials under nitrogen and lyophilized for 24 h. Shielded vials of the freeze-dried formulations were reconstituted with 5 mL of water for injection. Yttrium-90 labelling was carried out by adding 5–10 μL of $^{90}\text{YCl}_3$ in 0.05M HCl (~ 185 MBq).
- *Radiolabelling yield and RCP*: The labelling efficiency of ^{90}Y colloid particles was studied by conducting several experiments, by varying the different reaction parameters such as NaF concentration, temperature for labelling and incubation time. Radiochemical yields of various formulations were analysed using ITLC with saline as the eluant.
- *In vitro stability studies*: The in vitro stability of ^{90}Y radiolabelled colloid, stored at $2\text{--}8^\circ\text{C}$, was evaluated for a period of 72 h by measuring chromatographically its RCP at different times after preparation (ITLC SG/saline). The stability of ^{90}Y tin colloid in body fluids was assessed by measuring the release of ^{90}Y from the particles at 37°C for 5 d. To check the stability, 0.1 mL of the radiolabelled colloid was incubated with 1 mL of human plasma or human synovial fluid in a CO_2 incubator with 5% CO_2 atmosphere, at 37°C for 5 d. Human plasma and synovial fluid were obtained from normal volunteers and rheumatoid arthritis patients, respectively. The samples were centrifuged at different time points, and then the supernatant was separated and counted to estimate the extent of leaching out of the activity.
- *Particle size analysis*: The in vivo properties of a radiocolloid dispersion were determined by particle size, shape, charge and stability. The study explored the factors influencing the labelling yield and particle size distribution of ^{90}Y labelled tin colloid. Particle size was analysed in undiluted samples, at 20°C , using light scattering photon correlation spectroscopy (PCS), with a Zetasizer Nano ZS apparatus (Malvern Instruments Ltd), measuring particle sizes in the range 0.6 nm–6 μm .

— *Biological studies*: The whole animal study conformed to ethical guidelines and complied with the UK Biotechnology and Biological Sciences Research Council's guidelines on the use of living animals in scientific investigations. The local Animal Experiment Ethical Committee approved the use of animals for these studies. The biodistribution patterns of the labelled colloids prepared under optimized conditions were tested in healthy Wistar male rats (mean weight of 100 g). A volume of 0.1 mL of ^{90}Y colloid prepared with 5 mg of NaF was injected into the tail vein. The rats were sacrificed at different times. Samples of blood and organs were taken and weighed, and the radioactivity counted using a NaI(Tl) well counter under the same geometrical conditions. The percentages of injected dose per gram in each organ and blood were calculated by comparing their activities with appropriate standards of injected dose.

(b) Results and discussion

Radiochemical yields in the presence of the various mixtures of tin(II) fluoride and sodium fluoride increased when the radiolabelling was carried out at higher temperatures. The labelling yield was >97%.

In vitro stability experiments showed that there was no detectable dissociation of ^{90}Y from colloidal particles when stored at 4°C for 72 h, confirming that the metal remained firmly bound to the particles.

In vitro stability studies in body fluids confirmed that <2% and 2.5% of radioactivity leached from labelled tin colloid particles in human plasma and human synovial fluid after 5 d of incubation, respectively. The results are shown in Fig. 10.5.

Under well standardized conditions for preparation, the reproducibility of the particle size and its distribution was within 85–103 nm, which was a value that was considered acceptable.

Biodistribution results are shown in Fig. 10.6. The clearance from the liver was essentially complete within 1 h p.i. The liver uptake significantly decreased from 79.15%ID/organ \pm 3.74%ID/organ at 1 h p.i. to 3.79%ID/organ \pm 0.41%ID/organ at 72 h p.i. for colloids prepared at 95°C. Uptake of the colloid in the lungs and spleen, at 1 h p.i., was 7.95%ID/organ \pm 0.77%ID/organ and 10.57%ID/organ \pm 1.13%ID/organ, respectively. The uptake in other organs was insignificant. The uptake from lungs, spleen, stomach and intestine sharply decreased at 24 h p.i., while uptake by the kidneys, bone and blood increased. However, a significant decrease in whole body activity was confirmed at 72 h.

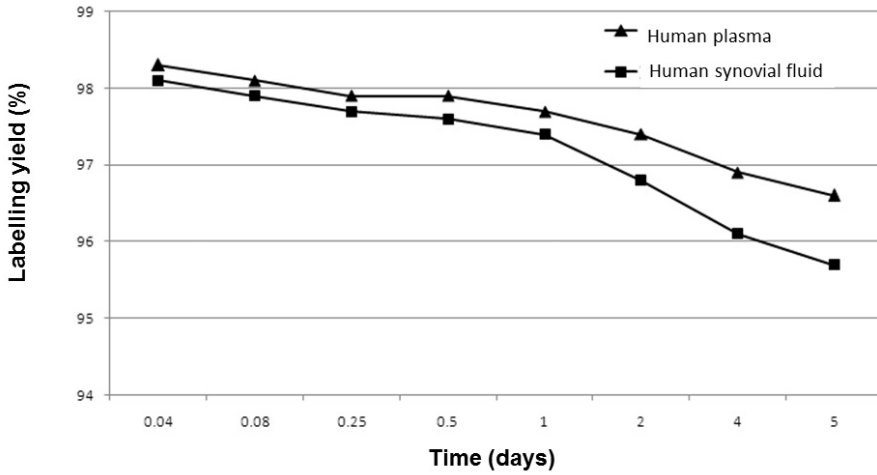


FIG. 10.5. In vitro stability of ⁹⁰Y tin colloids in human plasma and human synovial fluid for a period of 5 d at 37°C.

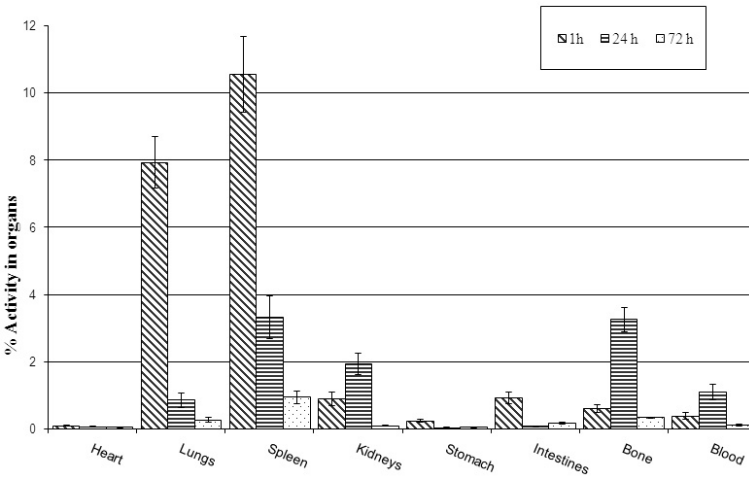


FIG. 10.6. Organ distribution study of ⁹⁰Y tin colloid at 1, 24 and 72 h postintravenous injection (mean ± SD, n = 3).

The synovial space of the rats was observed up to 72 h. There was no leakage into the inguinal lymph node or other lymph nodes. The knee radiopharmaceutical uptake was stable over a period of time. Whole body scans did not show accumulation of activity anywhere in the body (e.g. in the bone

or liver) (see Fig. 10.7). The results of organ distribution after intra-articular application of radiolabelled particles in rats confirmed that ^{90}Y tin colloids could be useful for radiosynovectomy.

10.3.3.2. Preparation of ^{90}Y microspheres of HSA for the treatment of HCC

Internal radionuclide therapy using ^{90}Y labelled microspheres is an alternative radiotherapeutic method for treatment of lung and liver metastases. For this purpose, biodegradable microspheres of HSA were labelled with ^{90}Y either directly or indirectly, by conjugation of DTPA prior to labelling using DTPA cyclic anhydride (cDTPA).

(a) Materials and methods

- *Preparation of ^{90}Y microspheres:* ^{90}Y microspheres were prepared in two different ways. The direct method was carried out by conjugation of DTPA to HSA microspheres followed by radiolabelling of microspheres and cDTPA with ^{90}Y . The indirect method for preparation of radioactive microspheres was conducted by first coupling cDTPA to HSA, followed by radiolabelling with ^{90}Y and, finally, by production of microspheres. The cDTPA was synthesized in house using the method of Eckelman et al. [10.9].
- *Preparation of microspheres and radiolabelling with ^{90}Y :* Albumin microspheres were prepared using the heat stabilized method as detailed in the following. A small amount of 20 wt% aqueous solution of HSA solution was added dropwise to 75 mL of cottonseed oil with continuous stirring.



FIG. 10.7. Scintigraphic image of a rat's knee after 2 h p.i. of ^{90}Y tin colloid.

The temperature of the oil bath was raised slowly to 170°C. The temperature was maintained for 3 h until the microspheres stabilized. The microspheres were filtered from the oil bath, washed twice with acetone and thrice with ether to remove any adherent oil. Washed particles were stored under ambient conditions for a few months without any modification. Particle size analysis was performed using PCS and scanning electron microscopy.

- *Conjugation of DTPA to HSA microspheres*: cDTPA dissolved in DMSO was added to 5–10 mg of the microspheres dissolved in 0.5 mL of 0.1M bicarbonate buffer, at pH8, with vigorous shaking and incubated for 10 min at room temperature. The final molar ratio of DTPA:microspheres was 50:1. The supernatant containing free DTPA was immediately removed by centrifugation at 2000 rev./min for 3 min. The pellet with microspheres conjugated to DTPA was washed with H₂O and then suspended in 1 mL of 0.1M sodium acetate buffer, at pH5.8, for radiolabelling.
- *Radiolabelling of microspheres and cDTPA with ⁹⁰Y*: Albumin microspheres, as well as microspheres conjugated to cDTPA, were suspended by sonication in 1 mL of 0.1M sodium acetate buffer at pH5.8. To this suspension, an appropriate volume of ⁹⁰YCl₃ in 0.05M HCl (37–50 MBq) was added and mixed in a thermomixer at 90°C for 30 min. Radiolabelling yield was determined by filtration of the final ⁹⁰Y microspheres or ⁹⁰Y cDTPA microsphere suspensions through a 0.2 μm nylon syringe filter, which selectively retained the microsphere bound ⁹⁰Y activity.
- *Preparation of radioactive ⁹⁰Y DTPA HSA microspheres*: Coupling of cDTPA to HSA was performed in the following way. The cDTPA in DMSO solution, prepared through a simple one step synthesis, was added to 2 mL of 20% HSA. Coupling was completed in 10 min at room temperature. The coupling was characterized using UV spectroscopy. Free DTPA was removed from DTPA coupled albumin by water dialysis overnight.
- *Radiolabelling with ⁹⁰Y*: An appropriate volume of ⁹⁰YCl₃ in 0.05M HCl (37–50 MBq) was added to a suspension of cDTPA coupled albumin. The suspension was shaken in a thermomixer at 90°C for 30 min. Purification was carried out by gel chromatography using a Sephadex G-25 column (0.8 cm × 30 cm), using water as the eluant. Yttrium-90 cDTPA HSA eluted out after 8 mL, while free ⁹⁰Y³⁺ was retained onto the column.
- *Microsphere preparation*: The method of preparation of radioactive microspheres was similar to the preparation of non-radioactive microspheres.

(b) Results and discussion

Healthy male Wistar rats (300–350 g) were used for imaging studies. A volume of 150 μL of sterile ^{90}Y microspheres (~ 18.5 MBq) was injected intravenously via the tail vein. Yttrium-90 labelled microspheres accumulated in the lungs within 2 h of injection. However, after 72 h, there was a marked reduction in lung activity and accumulation of ^{90}Y microspheres in the bone (see Fig. 10.8). Preliminary results of an organ distribution study for ^{90}Y microsphere cDTPA as well as radioactive ^{90}Y DTPA HSA microspheres have shown that lung uptake remained unchanged 72 h p.i., which further confirmed the stability of ^{90}Y microspheres.

10.3.3.3. Preparation of ^{90}Y colloids for radiosynovectomy: ^{90}Y HA

Radiosynovectomy is a type of radiotherapy used to relieve pain and inflammation in rheumatoid arthritis. Radiosynovectomy involves local intra-articular injection of suitable β emitting radionuclides in the form of radiocolloids or radiolabelled particulates into the affected synovial joints. These β emitting radionuclides penetrate only from fractions of a millimetre to a few millimetres and destroy the inflammatory tissue, thereby reducing swelling and pain. Few radionuclides, namely, ^{166}Ho , ^{153}Sm , ^{90}Y , ^{32}P , ^{198}Au and ^{186}Re , have been identified as potential radionuclides for radiation synovectomy in various

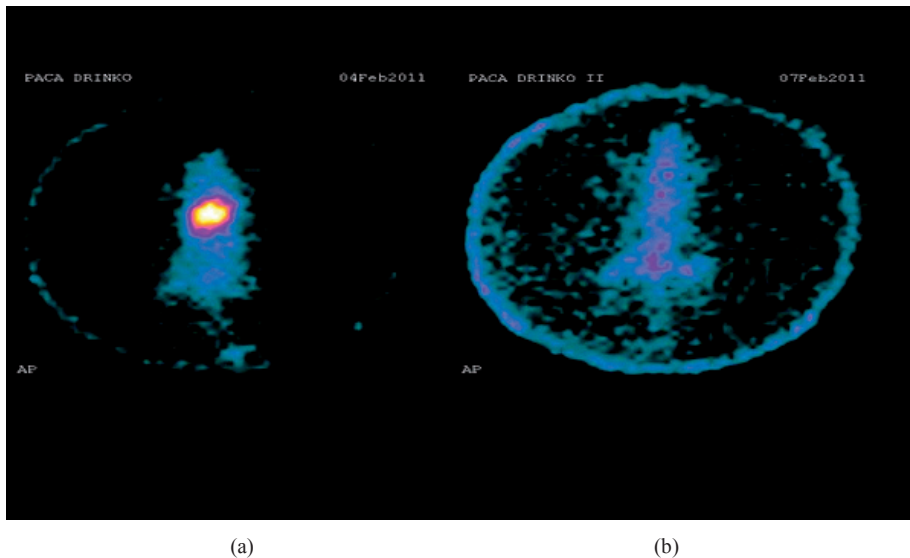


FIG. 10.8. Scintigraphic images of rats at: (a) 2 h p.i. and (b) 72 h p.i. of ^{90}Y microspheres.

particulate forms. Some newer radiopharmaceuticals could also be used for radiosynovectomy.

As a natural constituent of bone, HA was studied as a particulate carrier for β emitting radionuclides in radiation synovectomy. Particles were radiolabelled with ^{90}Y and their in vivo safety was studied following intra-articular injection into knees of normal rats. The objective was to examine the influence of different polyphosphates, such as HEDP, DPD and MDP, as chelators for ^{90}Y in radiolabelled calcium HA particles. In the experiments, HA particles of the 43–74 μm size range were chosen as particulate carriers. The labelling conditions were standardized to give the maximum yield, which ranged between 97% and 99%. The organ distribution studies were performed via two different methods of drug administration, namely, intravenous or intra-articular. The biological behaviour of radiolabelled particles ^{90}Y HA, ^{90}Y HEDP HA, ^{90}Y DPD HA and ^{90}Y MDP HA were compared in animal models.

(a) Materials and methods

Micro HA powder particles and DPD were synthesized in the Laboratory for Radioisotopes, Vinča Institute of Nuclear Sciences. The $^{90}\text{YCl}_3$ in 0.05M HCl was supplied by the Radioisotope Centre, Institute of Atomic Energy, POLATOM. HEDP and MDP were obtained from Sigma-Aldrich. The method is detailed in the following:

- *Preparation of ^{90}Y HA:* To a suspension of 5 mg of HA in 2 mL of double distilled water, 20–30 μL of $^{90}\text{YCl}_3$ (148–185 MBq) was added. The pH was adjusted to 7.0 using 0.5M NaOH. The solution was then thoroughly vortexed and incubated at 37°C for 60 min. The suspension was then centrifuged and the supernatant separated and counted. The radiolabelling yield was determined and the final suspension for injection was reconstituted in 3.0 mL of sterile saline.
- *Preparation of ^{90}Y polyphosphonate HA:* To a solution containing 3 mg of HEDP (DPD or MDP) in 2 mL of double distilled water, 20–30 μL of $^{90}\text{YCl}_3$ (148–185 MBq) was added and the pH was adjusted to 7.0 using 0.5M NaOH. The solutions were heated for 30 min at 95°C. After cooling, 5 mg of HA was added to the formulations and the mixtures were shaken at 37°C for 1 h. Subsequently, the procedure followed the same route as described for the preparation of ^{90}Y HA above.
- *Radiolabelling yield and RCP:* Radiolabelling yield was determined after centrifugation (3500 rev./min for 5 min) and careful separation of the supernatant. Radioactivity was measured for both the supernatant (free ^{90}Y)

and the pellet (particles of HA labelled with ^{90}Y). RCP was determined using paper chromatography with ITLC SG strips in 80% MeOH and saline.

- *In vitro stability studies*: The stability of ^{90}Y labelled particles was studied in saline as well as in 1% human serum at 37°C. Approximately 0.3 mL aliquots of ^{90}Y HA and/or ^{90}Y HEDP HA were dispensed into 1 mL of saline and human serum. After 24 h, 48 h and 5 d, the suspensions were vortexed thoroughly and centrifuged at 2000 rev./min for 5 min. The supernatant was removed and counted for any leakage of radioactivity from the particles.
- *Particle size analysis*: Particle size was analysed in undiluted samples, at 20°C, using a light scattering PCS instrument, Zetasizer Nano ZS (Malvern Instruments Ltd), which measures particles in the size range 0.6 nm–6 μm .
- *Biological studies*: Organ distribution was studied in Wistar rats under anaesthesia, after intravenous or intra-articular injection of ^{90}Y labelled particles.

(b) Results and discussion

Radiolabelling yields in the range 97–99% were achieved in all particle preparations, while RCP was >99%, as confirmed by ITLC SG in saline.

The stability of ^{90}Y labelled particles was studied in saline as well as in 1% human serum at 37°C. Experimental results showed that the ^{90}Y labelled particulates possess excellent in vitro stability with RCP >98% in both media at 37°C after 5 d.

The size distribution of synthesized HA particles (PCS method) is illustrated in Fig. 10.9, which shows that 75.2% of particles had a diameter of 1.37 μm and 24.8% had a diameter of 5.23 μm (average value of 2.73 μm).

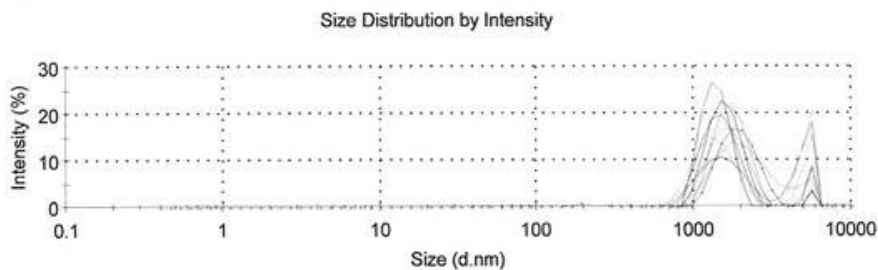


FIG. 10.9. Size distribution of synthesized HA particles (PCS method).

Organ biodistribution studies were performed in healthy Wistar rats (4 weeks old). After intravenous injection through the tail vein, and intra-articular injection, retention of ^{90}Y labelled particles in the animal model was observed up to 72 h. The clearance of ^{90}Y MDP HA particles (see Fig. 10.10) in the lungs reduced from 68.3%ID/g to 56.5%ID/g at 1–72 h, while for ^{90}Y HA, it reduced from 31.2%ID/g to 26.7%ID/g after 1 and 72 h. Furthermore, ^{90}Y HA was found to be less stable with 5.7%ID/g of leached activity accumulating in the bone after 72 h compared to ^{90}Y MDP HA and ^{90}Y DPD HA, which showed negligible activity in the bone after 72 h.

Organ distribution studies in rats were done also after intra-articular injection of ^{90}Y labelled particles, ^{90}Y HA and ^{90}Y polyphosphate HA. The results of intra-articular injected ^{90}Y HA are presented in Fig. 10.11. After intra-articular injection, biodistribution experiments in rats showed almost 99.1% of radioactive particles ^{90}Y and ^{90}Y HA, localized in the synovium for at least 96 h, with no detectable activity in the other organs.

The results demonstrate that the distribution of the radiolabelled particles in the organs depends on the mode of administration. Greater uptake of ^{90}Y HA and ^{90}Y HEDP HA was seen in the liver and spleen when injected intravenously. However, when the radiolabelled particles were administered intra-articularly in rats, almost 99.1% of ^{90}Y HEDP HA and ^{90}Y HA remained localized in the synovium for at least 96 h, with no detectable activity in other organs.

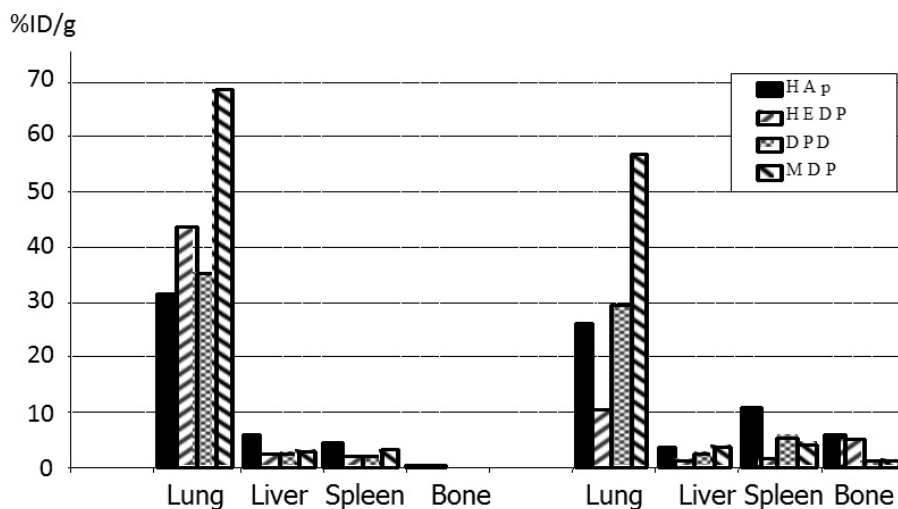


FIG. 10.10. Organ distribution study of ^{90}Y polyphosphate HA at 2 and 72 h after intravenous application (mean \pm SD, n = 3).

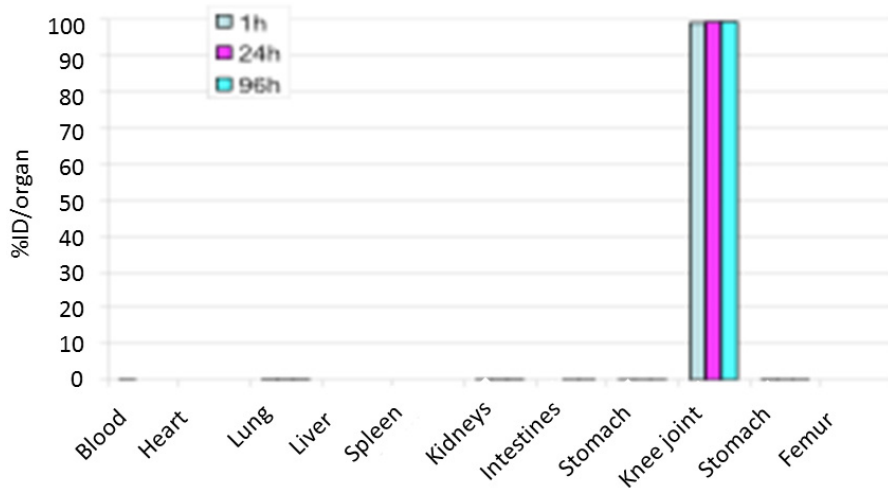


FIG. 10.11. Organ distribution study of ^{90}Y HA after intra-articular application.

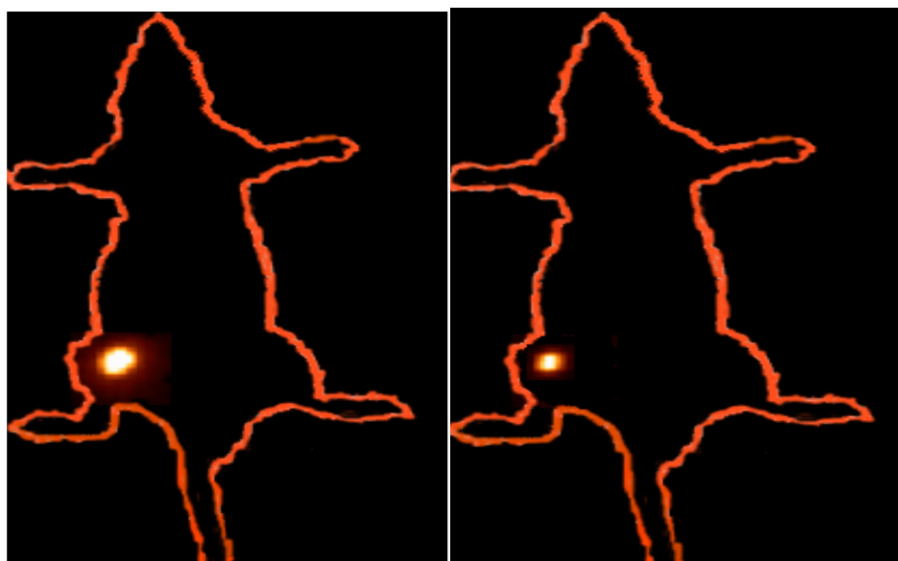


FIG. 10.12. Scintigraphic image of a knee of a rat at 2 h (left) and 72 h (right) after intra-articular injection of ^{90}Y HA.

Scintigraphic images of the knee of a rat at 2 and 72 h after intra-articular application of ^{90}Y HA colloid particles into the knee are shown in Fig. 10.12.

(c) Conclusion

The HA particles used for labelling were synthesized and characterized in the Laboratory for Radioisotopes, Vinča Institute of Nuclear Sciences. The present study has shown that ^{90}Y labelled HA particles could be prepared at a high yield and high RCP, and possess high in vitro stability at 37°C . Biological studies carried out in Wistar rats confirmed retention of injected radioactivity intra-articularly within the synovial cavity of normal animals after 96 h p.i. Stability of ^{90}Y HA complexes increased when polyphosphates such as HEDP, DPD and MDP were used as chelators.

10.3.4. Preparation and quality control of ^{90}Y DOTATATE

Yttrium-90 has been shown to be a very suitable radioisotope for the labelling of the modified somatostatin analogues ($\text{DOTA}^0\text{Phe}^1\text{Tyr}^3$) octreotide (DOTATOC) and ^{90}Y DOTATATE. Hence, ^{90}Y DOTATOC and ^{90}Y DOTATATE have been developed as the next generation of radiolabelled compounds for PRRT [10.10–10.13].

10.3.4.1. Materials and methods

Carrier free $^{90}\text{YCl}_3$ in 0.05M HCl with a radioactive concentration of 89.59 GBq/cm^3 was obtained from the Radioisotope Centre, Institute of Atomic Energy, POLATOM. DOTATATE in lyophilized form was provided by the same institute. The ligand [DOTA Tyr3] octreotate as TFA salt with a chemical purity $>95\%$ was obtained from Pi Chem. All other reagents and solvents were obtained from commercial sources.

Strontium-90 and ^{90}Y activities were measured in an ionization chamber (Capintec CRC-15 beta counting calibrator). For calibrating the ^{90}Y dose, a secondary calibration source of ^{90}Sr was used (radioactive solution ampoule No. BW/21/10/R₃-0.1, with an activity of $368.3 \pm 9.6\text{ kBq/g}$). Low level activity was measured in a NaI(Tl) scintillation counter (Wallac Comp Gamma Counter LKB) by measuring the bremsstrahlung radiation of ^{90}Sr and ^{90}Y . HPLC analysis of ^{90}Y DOTATATE was performed by HPLC (Hewlett Packard 1050) using a UV-visible and gamma flow detector (Raytest Austria GmbH), with an RP C18 column (250 mm \times 4.6 mm). Chromatographic separation was carried out using a SepPak C-18 column (Waters) activated by 95% $\text{C}_2\text{H}_5\text{OH}$.

Bremsstrahlung imaging of whole body scans (256 \times 256 matrix, 8 min acquisition/cm) 24 h after ^{90}Y DOTATATE injection, whole body scans (256 \times 256 matrix, 8 min acquisition/cm) and SPECT were performed using a dual head gamma camera (Siemens).

The procedure was as follows:

- Preparation and labelling of DOTATATE with ^{90}Y : The solution of DOTATATE was prepared under aseptic condition by dissolving [DOTA Tyr3] octreotate in ascorbic acid, at pH4.5. Aliquots of 0.5 mL were dispensed into glass vials and freeze-dried for 24 h. The final lyophilized sample contained 100 μg of DOTATATE and 50 mg of ascorbic acid. Reconstitution of the freeze-dried DOTATATE was done in the same way for DOTATATE obtained from the Radioisotope Centre, Institute of Atomic Energy, POLATOM, and for that prepared at the Laboratory for Radioisotopes, Vinča Institute of Nuclear Sciences. Sterile normal saline (0.5 mL) was added into the vials containing DOTATATE, mixed and then transferred into a vial containing $^{90}\text{YCl}_3$. Labelling of the peptide with ^{90}Y was carried out at 95°C for 30 min with constant stirring, in a temperature controlled heating bath. After 30 min, the vial was cooled with cold water, and acetic acid (50 mg/mL, pH4.5) was added as the stabilizer. The labelled compound was sterile filtered through 0.22 μm membrane filters (Millipore). The radioactivity of ^{90}Y labelled DOTATATE was 2–5.5 GBq per vial for commercial DOTATATE and 37 MBq for the same ligand prepared at Vinča Institute.
- Quality control of ^{90}Y DOTATATE: The RCP of the ^{90}Y labelled DOTATATE was determined using HPLC and solid phase purification using SepPak C-18 mini columns (cartridges). For SepPak purification, a SepPak C-18 mini column was activated with 5 mL of 95% ethanol and then washed with 10–15 mL of normal saline. Approximately 10–20 μL of ^{90}Y DOTATATE dissolved in 500 μL of normal saline was loaded onto the column and eluted first with 5 mL of normal saline (fraction A containing $^{90}\text{Y}^{3+}$) and then with 5 mL of 95% ethanol (fraction B containing ^{90}Y DOTATATE).

10.3.4.2. Results and discussion

A total of 59 batches of commercially available DOTATATE were labelled with $^{90}\text{YCl}_3$ (POLATOM) in a 5 year period. Among them, 53 batches were labelled following the protocol mentioned above in Section 10.4.4.1. RCP of ^{90}Y DOTATATE after SepPak purification showed that 49.0% of batches had RCP $\geq 99.0\%$, 73.6% $\geq 98\%$ and 84.9% $\geq 95.0\%$, whereas only 15.1% of all prepared batches had RCP $\sim 10\%$.

Table 10.5 represents the content of chemical impurities of ^{90}Y expressed in micrograms per millilitre (As, Cu, Fe, Ni, Pb and Zn) that could influence the labelling yield of ^{90}Y DOTATATE. It was observed that the content of the metals

TABLE 10.5. INFLUENCE OF CHEMICAL IMPURITIES ON LABELLING YIELD OF ⁹⁰Y DOTATATE*

Batch No.	Radioactivity (GBq)	RCP (%)	Cu (<1.0 µg/mL)	Ni (<1.0 µg/mL)	As (<1.0 µg/mL)	Pb (<5.0 µg/mL)	Fe (<10.0 µg/mL)	Zn (<10.0 µg/mL)
1/09	3.70	0.71	<0.3	<0.4	<1.0	<0.7	<0.8	8.5
2/09	5.55	0.11	<0.6	<0.6	<0.5	<3.9	1.1	5.6
4/10	3.70	1.52	<1.0	<0.2	<0.7	<1.3	<2.2	<2.5
5/10	3.70	0.29	<0.2	<0.4	<0.8	<0.9	<0.5	<0.3
6/10	5.55	1.10	<0.1	<0.5	<0.8	<0.6	<0.3	<1.0
9/10	3.70	0.51	<0.1	<0.5	<0.9	0.4	<0.3	<1.8
11/10	4.00	1.07	<0.3	<0.2	<0.9	<1.5	<0.2	<0.3
12/10	5.55	0.24	<0.3	<0.6	<1.0	<0.8	<0.2	<0.2
13/10	5.55	3.50	<0.3	<0.3	<1.0	<0.8	<0.1	<0.3
14/10	5.55	1.96	<0.2	<0.3	<0.9	<1.9	1.0	8.3
15/10	3.70	0.08	<0.5	<0.2	<0.8	<1.3	<0.2	<3.6
16/10	5.55	24.16	<0.1	<0.2	<1.0	<2.2	<0.1	<0.7

TABLE 10.5. INFLUENCE OF CHEMICAL IMPURITIES ON LABELLING YIELD OF ⁹⁰Y DOTATATE* (cont.)

Batch No.	Radioactivity (GBq)	RCP (%)	Cu (<1.0 µg/mL)	Ni (<1.0 µg/mL)	As (<1.0 µg/mL)	Pb (<5.0 µg/mL)	Fe (<10.0 µg/mL)	Zn (<10.0 µg/mL)
17/10	5.55	2.40	<0.3	<0.4	<1.0	<0.5	<0.4	<1.3
1/11	3.70	0.84	<0.4	<0.3	<0.4	<2.0	<2.6	<0.2
2/11	5.55	0.44	<0.4	<0.4	<1.0	<0.4	<0.5	<0.1
3/11	5.55	36.30	<1.0	<0.4	<1.0	<2.4	2.1	8.6
4/11	2.75	26.75	0.3	<0.8	<0.8	4.5	5.6	9.4
5/11	5.55	17.4	<0.2	<0.6	<0.9	<2.1	<0.6	<4.8
6/11	5.55	2.02	<0.2	<0.2	<1.0	<0.6	<0.1	<0.1
7/11	1.85	0.12	<0.4	<0.7	<1.0	<1.5	<0.3	<0.1
8/11	5.55	0.22	<0.5	<0.5	<1.0	<2.7	<0.6	<6.7
9/11	3.70	1.6	<0.4	<0.4	<0.8	<1.1	<0.7	<2.6
10/11	5.55	0.11	<0.2	<0.9	<0.5	<0.4	<4.1	<0.2
11/11	5.55	4.58	<0.5	<0.3	<1.0	<1.9	<2.2	<0.1

TABLE 10.5. INFLUENCE OF CHEMICAL IMPURITIES ON LABELLING YIELD OF ⁹⁰Y DOTATATE* (cont.)

Batch No.	Radioactivity (GBq)	RCP (%)	Cu (<1.0 µg/mL)	Ni (<1.0 µg/mL)	As (<1.0 µg/mL)	Pb (<5.0 µg/mL)	Fe (<10.0 µg/mL)	Zn (<10.0 µg/mL)
12/11	5.55	0.81	<0.1	<1.0	<0.8	<0.5	<1.0	<0.4
14/11	5.55	10.47	<0.4	<1.0	<1.0	<3.7	<0.3	<0.4
15/11	2.75	1.25	<0.4	<1.0	<1.0	<3.7	<0.3	<0.4
16/11	5.55	0.12	<0.4	<0.6	<1.0	<1.9	<0.2	<0.4
17/11	3.70	15.47	<0.1	<0.5	<0.4	<0.7	<0.3	<0.3
18/11	2.75	1.1	<0.1	<0.5	<0.4	<0.7	<0.3	<0.3
19/11	5.55	0.98	<0.4	<0.5	<1.0	<2.3	<0.4	<0.1
20/11	5.55	15.74	<0.5	<0.6	<1.0	<1.7	<0.2	<0.1
21/11	2.75	14.02	<0.3	<0.7	<1.0	<4.9	<0.9	<0.8

* DOTATATE and ⁹⁰YCl₃ were obtained from the Radioisotope Centre, Institute of Atomic Energy, POLATOM.

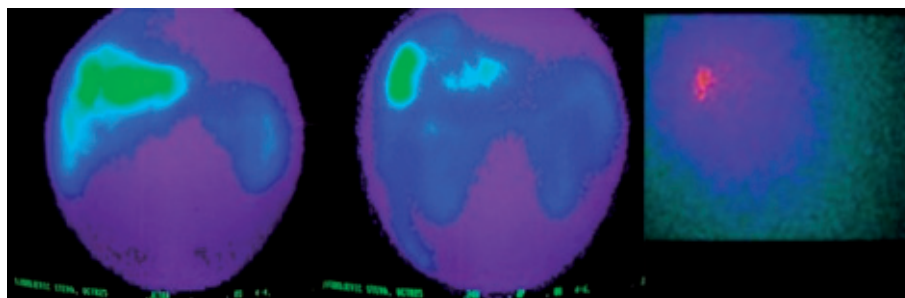
analysed using ICP OES was within the limits suggested by the manufacturer (As, Cu, Ni <1 µg/mL; Pb <5.0 µg/mL; Fe, Zn <10.0 µg/mL). Because $^{90}\text{YCl}_3$ was used for labelling within 4 d after the date of production and quality control, the content of chemical impurities with respect to ^{90}Y increased in time, which was reflected in the results of the quality control for ^{90}Y DOTATATE. It was observed that increasing the content of metals, especially Fe, Pb and Zn, concomitantly raised the percentage of free Y^{3+} . Because >15% of prepared batches had >10% of free Y^{3+} , it was obvious to conclude that in these preparations, the influence of metal ions was remarkable.

For application to patients, batches with RCP >98% without purification were used. The labelling efficiency of ^{90}Y DOTATATE after SepPak purification was $0.79\% \pm 0.58\%$.

A case study was conducted by V. Artiko, Institute of Nuclear Medicine, Clinical Centre of Serbia, Belgrade (Serbia), on a patient affected by characinoid metastases in the liver.

Therapy was carried out with 2.0–4.5 GBq of ^{90}Y DOTATATE per patient, in one cycle, with slow infusion in saline (150 mL/15 min), which lasted 4 h. Mixed amino acids (arginine and lysine) were infused to the patients 30 min prior to therapy. Whole body bremsstrahlung imaging collected 24 h after ^{90}Y DOTATATE administration, and SPECT imaging with ^{111}In pentetreotide and $^{99\text{m}}\text{Tc}$ tin colloid were performed using a dual head gamma camera, as shown in Fig. 10.13.

In a few areas where there was impairment of liver uptake of $^{99\text{m}}\text{Tc}$ tin colloids (greater in the lateral and medial part of the right upper lobe and less in the lower edge of the left lobe), there was an increased accumulation of ^{111}In pentetreotide and the therapeutic radiopharmaceutical ^{90}Y DOTATATE that bind to somatostatin receptors.

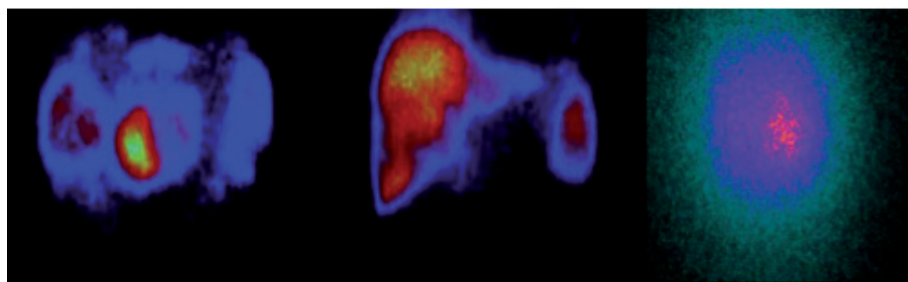


(a) Tc-99m tin colloid

(b) In-111 pentetreotide

(c) Y-90 DOTATATE

FIG. 10.13. SPECT imaging (a and b) and whole body bremsstrahlung imaging (c).



In-111 pentetretotide

Tc-99m tin colloid

Y-90 DOTATATE

FIG. 10.14. Anterior planar images of uptake by ^{111}In pentetretotide, $^{99\text{m}}\text{Tc}$ tin colloid and ^{90}Y DOTATATE in the same patient.

Anterior scintigraphy carried out using the somatostatin analogue ^{111}In pentetretotide, $^{99\text{m}}\text{Tc}$ tin colloid and bremsstrahlung radiation after the administration of therapeutic doses of ^{90}Y DOTATATE were performed in the same patients (see Fig. 10.14) and showed the following information: (i) high accumulation of pentetretotide visible in the middle region corresponded to the primary tumours in the pancreas (carcinoid), and smaller surrounding areas were associated with metastases in the liver and retroperitoneal lymph nodes; (ii) areas in the liver showed less accumulation of radiocolloids corresponding to metastases; and (iii) high accumulations of the therapeutic radiopharmaceutical were localized in the primary tumours of the pancreas, with moderate accumulation owing to metastases in the liver.

10.3.4.3. Conclusion

Radiopharmaceuticals for clinical use for PRRT in Serbia could be provided by using the proposed methodology. Despite insufficient data, beneficial effects on the clinical symptoms, hormone production and tumour proliferation were found without major clinical side effects. Thus, the first results in clinical application of these radiopharmaceuticals have shown that treatment with ^{90}Y DOTATATE is a feasible method and could be useful for the management of patients with inoperable or disseminated neuroendocrine tumours.

10.4. DEVELOPMENT OF $^{90}\text{Sr}/^{90}\text{Y}$ GENERATOR SYSTEMS

A $^{90}\text{Sr}/^{90}\text{Y}$ generator was developed to meet the demand of therapeutic applications in radiopharmaceutical research. An electrochemical method was

suggested for separation of pure ^{86}Y from ^{86}Sr and purification of ^{86}Y , which is an attractive radioisotope for PET [10.14–10.16]. Successful electrochemical separation of ^{90}Y from ^{90}Sr was presented by Chinol et al. [10.17], as well as by Chakravarty et al. [10.18] and the IAEA [10.19].

10.4.1. Materials

The following radioactive sources were obtained from the Radioisotope Centre, Institute of Atomic Energy, POLATOM: ^{90}Sr as strontium nitrate [$^{90}\text{Sr}(\text{NO}_3)_2$], in equilibrium with ^{90}Y in 1M HNO_3 , with specific activity 2.70 GBq/mg and a radioactive concentration of 9.24 GBq/cm³ and carrier free $^{90}\text{YCl}_3$ in 0.05M HCl solution with a radioactive concentration of 89.59 GBq/cm³. The potentiostat unit Potentiostat/Galvanostat/ZRA, series G 750 was equipped with licensed software FC 350 (Gamry Instruments Inc.).

The equipment for electrochemical separation consisted of an electrolysis cell made by the Faculty of Technology and Metallurgy, University of Belgrade (Serbia). Three electrodes were housed in a quartz cell fitted with an acrylic cap. Two of the electrodes (anode and cathode), with a surface area of 2 cm², were made of highly pure platinum plates that were made by the Institute for Mining and Metallurgy (Serbia). As a reference, a saturated calomel electrode (SCE) (Gamry Instruments Inc.) in a reference cell and connected by a Luggin capillary to the electrochemical cell was used (see Fig. 10.15). Highly pure argon gas was provided by a local supplier.

Radioactivity of ^{90}Sr and ^{90}Y was measured in an ionization chamber (Capintec CRC-15 beta counting calibrator) with a calibration factor. For calibrating ^{90}Y , a secondary calibration source of ^{90}Sr was used (radioactive solution ampoule No. BW/21/10/R₃-0.1, with an activity of 368.3 ± 9.6 kBq/g). Low level activity was measured using a NaI(Tl) scintillation counter (Wallac Comp Gamma Counter LKB) by measuring the bremsstrahlung radiation of ^{90}Sr and ^{90}Y .

10.4.2. Methods

10.4.2.1. Preparation of $^{90}\text{Sr}/^{90}\text{Y}$ generators

The $^{90}\text{Sr}/^{90}\text{Y}$ electrochemical generator was based on electrolysis of a mixture of ^{90}Sr and ^{90}Y as nitrate salts. The electrolysis was performed in a quartz cell with a volume of 100 cm³ loaded with 0.2 mL of $^{90}\text{Sr}(\text{NO}_3)_2$ in 1M HNO_3 (~1.85 GBq), in the presence of 50 mL of 0.003M HNO_3 as the electrolyte. The pH value was adjusted to 2.7 ± 0.2 prior to electrolysis with 3% ammonia. Before electrolysis, argon gas was bubbled for 15 min through a glass tube, which was

dipped into the electrolysis solution, and platinum electrodes were activated in 3M HNO₃.

The three electrode system was housed in quartz cells fitted with an acrylic cap. The two electrodes (anode and cathode), sealed in a glass holder, were fully immersed into the solution facing each other. They were maintained at a minimum distance, while the reference electrode (SCE) was kept very close to the cathode, but without contact.

10.4.2.2. *Electrochemical separation of ⁹⁰Y*

Electrolysis was performed in two steps. During the first step of electrolysis, ⁹⁰Y was separated from ⁹⁰Sr by selective electrodeposition of ⁹⁰Y on the platinum cathode. This was achieved by applying a fixed potential on the cathode of -2.5 V with respect to the SCE. Highly pure argon gas was continuously bubbled through the solution to vent gases such as H₂, and the solution was continuously mixed with a magnetic stirrer. The first electrolysis lasted for 90 min. At the end of the selective electrodeposition of ⁹⁰Y, the electrodes with an acrylic cap were removed from the quartz cell without switching off the power supply. The power supply was then switched off, and the cathode plate removed from the acrylic cap and washed with 10 mL of acetone. The cathode was then transferred to the second quartz cell.

During the second step of electrolysis (the 'purification step'), ⁹⁰Y was removed from the platinum electrode. In this step, the cathode from the first electrolysis containing ⁹⁰Y was used as the anode, and a new platinum electrode was used as the cathode. The electrodes were placed in a similar new electrolytic cell filled with 0.0003M NaNO₃ with the pH adjusted to 2.7 ± 0.2. This step of electrolysis was performed as galvanostatic electrolysis at a fixed potential of -2.5 V on the cathode with respect to the SCE for 45 min. Argon gas was continuously passed through the solution. During this electrolytic step, ⁹⁰Y was transferred from the first platinum electrode and deposited onto the new platinum electrode (cathode). After electrodeposition of ⁹⁰Y, the cathode was taken out without switching off the current, washed with 10 mL of acetone and subsequently dissolved by dipping it in a small volume of 0.5M HCl to obtain ⁹⁰Y as ⁹⁰YCl₃, which was suitable for labelling.

10.4.2.3. *Quality control of ⁹⁰Y*

The radionuclidic purity of the ⁹⁰Y solution was analysed using paper chromatography and ITLC. In paper chromatography, Whatman No. 1 paper (18 cm × 2 cm) and ITLC SG strips (14 cm × 1 cm) were used as the stationary phase and normal saline (0.9% NaCl) as the mobile phase. To determine the

radionuclidic purity of the ^{90}Y solution, the 'BARC technique' was also used. This method was a combination of solvent EPC [10.20] wherein Whatman No. 1 (18 cm \times 2 cm) paper chromatographic strips impregnated with KSM-17 at the point of spotting were used. On development with normal saline, ^{90}Sr moved to the solvent front, while ^{90}Y was retained at the point of spotting. The activity at the solvent front was estimated by cutting the chromatograms into 1 cm strips and measuring radioactivity in a dose calibrator. Radionuclidic purity was calculated as a percentage of the total activity spotted.

10.4.3. Results and discussion

10.4.3.1. Electrochemical separation of ^{90}Y

Although there are different methods of separation of ^{90}Y from the parent radionuclide ^{90}Sr reported in the literature [10.19], the $^{90}\text{Sr}/^{90}\text{Y}$ generator used an electrochemical method for separation of ^{90}Y . The electrolysis was carried out in an electrolytic quartz cell, prepared in the Laboratory for Radioisotopes, Vinča Institute of Nuclear Sciences (see Fig. 10.15(a)), as potentiostatic electrolysis with potential -2.500 ± 0.055 V with respect to the SCE. During the first electrolysis, the current was increased from 730 to 745 mA. The electrolytic potential at the platinum cathode was stable during the electrolysis, but could not be maintained at -2.50 V. It fell to -2.39 V, but was within the accepted limits of $\pm 0.2\%$ plus 5 mV, in constant voltage mode. The pH was adjusted to 2.7 ± 0.2 .

The second electrolysis was accomplished with a stable potential of -2.50 V on the platinum cathode and a constant current of 100 mA during the electrolysis. The solution was warmed up during electrolysis, and hence subsequent cooling of the electrolysis cell was necessary. Separation of H_2 gas was also detected (see Fig. 10.15(b)) and, therefore, stirring during the process was not required. These conditions ensured that the deposition yield was $>90\%$.

10.4.3.2. Quality control of ^{90}Y

Yttrium-90 exists in secular equilibrium with its parent isotope ^{90}Sr , which is a product of the fission reaction. Many impurities must be removed, and pure ^{90}Y has to be converted into an appropriate chemical form for application in medicine therapy. Radioactive ^{90}Sr , as $^{90}\text{Sr}(\text{NO}_3)_2$ in equilibrium with ^{90}Y in 1M HNO_3 from POLATOM, had a high radionuclidic purity ($>99.5\%$), as well as a high RCP. Strontium-90 breakthrough was the major problem often encountered with the $^{90}\text{Sr}/^{90}\text{Y}$ generator. Because ^{90}Sr is a bone seeker and the upper limit of

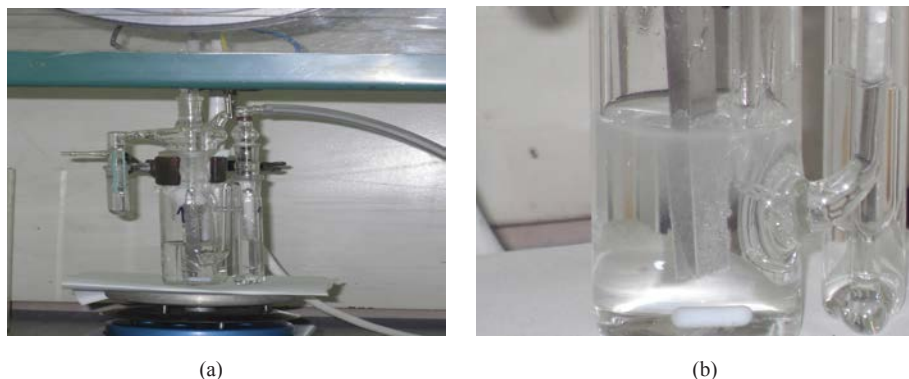


FIG. 10.15. (a) The electrolytic cell and (b) electrolytic separation of H_2 gas

^{90}Sr in ^{90}Y solution for human use was set at 74 kBq (2 mCi), the development of quality control methods was essential.

The radionuclidic purity of the ^{90}Y solution was analysed using paper chromatography and ITLC. Paper chromatography on Whatman No. 1 (18 cm \times 2 cm) and ITLC SG strips (14 cm \times 1 cm) using 0.9% saline solution was used for the analyses. In this method, ^{90}Sr moved to the solvent front, while ^{90}Y remained at the origin. The radionuclidic purity was calculated as a percentage of the total activity spotted.

Comparative results of RCP of ^{90}Y before and after electrolysis were obtained using paper chromatography (see Fig. 10.16), wherein two peaks were observed of ^{90}Sr and ^{90}Y at equilibrium (see Fig. 10.16(a)). The absence of a peak at 10 cm (see Fig. 10.16(b)), which represents free ^{90}Sr , indicated that separation of ^{90}Y from ^{90}Sr by electrochemical separation was successful.

The quality of separation was determined by measuring the radioactivity of ^{90}Y solution over time, following the half-life of ^{90}Y . The decay was followed for 31 d, which is ~ 11.6 half-lives of ^{90}Y . The absence of deviation in the lower part of the curve in Fig. 10.17 confirmed the absence of ^{90}Sr . The y axis is given as the logarithm of observed values.

To determine the radionuclide purity of the ^{90}Y solution, a combination of solvent extraction and EPC was used. This method is a sensitive and accurate analytical technique for estimation of the purity of ^{90}Y . The EPC pattern of ^{90}Y is shown in Fig. 10.18, wherein ^{90}Sr moved to the solvent front, while ^{90}Y was retained at the point of spotting. Radionuclide purity was calculated as the percentage of the total activity spotted, estimated by measuring radioactivity in a dose calibrator. These results revealed only a very low level of ^{90}Sr impurity ($<0.2\%$).

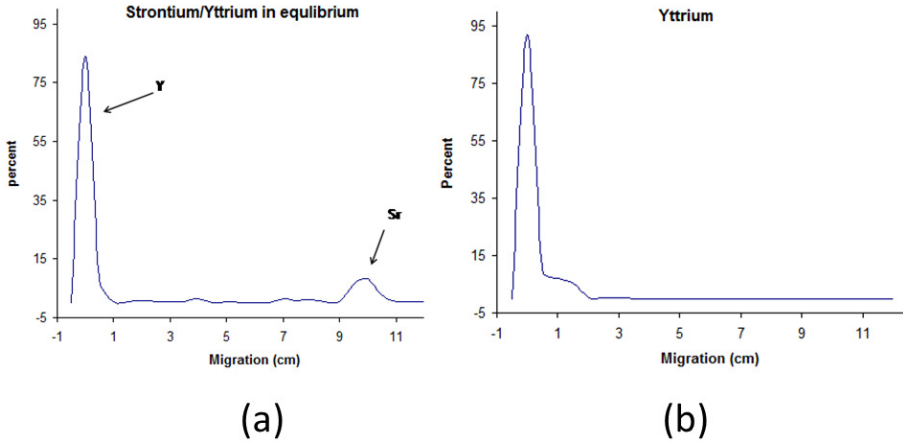


FIG. 10.16. (a) Strontium-90/yttrium-90 in equilibrium and (b) yttrium-90 after electrolysis.

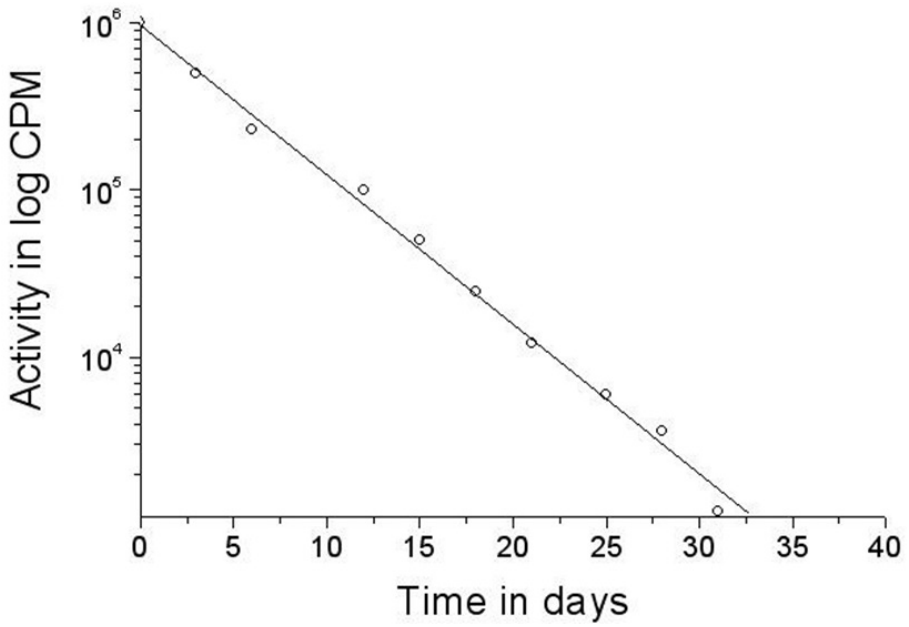


FIG. 10.17. Radioactive decay pattern of ^{90}Y prepared by the electrochemical separation method (> 11 half-lives).

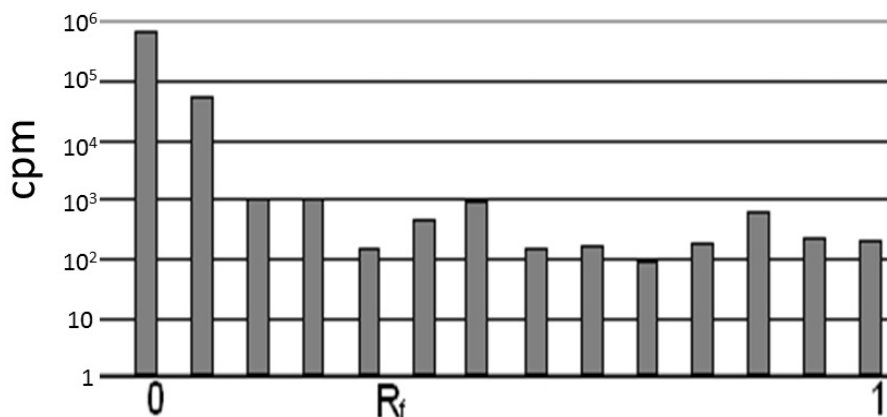


FIG. 10.18. EPC pattern of ⁹⁰Y sample.

10.4.4. Conclusion

In these experiments, ⁹⁰Sr in equilibrium with ⁹⁰Y with a relatively low activity (~1.85 GBq) was used. The efficiency of the ⁹⁰Sr/⁹⁰Y generator was ~96% of the theoretical value. The initial results confirmed the efficiency of the ⁹⁰Sr/⁹⁰Y electrochemical generator and allowed development of the electrochemical separation technique as a quality control method for ⁹⁰Y. The next step will involve production of higher levels of activity from the ⁹⁰Sr/⁹⁰Y generator for labelling and supply of ⁹⁰Y to the national nuclear medicine community of Serbia.

REFERENCES TO CHAPTER 10

- [10.1] MAUSNER, L.F., SRIVASTAVA, S.C., Selection of radionuclides for radioimmunotherapy, *Med. Phys.* **20** (1993) 503.
- [10.2] BRANS, B., LINDEN, O., GIAMMARILE, F., TENNVALL, J., PUNT, C., Clinical application of newer radionuclide therapies, *Eur. J. Cancer* **42** (2006) 994.
- [10.3] INTERNATIONAL ATOMIC ENERGY AGENCY, Comparative Evaluation of Therapeutic Radiopharmaceuticals, Technical Reports Series No. 458, IAEA, Vienna (2007).
- [10.4] KOTHARI, K., et al., "Preparation of ¹⁸⁶Re complexes of dimercaptosuccinic acid and hydroxy ethylidene diphosphonate", *Modern Trends in Radiopharmaceuticals for Diagnosis and Therapy*, IAEA-TECDOC-1029, IAEA, Vienna (1998) 539.

- [10.5] DJOKIĆ, D.J., JANKOVIĆ, D.L., NIKOLIĆ, N.S., Labeling, characterization, and in vivo localization of a new Y-90-based phosphonate chelate 2,3-dicarboxypropane-1,1-diphosphonic acid for the treatment of bone metastases: Comparison with Tc-99m-DPD complex, *Bioorga. Med. Chem.* **16** (2008) 4457.
- [10.6] DJOKIĆ, D., JANKOVIĆ, D., NIKOLIĆ, N., Preparation and in vivo evaluation of ⁹⁰Y-meso-dimercaptosuccinic acid (⁹⁰Y-DMSA) for possible therapeutic use: Comparison with ^{99m}Tc-DMSA, *Canc. Biother. Radiopharm.* **24** (2009) 129.
- [10.7] JANKOVIĆ, D., et al., Particle sizes analysis: ⁹⁰Y and ^{99m}Tc-labelled colloids, *J. Microsc.* **232** (2008) 601.
- [10.8] JANKOVIĆ, D.L., et al., ⁹⁰Y-labeled tin fluoride colloid as a promising therapeutic agent: Preparation, characterization, and biological study in rats, *J. Pharm. Sci.* **101** (2012) 2194.
- [10.9] ECKELMAN, W., KARESH, S., REBA, R., New compounds: Fatty acid and long chain hydrocarbon derivatives containing a strong chelating agent, *J. Pharm. Sci.* **64** (1975) 704.
- [10.10] OKARVI, S.M., Recent developments in ^{99m}Tc-labelled peptide-based radiopharmaceuticals: An overview, *Nucl. Med. Comm.* **20** (1999) 1093.
- [10.11] KWEKKEBOOM, D.J., KRENNING, P.E., DE JONG, M., Peptide imaging and therapy, *J. Nucl. Med.* **41** (2000) 1704.
- [10.12] DE JONG, M., KRENNING, E., New advances in peptide receptor therapy, *J. Nucl. Med.* **43** (2002) 617.
- [10.13] BREEMAN, W.A.P., DE JONG, M., VISSER, T.J., ERION, J.L., KRENNING, E.P., Optimising conditions for radiolabelling of DOTA-peptides with ⁹⁰Y, ¹¹¹In and ¹⁷⁷Lu at high specific activities, *Eur. J. Nucl. Med. Mol. Imaging* **30** (2003) 917.
- [10.14] REISCHL, G., ROSCH, F., MACHULLA, H.J., Electrochemical separation and purification of yttrium-86, *Radiochim. Acta* **90** (2002) 225.
- [10.15] YOO, J., et al., Preparation of high specific activity ⁸⁶Y using a small medical cyclotron, *Nucl. Med. Biol.* **32** (2005) 891.
- [10.16] INTERNATIONAL ATOMIC ENERGY AGENCY, Cyclotron Produced Radionuclides: Physical Characteristics and Production Methods, Technical Reports Series No. 468, IAEA, Vienna (2009) 244.
- [10.17] CHINOL, M., HNATOWICH, D.J., Generator produced yttrium-90 for radioimmunotherapy, *J. Nucl. Med.* **28** (1987) 1465.
- [10.18] CHAKRAVARTY, R., et al., Development of an electrochemical ⁹⁰Sr-⁹⁰Y generator for separation of ⁹⁰Y suitable for targeted therapy, *Nucl. Med. Biol.* **35** (2008) 245.
- [10.19] INTERNATIONAL ATOMIC ENERGY AGENCY, Therapeutic Radionuclide Generators: ⁹⁰Sr/⁹⁰Y and ¹⁸⁸W/¹⁸⁸Re Generators, Technical Reports Series No. 470, IAEA, Vienna (2009) 73.
- [10.20] PANDEY, U., DHAMI, P.S., JAGESIA, P., VENKATESH, M., PILLAI, M.R.A., A novel extraction paper chromatography (EPC) technique for the radionuclidic purity evaluation of ⁹⁰Y for clinical use, *Anal. Chem.* **80** (2008) 801.

Chapter 11

LOCAL DEVELOPMENT OF $^{90}\text{Y}/^{90}\text{Sr}$ GENERATORS AND ^{90}Y RADIOPHARMACEUTICALS IN THE SYRIAN ARAB REPUBLIC

T. YASSINE, H. MUKHALLALATI

Department of Chemistry,
Radioisotopes Section,
Atomic Energy Commission,
Damascus, Syrian Arab Republic

Abstract

Radiopharmaceuticals have shown promise in the field of therapy in the last decades. The use of generator produced radionuclides, such as ^{90}Y , has increased because of their unique properties. The focus of the work in this chapter has been the development of a ^{90}Y generator and related radiopharmaceuticals. A $^{90}\text{Sr}/^{90}\text{Y}$ generator was developed based on the isolation of ^{90}Y from ^{90}Sr using Sr-Spec resin packed in three columns. The resulting ^{90}Y solution was used for the preparation of therapeutic radiopharmaceuticals. In the $^{90}\text{Sr}/^{90}\text{Y}$ generator developed, a maximum of 200 mCi of ^{90}Sr was loaded onto the first column and ^{90}Y was eluted with 3M nitric acid. The middle two columns were used as purification barriers. The resulting eluate was evaporated and further purified by passing it through a cation exchange column for removal of trace elements. The final solution was concentrated and ^{90}Y obtained in the chloride form. The yield of ^{90}Y was ~90% with $\leq 10^{-6}\%$ ^{90}Sr . The quality of the ^{90}Y solution was tested in terms of radiochemical, radionuclidic and biological purities, which were found to be high. This reflected in obtaining high labelling efficiency and high quality of final radiopharmaceuticals, which included ^{90}Y EDTMP, ^{90}Y ferric hydroxide macroaggregates (FHMA), ^{90}Y DOTA-h-R3 antibody and ^{90}Y DOTA rituximab.

11.1. INTRODUCTION

In recent years, a number of new developments in targeted therapies using radiolabelled compounds have emerged. The application of energetic β and α emitting radionuclides in cancer therapy has been invaluable owing to their unique properties. Availability of large quantities of these radionuclides in high specific activity and with high radionuclide purity is essential for expanding the scope of targeted therapy. However, in developing countries, a lack of resources and non-availability of nuclear reactors have been the limiting steps to expanding the production of these radionuclides. Hence, the best alternative for the local production of such radionuclides is the use of generator technology.

Yttrium-90 is one of the radionuclides that has been playing an essential role in therapeutic nuclear medicine because of its unique properties. Yttrium-90 is a pure β emitter with a half-life of 64.1 h and emits high energy ($E_{\max} = 2.2$ MeV) and long range β particles that make it suitable for the irradiation of large tumour masses. It can be obtained with a high specific activity (2×10^{16} Bq/g) by isolation from the parent ^{90}Sr that is obtained from nuclear waste and has a very long half-life (~ 27 years).

A number of separation techniques have been used for isolation of ^{90}Y from ^{90}Sr , including solvent extraction, ion exchange SLM, electrochemical deposition and extraction chromatography. Each of these methods has its own advantages and disadvantages with respect to complex formation and purity of the final products. Of these, extraction chromatography has shown to be more reliable as it can be safely handled, thereby lowering radiation exposure. In addition, solid extractants such as Sr-Spec resin, which are highly selective for strontium, are used for selectively eluting ^{90}Sr and ^{90}Y with 3M nitric acid.

Yttrium-90 radiopharmaceuticals have been shown to play a very important role in radionuclide therapy, where receptor seeking molecules, such as peptides and MAbs, are used for delivering radioactivity to targeted cells or subcellular structures.

11.2. MATERIALS

11.2.1. Chemicals

Chimeric anti-CD20 rituximab MAb was provided by Roche (Roche Pharma Schweiz), and hR3 antibody was obtained from CIM. The p-SCN-Bz-DOTA (back-DOTA) and DOTA NHS ester were purchased from Macrocyclics Design Technologies. Yttrium-90 was obtained from a $^{90}\text{Sr}/^{90}\text{Y}$ generator produced at the Atomic Energy Commission of Syria (AECS), which was made up of Sr-Spec resin (crown ether [(4,4,(5)-di-t-butylcyclohexono-18-crown-6)] packed in three columns for separation and purification of $^{90}\text{Sr}/^{90}\text{Y}$. All other reagents were purchased from Aldrich or Sigma. The centrifuge filter devices were Amicon Ultra-15 (Millipore) filters (molecular weight cut-off MWCO = 30 000).

11.2.2. Equipment

For liquid scintillation counting of $^{90}\text{Sr}/^{90}\text{Y}$ solutions, an LS 6500 PACKMAN counter was used. A Waters 1525 HPLC with radio and UV detectors was used for chromatographic experiments.

- (a) The generator was prepared, investigated and validated for different parameters such as yield, breakthrough and its utility for the preparation of radiopharmaceutical products.
- (b) The design comprised three columns connected in series (length 21 cm, diameter 4 mm and 1 g of Sr-Spec in each column). The first column was used for absorbing ^{90}Sr , whereas the second and third columns were used as safety columns for further purification.
- (c) A stock solution of ^{90}Sr in 3M nitric acid was passed through the columns, whereby ^{90}Sr was retained in the column and ^{90}Y was eluted. Subsequently, ^{90}Sr was stripped from the column with dilute 0.05M nitric acid.

AG 50 resin was used for further purification to remove any traces of organic materials and trace elements [11.2, 11.3].

11.3.1.1. Purification of ^{90}Y eluate

This procedure was designed to remove as many impurities, such as ZrO^{2+} , Fe^{3+} , Cu^{2+} and Zn^{2+} , as possible, which could be present, along with ^{90}Y , during the production process. Briefly, the ^{90}Y solution was passed through a 9 cm long \times 0.4 cm wide column containing AG 50WX-12 resin in H^+ form followed by 15 mL of 0.5M H_2SO_4 to remove ZrO^{2+} . Subsequently, 40 mL of 2M HNO_3 was used to remove ^{90}Sr followed by 25 mL of 2M HCl to eliminate Fe^{3+} , Cu^{2+} , Zn^{2+} and other impurities. Finally, 12 mL of 4M HCl solution was passed through the column to elute purified ^{90}Y . The acid was removed by heating, and the ^{90}Y was dissolved in a small volume of 0.01M HCl solution [11.4]. Figure 11.2 illustrates the elution pattern of ^{90}Y through the three columns.

11.3.1.2. Stability of columns

To determine the reproducibility of the generator, experiments were carried out wherein the generator system was loaded with different quantities (25, 50, 100, 150 or 200 mCi) of ^{90}Sr , and the system was eluted every day with 20 mL of 3M nitric acid. The system was stable for up to one week (four elution processes after which ^{90}Sr breakthrough increased by a magnitude of ten). The resin column could be reused six to seven times if washed with 20 mL of 2% oxalic acid, 20 mL of water and finally with 20 mL of 0.01M EDTA.

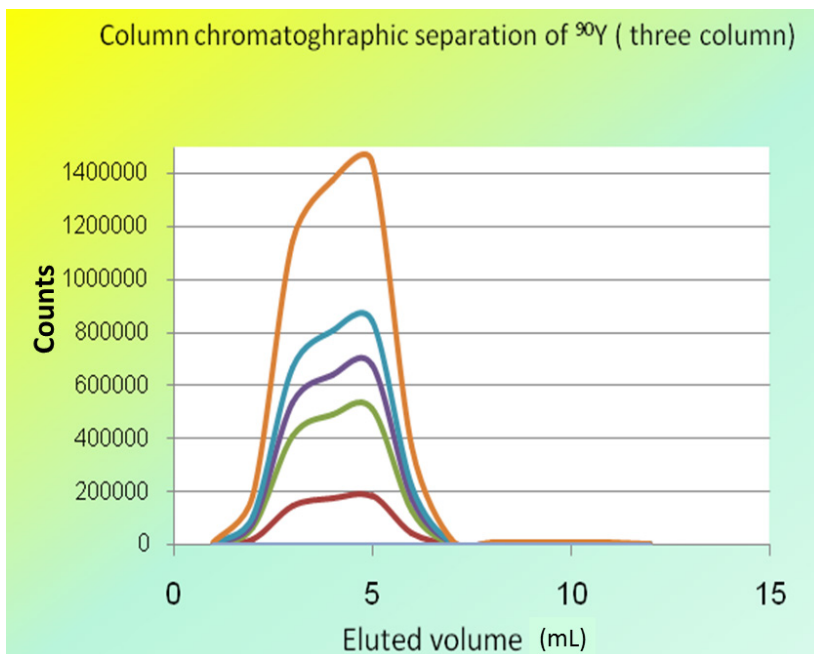


FIG. 11.2. Column chromatographic separation of ^{90}Y (three columns).

11.3.1.3. *Quality control of $^{90}\text{Sr}/^{90}\text{Y}$ generator*

An important issue related to the $^{90}\text{Sr}/^{90}\text{Y}$ generator was the quality control of the final ^{90}Y product. The most important concern was regarding ^{90}Sr breakthrough. Several methods were tested for ^{90}Sr assay as reported in the following.

- (a) EPC method for estimation of ^{90}Sr content in ^{90}Y chloride/acetate solutions

The following protocol was designed for estimation of the radionuclide purity of the ^{90}Y solution:

- *Preparation of test solution:* Take 15 mCi of ^{90}Y and dry it, add 50 μL of 0.5M ammonium acetate and divide the solution to obtain different activities such as 1, 2, 3, 4 and 5 mCi.
- *Preparation of test solution for EPC:* A 5 μL sample of each of the activities was applied on a KSM-17 spot on Whatman No. 1 chromatographic paper and allowed to dry completely.

— *Development of EPC:* The EPC was developed in ascending manner by inserting the paper in a chromatography jar containing 0.9% saline. After the solvent moved to the top, the paper was removed, cut into 1 cm segments and three segments of the solvent front. The paper strip was inserted in a liquid scintillation vial containing 10 mL of scintillation cocktail. The samples were counted for 5 min in an LSC. Each section of the front paper was inserted in a liquid scintillation vial and counted using an isotope counter.

The results demonstrated good reliability, as shown in Table 11.1.

TABLE 11.1. PAPER CHROMATOGRAPHY WITH DIFFERENT ACTIVITIES FOR ^{90}Y USING LIQUID SCINTILLATION CHROMATOGRAPHY

Activity of Y-90 (Bq (mCi))	Activity of Sr-90 (Bq)	Breakthrough (%)
3×10^7 (0.8)	1×10^2	3×10^{-4}
3×10^8 (1.25)	1×10^2	3×10^{-5}
6×10^8 (1.86)	1×10^2	1×10^{-5}
8×10^8 (2.3)	1×10^2	1×10^{-5}
1×10^9 (3.7)	2×10^3	2×10^{-4}

(b) Paper chromatography for standard solution of $^{90}\text{Sr}/^{90}\text{Y}$

This method was qualified by testing equilibrated $^{90}\text{Sr}/^{90}\text{Y}$ solution where 1.3 mCi (10 μL) was taken from the stock solution and diluted to 20 mL with 0.5M sodium acetate. A volume of 5 μL of the diluted solution was applied on the KSM-17 spot on the Whatman No. 1 chromatography paper and allowed to dry completely. The EPC was developed in an ascending manner by inserting the paper into a chromatography jar containing 0.9% saline. After development, the paper was removed, cut into two parts and counted by liquid scintillation using 10 mL of the scintillation cocktail. The samples were counted for 5 min in an LSC, and the ^{90}Sr breakthrough calculated ($^{90}\text{Sr}/^{90}\text{Y} = 1$), as shown in Fig. 11.3. Table 11.2 reports the paper chromatography results for the standard $^{90}\text{Sr}/^{90}\text{Y}$ solution. These results were further validated by counting a fraction of the solution after a two month decay.

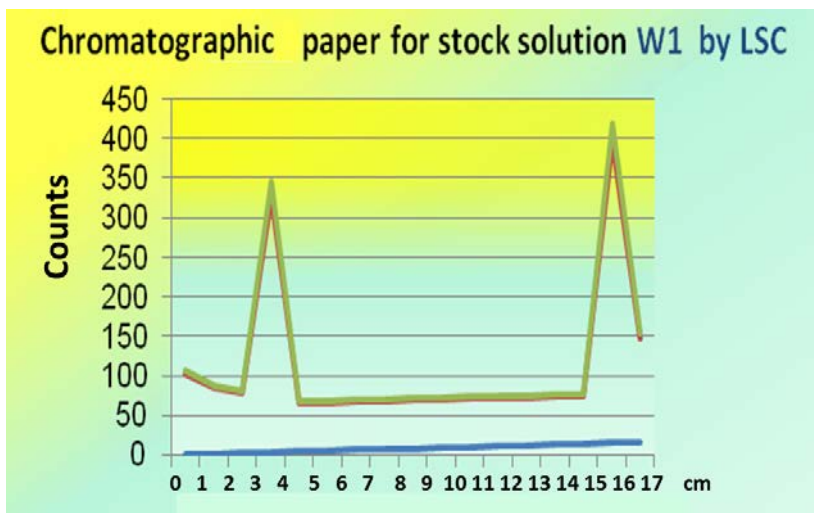


FIG. 11.3. Chromatography for the stock solution W1 using an LSC.

TABLE 11.2. PAPER CHROMATOGRAPHY FOR STANDARD SOLUTION OF $^{90}\text{Sr}/^{90}\text{Y}$

Standard solution Sr-90/Y-90 (Bq)	Activity of Sr-90 (Bq)	Activity of Y-90 (Bq)	Breakthrough (%)
15×10^8	7×10^8	5×10^8	1

- (c) Extraction chromatography using resin strontium selective extractant (Sr-Spec)

A known amount of eluted activity (3.2 mCi) of ^{90}Y was passed through a small Pyrex glass column containing 1 g of Sr-Spec and eluted with 15 mL 3M HNO_3 . The column was washed with 20 mL of 0.05M HNO_3 to elute ^{90}Sr . The 0.05M HNO_3 fraction collected from the column was used to assess the radionuclide purity of ^{90}Y using an LSC. This fraction contained >99% of the ^{90}Sr impurity. Ten microlitres from the ^{90}Sr fraction was mixed with 10 mL of the scintillation cocktail in a liquid scintillation vial, the ^{90}Sr activity measured using an LSC (LS 6500 PACKMAN) and the breakthrough calculated as $^{90}\text{Sr}/^{90}\text{Y} \leq 10^{-7}$, as shown in Fig. 11.4.

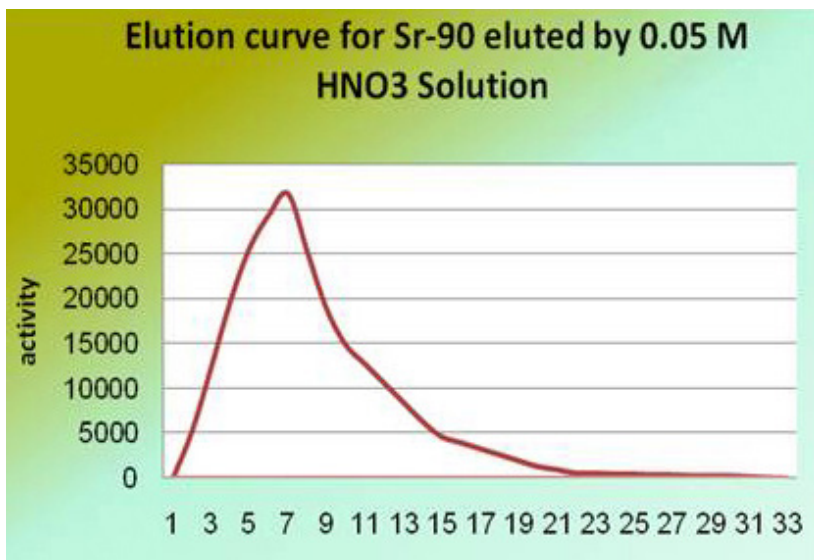


FIG. 11.4. Elution curve of ^{90}Sr eluted with 0.05M HNO_3 solution.

(d) Chemical purity of the final eluate

Chemical impurities such as trace metals and organic products were determined in the final solution after decay of ^{90}Y using ICP MS and liquid chromatography mass spectroscopy (MS) techniques. The liquid chromatographic assay did not show any organic contaminants. The amounts of trace metals in the final solution are shown in Table 11.3.

Elution profiles for the generator showed that >95% of the ^{90}Y was eluted with 10 mL of 3M nitric acid and no significant changes were observed when the same system was used up to six times for elution, as shown in Fig. 11.5. After each elution, the resin was washed with 20 mL of 2% oxalic acid and 20 mL of water, then with 20 mL of 0.01M EDTA.

The paper chromatography assay of the resulting ^{90}Y solution showed high purity, wherein ^{90}Sr was ~1 ppb. Breakthrough was $1.11 \times 10^{-8}\%$ when counted after a decay of two months.

TABLE 11.3. DETERMINATION OF TRACE METALS IN THE FINAL SOLUTION

Element	Sample concentration (ppb)	Element	Sample concentration (ppb)	Element	Sample concentration (ppb)
Li	2.88	As	0.39	Pr	1.14
Na	230.55	Se	≤0.000	Nd	0.3
Mg	≤0.000	Sr	0.1	Sm	0.29
Al	11.91	Ag	0.24	Eu	0.72
Ca	≤0.000	Cd	0.04	Gd	0.39
V	0.21	Cs	0.03	Tb	0.65
Mn	≤0.000	Pb	14.69	Dy	0.29

Elution curve for reusing

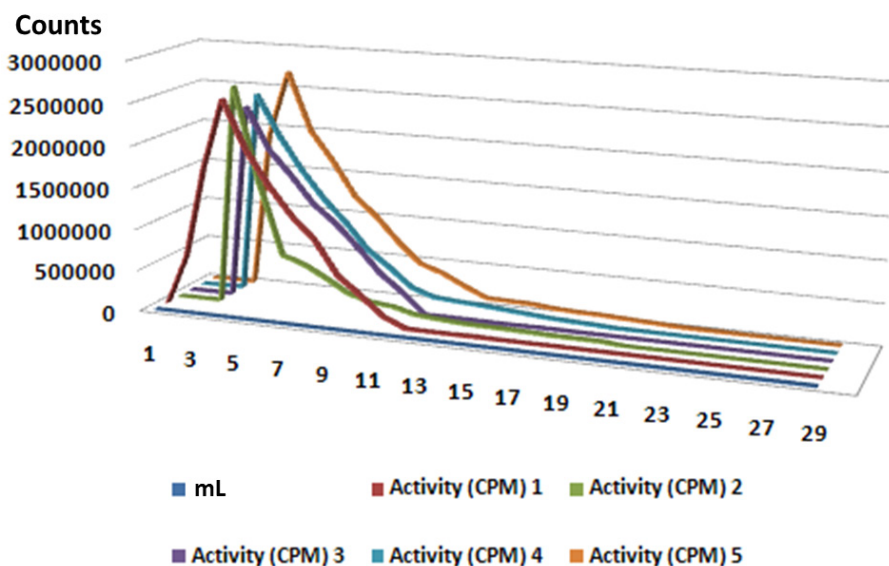


FIG. 11.5. Elution profiles collected on reused Sr-Spec resin.

11.4. YTTRIUM-90 MABs

The use of the MAb rituximab has become a standard mode of treatment for relapsed or refractory CD20 positive low grade NHL, along with chemotherapy. Rituximab is a chimeric antibody, discovered in 1990 by IDEC Pharmaceuticals. It possesses a high binding affinity to the CD20 antigen. The CD20 antigen is expressed on the surface of normal and malignant B lymphocytes, but not on stem cells or other healthy tissues. Rituximab kills CD20 positive B lymphocytes via a mechanism involving antibody dependent cytotoxicity. Over recent years, radioimmunotherapy has been used in the treatment of CD20 positive lymphomas. Most low grade NHLs that have relapsed or were refractory to standard therapies are eligible for radioimmunotherapy treatment. Radioimmunotherapy is used either alone or in combination with other therapies, with the aim of improving the efficacy of treatment. For this reason, β emitting radioisotopes have been linked to anti-CD20 antibodies. Lymphocytes and lymphoma cells are highly radiosensitive.

11.4.1. Preparation and characterization of ^{90}Y rituximab

Conjugation of rituximab with p-NCS-Bz-DOTA was carried out to obtain rituximab and DOTA NCS. Conjugation was also carried out with the NHS group activating one carboxylate to yield rituximab and DOTA NHS.

11.4.1.1. *Materials and methods*

Chimeric anti-CD20 rituximab MAb was provided by Roche Pharma Schweiz. The p-SCN-Bn-DOTA (back-DOTA) and DOTA NHS ester were purchased from Macrocyclics Design Technologies. Yttrium-90 was obtained from the $^{90}\text{Sr}/^{90}\text{Y}$ generator at AECS, and made up of a Sr-Spec resin (crown ether) packed into three columns for separation and purification of $^{90}\text{Sr}/^{90}\text{Y}$. All other reagents were purchased from Aldrich or Sigma. The centrifuge filter devices used were Amicon Ultra-15 filters, MWCO = 30 000 Da (Millipore).

Two activated DOTA moieties were available for the coupling reaction: DOTA NHS and DOTA SCN. Both conjugations were carried out at various molar DOTA:antibody ratios (40:1, 50:1, 80:1 and 100:1) to attain increased specific activities (2, 5, 10, 11 and 20 mCi/mg).

Commercially available rituximab (5 mg in 500 μL) was washed with 0.2M sodium carbonate, pH9, by centrifuging at 4°C at a speed of 4000 rev./min. This was mixed with DOTA NCS, and the reaction was allowed to continue overnight at room temperature with stirring. The buffer was changed to 0.5M sodium acetate buffer, pH7, which is more suitable for labelling, and the final immunoconjugate filtered in a volume of 1 mL.

This immunoconjugate solution (1 mL, 5 mg/mL) was prepared in a kit form by lyophilizing with 250 μ L of mannitol (80 mg/mL in distilled water). Both the immunoconjugate and mannitol solutions were filtered through sterile 0.45 μ m filters (Millipore) prior to lyophilization. On lyophilization, the final product has the appearance of a white pellet. For labelling, ^{90}Y was obtained from the $^{90}\text{Sr}/^{90}\text{Y}$ generator assembled at AECS. The generator was loaded with ~ 50 mCi of ^{90}Sr and the yield of ^{90}Y was ~ 45 mCi, equivalent to $>90\%$ elution efficiency.

Each labelling procedure was carried out at 42°C for 1 h with:

- (a) Two 700 μ L volumes of ^{90}Y activity of 2.8 mCi, pH5;
- (b) Two 100 μ L volumes of rituximab DOTA in acetate, pH7.5.

11.4.1.2. *Quality control*

- (a) HPLC

Quality control of the radiopharmaceutical was performed by HPLC using a 2.1 mm \times 200 mm Hypersil AA-ODS 5 μ m column with a flow rate of 0.4 m/min and wavelength $\lambda = 254$ nm. The mobile phase was 95% saline and 5% ACN, and the run was for 20 min. The analysis (HPLC) showed an overall RCP $\geq 95\text{--}98\%$.

- (b) TLC

ITLC SG (Gelman Sciences) paper chromatography was carried out using various mobile phases (saline, MeOH:ammonia 3:2, MeOH:ammonium acetate 1:1). ITLC radioactivity was analysed by cutting the strips into two segments and measuring the radioactivity using an LSC (Beckman), as shown in Figs 11.6–11.8. The RCP was observed to be 98.1%. In both reactions, carried out at a DOTA:antibody molar ratio of 100:1, specific activities of 10 and 20 mCi/mg with labelling yields of 99.8% and 99.5% were achieved, respectively. These data are reported in Table 11.4.

- (c) In vivo studies

Biodistribution studies of ^{90}Y DOTA NCS rituximab were carried out on healthy Albino rats. Rats weighing ~ 175 g were injected with 1 mCi (50 μ L) of the radioconjugate in acetate buffer, pH7.5. Biodistribution studies were carried out to confirm the in vivo stability of the radioimmunoconjugate, as shown in Fig. 11.9.

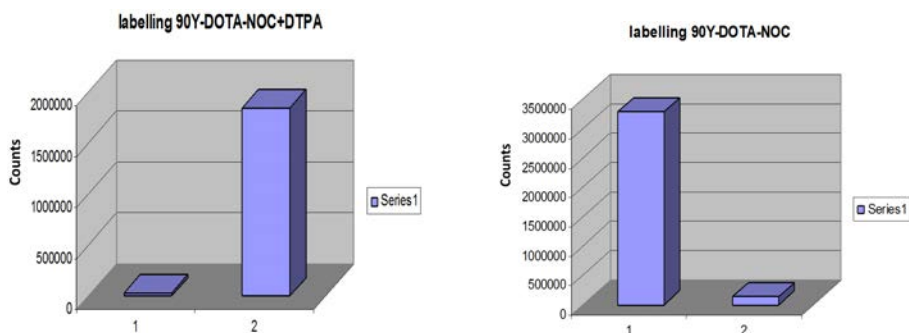


FIG. 11.6. RCP measured using ITLC SG eluted with saline.

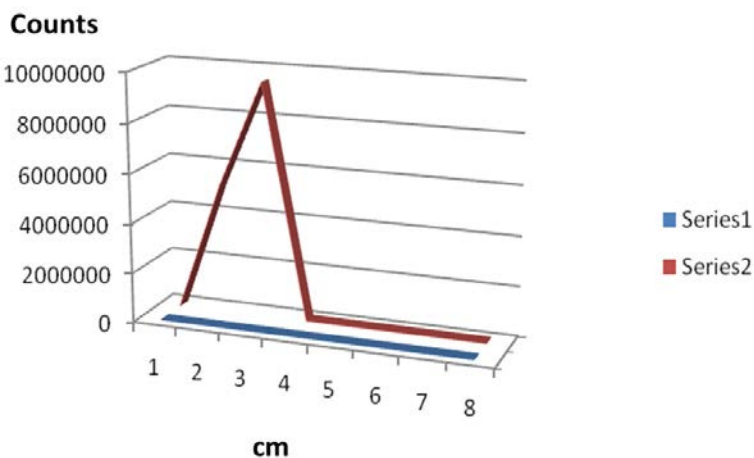


FIG. 11.7. RCP measured using ITLC SG eluted with MeOH:ammonia (3:2).

11.4.2. DOTA hR3 coupling and labelling with ^{90}Y

11.4.2.1. Materials and method

The hR3 antibody was obtained from CIM, p-SCN-Bn-DOTA and DOTA NHS ester were purchased from Macrocylics Design Technologies and ^{90}Y was obtained from a $^{90}\text{Sr}/^{90}\text{Y}$ generator assembled at AECS. All other reagents were purchased from Aldrich or Sigma. The centrifuge filter devices used were Amicon Ultra-15 filters (MWCO = 30 000 Da, Millipore).

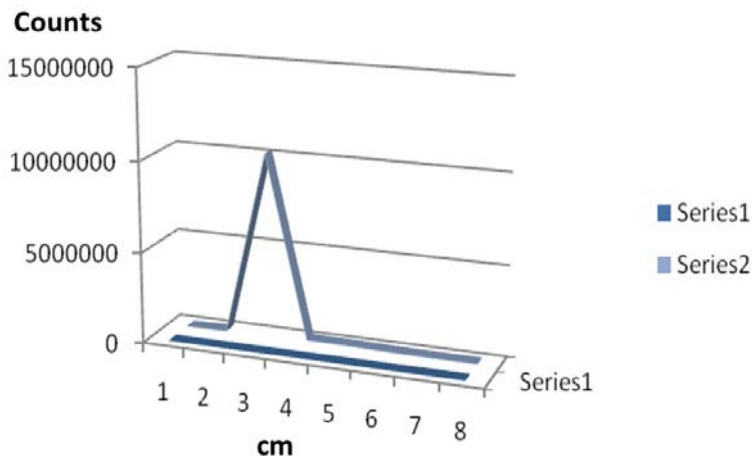


FIG. 11.8. RCP measured using ITLC SG eluted with MeOH:ammonium acetate (1:1).

TABLE 11.4. LABELLING EFFICIENCIES AND SPECIFIC ACTIVITIES AT VARIOUS DOTA:ANTIBODY MOLAR RATIOS

Antibody conjugate	Molar ratio	Labelling efficiency (%)	Specific activity (mCi/mg)
DOTA NCS rituximab	40:1	50	2
	50:1	66	2
	80:1	92	10
	100:1	99.5	10 20
DOTA NHS rituximab	40:1	43	2
	50:1	55	2
	80:1	45	5
	100:1	99.8	10
	100:1	99.8	20

Biodistribution of ^{90}Y -Rituximab

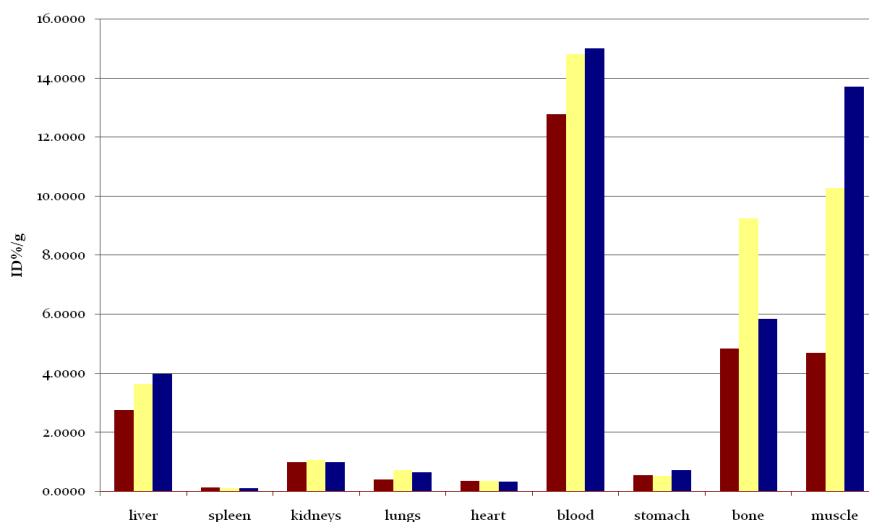


FIG. 11.9. Biodistribution of ^{90}Y DOTA (NCS) rituximab in healthy Albino rats.

DOTA hR3 was prepared by addition of 800 μL of hR3 pharmaceutical solution (5 mg/mL in phosphate buffer, pH8) into a glass tube, percolated with 5–5.6 mg of DOTA SCN in 0.1M phosphate buffer, pH8, at room temperature with continuous mild stirring and then kept in a fridge.

Labelling of the immunoconjugate DOTA hR3 with ^{90}Y was performed. The DOTA hR3 couplings were collected from a Sephadex G-50 column activated with 0.1M NH_4OAc after measurement using HPLC. Then, 200 μL of DOTA hR3 was withdrawn from all solutions and mixed with 150 μL of 0.25M ammonium acetate buffer and 150 μL of 2.0M ammonium acetate buffer, then added to 500 μL of $^{90}\text{YCl}_3$ (2.5 mCi) and incubated at pH7.5. The solution was gently stirred for 10 min, and radiolabelling was performed at 42°C for 1 h [11.5–11.7].

11.4.2.2. Quality control

(a) HPLC

Quality control of the final radiopharmaceutical was carried out using an HPLC (2.1 mm \times 200 mm) Hypersil AA-ODS 5 μm column with a flow rate of 0.4 mL/min, $\lambda = 254$ nm. The mobile phase was 95% saline and 5% ACN, and the

run was for 20 min. The overall RCP was ≥ 95 –98%, as illustrated in Fig. 11.10, while Fig. 11.11 represents the HPLC pattern for cold DOTA hr3 conjugate.

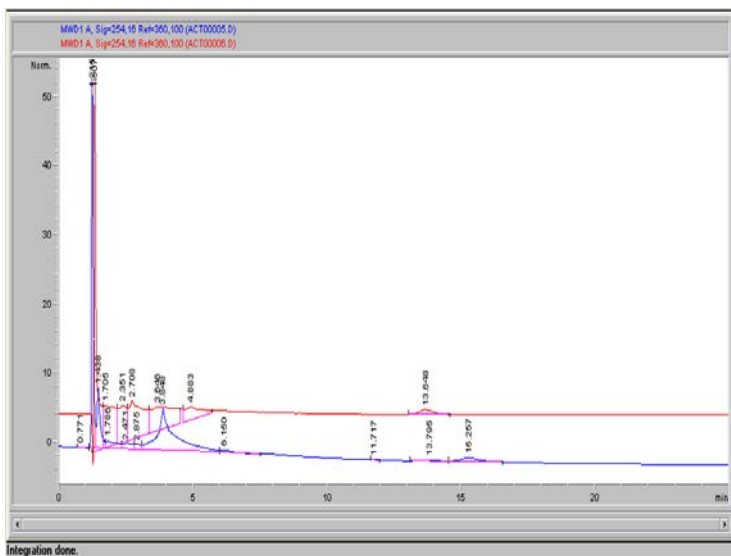


FIG. 11.10. HPLC pattern of ^{90}Y DOTA hr3.

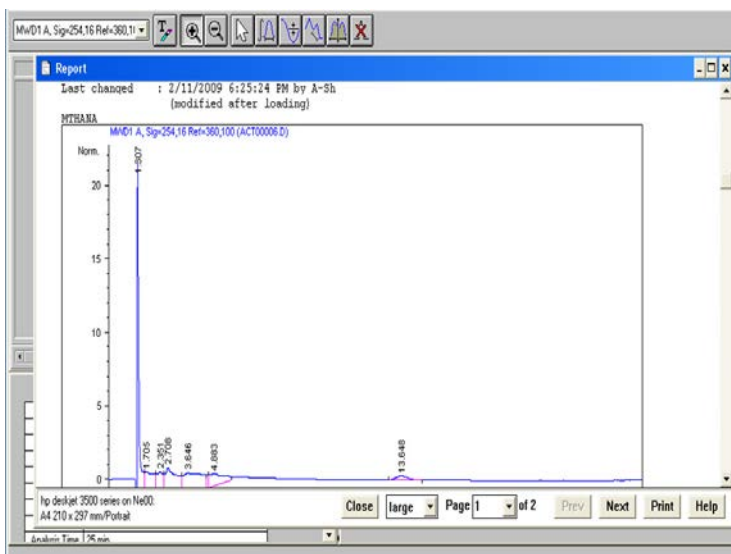


FIG. 11.11. HPLC pattern of cold DOTA hr3 immunoconjugate.

11.5. YTTRIUM-90 EDTMP

Bone metastases contribute to 25% of all cancer patients and hence it is essential to develop radiopharmaceuticals for the treatment of bone cancer. Yttrium-90 EDTMP is a specific bone seeking therapeutic agent, and careful evaluation of the injected dose into patients is a crucial requirement. Hence, it is very important to determine chemical purity and RCP of ^{90}Y EDTMP prior to injection [11.8].

11.5.1. Methods and results

11.5.1.1. Preparation of ^{90}Y EDTMP

Yttrium-90 labelled EDTMP was prepared by dissolving 150 mg of EDTMP in a 25% solution of NH_4OH , diluted to 10 mL with water and pH adjusted to ~8–8.5. A volume of 1 mL of this solution was labelled with 5 mCi of ^{90}Y , and then the pH was again adjusted to 6.5 using 0.1M ammonium chloride. The reaction was kept at room temperature for 15 min. The RCP was determined using an LS 6500 Beckman instrument.

(a) Procedure for purity determination

Take the labelled solution and measure it following the method described by Volkert et al. [11.9]. Test solution = 100 μL of ^{90}Y EDTMP + 10 mL (0.1M) HCl. Take 100 μL from the solution above and transfer it to column exchange Sephadex C-25 gel chromatography materials after washing with 0.9% NaCl (saline) (initial activity), which was eluted from the column. Free ^{90}Y stays in the column exchange. To remove the free ^{90}Y , wash the column again with 15–20 mL of saline (activity in column exchange). The RCP can be determined from:

$$\text{RCP}(\%) = \left(1 - \frac{\text{activity in column exchange}}{\text{initial activity}} \right) \times 100$$

11.5.1.2. Quality control

Paper chromatography with ^{90}Y labelled EDTMP was carried out using Whatman paper 3M as the stationary phase and $\text{NH}_4\text{OH}:\text{MeOH}:\text{H}_2\text{O}$, in the

ratio 0.2:2:4, as the mobile phase. Chromatography detected free ^{90}Y and ^{90}Y EDTMP, as shown in Figs 11.12 and 11.13, respectively. The RCP values in both cases were $\geq 98\%$.

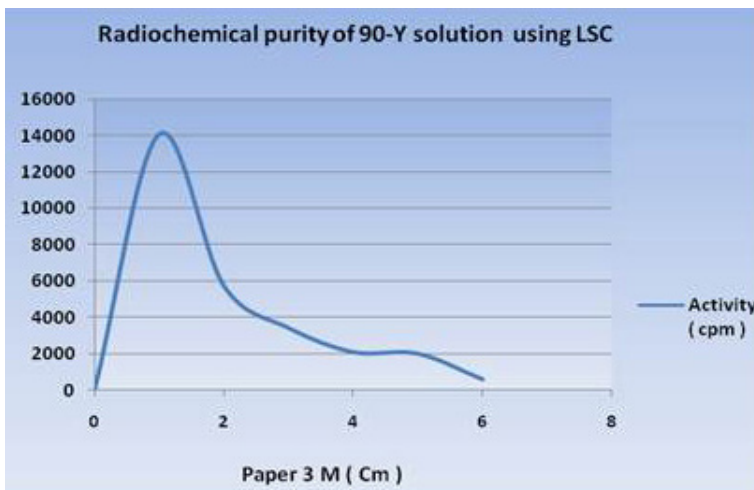


FIG. 11.12. RCP of ^{90}Y solution using ITLC Whatman paper 3M as the stationary phase and $\text{NH}_4\text{OH}:\text{MeOH}:\text{H}_2\text{O}$, in the ratio of 0.2:2:4, as the mobile phase.

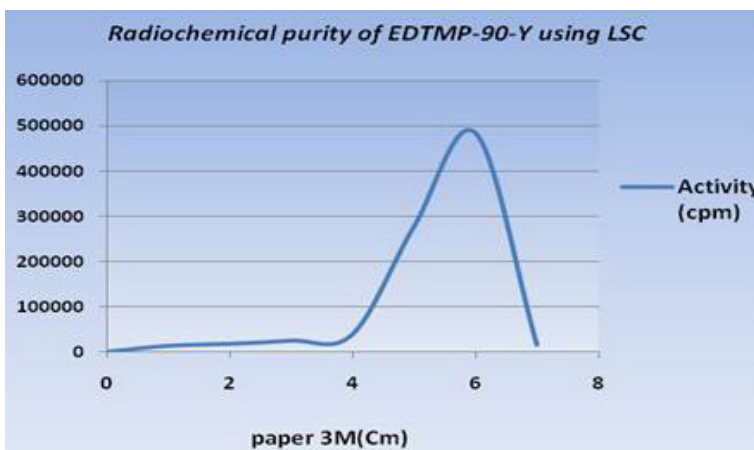


FIG. 11.13. RCP of ^{90}Y EDTMP using ITLC Whatman paper 3M as the stationary phase and $\text{NH}_4\text{OH}:\text{MeOH}:\text{H}_2\text{O}$, in the ratio of 0.2:2:4, as the mobile phase.

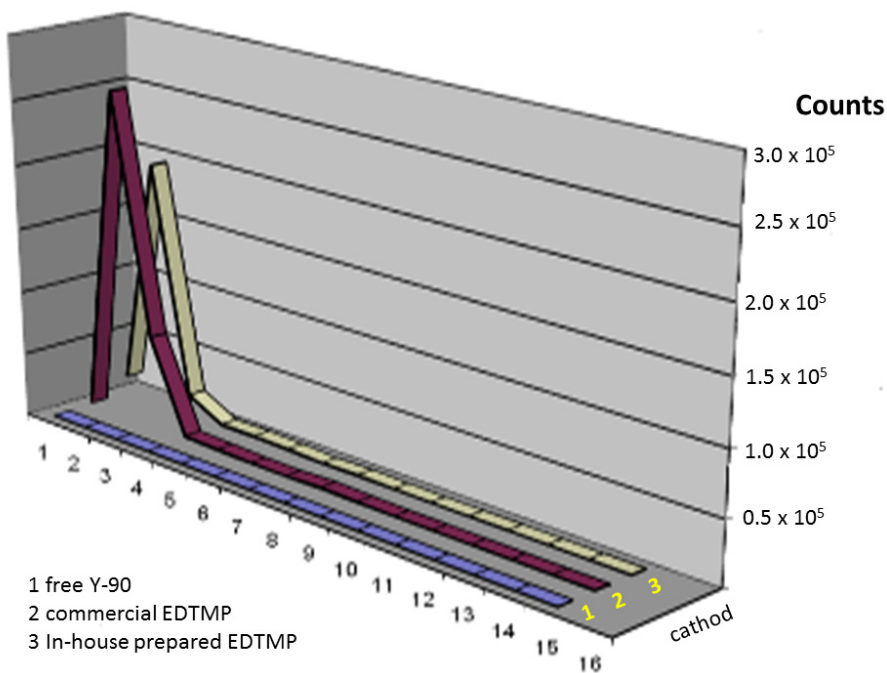


FIG. 11.14. Electrophoresis of ^{90}Y EDTMP after 20 d.

Electrophoresis of the labelled complex was carried out at 210 V for 1 h using a 0.025M phosphate buffer as the mobile phase. The results reported in Fig. 11.14 for the two types of EDTMP (local and commercial) showed that free ^{90}Y migrated to the cathode and ^{90}Y EDTMP to the anode. The RCP was $\sim 98\%$, and the results were reproducible [11.11, 11.12].

11.6. FHMA LABELLING WITH ^{90}Y

11.6.1. Methods and results

11.6.1.1. Preparation of ^{90}Y FHMA

Colloidal FHMA was prepared with a particle size in the range 2–10 μm and RCP $\geq 99\%$.

The starting (uncoated) super paramagnetic iron nanoparticles were prepared by mixing aqueous FeCl_3 with aqueous NH_4OH with stirring at room temperature for 15 min. A solution of FeCl_2 was then added and the mixture

poured into aqueous NH_4OH . The resulting magnetite precipitate was left for 15 min and repeatedly washed (7–10 times) with deionized water. Sodium citrate solution was added with stirring, and magnetite was oxidized by slow addition of a 5% aqueous solution of sodium hypochlorite. After applying the above procedure of repeated washing, the starting primary colloids were isolated [11.10].

The labelling with ^{90}Y was performed by co-precipitation of radioactive yttrium and ferric hydroxides under alkaline conditions. Briefly, 4.0 mL of 0.1M sodium citrate was added to 1 mL of $^{90}\text{YCl}_3$ (74–185 MBq) in a 10 mL vial followed by a previously prepared colloidal particulate, at room temperature. The resulting mixture was stirred vigorously under sonication and then centrifuged. Sodium citrate, 0.1M, was further added to 0.5 g of gelatin dissolved in 5 mL of saline, and the solution was stirred vigorously under sonication in a boiling water bath, before final addition of 1 mL of 5% aqueous sodium hypochlorite. The mixture was centrifuged at 3500 rev./min for 5 min, and the supernatant was removed and counted. The radiochemical yield was calculated as the percentage of radioactivity associated with the radiolabelled particles.

11.6.1.2. Particle size determination

A volume of 2 mL of saline was added to 1 mL of colloidal particles and stirred at 37°C . The particles were passed through filters of different sizes (0.2, 0.8, 2, 3, 5 and 10 μm), and collected fractions were evaluated for particle size determination. Preliminary estimates of particle sizes were carried out using an optical microscope and a scanning electron microscope, and >90% of particles were found to have sizes in the range 2–10 μm , as presented in Figs 11.15 and 11.16 [11.3].

11.6.1.3. Quality control

The RCP of ^{90}Y FHMA was determined by paper chromatography using Whatman No. 3 paper as the stationary phase and saline as the mobile phase. The RCP of ^{90}Y FHMA with gelatin was 99.2%, while without gelatin, it was 94.5%, as reported in Figs 11.17 and 11.18, respectively.

The RCP of ^{90}Y in saline was ~99.6%, as shown in Fig. 11.19.

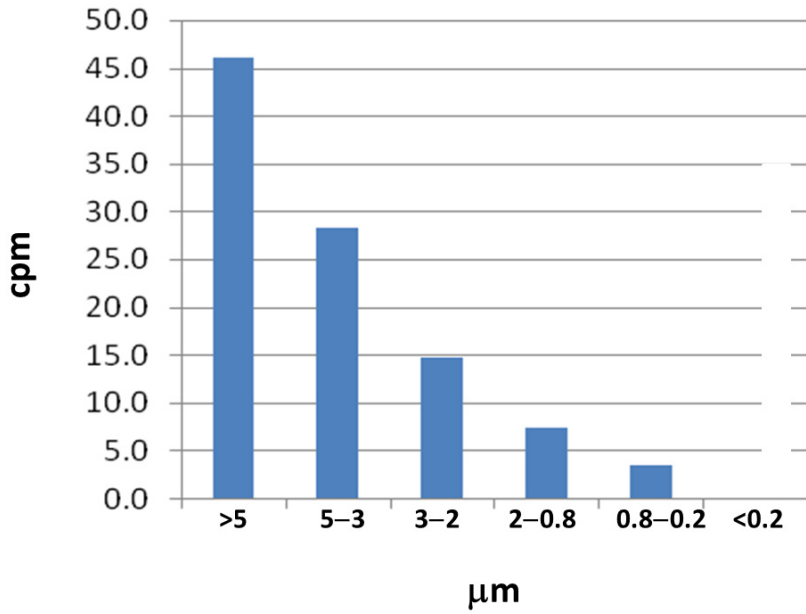


FIG. 11.15. Particle size distribution for ^{90}Y FHMA.

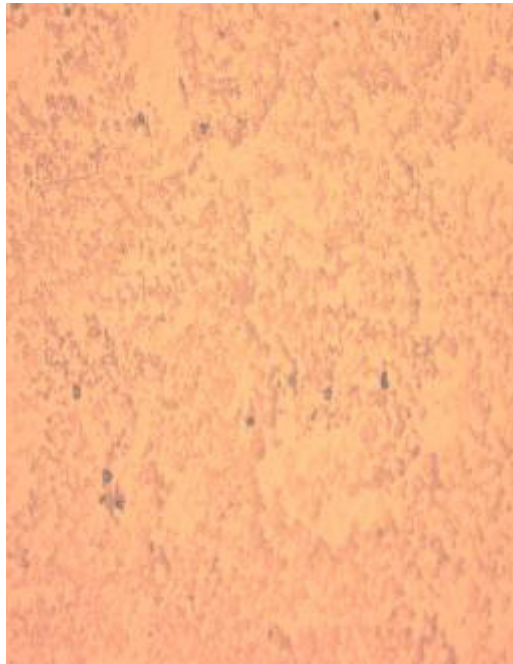


FIG. 11.16. Particle size of $2\ \mu\text{m}$ as viewed by an optical microscope.

chromatography paper y-colloid Y-FHMA

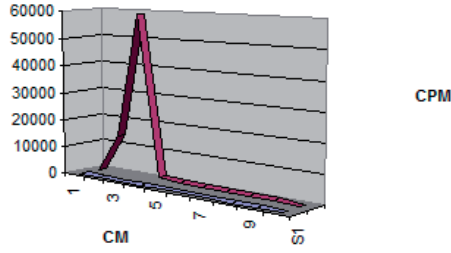


FIG. 11.17. RCP of ^{90}Y FHMA with gelatin.

Chromatography papery-colloid

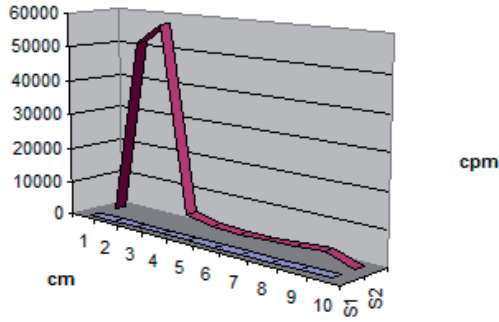


FIG. 11.18. RCP of ^{90}Y FHMA without gelatin.

Chromatography of Y-90

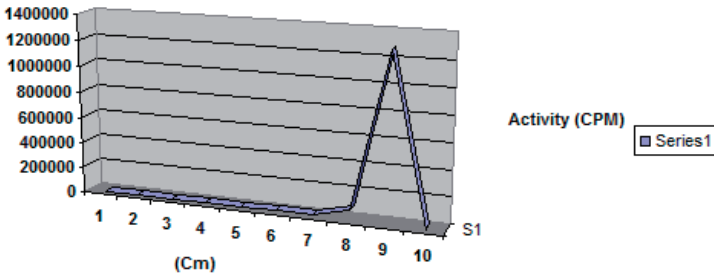


FIG. 11.19. RCP of ^{90}Y in saline.

11.7. CONCLUSION

During this CRP, a ^{90}Y generator and several radiopharmaceuticals were developed at AECS laboratories. An extraction chromatography generator was developed to give ~ 200 mCi of high quality ^{90}Y , and the ^{90}Sr impurity content was of the order of parts per billion. The resulting ^{90}Y was used for labelling various ligands and for preparing several radiopharmaceuticals such as ^{90}Y colloids, ^{90}Y EDTMP and ^{90}Y DOTA MABs (rituximab and nimotuzumab) [11.13].

ACKNOWLEDGEMENTS

The authors of this chapter appreciate the support of the IAEA in accomplishing this work. Thanks are due to the AECS, represented by I. Othman, for support. We are also grateful for all the technical assistance in the laboratory.

REFERENCES TO CHAPTER 11

- [11.1] HORWITZ, P.E., DIETZ, M.L., A process for the separation and purification of yttrium-90 for medical applications, United States patent application 8-095,555, Patents-US--A8095555 (1993).
- [11.2] CASTILLO, A.X., et al., Production of large quantities of ^{90}Y by ion-exchange chromatography using an organic resin and a chelating agent, *Nucl. Med. Biol.* **37** (2010) 935.
- [11.3] JALILIAN, A.R., et al., Preparation, quality control and biodistribution studies of two (^{111}In)-rituximab immunoconjugate, *Sci. Pharm.* **76** (2008) 151.
- [11.4] XIQUES, C.A., et al., An adapted purification procedure to improve the quality of ^{90}Y for clinical use, *Radiochim. Acta* **97** (2009) 739.
- [11.5] DENIS, R., et al., A new radio-immunoconjugate Y-90-DOTA-HR3: Synthesis and radiolabeling, *Nucleus* **41** (2007) 3.
- [11.6] SABBAH, E.N., et al., In vitro and in vivo comparison of DTPA- and DOTA-conjugated antiferritin monoclonal antibody for imaging and therapy of pancreatic cancer, *Nucl. Med. Biol.* **34** (2007) 293.
- [11.7] VENKATESH, M., USHA, C., PILLAI, M.R.A., " ^{90}Y and ^{105}Rh labelled preparations: Potential therapeutic agents", *Therapeutic Applications of Radiopharmaceuticals*, IAEA-TECDOC-1228, IAEA, Vienna (2001) 84.
- [11.8] CLUNIE, G., ELL, P.J., A survey of radiation synovectomy in Europe, *Eur. J. Nucl. Med.* **22** (1995) 970.
- [11.9] VOLKERT, W.A., et al., Radiolabeled phosphonic acid chelates: Potential therapeutic agents for the treatment of skeletal metastases, *J. Nucl. Med.* **14** (1989) 799.

- [11.10] MALJA, S., et al., “⁹⁰Y-preparation and some preliminary results on labelling of radiopharmaceuticals”, Therapeutic Applications of Radiopharmaceuticals, IAEA-TECDOC-1228, IAEA, Vienna (2001) 69.
- [11.11] ARGUELLES, M.G., LUPPIBERLANGA, I.S., TORRES, E.A., RUTTY SOLA, G.A., RIMOLDI, G., “Preparation and biological behavior of samarium-153-hydroxyapatite particles for radiation synovectomy”, Modern Trends in Radiopharmaceuticals for Diagnosis and Therapy, IAEA-TECDOC-1029, IAEA, Vienna (1998) 531.
- [11.12] FERRO-FLORES, G., et al., Kit preparation of ¹⁵³Sm-EDTMP and factors affecting radiochemical purity and stability, J. Radioanal. Nucl. Chem. 204 (1996) 303.
- [11.13] KOZAK, R.W., et al., Nature of the bifunctional chelating agent used for radio immunotherapy with Y-90 monoclonal antibodies – critical factors in determining in vivo survival and organ toxicity, Cancer Res. **49** (1989) 2639.

Chapter 12

DEVELOPMENT OF $^{90}\text{Sr}/^{90}\text{Y}$ GENERATORS AND RADIOPHARMACEUTICALS USING ^{90}Y

N. PORAMATIKUL

Research and Development Group,
Thailand Institute of Nuclear Technology,
Bangkok, Thailand

J. SANGSURIYAN

Radioisotope Center,
Thailand Institute of Nuclear Technology,
Bangkok, Thailand

W. SRIWEING

Research and Development Group,
Thailand Institute of Nuclear Technology,
Bangkok, Thailand

P. KAEOPOOKUM

Research and Development Group,
Thailand Institute of Nuclear Technology,
Bangkok, Thailand

A. CHANTAWONG

Research and Development Group,
Thailand Institute of Nuclear Technology,
Bangkok, Thailand

S. YASET

Research and Development Group,
Thailand Institute of Nuclear Technology,
Bangkok, Thailand

Abstract

Two types of $^{90}\text{Sr}/^{90}\text{Y}$ generators, an extraction system and an ion exchange system, have been designed and fabricated. The generator module was operated manually and the performance evaluated. The $^{90}\text{Sr}/^{90}\text{Y}$ extraction generator system has been developed for use

with high activities of ^{90}Sr up to 93 mCi. This $^{90}\text{Sr}/^{90}\text{Y}$ extraction generator was operated for six cycles, giving a mean ^{90}Y production yield of 65.8% (47.6–86.0 mCi). After purification using cation exchange chromatography, the RCP of ^{90}Y under acetate form was >99% using TLC and the ^{90}Sr breakthrough was $<1.4 \times 10^{-5}\%$ using EPC. The ^{90}Sr breakthrough was confirmed using ^{90}Sr counting after decay for 45 d and found to be $\leq 8 \times 10^{-6}\%$. Yttrium-90 labelling with DOTATE peptide showed moderate yields ranging between 60% and 85% using ITLC and HPLC, whereas some batches showed yields as low as 10–30%.

12.1. EXPERIMENTS

12.1.1. Design and fabrication of generators

12.1.1.1. Generator process design

The $^{90}\text{Sr}/^{90}\text{Y}$ extraction generator and $^{90}\text{Sr}/^{90}\text{Y}$ ion exchange generator were designed with some modifications according to the methods described in Refs [12.1–12.3], as shown in Figs 12.1 and 12.2.

12.1.1.2. Radiation shielding box

A shielded box was designed for the generator to protect the operator from high energy β rays from both ^{90}Y ($E_{\beta \text{ max}} = 2.2 \text{ MeV}$) and ^{90}Sr ($E_{\beta \text{ max}} = 0.54 \text{ MeV}$) and their bremsstrahlung radiation. A small glovebox with a 0.8–1.5 mm thick acrylic sheet was made for the generator and purification systems and a stainless steel box was used for fixing the column inside the acrylic box. The front wall and bottom of the box were lined with 2 mm thick lead sheet to shield bremsstrahlung radiation. The glovebox was installed inside a fume hood, which was connected to an exhaust filter system (high efficiency particulate and charcoal filters). The generator system was manually operated through two gloveports using long forceps and tweezers.

12.1.1.3. Equipment

All glassware used was of high grade borosilicate glass and was acid washed before use. A polypropylene (Eichrom Technologies) column and a sterile, disposable polystyrene three way valve were used. All tubing used was silicone tubing of pharmaceutical grade, except that used for concentrated acids, in which polytetrafluoroethylene (PTFE) tubing was used. Drying of the solution was carried out in a specifically made pear shaped flask with stainless steel or aluminium heating blocks kept in the glovebox. The temperature was controlled using a temperature controller and monitored from the outside.

12.1.1.4. Acid vapour trap and radioactive waste collection

Because of the long half-life of ^{90}Sr , acid vapour and other radioactive wastes were collected in a closed system after decreasing their volume. Acid vapour from the evaporation flask was evacuated using polyvinyl chloride tubing with an air jet pump (activated by compressed air) and trapped in an acid scrubber unit kept outside the fume hood. The unit had continuous circulating water from a storage tank and the drain returned to the tank. Other radioactive wastes in the process box were then washed and kept in a 20 L storage vessel under the fume hood, with the drainage port located on the box floor.

12.1.2. Strontium-90/yttrium-90 extraction generator

Three columns of strontium resin (Eichrom Technologies) were connected in tandem. A concentration of 3M HNO_3 was used as the eluent for ^{90}Y extraction and 0.05M HNO_3 for ^{90}Sr recovery. The flow rate of the peristaltic pump was set at 0.5 mL/min and ^{90}Y was collected for 30 mL in an evaporating flask, which was subsequently heated to dryness. The residue containing the ^{90}Y product was dissolved with 0.05M HCl. Strontium-90 adsorbed in the first and second columns was recovered with 0.05M HNO_3 (30 mL each) and collected in another evaporation flask, which was then heated to almost dryness for the next cycle. Strontium-90 was used at the tracer level (300–400 μCi) and the low level (6–8 mCi) to monitor the elution characteristics and for evaluation of the generator performance, respectively.

12.1.3. Strontium-90/yttrium-90 ion exchange generator

Two ion exchange resin columns (Dowex 50WX8, 100–200 mesh, H^+ form) were connected in tandem. Strontium-90 was dissolved in 0.003M EDTA, pH4.5, and loaded onto the first column. The generator was eluted with 40 mL of this buffer into an evaporating flask to enable collection of ^{90}Y in the form of the ^{90}Y EDTA complex. The eluate was subsequently digested with concentrated H_2SO_4 /concentrated HNO_3 by heating (300°C) to dryness. This ^{90}Y was preconditioned for purification by redissolving it in 0.05M HCl. Strontium-90 from the first column was recovered by washing with 20 mL of 2M HNO_3 and 20 mL of 4M HCl and subsequently collected in another evaporating flask. This was then heated to almost dryness for the next cycle. The amount of ^{90}Sr activity loaded was the same as that used in the $^{90}\text{Sr}/^{90}\text{Y}$ extraction generator.

12.1.4. Development of a high activity $^{90}\text{Sr}/^{90}\text{Y}$ generator

The $^{90}\text{Sr}/^{90}\text{Y}$ extraction generator system was developed for use with high activity ^{90}Sr (see Fig. 12.1(a)). The generator was first loaded with 93.0 mCi of ^{90}Sr (supplier calibrated) on 30 July 2011, and the system was operated on a 1–3 week cycle using the same method.

12.1.5. Yttrium-90 purification

Purification of ^{90}Y product was carried out using the method described previously [12.4, 12.5]. AG 1-X8 resin (Bio-Rad) was used as the stationary phase in cation exchange chromatography for the purification of the ^{90}Y crude product from each generator system. One column of 5 mm \times 200 mm was fixed in the stainless steel box kept inside the acrylic box. Washing to remove any metal impurities and ^{90}Sr contaminants was done with 20 mL of 0.5M H_2SO_4 , 20 mL of 2M HNO_3 and 20 mL of 2M HCl . The purified ^{90}Y product was collected with 30 mL of 4M HCl as the eluent, evaporated to dryness and finally redissolved in 0.05M HCl .

12.1.6. Quality control of ^{90}Y

The RCP of purified ^{90}Y was tested using TLC. A small amount of sample was made into acetate form with 0.5M NaOAc and analysed using the ITLC SG/0.9% NaCl system. The ITLC plate was counted for radioactivity, and the percentage calculated as ^{90}Y acetate. The radionuclidic purity of ^{90}Y (^{90}Sr breakthrough) was evaluated by modified EPC [12.6–12.8] using Whatman No. 3 paper. One drop (5 μL) of 0.1M 2-ethylhexyl-phosphoric acid was applied on the strip followed by 5 μL of the ^{90}Y sample. This was developed with 0.3M HNO_3 wherein ^{90}Y will remain at the origin and ^{90}Sr moves to the solvent front. The strips were cut and counted in an LSC. To confirm the EPC results, the same amount of samples was kept for ^{90}Sr counting after decay of ^{90}Y for ≥ 45 d.

12.1.7. Radiation dose rate

Radiation dose rates during generator operation at low (6–8 mCi) and high (93.0 mCi) ^{90}Sr activity loads were monitored using survey meters inside and outside the gloveboxes to assess the radiation safety of the systems.

12.1.8. Yttrium-90 peptide labelling

Five to ten millicuries of ^{90}Y in 300 μL and 350 μL 0.5M NH_4OAc were added to 20 μg of DOTATATE in a polypropylene tube, pH adjusted to 5.0–5.5, then heated at 90°C for 5 min in a water bath. After cooling for 5 min, the labelling yields were determined using TLC (ITLC SG/0.05M EDTA system) and a HPLC column (Agilent Technologies, Series 1200: C18, 5 μm , 4.6 mm \times 250 mm, mobile phase: A = 0.1% TFA/ H_2O , B = ACN; flow rate: 1 mL/min; analysis time: 30 min; detector: UV/ γ (NaI)).

12.2. RESULTS

12.2.1. Fabrication and processing of generator modules

Acrylic box containments with lead shielding for modules of the two generator systems and for purification parts were fabricated. The generator system was integrated in one main box for ^{90}Y processing and one small side box for ^{90}Sr recovery, as shown in Figs 12.1 and 12.2. The system was placed in a fume hood and manually operated. The processing time required for one cycle was ~ 3 h. The ^{90}Y purification part (on the right hand side of Fig. 12.2), which contained one cation exchange chromatography column, was placed in a separate shielded box for convenient operation owing to its short half-life compared to ^{90}Sr in the generator box.

12.2.2. Generator elution profiles

Elution profiles of ^{90}Y from extraction generator and ion exchange generator systems were monitored by counting each fraction in a Geiger–Müller (GM) counter, as shown in Fig. 12.3. The volumes of ^{90}Y fraction collected from each generator type were 30 and 40 mL, respectively.

12.2.3. Yttrium-90 yields and quality control

The yields of ^{90}Y from the extraction generator and the ion exchange generator loaded with a low activity of ^{90}Sr were 3.56–3.80 mCi and 0.53–1.42 mCi, respectively. For the $^{90}\text{Sr}/^{90}\text{Y}$ extraction generator with a high activity of ^{90}Sr (93 mCi), the yield of ^{90}Y was 47.6–86.0 mCi (see Fig. 12.4), with a mean generator yield of 65.8%.

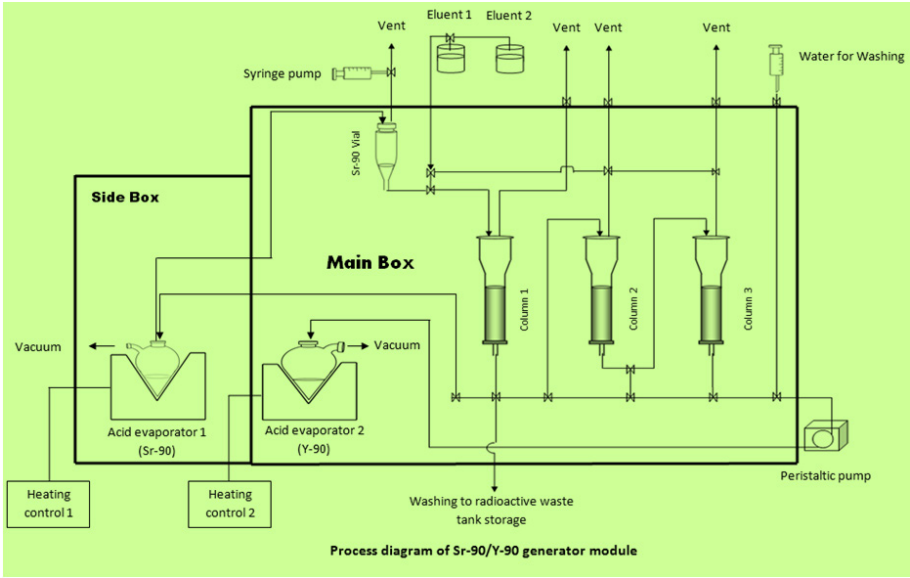


FIG. 12.1. Schematic diagram of the $^{90}\text{Sr}/^{90}\text{Y}$ extraction generator.

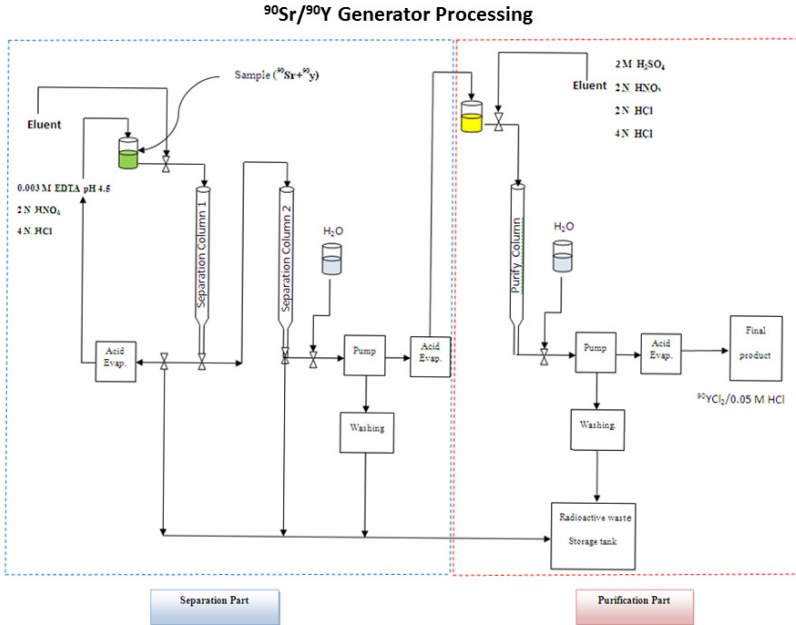


FIG. 12.2. Schematic diagram of the $^{90}\text{Sr}/^{90}\text{Y}$ ion exchange generator.

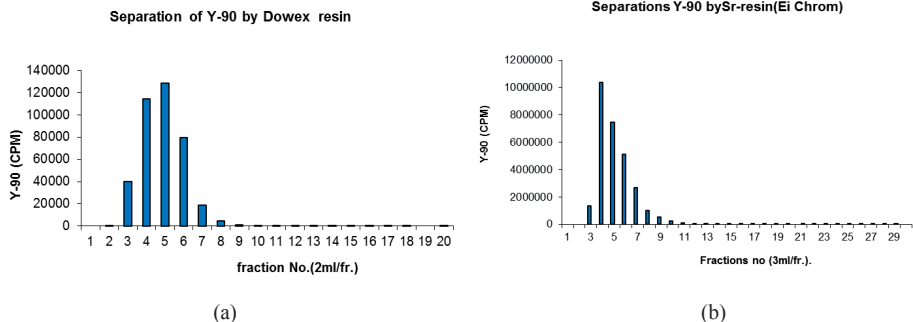


FIG. 12.3. Yttrium-90 elution profile of (a) $^{90}\text{Sr}/^{90}\text{Y}$ extraction generator and (b) $^{90}\text{Sr}/^{90}\text{Y}$ ion exchange generator.

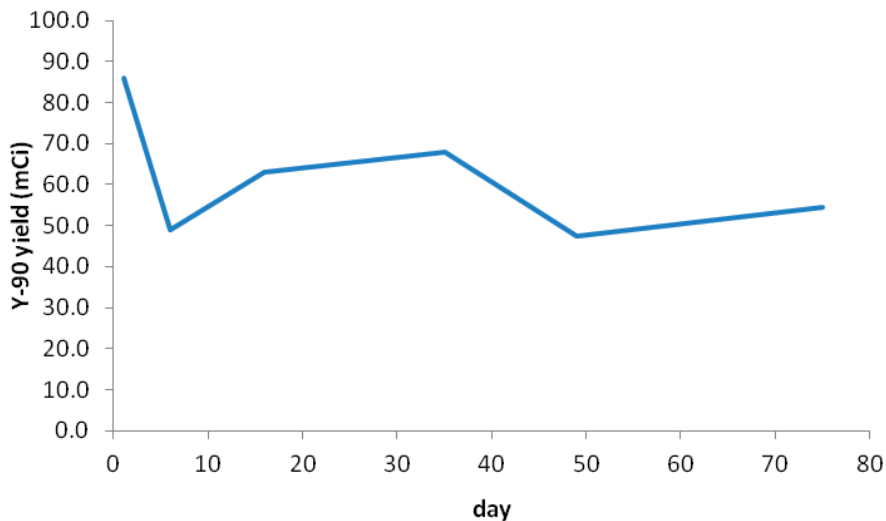


FIG. 12.4. Generator yields of $^{90}\text{Sr}/^{90}\text{Y}$ extraction generator with 93.0 mCi of ^{90}Sr (first load 30 July 2011).

The mean yield of ^{90}Y was 84.9% and the RCP of ^{90}Y as ^{90}Y acetate was 99.47% when determined using TLC. Strontium breakthrough by EPC was found to be $1.4 \times 10^{-5}\%$ (see Fig. 12.5). Contamination by ^{90}Sr , determined by counting ^{90}Sr activity in a GM counter after the decay of ^{90}Y (≥ 45 d), was found to be 4×10^{-5} to 2×10^{-6} mCi and 8×10^{-6} to 6.9×10^{-7} mCi for ^{90}Y products before and after purification, respectively.

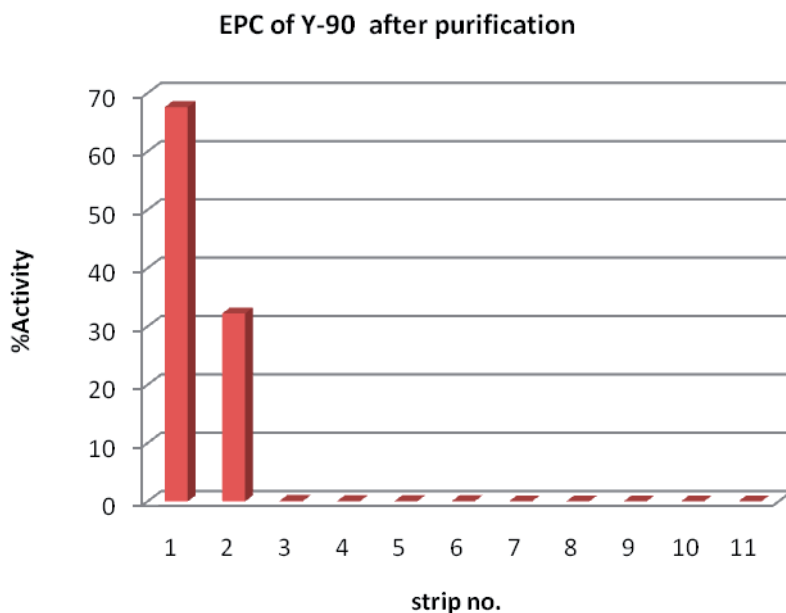


FIG. 12.5. EPC chromatogram of purified ^{90}Y collected using an LSC.

12.2.4. Radiation dose rate

The radiation dose rates while processing low ^{90}Sr (6–8 mCi) activity in the extraction generator, ion exchange generator and purification box were 1.2 and 0.1 mSv inside and outside (contact front) the box, respectively. The dose rate at the operator position for the $^{90}\text{Sr}/^{90}\text{Y}$ extraction generator with high ^{90}Sr activity loaded was approximately in the same range.

12.2.5. Yttrium-90 DOTATATE labelling yields

Labelling yields of ^{90}Y DOTATATE as determined using TLC and HPLC were 60–85%. In some batches, low yields of 10–39% were also found. The retention times for free ^{90}Y and ^{90}Y DOTATATE in the HPLC system were 4.7 and 9.5 min, respectively (see Fig. 12.6).

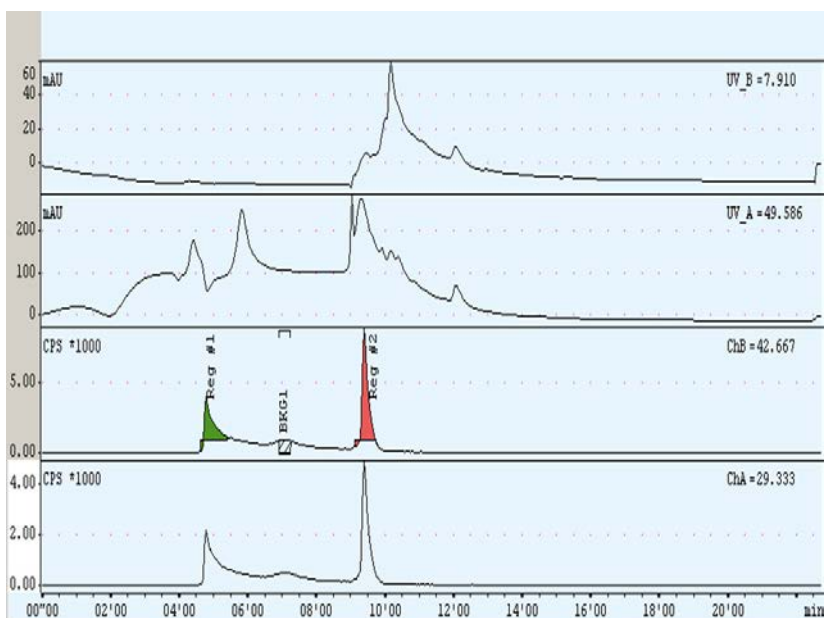


FIG. 12.6. HPLC of ^{90}Y DOTATATE.

12.3. CONCLUSION

The main conclusions from this study are the following:

- Design and fabrication of generator processing were completed;
- Processing and evaluation of the extraction generator were satisfactory;
- Processing of the ion exchange generator needs to be optimized: because some ^{90}Sr was adsorbed in the column, there was a loss of ^{90}Sr during processing;
- The yield with the extraction generator was 65.8%, while the yield with the ion exchange generator was low;
- After purification, the yield of ^{90}Y was 84.9% with RCP >99.5% and strontium breakthrough of $8 \times 10^{-6}\%$ or lower;
- The in house produced ^{90}Y could be used for labelling DOTATATE with ~85% labelling efficiency.

REFERENCES TO CHAPTER 12

- [12.1] CASTILLO, A.X., et al., Production of large quantities of ^{90}Y by ion-exchange chromatography using an organic resin and a chelating agent, *Nucl. Med. Biol.* **37** (2010) 935.
- [12.2] WIKE, J.S., GUYER, C.E., RAMEY, D.W., PHILLIPS, B.P., Chemistry for commercial scale production of yttrium-90 for medical research, *Appl. Radiat. Isot.* **41** (1990) 861.
- [12.3] DIETZ, M.L., HORWITZ, E.P., Improved chemistry for the production of yttrium-90 for medical application, *Int. J. Radiat. Appl. Instrum. Appl. Radiat. Isot.* **43** (1992) 1093.
- [12.4] STRELOW, F.W.E., RETHEMEYER, R., BOTHMA, C.J.C., Ion-exchange selectivity scales for cations in nitric acid and sulfuric acid media with a sulfonated polystyrene resin, *Anal. Chem.* **37** (1965) 106.
- [12.5] CHINOL, M., HNATOWICH, D.J., Generator-produced yttrium-90 for radioimmunotherapy, *J. Nucl. Med.* **28** (1987) 1456.
- [12.6] PORAMATIKUL, N., SANGSURIYAN, J., SRIWIENG, W., CHANTHAWONG, A., YASET, S., "Development of an early detection method to quantify contaminated Sr-90 in Y-90 for therapeutic radiopharmaceuticals", *Proc. Siam Physics Congress, Kanchanaburi, Thailand, March 2010.*
- [12.7] PORAMATIKUL, N., SANGSURIYAN, J., SRIWIENG, W., "Validation of extraction paper chromatography as a quality control technique for analysis of Sr-90 in Y-90 product", *Proc. 11th Nuclear Science and Technology Conf., Bangkok, Thailand, July 2009.*
- [12.8] PANDEY, U., DHAMI, P.S., JAGASIA, P., VENKATESH, M., PILLAI, M.R.A., Extraction paper chromatography technique for the radionuclidic purity estimation of ^{90}Y , *Anal. Chem.* **80** (2008) 801.

Chapter 13

BIFUNCTIONAL BISPHOSPHONATE COMPLEXES OF ^{99m}Tc AND ^{188}Re FOR DIAGNOSIS AND THERAPY OF BONE METASTASES

R.T.M. DE ROSALES, D.J. BERRY, P.J. BLOWER
Division of Imaging Sciences and Biomedical Engineering,
King's College London,
St Thomas' Hospital,
London, UK

Abstract

A simple method to purify the rhenium tricarbonyl precursor for labelling small molecules and biomolecules with ^{188}Re is reported in this chapter. The synthesis of a new radiopharmaceutical for the radionuclide therapy of bone metastases and of the corresponding ^{99m}Tc analogue is also described. In contrast with the clinically approved $^{186/188}\text{Re}$ HEDP, this new ^{188}Re agent forms an inert, single species that has been well characterized and displays superior stability, selective bone targeting and retention properties. Similarly, a new bone seeking ^{99m}Tc tracer prepared using the ^{99m}Tc nitrido core as a prerduced intermediate shows prolonged retention in bone and higher stability and binding to serum proteins compared to ^{99m}Tc MDP.

13.1. INTRODUCTION

1,1-Bisphosphonates are a family of compounds that are extensively used in the management of disorders of bone metabolism [13.1]. They accumulate in areas of high bone metabolism, such as bone metastases, and consequently have been receiving increasing attention as molecular imaging probes and pain palliation treatments [13.2]. Imaging of bone metastases with bisphosphonates using SPECT or planar scintigraphy is one of the most common clinical imaging procedures. Beta emitting analogues capable of producing a therapeutic effect have also been developed [13.3]. In particular, the rhenium compounds $^{186/188}\text{Re}$ HEDP have shown promise as palliative agents for bone metastases in recent clinical trials [13.4]. The radiochemicals consist of a complex of a bisphosphonate (e.g. MDP) with γ (^{99m}Tc) or β ($^{186/188}\text{Re}$) emitters.

Despite the proven clinical success of $^{99m}\text{Tc}/^{188/186}\text{Re}$ bisphosphonates, these radiopharmaceuticals are far from optimal, from the chemical and pharmaceutical points of view. For example, despite decades of clinical use, their structures and compositions remain unknown. A critical review of the literature reveals that the ^{99m}Tc MDP preparation used in clinical practice is composed of a mixture of anionic polymers of different properties [13.5]. A particular concern is that the in vivo stability of $^{186/188}\text{Re}$ bisphosphonates does not adequately match their physical half-lives, and a large fraction of the injected complex degrades to perrhenate in vivo within 24 h, leading to reduced bone uptake and higher soft tissue doses [13.6]. Furthermore, $^{186/188}\text{Re}$ bisphosphonates are not chemically analogous to their technetium counterparts and do not target bone metastases unless additional ‘carrier’ non-radioactive rhenium is added [13.7]. Consequently, there is a need for rational design of $^{186/188}\text{Re}$ labelled bisphosphonate derivatives to improve specificity and reduce soft tissue and bone marrow doses during radionuclide therapy.

In current technetium rhenium bisphosphonate complexes, the bisphosphonate acts as both the chelator and the targeting group. Each role, however, may compromise the other because bisphosphonates are excellent bone seeking agents but poor rhenium chelators. To improve upon current $^{186/188}\text{Re}$ bisphosphonates, a more logical approach is the use of targeted bifunctional ligands in which the targeting (bisphosphonate) and metal chelating groups are separated within the molecule so that they can each function independently and effectively. A few recent reports describe such a bisphosphonate chelator bifunctional approach [13.8, 13.9]. These bisphosphonate conjugates, however, require complicated multistep synthetic strategies, show high plasma protein binding and often form enantiomeric mixtures. Herein reported, is a new chelator bisphosphonate conjugate **3** (DPA bisphosphonate) that is synthesized using mild aqueous conditions in one step from commercially available compounds. In addition, **3** efficiently complexes with the $\text{M}(\text{CO})_3^+$ core **4** ($\text{M} = \text{Tc}, \text{Re}$) to form single, well defined isostructural technetium rhenium complexes **5** and **6** with no detectable protein binding that efficiently accumulate in bone tissue in vivo. A second new chelator **7** (DTC bisphosphonate) is herein reported, which comprises a dithiocarbamate linked to a bisphosphonate group, which forms a stable complex with the $^{99m}\text{Tc}(\text{V})$ nitride core **8** to give a bis(bisphosphonate) complex **9** that also accumulates efficiently in bone in vivo.

Our approach requires the bisphosphonate part of the molecule to be separated from the chelator by a spacer, to avoid any bisphosphonate–metal interactions. In addition, the radionuclide must selectively coordinate with the chelating group, not the bisphosphonate, and must remain inert under in vivo conditions. The organometallic precursor *fac*- $[\text{M}(\text{CO})_3(\text{H}_2\text{O})_3]^+$ ($\text{M} = \text{Tc}, \text{Re}$) (**4**, see Fig. 13.1), pioneered by Jaouen et al. and Alberto et al., facilitates the

latter requirement [13.10]. When the three labile water molecules are displaced by an appropriate ligand system, the d^6 low spin octahedral Tc(I) Re(I) centre formed is protected from oxidation and ligand substitution. Furthermore, imaging probes containing a coordinatively saturated *fac*-[M(CO)₃]⁺ core have shown high *in vivo* inertness and negligible binding to human serum proteins [13.11]. Particularly favourable ligands for [M(CO)₃]⁺ are N₃ tridentate chelators containing two sp² N-heterocycles, such as DPA [13.12]. As the targeting vector, an alendronate (**2**, see Fig. 13.1), a clinically approved bisphosphonate, was selected that binds avidly to HA, the main component of bone mineral [13.13]. Furthermore, **2** provides an amino group conveniently separated from the bisphosphonate group by a spacer, allowing facile one step conjugation of two picolyl units to form a DPA group see Fig. 13.1).

Two major obstacles were encountered during the development of DPA ale (**3**, see Fig. 13.1(a)). First is the insolubility of alendronate in organic solvents, which complicates conjugation reactions. Second, the high basicity of its amino group (acid dissociation constant $pK_a = 12.7$) inhibits nucleophilic attack by alendronate using standard organic bases [13.14]. Important factors to overcome

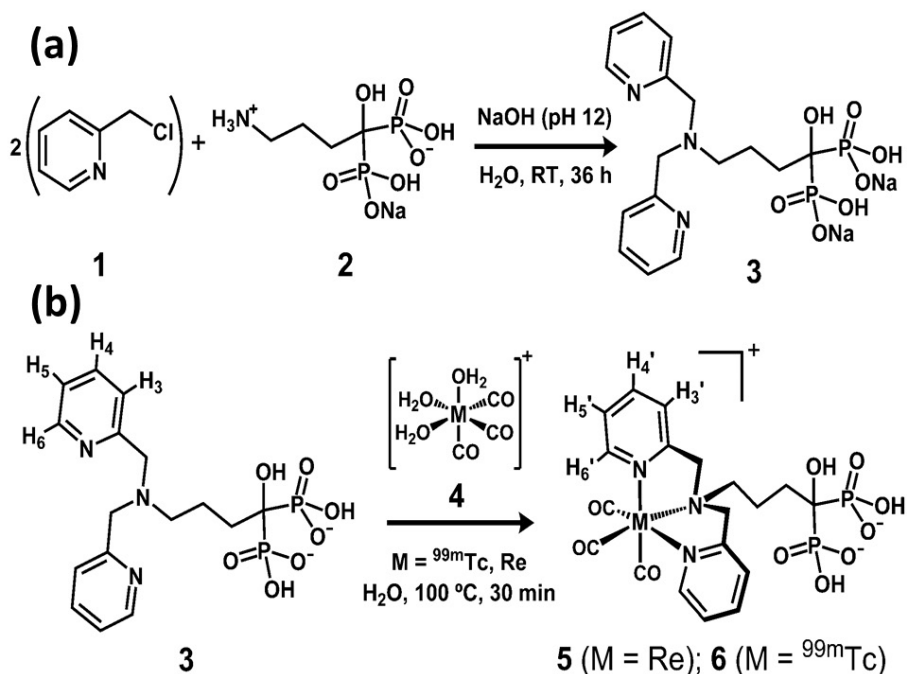


FIG. 13.1. Schematic diagram of the synthesis of bisphosphonate ligands and Tc(I)/Re(I) complexes.

these barriers are pH and the concentration of the base. Using strong organic bases such as triethylamine was unsuccessful. High concentrations of inorganic bases and high temperatures, however, led to hydrolysis of 2-picolyl chloride (**1**, see Fig. 13.1(a)) and rearrangements of the bisphosphonate [13.15]. It was found that using water as the solvent and maintaining the pH of the solution at 12 with a minimum amount of NaOH was sufficient to drive the reaction to completion after 36 h at room temperature, without detectable hydrolysis or bisphosphonate rearrangements. The yield of **3** was >90% using RP HPLC.

13.2. MATERIALS AND RESULTS

13.2.1. Technetium-99m and $^{187/185}\text{Re}$ studies with DPA bisphosphonate **3**

The complexation of **3** with *fac*- $[\text{Re}(\text{CO})_3]^+$, and its solution properties, were examined using HPLC (see Fig. 13.2) and nuclear magnetic resonance (NMR) spectroscopy, MS and IR spectroscopy. The aim was to determine

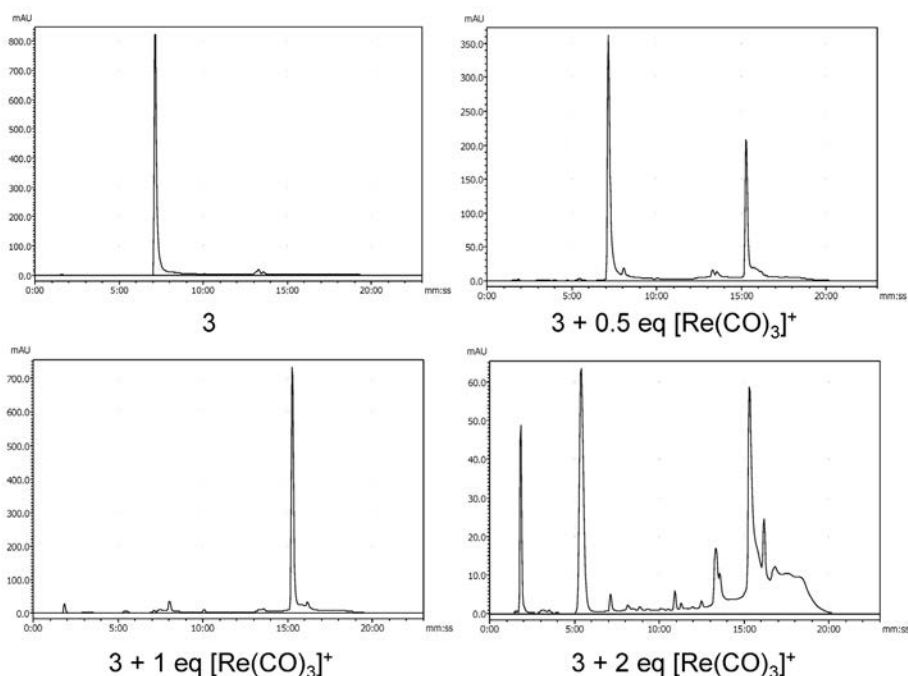


FIG. 13.2. RP HPLC chromatograms of **3** (top left) and **3** plus increasing amounts of $[\text{Re}(\text{CO})_3]^+$.

whether the organometallic core selectively coordinated the chelating DPA group. NMR spectroscopy and HPLC titration studies revealed that $fac\text{-}[\text{Re}(\text{CO})_3(\text{H}_2\text{O})_3]^+$ stoichiometrically binds **3** in the designed facial conformation when <1.5 equivalents of $fac\text{-}[\text{Re}(\text{CO})_3(\text{H}_2\text{O})_3]^+$ were used. The presence of a single species corresponding to **5** in solution was confirmed using $^1\text{H}/^{31}\text{P}$ NMR spectroscopy and HPLC (see Fig. 13.2). High resolution electron spray ionization MS also demonstrates the formation of the desired product. Upon addition of ≥ 1.5 equivalents of the metal reagent, new ^{31}P NMR signals appeared, accompanied by a general upfield shift of the aromatic protons in the ^1H NMR spectrum, strongly suggesting coordination of metal centres to the bisphosphonate group. These putative multinuclear species, however, do not form during radiosynthesis because the concentration of ligand always exceeds that of the radionuclide by several orders of magnitude. Complex **3** in concentrations as low as 10^{-5}M ($0.7\ \mu\text{g}$ per labelling) can be efficiently labelled with $fac\text{-}[^{99\text{m}}\text{Tc}(\text{CO})_3]^+$ in water to form **6** ($>98\%$ radiochemical yield, $22\ \text{GBq}/\text{mg}$). RP HPLC analyses show that **5** and **6** coeluted, demonstrating their analogous structure (see Fig. 13.3).

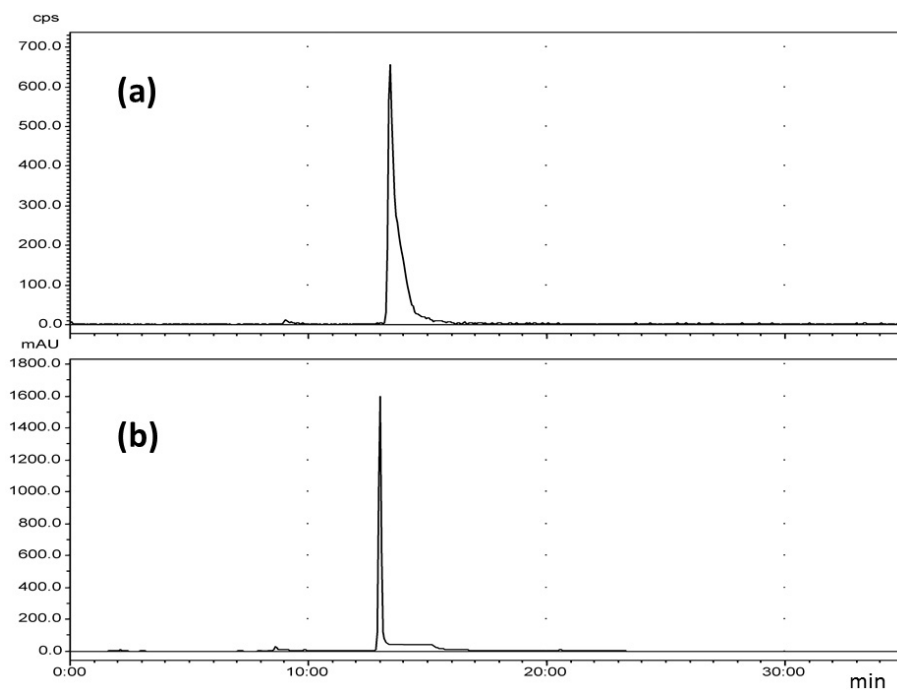


FIG. 13.3. RP HPLC chromatograms (method B) of (a) **6**, γ detection, 13.26 min and (b) **5**, UV detection, 13.14 min. The difference in retention time observed (12 s) is because of the lag time between the in line γ and UV detectors.

One of the factors that makes **2** one of the most potent bisphosphonate drugs is its high skeletal uptake and retention, which is directly related to its affinity towards HA [13.13]. The affinities and selectivities of **6** and ^{99m}Tc MDP towards several calcium salts were evaluated using an in vitro assay. As shown in Fig. 13.4, **6** binds HA selectively with very high affinity (>80% binding). On the other hand, ^{99m}Tc MDP is less selective and binds HA and calcium oxalate (CO) with lower affinity (~40% binding). Remarkably, **6** shows higher affinity for HA, despite having a concentration of competitive inhibitor (in the form of non-labelled bisphosphonate) approximately 10 times higher than in the ^{99m}Tc MDP preparation [13.16].

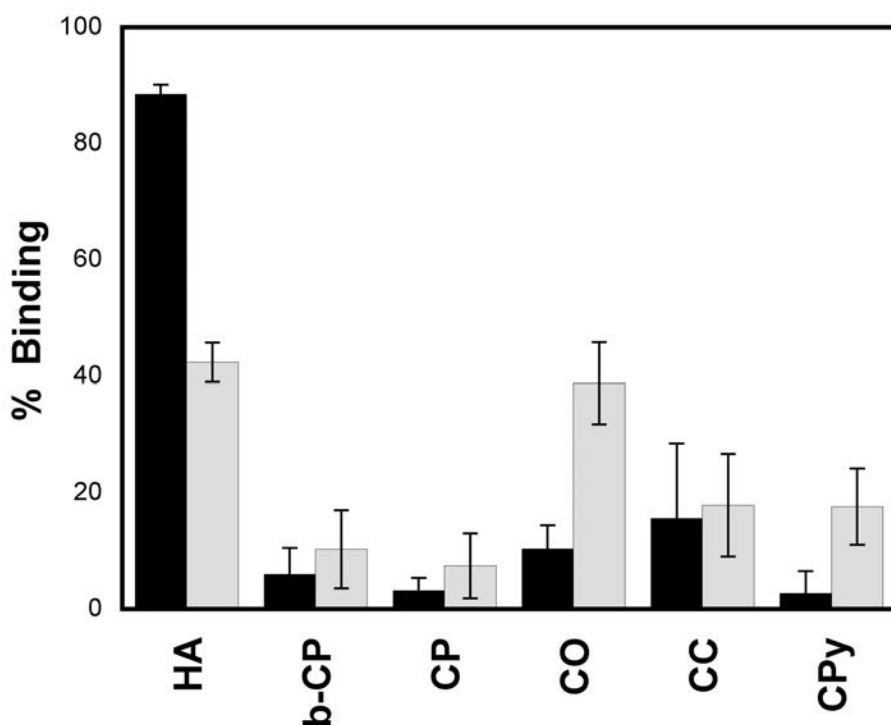


FIG. 13.4. In vitro calcium salt binding study in 50mM Tris pH6.9 at room temperature to compare the binding of **6** (black bars) and ^{99m}Tc MDP (grey bars) to different calcium salts after 1 h (1 mg/mL): HA; β -tricalcium phosphate (b-CP); calcium phosphate (CP); calcium oxalate (CO); calcium carbonate (CC) and calcium pyrophosphate (CPy).

The fate of a targeted imaging probe or radiopharmaceutical in blood is one of the most important factors during preclinical development of radiopharmaceuticals. Strong binding to serum proteins such as albumin often delays blood clearance, leading to low target to background ratios [13.11]. Previous chelator bisphosphonate conjugates have shown high binding to serum proteins [13.9]. Furthermore, human plasma enzymes may decompose exogenous compounds. Complex **6** showed negligible binding to serum proteins and no decomposition after incubation with human plasma for at least 18 h (see Fig. 13.5). On the other hand, ^{99m}Tc MDP remained mostly bound to serum proteins throughout the 18 h incubation.

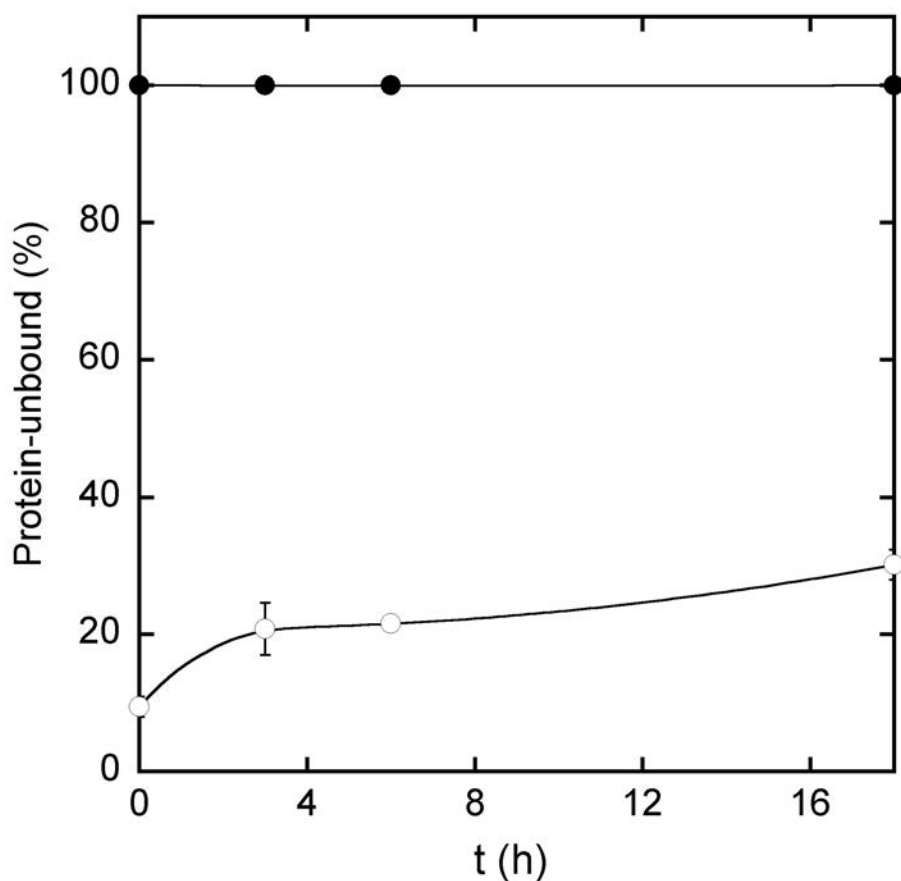


FIG. 13.5. Serum protein binding study of **6** (black circles) and ^{99m}Tc MDP (empty circles).

In vivo imaging studies with **6** were carried out on adult BALB/C female mice using a nanoSPECT/CT animal scanner. Control imaging studies were also performed using ^{99m}Tc MDP. Complex **6** shows essentially identical bone uptake to ^{99m}Tc MDP, demonstrating its usefulness as a bone seeking agent (see Figs 13.6 and 13.7). Biodistribution studies were performed ex vivo to quantify the uptake of the two tracers in bone and soft tissue organs (see Fig. 13.6). As expected, the bone uptake of both compounds was very high, with 27–30%ID/g in the femur. Imaging shows that this uptake was in fact confined to the joints, where active remodelling occurs. Liver and lower gastrointestinal uptakes, while very low, were slightly higher with **6** (2.5%ID/g) than with ^{99m}Tc MDP (0.4%ID/g), which is consistent with the more lipophilic nature of the tricarbonyl core compared to MDP. An advantage of using bifunctional compounds is that properties such as lipophilicity may be tuned by using, for example, different spacers and/or chelators.

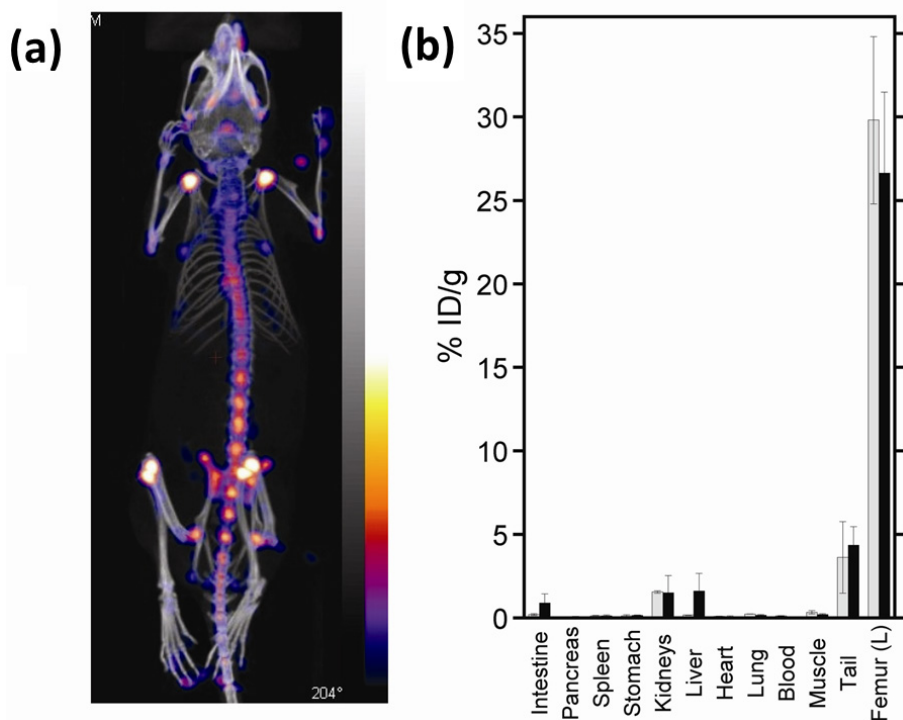


FIG. 13.6. (a) SPECT (colour)/CT (grey scale) image showing the high uptake of **6** in bone tissue, particularly at the joints. (b) Biodistribution profile of **6** (black bars) and ^{99m}Tc MDP (grey bars) at $t = 6.5$ h p.i.

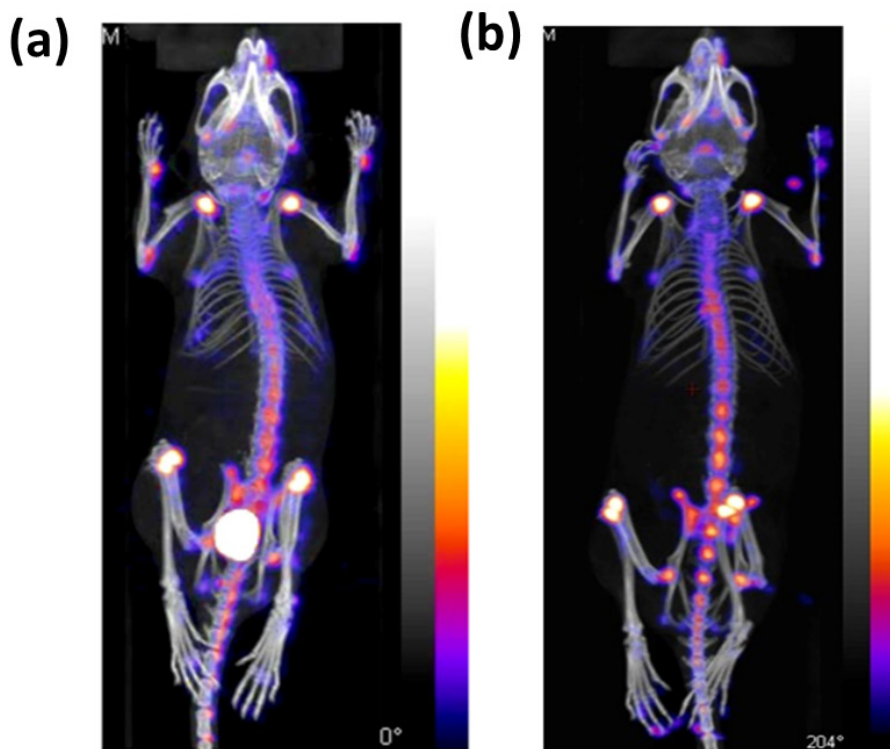


FIG. 13.7. SPECT/CT images showing the essentially identical bone uptake of: (a) ^{99m}Tc MDP and (b) **6** in mice.

13.2.2. Rhenium-188 studies with DPA bisphosphonate

The synthesis, characterization and preclinical in vivo studies of its ^{188}Re complex, $^{188}\text{Re}(\text{CO})_3$ DPA ale (**5**, see Fig. 13.8, *vide infra*), in comparison with ^{188}Re HEDP, are described to evaluate its potential as a new improved radiopharmaceutical for the therapy of bone metastases. Complex **5** was easily made from generator eluted $^{188}\text{ReO}_4^-$ in two steps (see Fig. 13.8). The precursor *fac*- $^{188}\text{Re}(\text{CO})_3(\text{H}_2\text{O})_3^+$ (**4**, see Fig. 13.8) was synthesized following the method of Salmain et al. [13.17]. The radiochemical yields of **4** ranged between 80% and 85%, in agreement with the published method, with the remaining by-products being unreduced and/or reoxidized $^{188}\text{ReO}_4^-$ and colloidal $^{188}\text{ReO}_2$. A new purification method was required because it was not described in the original report. It was reasoned that ionic chromatography could be used to separate the two by-products based on their ionic and colloidal characters. Thus, the crude solution was passed through a system composed of two solid phase extraction

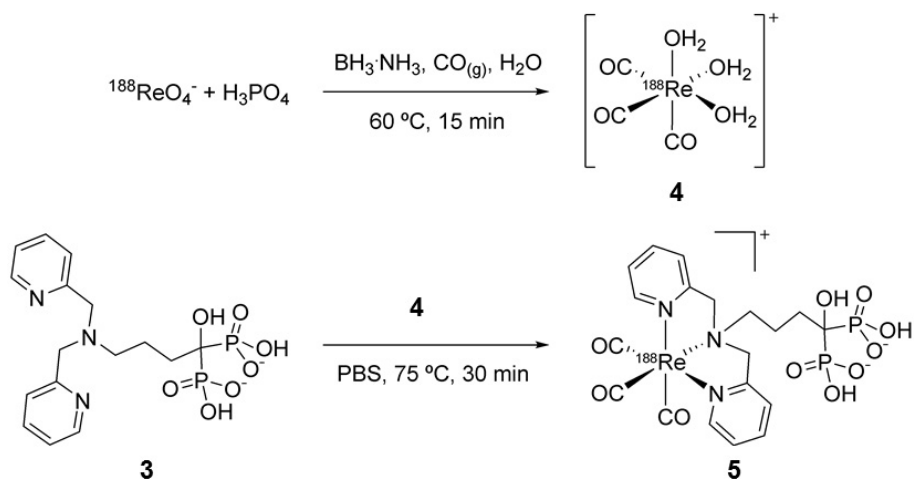


FIG. 13.8. Preparation ^{188}Re radiopharmaceuticals with bisphosphonate ligands.

columns connected in series, an OnGuard II Ag column (Dionex) to remove chloride ions from the saline solution followed by a strong anion exchange (SAX) column (SAX Varian Bond Elut, 100 mg) to retain $^{188}\text{ReO}_4^-$. Using this system, **4** can be obtained in the eluate in good radiochemical yields (65%, based on initial $^{188}\text{ReO}_4^-$ activity) and excellent purities ($\geq 99\%$) (see Fig. 13.9). The OnGuard II Ag column was proven necessary to remove the chloride ions from the saline solution that otherwise compete with $^{188}\text{ReO}_4^-$ in the SAX column, at the expense of **4** being retained to some extent in the OnGuard II Ag column (10%). Attempts to release trapped **4** using increasing concentrations of NaCl were unsuccessful, suggesting the interaction between **4** and the OnGuard II Ag column is not ionic.

Complex **5** was synthesized by mixing a solution of freshly made **4** (100 μL , 150 MBq) with **3** (0.01 mg/mL in PBS, 100 μL) in a N_2 purged vial followed by heating at 75°C for 30 min. RP HPLC analysis of the reaction solution revealed the formation of **5** with a specific activity of 18.8 GBq/mg and $\geq 96\%$ radiochemical yield, with the remainder of the activity being $^{188}\text{ReO}_4^-$. In contrast to $[\text{}^{99\text{m}}\text{Tc}(\text{CO})_3(\text{OH}_2)_3]^+$, reoxidation of **4** to $^{188}\text{ReO}_4^-$ during labelling conditions has been observed previously with other ligands, and can be rationalized to be the result of the lower redox potential of rhenium compared to that of technetium [13.17–13.19]. Longer reaction times (up to 60 min) and lower reaction temperatures (60°C) led to lower yields of **5**. A comparison with the chromatogram of the well characterized non-radioactive $\text{Re}(\text{CO})_3$ DPA ale complex, and its $^{99\text{m}}\text{Tc}$ analogue, demonstrates the formation of the desired compound as a single species (see Fig. 13.10) [13.20].

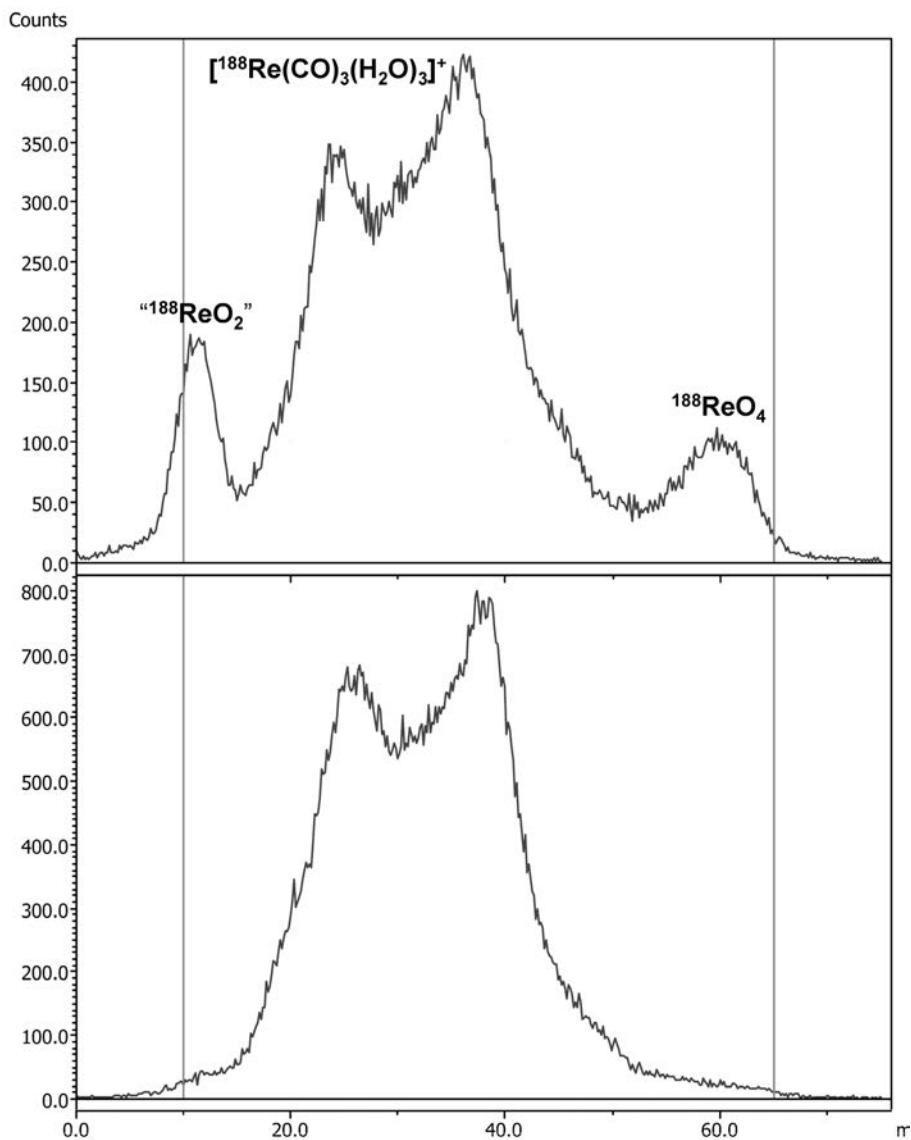


FIG. 13.9. TLC SG analyses of $[^{188}\text{Re}(\text{CO})_3(\text{H}_2\text{O})_3]^+$ (**4**) in the crude reaction solution (top) and after purification (bottom). Vertical lines indicate the origin and solvent front. Using $\text{MeOH}:\text{HCl}_{\text{conc}}$ (99%:1%) as the mobile phase, $^{188}\text{ReO}_2$ colloids appear at $R_f = 0.05$, **4** appears as two broad peaks with $R_f = 0.20\text{--}0.50$ and $^{188}\text{ReO}_4^-$ appears at $R_f = 0.90$.

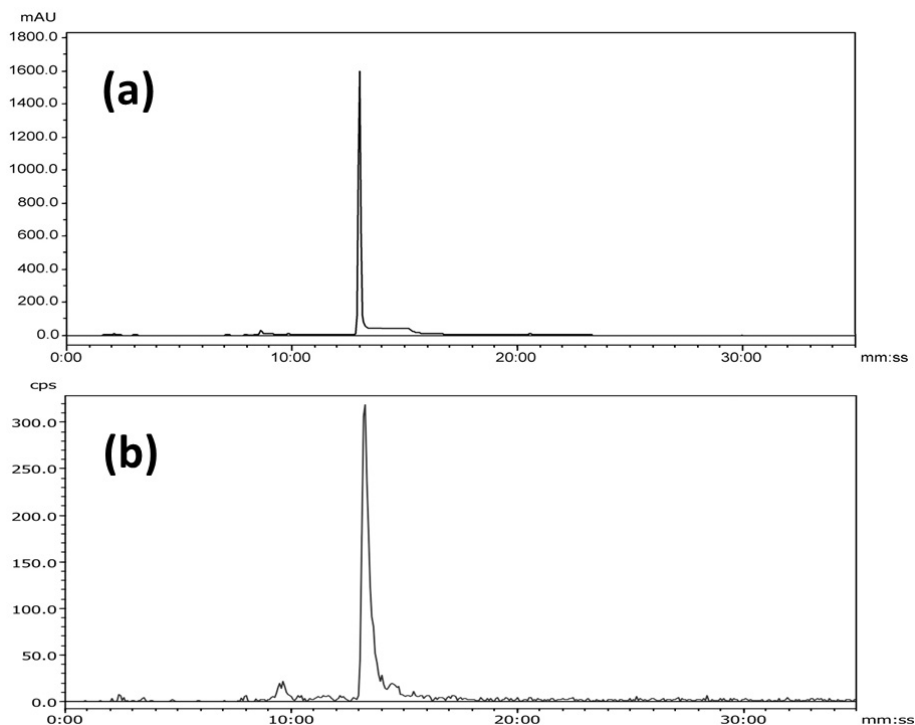


FIG. 13.10. RP HPLC chromatograms of non-radioactive $\text{Re}(\text{CO})_3$ DPA ale: (a) UV detection (254 nm), $t_R = 13.14$ min and 5; (b) β detection, $t_R = 13.12$ min). The difference in peak width is because of the larger cell volume of the γ/β detector.

To achieve the maximum therapeutic efficiency, ^{188}Re compounds must remain stable and bound to the target during at least one to three half-lives of ^{188}Re (16.9 h). One of the most important drawbacks of ^{188}Re HEDP is its lack of stability both in vivo and in vitro. To assess the in vitro stability of **5** in comparison with ^{188}Re HEDP, both compounds were incubated in PBS for 48 h at 37°C . RP HPLC and TLC analyses demonstrated that **5** did not degrade over this time, whereas most of the ^{188}Re HEDP oxidized to $^{188}\text{ReO}_4^-$ (up to 75%) (see Fig. 13.11).

Incubation of both compounds in human serum showed that most of the radioactivity from the ^{188}Re HEDP sample remains bound to serum proteins during the first 24 h. After this time, $\sim 70\%$ of the radioactivity was free in solution. ITLC analyses demonstrated, however, that the non-protein bound radioactivity was $^{188}\text{ReO}_4^-$, the decomposition product of ^{188}Re HEDP. Complex **5**, on the other hand, remained non-protein bound and unmodified throughout the 48 h incubation period (see Fig. 13.11).

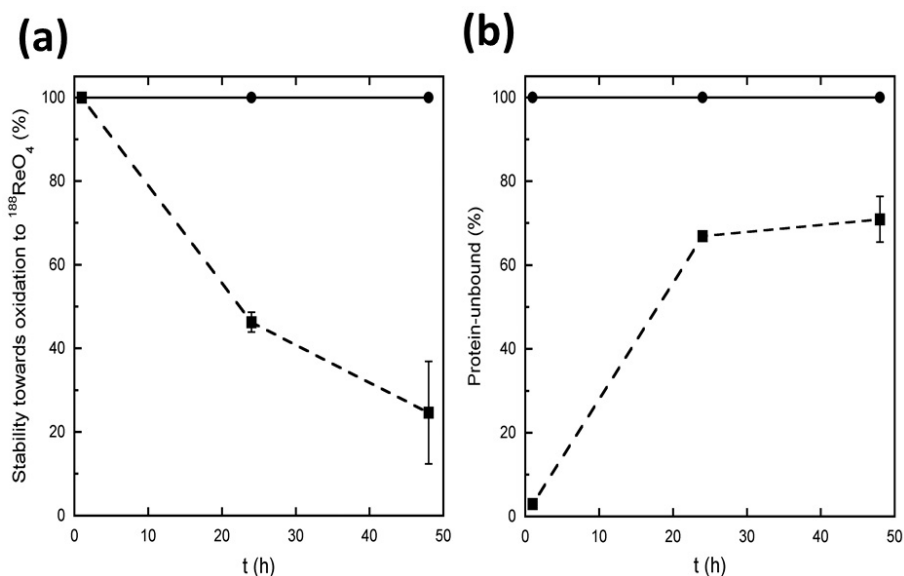


FIG. 13.11. Stability study (towards oxidation to $^{188}\text{ReO}_4^-$) in (a) PBS and (b) serum protein binding study of **5** (black circles) and ^{188}Re HEDP (black squares).

In vivo imaging studies with **5** and ^{188}Re HEDP were carried out at 1, 5, 24 and 48 h p.i. with adult BALB/c female mice using a nanoSPECT/CT scanner (see Fig. 13.12). These studies confirmed the ability of **5** to accumulate in areas of metabolically active bone such as the joints, while soft tissue organ uptake was very low throughout the experiment. Quantification of the images provided an interesting comparison of the pharmacokinetics of each compound (see Fig. 13.13). Thus, both compounds show an increase in uptake in the knee for the first 5 h. After this time, however, the uptake of **5** increased during the next 24 h, whereas that of ^{188}Re HEDP diminished until the end of the 48 h experiment. It was proposed that the increased uptake in bone of **5** during the first 24 h is the result of recycling of the unmetabolized, chemically intact complex from soft tissues, coupled with its excellent retention and slow release from bone compared to ^{188}Re HEDP. This is in agreement with the biodistribution profiles at 48 h (vide infra), as well as with previous in vitro experiments with its $^{99\text{m}}\text{Tc}$ analogue, demonstrating the superior capabilities of rhenium technetium DPA ale for binding, and remaining bound, to the main component of bone mineral (HA) [13.21].

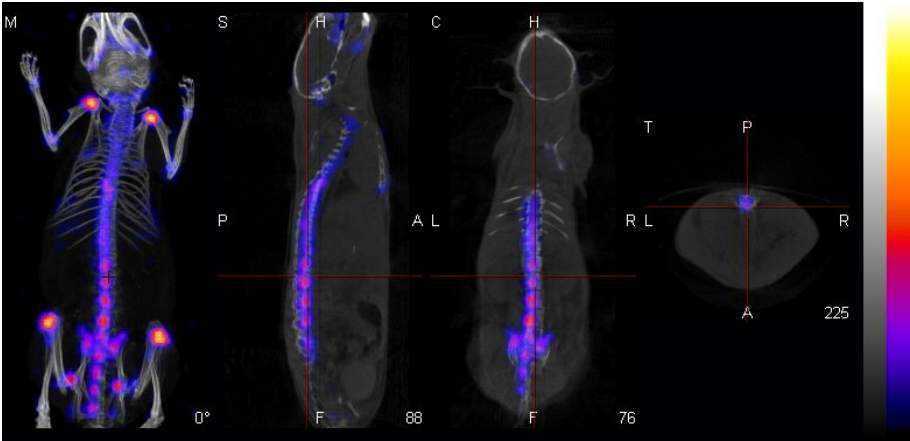


FIG. 13.12. SPECT (colour)/CT (grey scale) image taken 24 h p.i. showing the high uptake of ^{188}Re in bone tissue, particularly at the joints. From left to right, maximum intensity projection (M), sagittal (S), coronal (C) and transverse (T) sections.

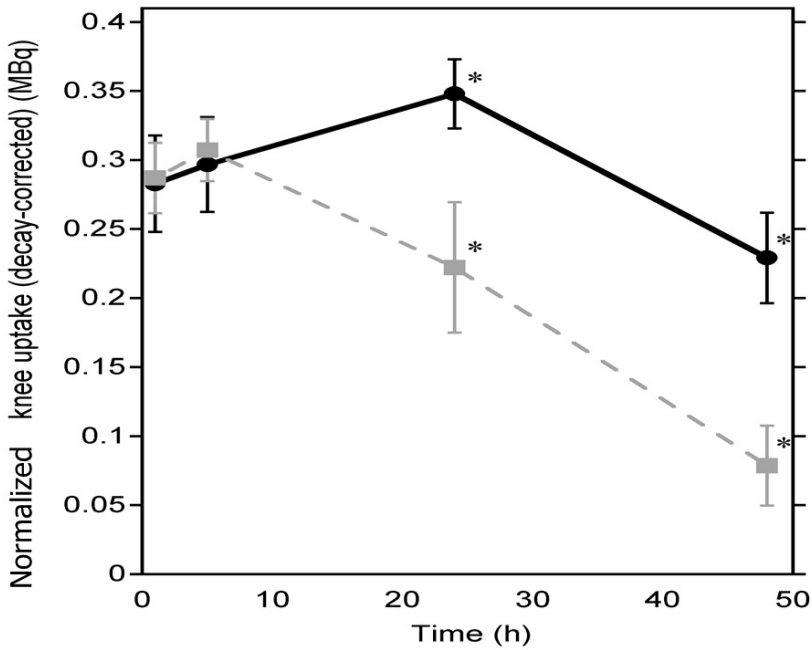


FIG. 13.13. Uptake in the left knee (decay corrected) after injection of 5 (33 MBq, black circles, continuous line) or ^{188}Re HEDP (29 MBq, grey squares, dashed line) obtained from region of interest analysis of the imaging data. The data from 5 were scaled by a factor of 29/33 to take into account the different injected activity. Values represent the mean \pm SD ($n = 3$ mice). * indicates a significant difference ($P < 0.05$, Student's paired t -test) between the two radiotracers.

Ex vivo biodistribution studies at 48 h demonstrate that **5** exhibits higher uptake in bone tissue than ^{188}Re HEDP ($21.2\% \text{ID/g} \pm 6.6\% \text{ID/g}$ for **5**; cf. $13.4\% \text{ID/g} \pm 0.2\% \text{ID/g}$ for ^{188}Re HEDP), consistent with its higher stability and/or better targeting properties (see Fig. 13.14). As shown in the above mentioned imaging studies, soft tissue uptake was very low for both compounds, with most organs having an uptake of $<0.6\% \text{ID/g}$. Complex **5** consistently shows higher uptake than ^{188}Re HEDP in these organs, especially in the liver ($0.96\% \text{ID/g} \pm 0.2\% \text{ID/g}$). This may be explained by the lipophilic nature of the tricarbonyl core. An interesting exception, however, is the lower uptake of **5** in the thyroid. This was attributed to the tendency of ^{188}Re HEDP, but not **5**, to decompose into $^{188}\text{ReO}_4^-$, which is known to be taken up by NIS expressing organs such as the thyroid [13.21–13.29].

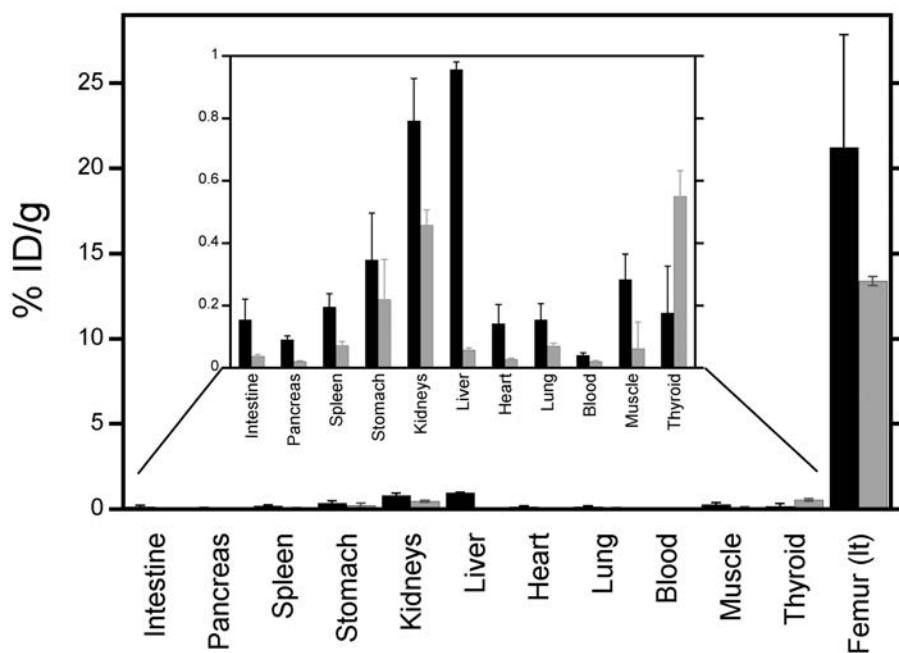


FIG. 13.14. Biodistribution profile of **5** (black bars) and ^{188}Re HEDP (grey bars) at $t = 48$ h p.i. Values represent the mean \pm SD ($n = 3$ mice).

13.2.3. Dithiocarbamate bisphosphonate conjugates

A new bifunctional ligand **7**, comprising a bisphosphonate group conjugated to a dithiocarbamate, was synthesized with a view to preparing bis(bisphosphonate) complexes using the pentavalent rhenium and technetium nitride cores (see Fig. 13.15). The methodology for the ligand synthesis has been described previously [13.30–13.32]. The solution of **6** used in these studies contained 10 times more non-labelled bisphosphonate than there was in the ^{99m}Tc MDP solution. To test the inhibition properties of **3**, the same binding studies were carried out with HA and CO in the presence of an excess of **3**, resulting in the complete inhibition of binding of **6**.

Radiolabelling to produce the ^{99m}Tc complex **9** was achieved by first making a $\text{Tc} \equiv \text{N}^{2+}$ intermediate [13.22, 13.23] as follows. Succinic dihydrazide (2.5 mg) and 1,2-diaminopropane- $\text{N},\text{N},\text{N}',\text{N}'$ -tetraacetic acid DPTA (1 mg) were dissolved in 0.5 mL saline. Technetium-99m pertechnetate generator eluate (700 MBq, 0.12 mL) was then added, followed by 30 μL of a 10 mg/mL solution of SnCl_2 in 0.05M HCl. The mixture was then incubated with shaking at room temperature for 30 min. After this time, TLC was performed using aluminium backed SG plates in a solvent system of 6:3:3:1 ethanol:chloroform:toluene:0.5M ammonium acetate, in which pertechnetate had $R_f = 0.5$ and was shown to be absent. A volume of 300 μL of the $^{99m}\text{TcN}^{2+}$ intermediate thus prepared was added to 200 μL of 50mM sodium carbonate buffer containing 0.5 mg of the DTC bisphosphonate ligand **7**, followed by shaking at 60°C for 25 min to give **9**. TLC was performed (silica on alumina TLC) using MeOH and 1% of 60% HEDP solution. Here, 97% of the activity was retained at the origin, showing that only 3% of the activity

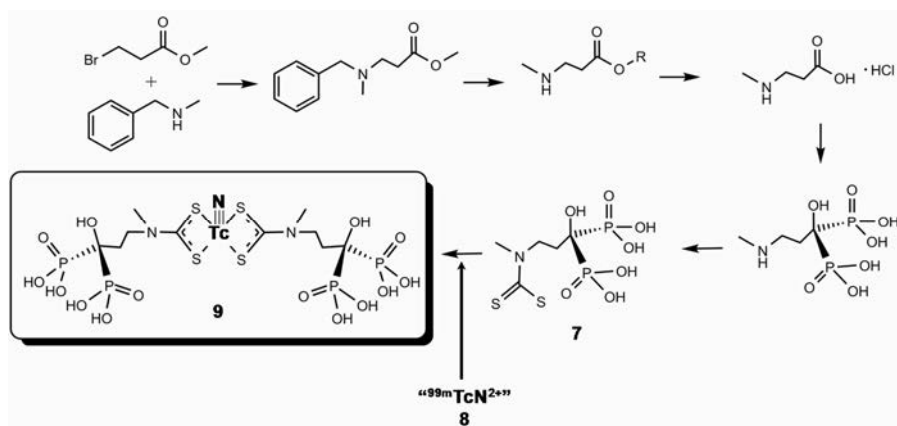


FIG. 13.15. Synthesis of dithiocarbamate bisphosphonate ligand **7** and its ^{99m}Tc complex **9**.

was in the form of either pertechnetate or $^{99m}\text{TcN}^{2+}$. For biological evaluation, 80 μL of 0.1N HCl was added to 200 μL of the product solution to adjust the pH to between 6.7 and 7.0, giving a final activity 101 MBq in 280 μL .

The affinity of **9** for calcium based minerals including HA was assessed by incubating the tracer with 1 mg/mL solutions of the salts in tris buffer (50mM, pH6.9), followed by centrifugation, using the ^{99m}Tc nitride intermediate **8** as a negative control, which showed negligible binding to all minerals. The ^{99m}TcN DTC bisphosphonate complex **9** showed high percentage incorporation into all minerals, especially HA (~90%) (see Fig. 13.16). The binding to HA was also measured using human serum as the incubation medium and compared with ^{99m}Tc MDP. Complex **9** retained much higher affinity for HA in the serum than did ^{99m}Tc MDP (see Fig. 13.17).

The affinity for HA in serum over a prolonged period (24 h) suggests that **9** should be evaluated in vivo as a bone targeting tracer. Accordingly, mice were given tail vein injections of 40 MBq **9** (volume = 0.1 mL) and scanned using a nanoSPECT scanner for up to 6 h. The affinity for bone and low soft tissue uptake was evident (see Fig. 13.18), while both bone uptake and renal clearance were slower than for the commercial radiopharmaceutical ^{99m}Tc MDP (see Fig. 13.19), which was studied in parallel as a standard reference bone imaging agent. Although uptake in bone was slower, the absolute percentage of injected dose per gram eventually reached significantly higher levels than for ^{99m}Tc MDP.

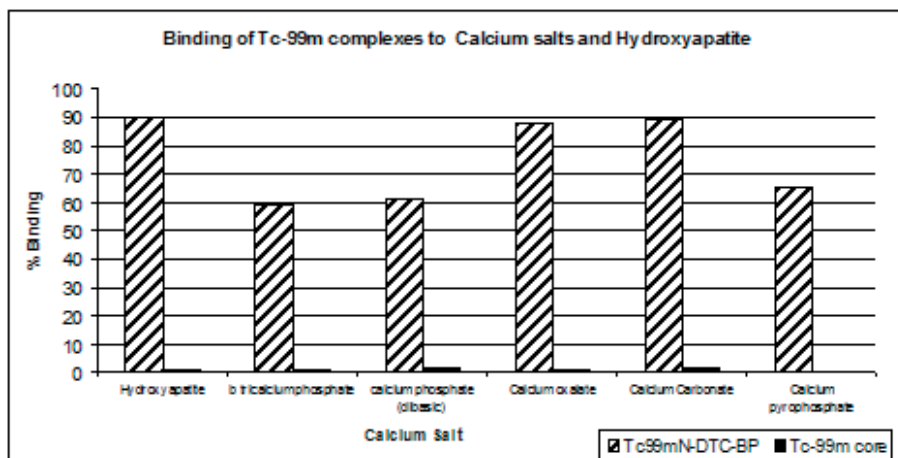


FIG. 13.16. Binding of ^{99m}Tc bisphosphonate conjugate **9** to calcium salts.

MDP and Bisphosphonate comparison (HA binding)

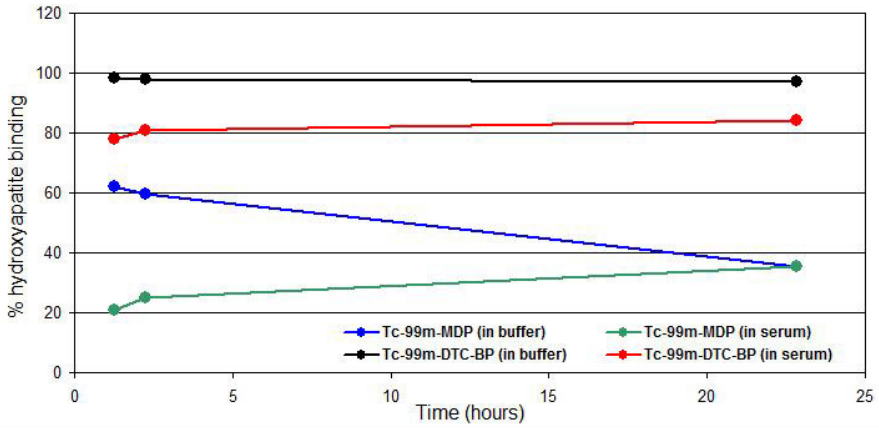


FIG. 13.17. Binding to HA in serum: comparison of **9** with ^{99m}Tc MDP.

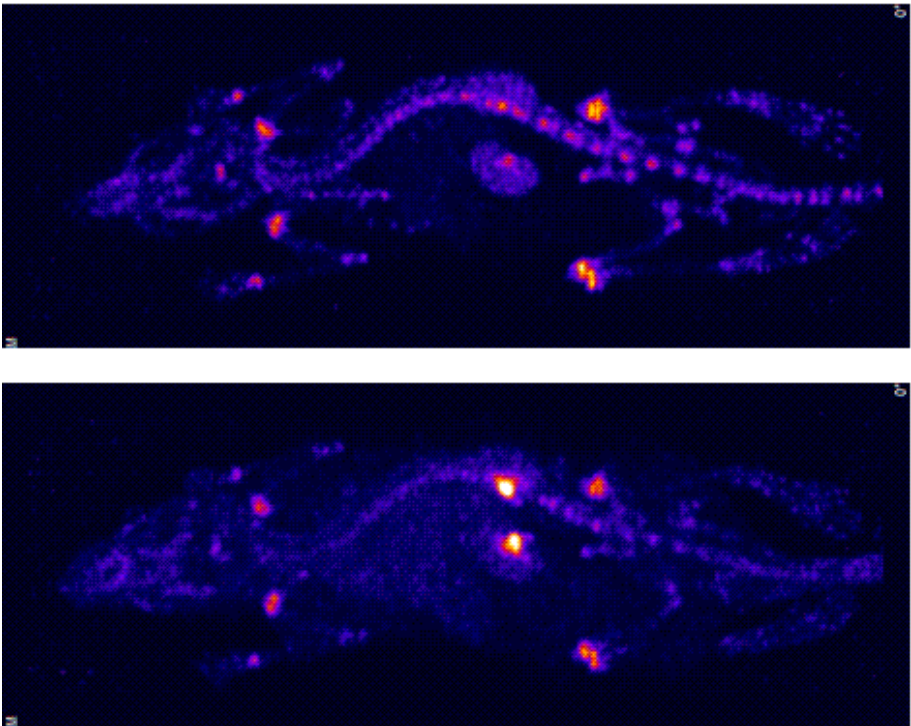


FIG. 13.18. NanoSPECT scans of two mice 6 h after injection of ^{99m}Tc MDP (top) and **9** (bottom).

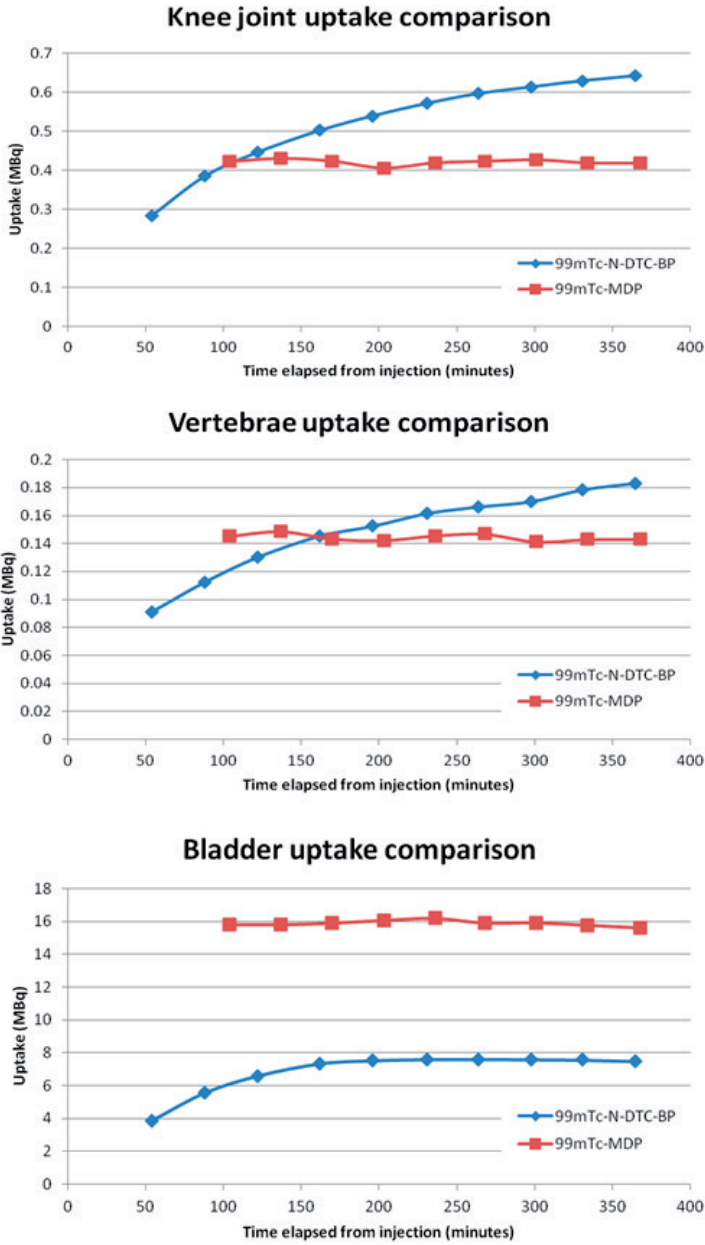


FIG. 13.19. Absolute uptake of ^{99m}Tc in bone, and accumulation in bladder, after injection of 40 MBq of ^{99m}Tc -N-DTC-BP and 40 MBq of ^{99m}Tc -MDP in mice.

13.3. CONCLUSION

In conclusion, this chapter describes a simple and convenient method to purify the rhenium tricarbonyl precursor **4** that will facilitate the labelling of other small molecules and biomolecules such as His-tagged peptides/proteins with ^{188}Re in high radiochemical yields and purities [13.24]. Also described here is the synthesis of **5** as a new radiopharmaceutical for the radionuclide therapy of bone metastases, and its technetium analogue **6**. Complex **5** can be easily synthesized with high specific activity in two steps using a kit based methodology and, in contrast with the clinically approved $^{186/188}\text{Re}$ HEDP, it forms an inert, single species that has been well characterized. The strategy of using a designed chelating agent for rhenium rather than relying on the chelating properties of the bisphosphonate group is vindicated in that **5** displays superior stability, bone targeting and retention properties. Complex **5** is therefore an attractive candidate for further clinical studies.

Similarly, the new $^{99\text{m}}\text{Tc}$ tracer **9** shows prolonged retention in bone and higher stability and binding to HA in serum compared to $^{99\text{m}}\text{Tc}$ MDP. Because of the selection of a stable, well characterized metal core in which the technetium and rhenium complexes are known to behave analogously and retain structural integrity, the ^{188}Re complex is expected to behave similarly and deserves investigation as a potential therapeutic radiopharmaceutical.

ACKNOWLEDGEMENTS

This work was supported by Cancer Research UK (grant C789/A7649) and conducted within the King's College London–UCL Comprehensive Cancer Imaging Centre supported by Cancer Research UK and the Engineering and Physical Sciences Research Council, in association with the Medical Research Council and the Department of Health (UK). This collaborative study was performed within the framework of the European Cooperation in Science and Technology action BM0607 on targeted radionuclide therapy. The nanoSPECT scanner was funded by an equipment grant from the Wellcome Trust. We thank K. Sunassee and S. Clarke for assistance with nanoSPECT imaging.

REFERENCES TO CHAPTER 13

- [13.1] FLEISH, H., *Bisphosphonates in Bone Disease: From the Laboratory to the Patient*, Parthenon Publishing Group, London (1995).

- [13.2] ZHANG, S., GANGAL, G., ULUDAG, H., 'Magic bullets' for bone diseases: Progress in rational design of bone-seeking medicinal agents, *Chem. Soc. Rev.* **36** (2007) 507.
- [13.3] LEWINGTON, V.J., Bone-seeking radionuclides for therapy, *J. Nucl. Med.* **46** (2005) 38S.
- [13.4] DE KLERK, J.M.H., et al., Phase I study of rhenium-186-HEDP in patients with bone metastases originating from breast cancer, *J. Nucl. Med.* **37** (1996) 244.
- [13.5] HSIEH, B.T., et al., Comparison of various rhenium-188-labeled diphosphonates for the treatment of bone metastases, *Nucl. Med. Biol.* **26** (1999) 973.
- [13.6] LIEPE, K., KROPP, J., RUNGE, R., KOTZERKE, J., Therapeutic efficiency of rhenium-188-HEDP in human prostate cancer skeletal metastases, *Br. J. Cancer* **89** (2003) 625.
- [13.7] MAXON, H.R., et al., Rhenium-186(Sn)HEDP for treatment of painful osseous metastases — results of a double-blind crossover comparison with placebo, *J. Nucl. Med.* **32** (1991) 1877.
- [13.8] PALMEDO, H., et al., Remission of bone metastases after combined chemotherapy and radionuclide therapy with Re-186 HEDP, *Clin. Nucl. Med.* **23** (1998) 501.
- [13.9] TIAN, M., ZHANG, H., LI, S., ENDO, K., TANADA, S., Rhenium-188 HEDP for the palliation of painful bone metastases, *J. Clin. Oncol.* **22** (2004) 766S.
- [13.10] HANDELAND, Å., LINDEGAARD, M.W., HEGGLI, D.E., Biodistribution of anionic separated MDP complexes from different MDP preparations, *Eur. J. Nucl. Med.* **15** (1989) 609.
- [13.11] DE KLERK, J.M.H., et al., Pharmacokinetics of Re-186 after administration of rhenium-186-HEDP to patients with bone metastases, *J. Nucl. Med.* **33** (1992) 646.
- [13.12] CHUNG, Y.S., et al., Effect of carrier on labeling and biodistribution of Re-188-hydroxyethylidene diphosphonate (HEDP) in mice and rats, *J. Nucl. Med.* **39** (1998) 1037.
- [13.13] OGAWA, K., et al., Development of a rhenium-186-labeled MAG3-conjugated bisphosphonate for the palliation of metastatic bone pain based on the concept of bifunctional radiopharmaceuticals, *Bioconjug. Chem.* **16** (2005) 751.
- [13.14] EL-MABHOUH, A., ANGELOV, C., McEWAN, A., JIA, G., MERCER, J., Preclinical investigations of drug and radionuclide conjugates of bisphosphonates for the treatment of metastatic bone cancer, *Cancer Biother. Radiopharm.* **19** (2004) 627.
- [13.15] EL-MABHOUH, A., MERCER, J.R., Re-188-labeled bisphosphonates as potential bifunctional agents for therapy in patients with bone metastases, *Appl. Radiat. Isot.* **62** (2005) 541.
- [13.16] OGAWA, K., MUKAI, T., INOUE, Y., ONO, M., SAJI, H., Development of a novel Tc-99m-chelate-conjugated bisphosphonate with high affinity for bone as a bone scintigraphic agent, *J. Nucl. Med.* **47** (2006) 2042.
- [13.17] SALMAIN, M., GUNN, M., GORFTI, A., TOP, S., JAOUEN, G., Labeling of proteins by organometallic complexes of rhenium (I) – synthesis and biological-activity of the conjugates, *Bioconjug. Chem.* **4** (1993) 425.

- [13.18] ALBERTO, R., et al., A novel organometallic aqua complex of technetium for the labeling of biomolecules: Synthesis of $[\text{}^{99\text{m}}\text{Tc}(\text{OH}_2)_3(\text{CO})_3]^+$ from $[\text{}^{99\text{m}}\text{TcO}_4]^-$ in aqueous solution and its reaction with a bifunctional ligand, *J. Am. Chem. Soc.* **120** (1998) 7987.
- [13.19] SCHIBLI, R., et al., Influence of the denticity of ligand systems on the in vitro and in vivo behavior of Tc-99m(I)-tricarbonyl complexes: A hint for the future functionalization of biomolecules, *Bioconjug. Chem.* **11** (2000) 345.
- [13.20] BANERJEE, S.R., et al., Bifunctional single amino acid chelates for labeling of biomolecules with the $\{\text{Tc}(\text{CO})_3\}^+$ and $\{\text{Re}(\text{CO})_3\}^+$ cores. Crystal and molecular structures of $[\text{ReBr}(\text{CO})_3(\text{H}_2\text{NCH}_2\text{C}_5\text{H}_4\text{N})]$, $[\text{Re}(\text{CO})_3\{\text{(C}_5\text{H}_4\text{NCH}_2)_2\text{NH}\}]\text{Br}$, $[\text{Re}(\text{CO})_3\{\text{(C}_5\text{H}_4\text{NCH}_2)_2\text{NCH}_2\text{CO}_2\text{H}\}]\text{Br}$, $[\text{Re}(\text{CO})_3\{\text{X}(\text{Y})\text{NCH}_2\text{CO}_2\text{CH}_2\text{CH}_3\}]\text{Br}$ (X=Y=2-pyridylmethyl; X=2-pyridylmethyl, Y = 2-(1-methylimidazolyl)methyl; X=Y=2-(1-methylimidazolyl)methyl), $[\text{ReBr}(\text{CO})_3\{\text{(C}_5\text{H}_4\text{NCH}_2)_2\text{N}(\text{CH}_2\text{C}_4\text{H}_3\text{S})\}]$, and $[\text{Re}(\text{CO})_3\{\text{(C}_5\text{H}_4\text{NCH}_2)_2\text{N}(\text{CH}_2\text{C}_4\text{H}_3\text{S})(\text{CH}_2\text{CO}_2)\}]$, *Inorg. Chem.* **41** (2002) 6417.
- [13.21] NANCOLLAS, G.H., et al., Novel insights into actions of bisphosphonates on bone: Differences in interactions with hydroxyapatite, *Bone* **38** (2006) 617.
- [13.22] KUBÍČEK, V., KOTEK, J., HERMANN, P., LUKEŠ, I., Aminoalkyl bis (phosphonates): Their complexation properties in solution and in the solid state, *Eur. J. Inorg. Chem.* **2007** (2007) 333.
- [13.23] LECOUEVEY, M., LEROUX, Y., Synthesis of 1-hydroxy-1,1-bisphosphonates, *Heteroat. Chem.* **11** (2000) 556.
- [13.24] SCHIBLI, R., et al., Steps toward high specific activity labeling of biomolecules for therapeutic application: Preparation of precursor $[\text{}^{188}\text{Re}(\text{H}_2\text{O})_3(\text{CO})_3]^+$ and synthesis of tailor-made bifunctional ligand systems, *Bioconjug. Chem.* **13** (2002) 750.
- [13.25] PARK, S.H., SEIFERT, S., PIETZSCH, H.J., Novel and efficient preparation of precursor $[\text{}^{188}\text{Re}(\text{OH}_2)_3(\text{CO})_3]^+$ for the labeling of biomolecules, *Bioconjug. Chem.* **17** (2006) 223.
- [13.26] DE ROSALES, R.T.M., et al., $^{188}\text{Re}(\text{CO})_3$ -dipicolylamine-alendronate: A new bisphosphonate conjugate for the radiotherapy of bone metastases, *Bioconjug. Chem.* **21** (2010) 811.
- [13.27] DE ROSALES, R.T.M., FINUCANE, C., MATHER, S.J., BLOWER, P.J., Bifunctional bisphosphonate complexes for the diagnosis and therapy of bone metastases, *Chem. Commun.* (2009) 4847.
- [13.28] RIESE, C.G.U., SEITZ, S., SCHIPPER, M., BEHR, T., Effective treatment of pancreatic neuroendocrine tumours transfected with the sodium iodide symporter gene by ^{186}Re -perrhenate in mice, *Eur. J. Nucl. Med. Mol. Imaging* **36** (2009) 1767.
- [13.29] WAIBEL, R., et al., Stable one-step technetium-99m labeling of His-tagged recombinant proteins with a novel Tc(I)-carbonyl complex, *Nat. Biotechnol.* **17** (1999) 897.
- [13.30] DEMAIMAY, F., et al., Rhenium-188 and technetium-99m nitridobis (N-ethoxy-N-ethylthiocarbamate) leucocyte labelling radiopharmaceuticals: $[\text{Re-188-N}(\text{NOET})_2]$ and $[\text{Tc-99m-N}(\text{NOET})_2]$, NOET = Et(EtO)NCS₂: Their in vitro localization and chemical behavior, *Nucl. Med. Biol.* **24** (1997) 701.

- [13.31] DE ROSALES, R.T.M., et al., Synthesis of $^{64}\text{Cu}(\text{II})$ -bis(dithiocarbamate-bisphosphonate) and conjugation with superparamagnetic iron oxide nanoparticles: In vivo evaluation as dual-modality PET-MRI agent, *Angew. Chem. Int. Ed.* **123** (2011) 5623.
- [13.32] STALTERI, M.A., et al., Uptake of Tc-99m-nitrido dithiocarbamate complexes by tumour cells, *Nucl. Med. Commun.* **18** (1997) 870.

Chapter 14

DEVELOPMENT OF $^{90}\text{Sr}/^{90}\text{Y}$ GENERATOR SYSTEMS BASED ON SLM TECHNIQUES FOR RADIOLABELLING OF THERAPEUTIC BIOMOLECULES WITH ^{90}Y

N.T. THU, D. VAN DONG, B. VAN CUONG, C. VAN KHOA, V.T. CAM HOA
Nuclear Research Institute,
Dalat, Viet Nam

Abstract

Yttrium-90 is one of the most useful radionuclides for radioimmunotherapeutic applications, especially for labelling peptides and antibodies. Studies were carried out to develop a $^{90}\text{Sr}/^{90}\text{Y}$ generator system based on the SLM technique. Two stages of $^{90}\text{Sr}/^{90}\text{Y}$ generator systems were developed at different activity levels of 5, 20, 50 and 100 mCi and operated with semiautomation in sequential mode. In the first stage of the system, PC88A based SLM was used, which transported ^{90}Y from a nitric acid medium containing 0.01–4M HNO_3 . In the second stage, the ^{90}Y from the first stage was transferred to the first compartment of the second stage using carbamoylmethyl phosphine oxide (CMPO) based SLM where 1M acetic acid was used as the receiving phase for ^{90}Y . Quality control was carried out for the products of ^{90}Y using EPC with paper chromatography and Tec control chromatography. Peptides and antibodies were labelled using the ^{90}Y product obtained from the generator developed in house.

14.1. INTRODUCTION

Yttrium-90 is a useful radionuclide used for therapy in nuclear medicine. It has good physical characteristics and stable binding properties with many chelating agents. Yttrium-90 is a pure β emitter ($T_{1/2} = 64.1$ h, $E_{\beta, \text{max}} = 2.2$ MeV) that is formed by the decay of ^{90}Sr . To separate this radionuclide in a carrier free form from the parent ^{90}Sr , many techniques have been proposed, and a few of them are still being used. Methods based on ion exchange, extraction chromatography and solvent extraction have been reported [14.1, 14.2]. The most important issue in the development of this generator system that needs to be addressed is the purity of ^{90}Y , especially from ^{90}Sr , which is a bone seeker [14.3].

The activity due to ^{90}Sr should be $<0.001\%$. No convenient generator system has been available until now that can ensure the continuous availability of ^{90}Y for radiotherapeutic applications. Herein, the SLM technology developed in India was chosen for the separation of ^{90}Y for radiopharmaceutical application [14.4]. In recent years, advances in understanding tumour biology and the developments in peptide chemistry and MAb technology have created new opportunities for the development of therapeutic radiopharmaceuticals and widened the scope of radionuclide therapy. In particular, ^{90}Y radiopharmaceuticals have been used for treating NHL, HCC and malignant cancer [14.5–14.8]. During the CRP, rituximab, DOTATATE, albumin microspheres and microaggregated albumin were used for labelling with in house produced ^{90}Y .

14.2. MATERIALS

The materials provided by the IAEA included 3.7 GBq of ^{90}Sr in 1.5M HNO_3 solution with a radionuclidic purity of $>99.9\%$ and a specific activity >50 Ci/g, produced at IDB Holland. DOTATATE was received from M. Chinol, European Institute of Oncology. A double glass cell was gifted by M. Venkatesh, BARC. Albumin microspheres were obtained from R. Mikołajczak, POLATOM. The chemicals purchased included PC88A from Daihachi Chemicals Industry Co. Ltd; a PTFE membrane with 0.45 μm pore, 47 mm diameter from Merck, PTFE coated magnetic stirrers, DOTA CAS No. 127985-74-4, Macrocyclic, product B-205; and cetyl (phenyl)-N,N-diisobutyl CMPO, CAS No. 83242-95-9, lot No. A4546029. Other chemicals such as DTPA, nitric acid, acetic acid, sodium hydrophosphate and sodium acetate were analytical grade.

14.3. METHODS

14.3.1. Preparation of $^{90}\text{Sr}/^{90}\text{Y}$ generator systems based on the SLM technique

14.3.1.1. Setting up of the $^{90}\text{Sr}/^{90}\text{Y}$ generator systems

Based on the SLM $^{90}\text{Sr}/^{90}\text{Y}$ generator technology successfully developed at BARC, a similar $^{90}\text{Sr}/^{90}\text{Y}$ generator system based on the SLM technique was built in house for routine separation of carrier free ^{90}Y . Four glass cells were connected together with magnetic stirrers, as shown in Fig. 14.1. The solvent impregnated PTFE membranes were incorporated in between the chambers. In the first stage, diluted PC88A was used as the carrier, and in the second stage,

0.8M CMPO in n-dodecane was used as the carrier. For solvent impregnation, PTFE supports were cut to the diameter of the glass cell and kept immersed in the solvent overnight. Before use, they were washed with deionized water and tightly assembled into the generator set-up. The PC88A based SLM was inserted and tightly fixed in between the first and second compartment. In the same way, the CMPO impregnated PTFE was inserted and tightly fixed between the third and fourth compartments. The generator was housed in a polymethyl methacrylate box inside a fume hood to protect from any radioactivity contamination. The first compartment was filled with 5 mL of 0.1M HNO₃ containing a ⁹⁰Sr/⁹⁰Y mixture (pH1–2), the second compartment was filled with 5 mL of 4M HNO₃, the third compartment was filled with 5 mL of 4M HNO₃ and the fourth compartment was filled with 5 mL of 1M acetic acid. To introduce the solution into the chamber or collect the liquid product from the chamber, Teflon tubes of small diameter, ~2 mm were connected between the chambers, as shown in Fig. 14.1. The solutions in the chambers were stirred using PTFE coated magnetic stirring bars. The generator set-up was placed on the magnetic stirring system. The system was run at different activity levels of 5, 20, 50 and 100 mCi. The SLM based ⁹⁰Sr/⁹⁰Y generator system for 100 mCi levels in a semiautomation sequential mode was developed to produce highly pure ⁹⁰Y that can be used in the preparation of radioimmunoconjugates and radiopharmaceuticals.

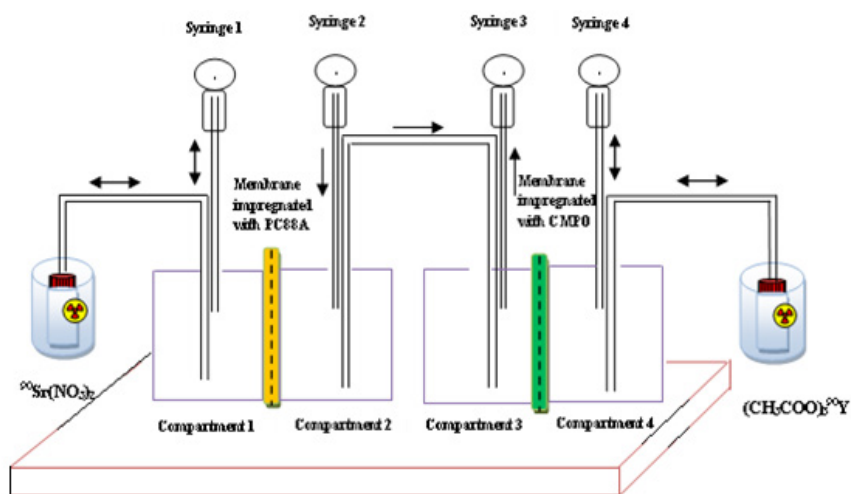


FIG. 14.1. General scheme of the ⁹⁰Sr/⁹⁰Y generator using SLM technology.

14.3.1.2. Operation of the $^{90}\text{Sr}/^{90}\text{Y}$ generator

The transport of β activity was investigated as a function of time. The experiments were carried out at an activity level of 100 mCi. The activity data were used to evaluate the separation yields. Three set of experiments were carried out under identical experimental conditions. The system was operated continuously for ~ 6 h in the first stage. Five millilitres of ^{90}Sr was transferred from the original solution vial into the first chamber by pulling up syringe No. 1. Over time, the β activity owing to ^{90}Y was transported from the first to the second chamber across the PC88A based liquid membrane. In the next step, syringe No. 2 was pushed down or syringe No. 3 pulled up, whereby ^{90}Y in 4M HNO_3 was transported into the third chamber that contained CMPO based SLM and 1M acetic acid as the receiving phase. The second stage was also operated continuously for ~ 6 h. Finally, the entire product containing ^{90}Y in acetic acid was taken out for quality control.

14.3.1.3. Quality control of ^{90}Y collected from the $^{90}\text{Sr}/^{90}\text{Y}$ generator

(a) Measurement of ^{90}Y radioactivity and evaluation of the separation yield

Yttrium-90 solution eluted from the $^{90}\text{Sr}/^{90}\text{Y}$ generator was measured using the LSC Aloka 6100 and a GM counter system. Five microlitre aliquots of the ^{90}Y solution were added into a scintillation vial, which contained 10 mL of cocktail and counted using the LSC. For comparison, 10 μL aliquots of diluted ^{90}Y sample were placed on the stainless steel dish and counted on the UMF-2000 counter.

(b) Quality control of ^{90}Y

To evaluate the radionuclide purity of ^{90}Y acetate, the EPC method was adopted by using PC88A as the chelating agent. The EPC technique was performed on different kinds of chromatography paper such as Whatman No. 1, ITLC paper or Tec control chromatography paper, BIODEx 150-771. Whatman No. 1 paper was cut into 12 cm \times 1 cm sizes and BIODEx strips were ready to use. In these quality control tests, ~ 5 –10 μL of PC88A was spotted between the second and third segment of the Whatman No. 1/ITLC paper (spot diameter = 1 cm). After drying, 5 μL of the ^{90}Y sample was spotted over the PC88A spot. Two sets from each type of chromatography paper were prepared. The papers were developed in a saline 0.9% solution. The developing time was 30 min for Whatman No. 1 paper and 4 min for ITLC paper. For the ^{90}Y radioactivity measurement at the origin and ^{90}Sr radioactivity at the solvent front, strips were placed in 10 mL liquid

scintillation vials and counted. The measured counts were directly compared to the total activity spotted to obtain the radionuclide impurity in ^{90}Y .

As an alternative quality control technique, 5 μL of PC88A was spotted on the bottom line of the BIODEx strip (0.7 cm \times 5.8 cm), to which 5 μL of the ^{90}Y sample was added. The chromatography was developed in 0.9% NaCl. The chromatography time was \sim 2 min and the strips were dried and cut at the centre. The ^{90}Y remained at the point of spotting, while the ^{90}Sr migrated to the solvent front. The strips were either counted using a GM counter or an LSC.

14.3.2. Labelling of rituximab with ^{90}Y

For DTPA rituximab preparation, the method described by Hnatowich et al. was used [14.7]. The cDTPA (0.1 mg/mL) was dissolved in chloroform and degassed under a stream of nitrogen for 30 min. Rituximab solution in a 0.05M bicarbonate buffer was immediately added and mixed for 1 min at room temperature. Rituximab at different concentrations (5 and 10 mg/mL) was coupled with the cDTPA at molar ratios (cDTPA:rituximab) of 1:1, 3:1, 5:1, 10:1 and 20:1. The DTPA rituximab conjugate was labelled with ^{90}Y in 0.5M acetate buffer, pH5, at room temperature and purified using Sephadex G-25 to determine the coupling efficiency. After purification, the RCP of ^{90}Y DTPA rituximab was determined using ITLC and developed in 0.1M acetate buffer, pH6, as the mobile phase. Biodistribution studies in normal mice were carried out using these radioimmunoconjugates.

For DOTA rituximab preparation, the bifunctional chelator p-NCS-Bz-DOTA was dissolved in DMSO and then conjugated to rituximab. The antibody was diluted with phosphate buffer to obtain a concentration of 5 mg/mL. The pH was adjusted to 8.5 with 1M NaOH. A solution of the chelator in DMSO was added to the antibody solution at 1, 5, 25, 50 and 100 equivalents of chelate/antibody. The reaction was allowed to proceed overnight at 37°C. After incubation, the antibody solution was left at room temperature.

The number of chelate molecules conjugated to the antibody was determined using ^{90}Y . Yttrium-90 in the form of acetate (1 mCi/mg) was directly added to the tubes containing the DOTA rituximab conjugate, and the solution was adjusted to pH6 using acetic acid. The reaction mixture was incubated at 37°C for 60 min. RCP was analysed using BIODEx strips and 0.9% NaCl as the mobile phase. Unbound ^{90}Y migrated to the solvent front, while ^{90}Y DOTA rituximab remained at the origin. The percentage of ^{90}Y DOTA rituximab was determined, and the mean number of DOTA groups attached to each molecule of rituximab was also determined.

For radiolabelling of the DOTA rituximab conjugate with ^{90}Y , in each reaction vial, 100 μL of 0.5M acetate buffer, pH6, and 100 μg of the conjugated

antibody were taken, to which ^{90}Y acetate was added to obtain a specific activity of >37 MBq/mg and incubated at 37°C for 60 min. The radioimmunoconjugate was purified using a G-25 Sephadex column previously equilibrated and stabilized with 0.9% NaCl. Fractions of 1 mL were collected and counted.

14.3.3. Labelling of DOTATATE with ^{90}Y

DOTATATE in the lyophilized form was dissolved in water to a concentration of 1 mg/mL. Yttrium-90 obtained from the $^{90}\text{Sr}/^{90}\text{Y}$ generator based on SLM as ^{90}Y acetate was used. A gentisic acid solution (0.33 g of sodium acetate, 0.4 g of 2,5-dihydroxybenzoic acid, 250 μL of saturated NaOH and 10 mL of sterile water, pH5) was prepared. Optimization experiments to determine the optimal pH were performed using 10 μg of peptide and 37 MBq of ^{90}Y at 90°C for 30 min at different pH values.

In the protocol used for radiolabelling, 10 μg (10 μL) of DOTATATE was added to 50 μL gentisic acid and 37 MBq of ^{90}Y acetate at pH4.5–5. The reaction mixtures were incubated for 30 min at 90°C followed by quality control procedures. After incubation and cooling at room temperature, 20 μL of the labelled peptide was mixed with 200 μL of 0.25mM DTPA and passed through a SepPak C18 cartridge and compared with paper chromatography using 10% sodium acetate and MeOH (30:70). The stability of ^{90}Y DOTATATE was tested for 5 d.

14.3.4. Labelling of albumin macroaggregates with ^{90}Y

A direct method was used to label albumin with ^{90}Y . Both in house prepared albumin and commercial (MAASOL, GE Healthcare) albumin were used. The preparation of wet albumin particles with sizes in the range 10–30 μm was carried out at the Nuclear Research Institute (Viet Nam). A solution of 0.16% HSA, pH4.6, was suspended in 5% NaCl, pH6, at 80°C with stirring. The microaggregated albumin particle sizes ranged from 10 to 30 μm . The suspended albumin particles were centrifuged at 3000 rev./min for 5 min. The pelleted particles were resuspended with 0.8M sodium dihydrophosphate. Two milligrams of albumin particles were mixed with 0.5 mg of stannous chloride dihydrate in 2M HCl and the pH adjusted to 5.0 with 2M NaOH. The sizes of the particle were examined using an optical microscope and a haemocytometer. The mixture was washed three times with PBS, pH7.2, by centrifugation and resuspension in a 0.5M sodium acetate buffer, pH6. Yttrium-90 in 1M acetic acid was collected from the $^{90}\text{Sr}/^{90}\text{Y}$ generator at a concentration of 296 MBq/mL. The radiolabelling of the particles with ^{90}Y was performed at pH5.5 in an acetate buffer with agitation for 60 min at room temperature. The labelled albumin suspensions were

centrifuged at 6000 rev./min for 15 min. Labelling yields were controlled using centrifugation, filtration and comparison with paper chromatography developed with tris-acetic EDTA.

For preparation and labelling of p-NCS-Bz-DOTA albumin conjugation, p-NCS-Bz-DOTA was dissolved in DMSO. The ligand was then conjugated to albumin microspheres. Six milligrams of albumin was diluted with phosphate buffer, pH7.2, to make a 6 mg/mL solution. A solution of the chelator in DMSO was added to the 100 µg albumin solution at 1, 5, 20, 50 and 100 equivalents of chelate:albumin. The reaction was allowed to proceed overnight at 37°C. The suspended albumin particles were centrifuged at 3000 rev./min for 5 min. The particles were reconstituted in 0.5M acetate buffer, pH6. The radionuclide ⁹⁰Y acetate (1 mCi/mg) was directly added to the tubes containing the conjugate. The reaction mixture was incubated at 37°C for 60 min or 90°C for 30 min. The solution was analysed using BIODEx strips and saline as the mobile phase. Unbound ⁹⁰Y migrated to the solvent front, whereas ⁹⁰Y DOTA albumin remained at the origin. The activity of each portion of the strip was measured using a β counter. Yttrium-90 DOTA albumin was dialysed in the tris-acetate buffer at room temperature with buffer changes. Thereafter, the ⁹⁰Y DOTA albumin was recovered from the dialysis bag and resuspended in 0.1M acetate buffer.

14.4. RESULTS

14.4.1. Preparation of ⁹⁰Sr/⁹⁰Y generator systems based on the SLM technique

Studies of the preparation of ⁹⁰Sr/⁹⁰Y generator systems based on the SLM technique were carried out either by setting up or upgrading the generator system that was amenable to generate ⁹⁰Y at 5, 20, 50 and 100 mCi levels for routine application in radiopharmaceutical centres. The generator system was operated under semiautomation in sequential mode, wherein the highest separation yield was 93% as compared to independent operations.

14.4.1.1. The ⁹⁰Sr/⁹⁰Y generator

Stage I of the ⁹⁰Sr/⁹⁰Y generator needed to be operated for 5–6 h. The solution was then transferred from the second chamber to the third chamber using syringe 2 or syringe 3. In stage I, the separation yield was determined and found to be ~80–93%. In stage II, transport of ⁹⁰Y was 90% in ~4–5 h. Quality control of ⁹⁰Y was carried out using the EPC technique as well as the radioactive decay method, followed by half-life measurement. After second stage

operation, radiopharmaceutical grade ^{90}Y acetate could be collected and used for radiolabelling biomolecules.

14.4.1.2. Operation of the stage I $^{90}\text{Sr}/^{90}\text{Y}$ generator at 5, 20, 50 and 100 mCi levels

In the first stage, the pH of the $^{90}\text{Sr}/^{90}\text{Y}$ mixture was adjusted to 1–2, as described previously in Section 14.4.1, and used as a feed in compartment 1. A PTFE support, after impregnation with concentrate PC88A, was used for selective transport of ^{90}Y at 5, 20 and 50 mCi levels. The separation yields were ~60–80% of ^{90}Y . In the case of separation of 100 mCi of ^{90}Sr , the membrane PTFE was impregnated with 60% PC88A in n-dodecane. Nitric acid, 4.0M, was used as the receiver phase. Approximately 6 h was taken to transport 93.61% ^{90}Y activity in 4M HNO_3 . The percentage of β activity owing to ^{90}Y transported in compartment 2 was 93.19%. After 6 h, the separation yield in stage I was 93.2%. Transfer of the feed solution in compartment 1 from the glass vial (kept inside the lead chamber) was carried out using a semiautomated system consisting of silicon tubing attached to a syringe at one end and a rubber cork at the sampling ports. Figure 14.2 shows the activity profile as a function of time using the SLM generator developed in house at 5, 20 and 50 and 100 mCi levels. The separation yield was lower with the PTFE membrane impregnated with concentrated PC88A compared to the membrane impregnated with diluted PC88A.

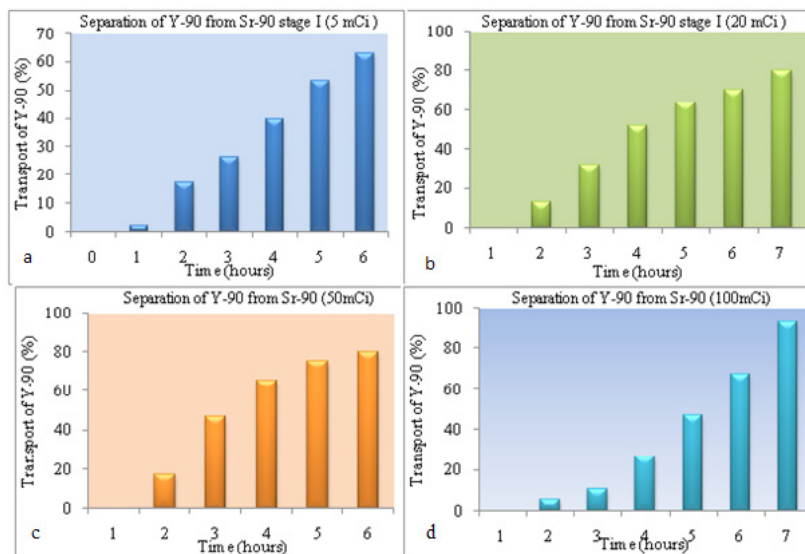


FIG. 14.2. Transport of ^{90}Y from the $^{90}\text{Sr}/^{90}\text{Y}$ mixture at 5, 20, 50 and 100 mCi levels in stage I.

Figure 14.3 shows the results of transport studies carried out for ^{90}Y as a function of PC88A concentration on the PTFE support. In these studies, the concentration of the carrier was 60% in n-dodecane and undiluted PC88A. Transport of ^{90}Y was carried out from a feed solution in 0.1M HNO_3 spiked with ^{90}Y , whereas the acidity of the strippant was kept at 4M HNO_3 . From the results, it is observed that when the carrier was diluted to 60%, the transport of ^{90}Y across the membrane was higher.

Figure 14.4 shows a decrease of ^{90}Y in the feed and an increase of ^{90}Y in the receiver. The figure indicates that there is higher transport of ^{90}Y at 6 h into the receiver with 4M HNO_3 .

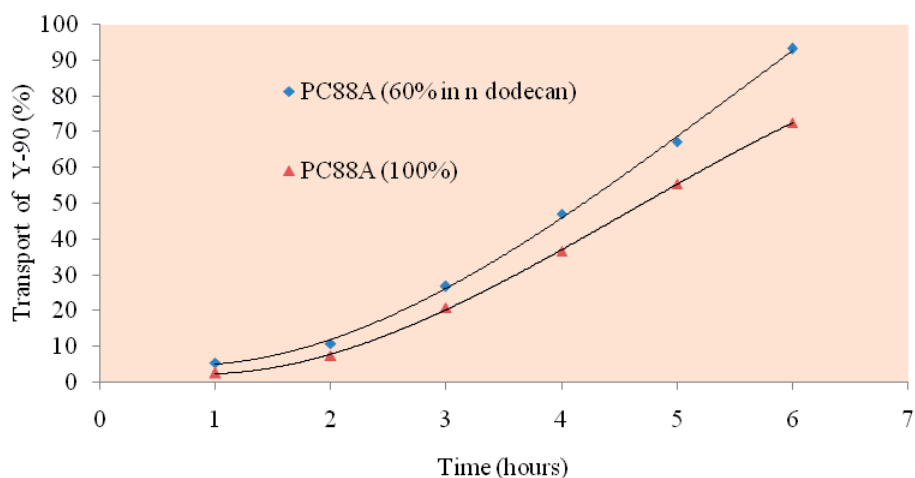


FIG. 14.3. Transport of ^{90}Y using an impregnated PTFE support with 60% and undiluted PC88A.

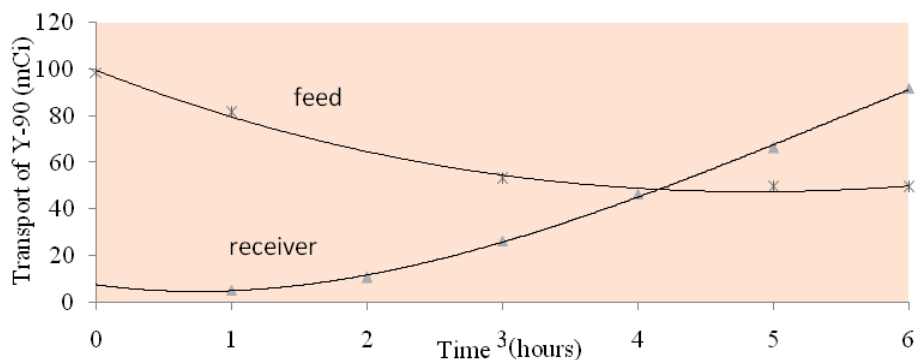


FIG. 14.4. Transport of ^{90}Y from $^{90}\text{Sr}/^{90}\text{Y}$ mixture at 100 mCi level in stage I.

14.4.1.3. Operation of the stage II $^{90}\text{Sr}/^{90}\text{Y}$ generator at 100 mCi level

A similar mechanism was used for transferring the ^{90}Y product in 4M HNO_3 from the first stage to the second stage. The system was shown in Fig. 14.1. In stage II, 4M HNO_3 containing ^{90}Y was removed from compartment 2 and introduced into compartment 3 of the second stage wherein 0.8M CMPO in n-dodecane based SLM was used to selectively transport ^{90}Y to compartment 4, which had 1M CH_3COOH as the receiver phase. The results of ^{90}Y transport in stage II are given in Fig. 14.5. The separation yield in the second stage was found to be 90.45% at 4 h. Figures 14.5 and 14.6 show the transport of ^{90}Y from the feed of stage II containing ^{90}Y in 4M HNO_3 at 20 and 100 mCi levels. The data show that the transport of ^{90}Y was >90% after 4 h under the experimental conditions.

In the second set of experiments under the same conditions, the membrane was impregnated with concentrated tributylphosphate (TBP) and inserted between compartment 3 and compartment 4. Figure 14.7 shows the results of transport studies carried out for ^{90}Y as a function of CMPO and TBP on the PTFE support. In these studies, the transport of ^{90}Y through the PTFE membrane impregnated with 0.8M CMPO was higher compared to the transport of ^{90}Y through the PTFE membrane impregnated with TBP. These studies clearly indicate that CMPO can be used as a carrier for the separation of carrier free ^{90}Y in stage II of the SLM based generator system. The second stage of the system can be operated safely to generate carrier free ^{90}Y . The above results indicate that the overall separation yield of ^{90}Y is >84% using the SLM generator system.

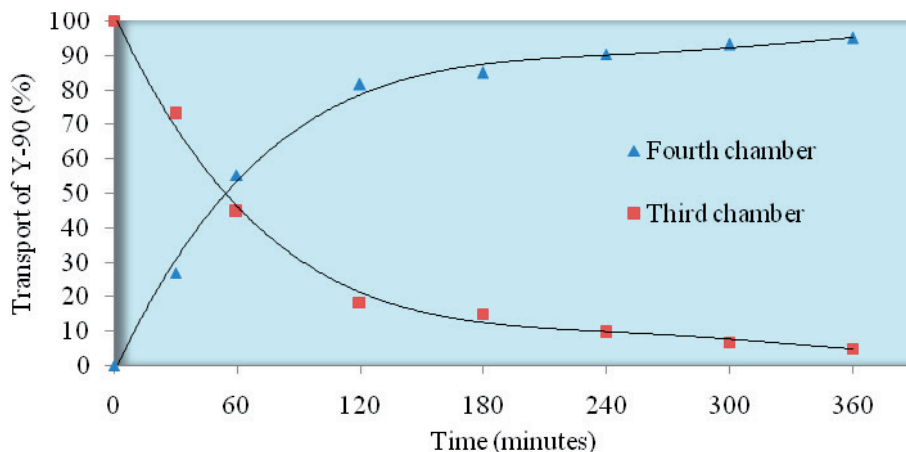


FIG. 14.5. Transport of ^{90}Y in stage II (20 mCi).

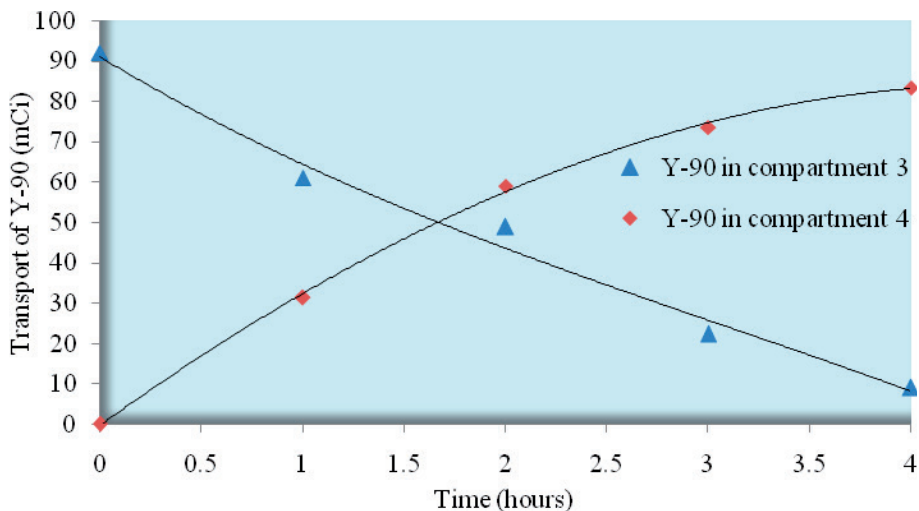


FIG. 14.6. Transport of ⁹⁰Y in stage II (100 mCi).

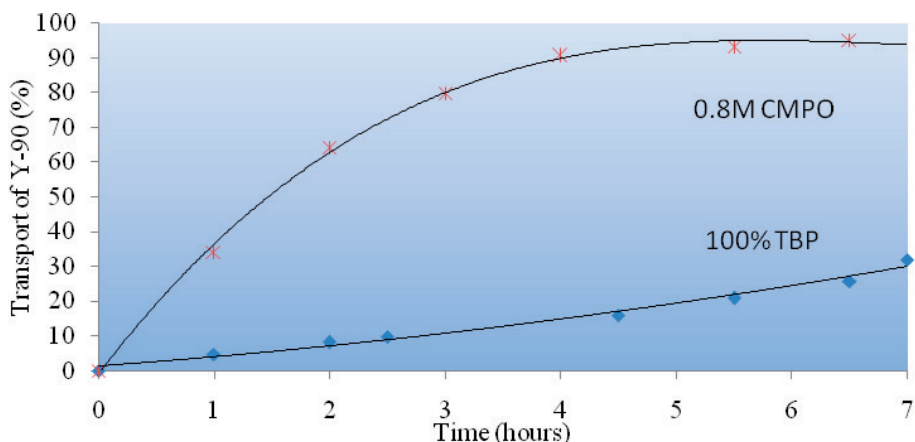


FIG. 14.7. Transport of ⁹⁰Y in stage II using 0.8M CMPO and 100% TBP.

14.4.1.4. Quality of ⁹⁰Y

Table 14.1 presents the chromatography systems that were tested for determination of radionuclidic purity of ⁹⁰Y. For the EPC technique, BIODEx strips were used instead of Whatman No. 1 paper. This material had many advantages, and the strips were hard, thick and easy to handle. A 0.9% sodium chloride solution was used as the solvent and the chromatogram could be developed in only 2 min instead of the 30 min needed for Whatman No. 1 paper.

A typical EPC pattern for a ^{90}Y product indicating the retention of the spotted activity is shown in Fig. 14.8.

Figure 14.9 illustrates how the BIODEx strips were prepared for experiments. The PC88A applied onto the strip was easily absorbed, although it was very viscous. The activities on both segments of the strip were counted using a β counter. The segment, which contained very low levels of ^{90}Sr , was counted in an LSC. Table 14.2 shows the values of ^{90}Sr radioactivity determined in the ^{90}Y product solution (37 MBq/mL). The calculated radionuclidic purity for the five different batches tested was, in each case, >99.999% (^{90}Sr content in the product was always <0.001%).

TABLE 14.1. SOLVENTS FOR TESTING RADIONUCLIDIC PURITY OF ^{90}Y AND R_f VALUES

Solvents	R_f
NaCl 0.9%	0.9–1.0
0.1M sodium acetate	0.9–1.0
Tris-acetic EDTA	0.9–1.0
Ammonium acetate 10%:MeOH (30:70 vol.%)	0.0
Tris-NaCl EDTA	0.9–1.0

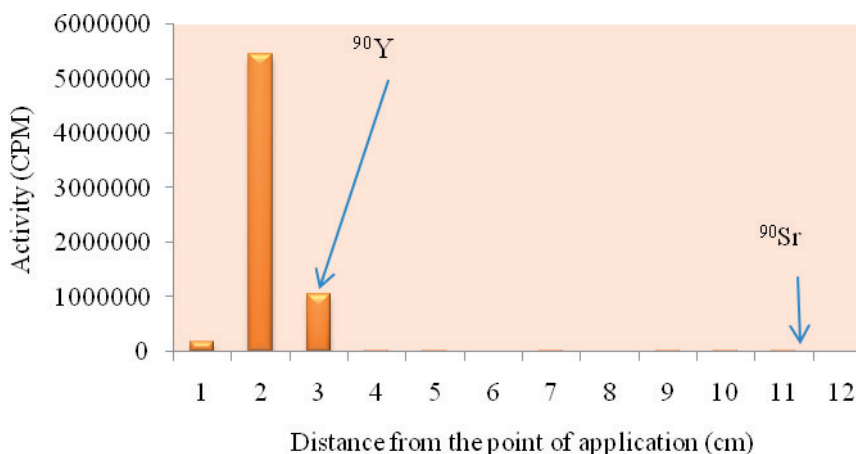


FIG. 14.8. EPC of ^{90}Y product.



FIG. 14.9. BIODEX strips.

TABLE 14.2. STRONTIUM-90 ACTIVITY IN THE ^{90}Y SOLUTION USING BIODEX STRIPS

Batch No.	EPC method (1 mCi/mL)	
	Sr-90 (Bq)	Y-90 (Bq)
01	1.55	1.85×10^5
02	1.95	1.85×10^5
03	0.93	1.85×10^5
04	0.57	1.85×10^5
05	1.48	1.85×10^5

The radionuclidic purity of ^{90}Y was assayed using the radiometric method. The β activity of the product was plotted as a function of time. Figure 14.10 represents the decay curve wherein the half-life of 64 h confirms the absence of other radionuclides except ^{90}Y in the product. The initial β activity was found to decay exponentially to the background activity after ~ 624 h.

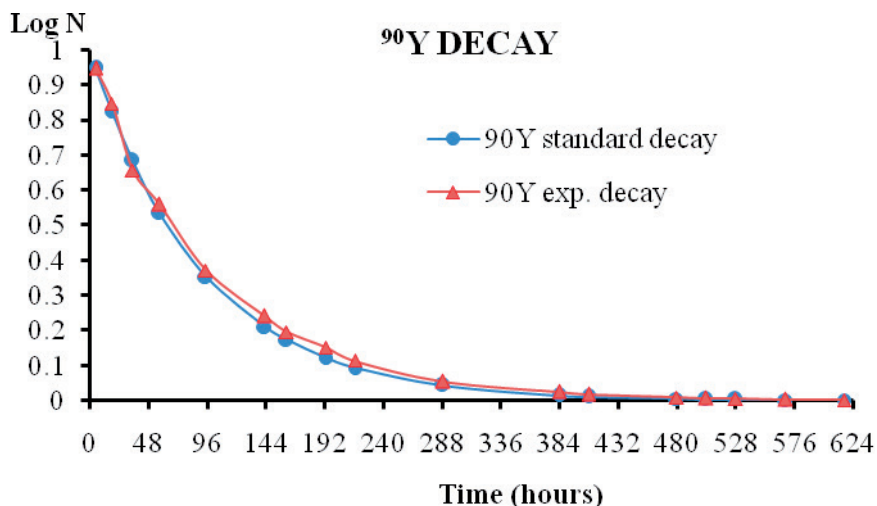


FIG. 14.10. Decay curve of carrier free ^{90}Y product from the SLM based $^{90}\text{Sr}/^{90}\text{Y}$ generator.

14.4.2. Results of the preparation and quality control of ^{90}Y rituximab

14.4.2.1. Results of DTPA rituximab

(a) Preparation and labelling of DTPA rituximab conjugate

The coupling efficiencies of cDTPA to rituximab at molar ratios of 1, 3, 5, 10 and 20 with rituximab concentrations of 5 and 10 mg/mL were ~82.0–53.5% and ~78.2–24.4%, respectively (see Fig. 14.11). The coupling efficiency of ~63% at a 3:1 molar ratio shows a mean of two DTPA groups per antibody molecule. The conjugation mixture was diluted to ~0.2 mL with bicarbonate buffer and loaded onto a PD-10 column (Sephadex G-25, Pharmacia Biotech).

After purification, the DTPA rituximab conjugate was labelled with ^{90}Y in 0.5M acetate buffer, pH5, at room temperature. The reaction time ranged from 1–150 min, and the labelling yield was ~99% (see Table 14.3).

(b) Quality control of ^{90}Y DTPA rituximab

The RCP of ^{90}Y DTPA rituximab determined using ITLC developed in 0.1M acetate, pH6, was >99% (see Fig. 14.12). The product ^{90}Y DTPA rituximab was also stable in vitro (RCP >98%) up to 6 d when incubated in human serum at 37°C.

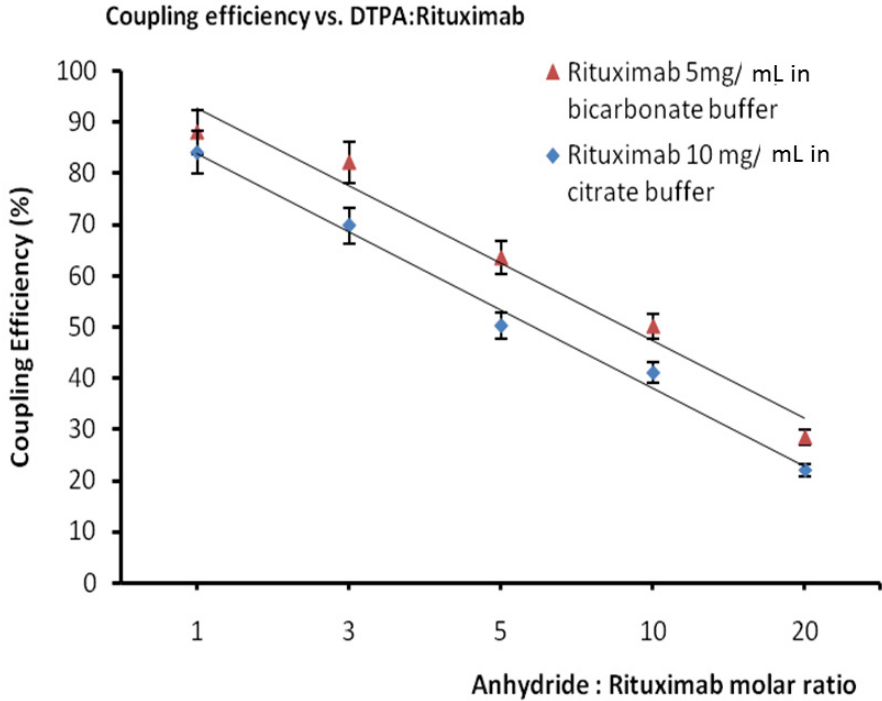


FIG. 14.11. Coupling efficiency of cDTPA to rituximab

TABLE 14.3. REACTION TIME OF DTPA RITUXIMAB

Reaction time (min)	1	3	5	7	10	20	60	120	150
Efficiency (%)	99.5	99.5	99.6	99.7	99.8	99.8	99.8	99.8	99.8

Biodistribution of ^{90}Y DTPA rituximab was investigated in normal mice. After tracer injection in the tail vein, mice were sacrificed at designated time intervals, and organs were removed and counted. The percentage of injected dose per gram of tissue was calculated as shown in Table 14.4. Uptake in the bone was high, even after 2 d of injection.

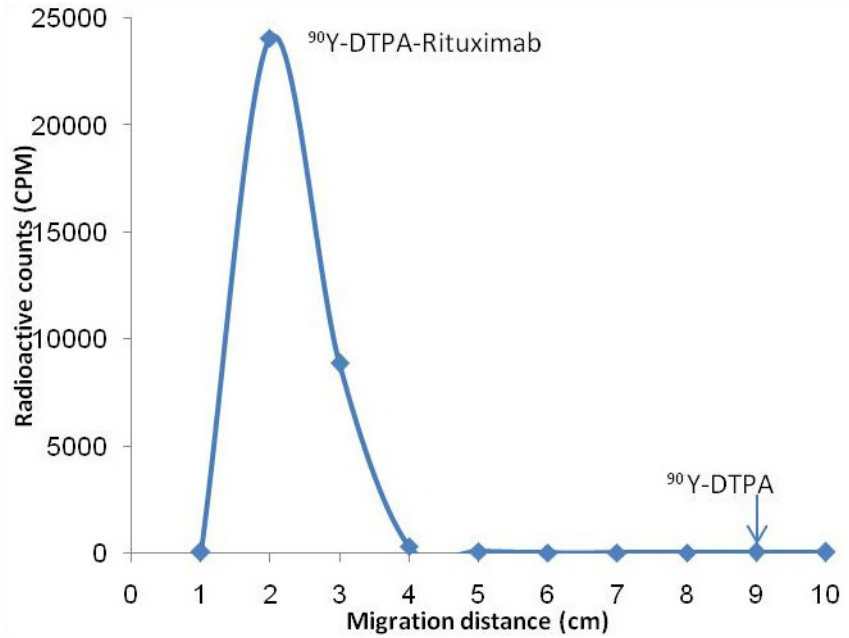


FIG. 14.12. ITLC of ⁹⁰Y rituximab.

TABLE 14.4. BIODISTRIBUTION OF ⁹⁰Y DTPA RITUXIMAB IN NORMAL MICE (%ID/G ± SD) (N = 5)

Tissue	1 h	6 h	24 h	72 h	120 h
Liver	0.72 ± 0.14	4.45 ± 1.15	5.31 ± 0.76	4.23 ± 1.81	6.22 ± 3.17
Spleen	0.09 ± 0.04	0.24 ± 0.23	0.34 ± 0.12	0.22 ± 0.07	0.30 ± 0.16
Kidneys	0.51 ± 0.17	2.66 ± 1.40	1.95 ± 0.72	1.26 ± 0.56	1.37 ± 0.75
Lungs	0.17 ± 0.02	0.70 ± 0.06	1.75 ± 1.15	0.41 ± 0.20	1.93 ± 2.47
Heart	0.25 ± 0.18	0.40 ± 0.13	0.43 ± 0.07	0.23 ± 0.06	1.27 ± 1.60
Blood	3.20 ± 1.09	13.59 ± 1.08	15.16 ± 2.86	9.56 ± 3.61	3.01 ± 1.37
Stomach	0.66 ± 0.15	0.58 ± 0.08	1.08 ± 0.18	1.27 ± 0.27	3.19 ± 0.54
Bone	4.68 ± 0.79	6.64 ± 2.32	23.92 ± 7.93	38.37 ± 7.68	29.52 ± 9.17
Muscle	4.23 ± 1.62	8.40 ± 3.22	12.86 ± 3.58	9.93 ± 3.15	7.63 ± 2.48

14.4.2.2. Results of ^{90}Y DOTA rituximab

(a) Preparation and labelling of p-SCN-Bn-DOTA rituximab conjugate

The optimal conditions for chelator conjugation were determined after incubating 100 μg rituximab with increasing amounts of p-SCN-Bn-DOTA at 25°C or 37°C overnight. A molar ratio of 50:1 was used to achieve a conjugation of two to three groups of DOTA per antibody. Incubation overnight at 37°C yielded 3.04 molecules of p-SCN-Bn-DOTA per antibody. The labelling reaction was performed in 0.5M acetate buffer, pH6, using 10 μg of antibody with 370 kBq of ^{90}Y followed by incubation at 37°C for 60 min. The radioimmunoconjugate was analysed using BIODEx strips where the radiolabelled rituximab had $R_f = 0$, while unbound ^{90}Y had $R_f = 1$. The labelling efficiency was >98%. A schematic representation of the antibody labelling procedure with ^{90}Y through p-SCN-Bn-DOTA is given in Fig. 14.13.

14.4.3. Results of ^{90}Y DOTATATE

DOTATATE could be labelled with ^{90}Y with high radiochemical yields. The optimum pH was in the range 4–5, as shown in Fig. 14.14, and the labelling yield was >98% at 20–60 min incubation (see Table 14.5). The RCP of ^{90}Y DOTATATE was 99%. In vitro stability of ^{90}Y DOTATATE was evaluated after labelling wherein the labelling mixtures were stored at 4°C with gentisic acid and at 37°C with human serum for 24, 42, 72 and 96 h. The stability results are shown in Table 14.6.

14.4.4. Results of the preparation of ^{90}Y aggregated albumin

The diluted albumin particles in 0.5M acetate buffer, pH6, were labelled with ^{90}Y acetate using the direct method. The radioactivity of ^{90}Y was measured using β and γ counters. The labelling yields of ^{90}Y albumin and ^{90}Y MAASOL were >80% (see Fig. 14.15).

The incubation time for the labelled reaction was ~60 min. However, labelling yields were not much different between the incubation times from 15–60 min (see Fig. 14.16). A suitable solvent for paper chromatography and ITLC of labelled microaggregated albumin and ^{90}Y acetate was tris-acetic EDTA. Here, the unbound ^{90}Y migrates to the solvent front ($R_f = 0.9$ –1.0), and the radiolabelled albumin particles remain at the origin ($R_f = 0$).

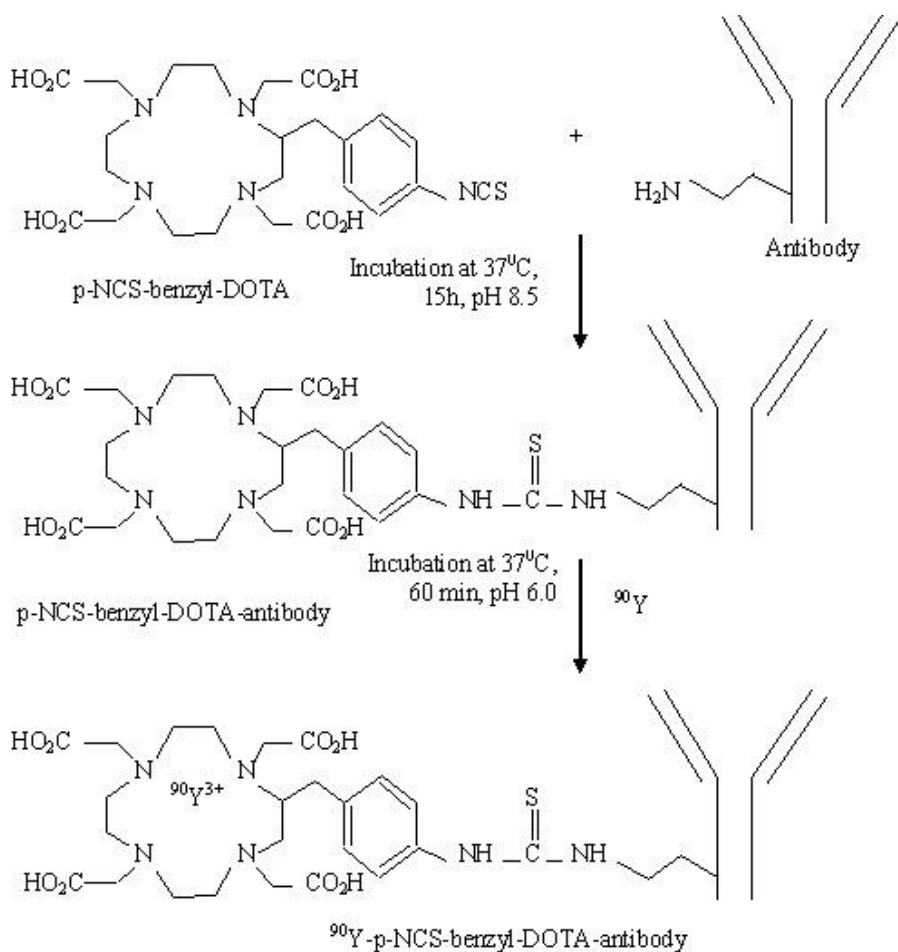


FIG. 14.13. Reaction scheme for labelling the antibody with ^{90}Y .

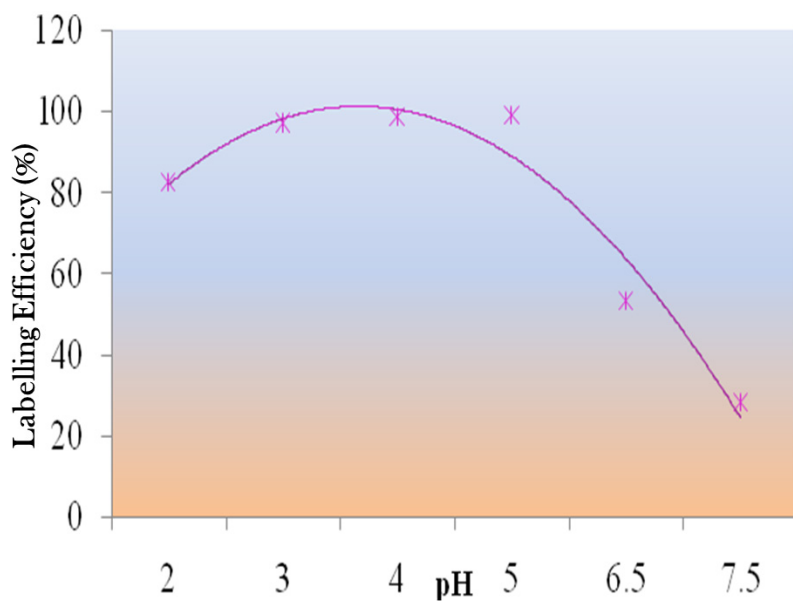


FIG. 14.14. Optimization of pH of ⁹⁰Y DOTATATE.

TABLE 14.5. LABELLING YIELDS OF ⁹⁰Y DOTATATE AS A FUNCTION OF TIME AND TEMPERATURE

Temperature (°C)	RCP (%) 1 min	RCP (%) 20 min	RCP (%) 30 min	RCP (%) 45 min	RCP (%) 60 min
4	14.3	24.4		22.5	2.1
24	14.3	17.4		18.9	4.3
37	14.3	24.1		28.6	17.9
70	14.3	34.9		91.3	95.2
90	14.3	98.0	99.7	99.8	99.8

TABLE 14.6. STABILITY (%) OF ^{90}Y DOTATATE IN HUMAN SERUM AT 37°C AND IN GENTISIC ACID AT 4°C

Time (h)	Human serum	Gentisic acid
1	99.98	99.80
4	99.90	99.60
5	98.59	98.55
48	96.20	95.41
72	95.01	92.60
96	94.38	92.03

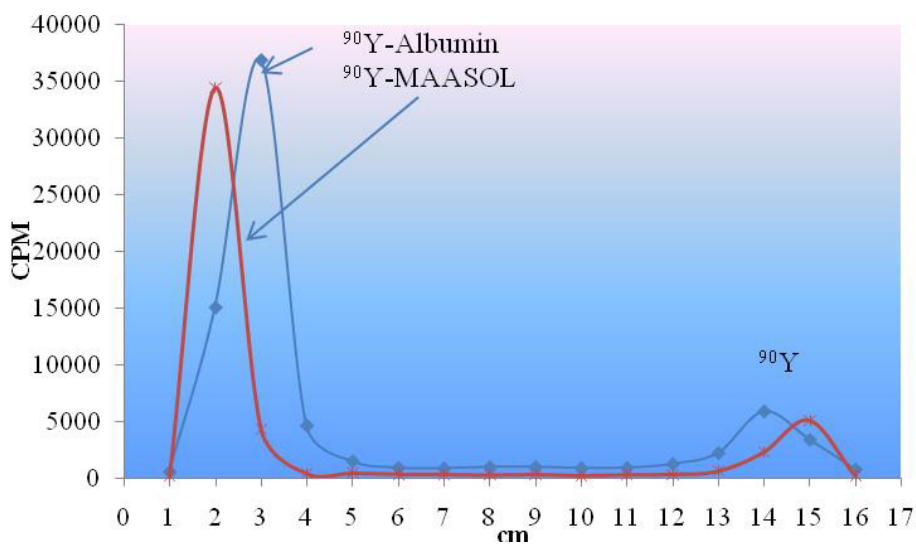


FIG. 14.15. Labelling yield of ^{90}Y albumin.

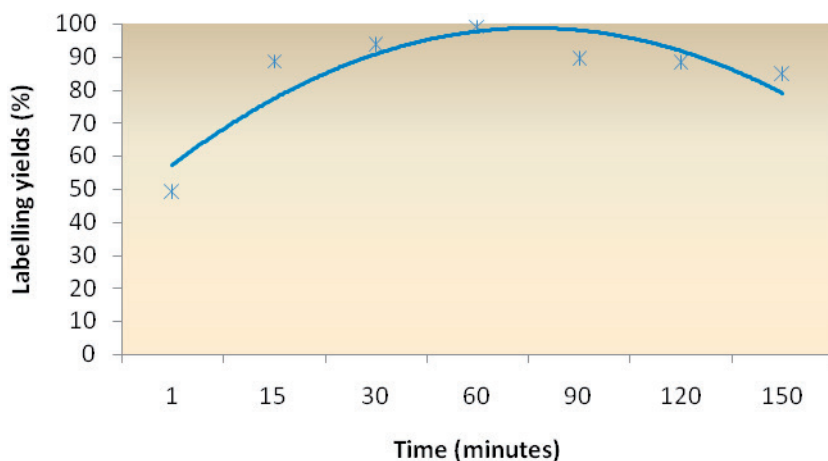


FIG. 14.16. Labelling yield of ⁹⁰Y albumin as a function of incubation time.

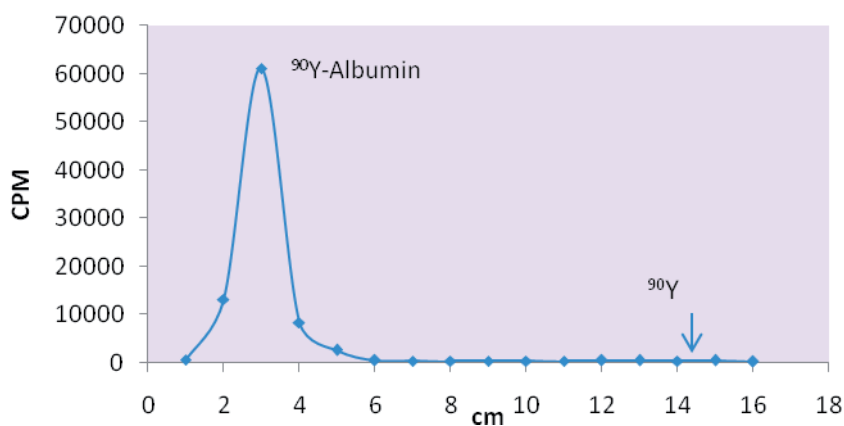


FIG. 14.17. RCP of ⁹⁰Y albumin.

The RCP of ⁹⁰Y albumin was carried out using ITLC and developed in tris-acetic EDTA buffer with >98% purity (see Fig. 14.17). MAASOL was also labelled with ⁹⁰Y in the same way, with a purity of 98%.

The sizes of ⁹⁰Y albumin particles were compared with the albumin particles in the original solution to ensure that they did not change during labelling treatment (see Fig. 14.18).

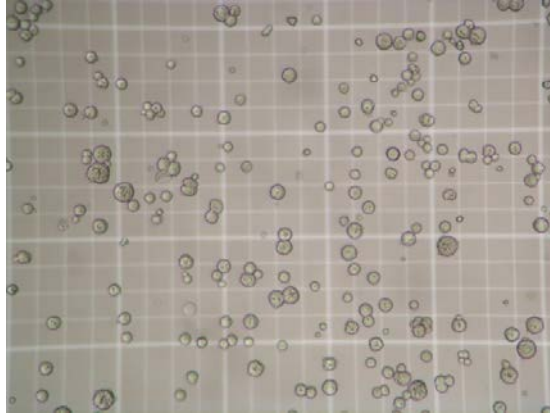


FIG. 14.18. Microsphere albumin size 10–30 μm .

Figure 14.19 shows ^{90}Y labelling yield of the benzyl DOTA albumin conjugate in 0.5M acetate buffer, pH6, at 37°C for 60 min and at 90°C for 30 min. Labelling yields were >80% at all benzyl DOTA albumin conjugate ratios from 1:1, 5:1, 20:1, 50:1 to 100:1. Labelling yields of the benzyl DOTA albumin conjugate with ^{90}Y at 37°C for 60 min were >5–6% in comparison with incubation at 90°C for 30 min.

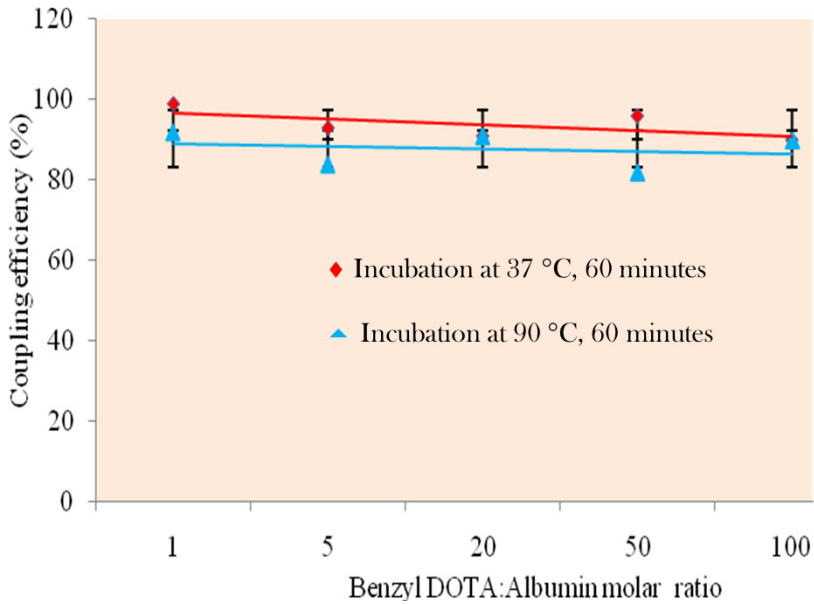


FIG. 14.19. Conjugation of benzyl DOTA albumin.

14.5. CONCLUSION AND SUGGESTIONS

The work in this chapter has been carried out according to the scope of the work plan developed in the CRP. This included the preparation of a $^{90}\text{Sr}/^{90}\text{Y}$ generator using SLM technology and the development of a two stage SLM based $^{90}\text{Sr}/^{90}\text{Y}$ generator in a semiautomation sequential mode. The production of carrier free ^{90}Y from this system was successfully developed in house. In addition, the validation of quality control methods for ^{90}Y extracted from this $^{90}\text{Sr}/^{90}\text{Y}$ generator was developed based on the EPC method using modified paper chromatography and various solvents. Yttrium-90 was obtained with a high radionuclidic purity and could be used for the preparation of radiopharmaceuticals.

Yttrium-90 rituximab was labelled with ^{90}Y obtained from a $^{90}\text{Sr}/^{90}\text{Y}$ generator. Rituximab was conjugated to the cDTPA and p-NCS-Bz-DOTA chelating agents, and the labelling conditions, quality control and biodistribution optimized. The preparations of ^{90}Y DOTATATE and ^{90}Y albumin particles were studied. To determine the RCP of ^{90}Y albumin particles, a new solvent using a tris-acetate system as the mobile phase in paper chromatography and ITLC was used. The stability of the labelled compounds was investigated. Stability testing and biodistribution analysis of ^{90}Y DOTA benzyl rituximab and ^{90}Y DOTA benzyl albumin microspheres will be completed in the future.

ACKNOWLEDGEMENTS

The authors of this chapter wish to thank the IAEA for support in carrying out the research. The authors are grateful to experts from BARC for help in upgrading the generator and quality control methods to check the purity of ^{90}Y . The authors are also thankful to M. Chinol for valuable suggestions in the labelling techniques and preclinical studies.

REFERENCES TO CHAPTER 14

- [14.1] CHINOL, M., HNATOWICH, D.J., Generator produced yttrium-90 for radioimmunotherapy, *J. Nucl. Med.* **28** (1987) 1465.
- [14.2] CHINOL, M., FRANCESCHINI, R., PAGANELLI, G., PAIANO, A., "Simple production of yttrium-90 in a chemical form suitable to clinical grade radioconjugates", *Radioactive Isotopes in Clinical Medicine and Research, Proc. 22nd Int. Badgastein Symp. Series* (BERGAMANN, H., KROISS, A., SINZINGER, H., Eds), Springer (1997) 327.

- [14.3] PANDEY, U., DHAMI, P.S., JAGESIA, P., PILLAI, M.R., Extraction paper chromatography technique for the radionuclide purity evaluation of ^{90}Y for clinical use, *Anal. Chem.* **80** (2008) 801.
- [14.4] NAIK, P.W., et al., Separation of carrier-free ^{90}Y from ^{90}Sr by SLM technique using D2EHDP in N-dodecane as carrier, *Sep. Sci. Technol.* **45** (2010) 554.
- [14.5] KNOX, S.J., et al., Yttrium-90 labeled anti-CD20 monoclonal antibody therapy of recurrent B-cell lymphoma, *Clin. Cancer Res.* **2** (1996) 457.
- [14.6] SAHA, G.B., *Fundamentals of Nuclear Pharmacy*, 3rd edn, Springer, New York (2000).
- [14.7] HNATOWICH, D.J., LAYNE, W.W., CHILDS, R.L., Radioactive labeling of antibody: A simple and efficient method, *Science* **220** (1983) 613.
- [14.8] WATANABE, N., et al., Yttrium-90 labeled human macroaggregated albumin for internal radiotherapy: Combined use with DTPA, *Nucl. Med. Biol.* **26** (1999) 847.

Annex

PROTOCOLS DEVELOPED UNDER THE COORDINATED RESEARCH PROJECT DEVELOPMENT OF THERAPEUTIC RADIOPHARMACEUTICALS BASED ON ¹⁸⁸Re AND ⁹⁰Y FOR RADIONUCLIDE THERAPY

A-1. STRONTIUM-90 DETERMINATION IN ⁹⁰Y BY EXTRACTION PAPER CHROMATOGRAPHY (CONTRIBUTION FROM BHABHA ATOMIC RESEARCH CENTRE, INDIA)

A-1.1. Introduction

Yttrium-90 based therapeutic radiopharmaceuticals are widely used for cancer treatment and therapy of other diseases such as rheumatoid arthritis. An important condition for the use of ⁹⁰Y eluate obtained from ⁹⁰Sr/⁹⁰Y generators is that it should be devoid of any ⁹⁰Sr because this long lived radioisotope (~28.8 years) accumulates in bone. The maximum permissible body burden of ⁹⁰Sr is only 74 kBq (2 µCi) [A-1]. The ⁹⁰Sr impurity level in ⁹⁰Y is quoted by manufacturers as being ≤740 kBq (20.0 µCi) of ⁹⁰Sr per 37 GBq (1 Ci) of ⁹⁰Y [A-2, A-3]. To measure this level of purity, the ability to detect ≤20 disintegrations/s of ⁹⁰Sr in 1 × 10⁶ disintegrations/s of ⁹⁰Y is required.

The Bhabha Atomic Research Centre (BARC), India, method for estimating the radionuclidic purity of ⁹⁰Y is based on the extraction paper chromatography (EPC) technique [A-4]. The EPC technique is a combination of solvent extraction and paper chromatography techniques. A chromatography paper impregnated with a ⁹⁰Y specific chelate, 2-ethylhexyl, 2-ethylhexyl phosphonic acid (KSM-17), at the point of application is used as the support for chromatography. Owing to its selective retention by KSM-17, Y³⁺ remains at the point of spotting, while Sr²⁺ moves with the solvent front. The activity at the solvent front is estimated using a liquid scintillation counter (LSC) and compared with the total spotted activity. The following procedure is adapted from Ref. [A-5].

A-1.2. Materials

The KSM-17 used in these studies was synthesized at BARC [A-6]. The commercially available reagent equivalent to KSM-17 is 2-ethylhexyl-phosphoric acid mono-2-ethylhexyl ester (Daihachi Chemical Industry Co. Ltd). The scintillation cocktail was prepared from 900 mL of dioxane, 100 g of

naphthalene and 1.2 g of 2,5-diphenyloxazole. Paper chromatography strips from Whatman were used for the assay.

A-1.3. Methods

The EPC technique was performed as described in the following steps:

- *Step 1: Preparation of test solution.* A test solution of 100 μL of ^{90}Y acetate with a radioactivity concentration of 37 MBq/mL (1.0 mCi/mL) was prepared by dilution of the bulk solution with 0.5M ammonium acetate.
- *Step 2: Preparation of EPC paper.* Whatman No. 1 chromatography paper (12 cm \times 1 cm) marked in 1 cm segments along the longest dimension was used, with 10 μL of KSM-17 applied between the second and third segments, and then allowed to dry in air.
- *Step 3: EPC.* A 5 μL sample of the test solution prepared in step 1 was applied to the KSM-17 spot on the EPC paper and allowed to dry in air. Then, the EPC was developed by ascending chromatography using 0.9% saline as the solvent. After the solvent had moved to the top, the paper was removed and cut into 1 cm segments. Three segments of the solvent front were inserted in a liquid scintillation vial containing 10 mL of the scintillation cocktail. It should be noted that the paper has to be segmented beginning at the solvent front and moving backwards. The activity at the point of spotting is very high, and contamination of the scissors owing to contact with this activity might increase the activity of subsequent strips. The samples were counted for 60 min. The counting must be done immediately (within a couple of hours after completion of the experiment) because the counts in the ^{90}Sr fraction will continue to increase during storage owing to growth of ^{90}Y . For example, ^{90}Y grows to 2% of its maximum value in 2 h, to $\sim 23\%$ in 1 d and to $\sim 40\%$ in 2 d. Therefore, the amount of ^{90}Sr will be overestimated if a time lag occurs between the development of the paper strip and sample counting.
- *Step 4: Calculation of results.* In the following representative example, the test solution contained 37 MBq/mL (1.0 mCi/mL) and so the original activity used in the EPC was 1.85×10^5 Bq (5 μCi). Using the efficiency of the counter, the activity at the solvent front of the paper strip was calculated and, accordingly, the percentage of radionuclidic impurity was calculated from the above results. As a model calculation, if 6000 counts are obtained at the solvent front for a 60 min counting time, these correspond to 100 counts/min. Assuming 90% efficiency of the counter, the resulting activity is 111 disintegrations/min (1.85 Bq). It follows that the radionuclidic impurity is 0.001%, and the radionuclidic purity of the

product is 99.999%. Thus, the solution contains 370 kBq (10 μ Ci) of ^{90}Sr in 37 GBq (1 Ci) of ^{90}Y .

- *Step 5: Setting the ^{90}Sr impurity limit for the ^{90}Y eluate.* The ^{90}Sr impurity limit quoted by most commercial manufacturers is 740 kBq (20 μ Ci) of ^{90}Sr per 37 GBq (1 Ci) of ^{90}Y , which corresponds to 3.7 Bq or 222 disintegrations/min of ^{90}Sr per 185 kBq (5 mCi) of the spotted solution. Hence, a value ≤ 222 disintegrations/min in the solvent front corresponds to ^{90}Sr contamination ≤ 740 kBq (20 μ Ci) per 37 GBq (1 Ci) of ^{90}Y . In this condition, the product can be considered to meet the required standard specifications. If necessary, lower cut-off limits can also be set, based on the above method.
- *Step 6: Validation of the technique.* This is an optional step to be followed for validation of the EPC technique. A 5 mL aliquot of the test solution is dispensed into a liquid scintillation vial. The vial is marked with the batch number and stored for ~ 60 d, by which time, it is expected that 99.99999% of the ^{90}Y decays, and only ^{90}Sr contamination is present. At this point, any ^{90}Sr present will be in secular equilibrium with ^{90}Y . The vial is then counted in an LSC for 60 min. The counts correspond to any ^{90}Sr contamination and an equal amount of ^{90}Y . If gross counting is performed to include both ^{90}Y and ^{90}Sr windows, the activity measured can be halved to obtain the ^{90}Sr activity (assuming that there is not much difference in the efficiency for ^{90}Sr and ^{90}Y). The activity thus calculated for ^{90}Sr should be equal to the activity in the solvent front obtained during the EPC (step 4 above).

A-2. STRONTIUM-90 DETERMINATION IN ^{90}Y BY SOLID PHASE EXTRACTION (CONTRIBUTION FROM EUROPEAN INSTITUTE OF ONCOLOGY, ITALY)

A-2.1. Introduction

Usually, the determination of ^{90}Sr impurities is carried out by liquid scintillation counting after decay of the majority of ^{90}Y , which would interfere with the measurement. However, to use the ^{90}Y eluate obtained from a $^{90}\text{Sr}/^{90}\text{Y}$ generator in patients, the radionuclidic purity determination must be carried out in a freshly eluted ^{90}Y sample. In the frame of this coordinated research project, efforts have been devoted to the development of a simple and efficient method to assess whether the ^{90}Y solution meets the clinical requirements immediately after elution from the generator, prior to proceeding to radiopharmaceutical preparation (i.e. an absolute ratio of activities of 10^{-7} at time of administration [A-7].)

A-2.2. Materials

The method for separation of ^{90}Sr from ^{90}Y eluate is based on the commercially available strontium resin obtained from Eichrom Technologies. This is an extraction chromatography resin coated with a 1.0M solution of the crown ether 4,4'(5')-di-butylcyclohexane 18-crown-6 1.0 in 1-octanol as the extracting system. This extractant has different stability constants (pH dependent) for different cations, which is a property resulting from both steric interactions with the cavity of the 18-crown-6 ether and electrostatic forces between the oxygens of the ether and the cations dissolved in the mobile phase. In particular, this strontium resin has a high stability constant for Sr^{2+} at low pH (high acidic concentration), whereas in the same conditions, the stability constant for Y^{3+} is very low.

In the initial experiments, the solution containing ^{90}Sr and ^{90}Y was loaded onto a strontium resin minicolumn (2 mL cartridge), the ^{90}Y was eluted with two fractions of 5 mL of 8.0M HNO_3 to collect the ^{90}Y , and then the two fractions were eluted with 5 mL of 0.01M HNO_3 , each to recover the ^{90}Sr from the column. According to Eichrom Technologies specifications, this procedure should allow collection of pure solutions of each radionuclide. Unfortunately, this was not confirmed in the liquid scintillation counting and spectrometric analysis. This led to improvements of the conditions for separation, as published earlier [A-8] and presented in the method below.

A-2.3. Method

The technique was performed as described in the following steps:

- (a) *Column preparation:* 4 mL of the Eichrom Technologies strontium resin prepared according to manufacturer recommendations was loaded onto a chromatographic column (dimensions of 1 cm \times 5 cm).
- (b) *Elution procedure:* The ^{90}Y - ^{90}Sr eluate mixture was loaded onto the freshly prepared strontium resin column. Two 5 mL fractions of HNO_3 (8.0M) were successively passed through the column. Activity corresponding to ^{90}Y was recovered almost quantitatively in the first 5 mL fraction. The elution with HNO_3 (8.0M) was continued by collecting and counting smaller portions of the second fraction until the ^{90}Y radioactivity was below the detection limit, thus indicating that ^{90}Y will not interfere with the subsequent counting of ^{90}Sr . Finally, ^{90}Sr was stripped from the column by successively passing two 5 mL fractions of HNO_3 (0.01M). These solutions were collected and counted and the ratio ^{90}Sr : ^{90}Y calculated.

A-2.4. Conclusion

Using the described chromatographic system, it was possible to determine ^{90}Sr by measuring the fractions eluted with 0.01M HNO_3 , after the complete recovery of ^{90}Y in the first fractions by 8.0M HNO_3 .

A-3. STRONTIUM-90 DETERMINATION IN ^{90}Y ELUATES USING DGA RESIN (CONTRIBUTION FROM NATIONAL CENTRE FOR NUCLEAR RESEARCH, RADIOISOTOPE CENTRE, POLATOM, POLAND)

A-3.1. Introduction

Another approach to separate ^{90}Sr from ^{90}Y eluates was based on the use of the new extraction chromatography resin DGA (Eichrom Technologies). DGA resin is an extraction chromatographic system in which the extractant material is N,N,N',N'-tetra-n-octyldiglycolamide, bearing a linear chain (C8) of carbon methyl groups as lateral R substituents (DGA resin, normal). This resin has a high capacity for selective adsorption of strontium [A-9].

A-3.2. Method

The procedure for separation is described in the following:

- (a) *Column preparation:* A chromatographic column containing 100 mg of DGA resin was prepared according to manufacturer recommendations.
- (b) *Elution procedure:* A volume of 0.030 mL of ^{90}Y solution (200 ± 5 MBq as measured using a calibrated ionization chamber) was loaded onto the column and instantly rinsed successively with 4 mL of 5M HNO_3 , 2 mL of 5M HNO_3 and 2 mL of 0.1M HNO_3 . The flow rate was 1.0 mL/min. The three successive elutions led to collections of three corresponding fractions from the column:
 - (i) Fraction I: volume = 8 mL (including loaded volume sample and 4 mL of 5M HNO_3 from the first elution);
 - (ii) Fraction II: volume = 2 mL of 5M HNO_3 from the second elution;
 - (iii) Fraction III: volume = 2 mL of 0.1M HNO_3 from the third elution.

Activity was measured by transferring ~1 g aliquots by weight from each fraction into 20 mL LSC vials. Deionized water (1.5 mL) and 10 mL of Ultima Gold AB liquid scintillator were added to each vial. Measurements were carried

out using a Wallac 1411 spectrometer or similar instrument, and results were used to calculate the $^{90}\text{Sr}:$ ^{90}Y activity ratio.

A-3.3. Conclusion

When separation is properly accomplished, fraction I should contain the total ^{90}Sr activity with only a few ^{90}Y counts originating from the decay of ^{90}Sr occurring during collection and measurement. Fractions II and III should not contain any radioactivity, and their spectra should show pure background only. The calculation of ^{90}Sr activity should be performed based on the obtained spectra and taking into account the dilution factor for each fraction.

A-4. YTTRIUM-90 RADIOLABELLING OF BIOTIN DOTA (CONTRIBUTION FROM EUROPEAN INSTITUTE OF ONCOLOGY)

A-4.1. Introduction

Yttrium-90 1,4,7,10-tetraazacyclododecane 1,4,7,10-tetraacetic acid (DOTA) biotin was prepared by adding an equal volume of sodium acetate (1.0M, pH5.0) to the $^{90}\text{YCl}_3$ vial (concentration 37–74 GBq/mL in 0.05M HCl) containing 2.96–4.44 GBq of ^{90}Y followed by 1.0 mg of biotin DOTA dissolved in 0.5 mL of saline (recommended specific activity of 3.7 GBq/mg). After mixing, the reaction vial was incubated for 30 min at 95°C. Aliquots of the mixture were drawn at defined time intervals to determine the radiochemical purity (RCP).

A-4.2. Procedure

The technique was performed as described in the following steps:

- (a) Measure the ^{90}Y activity in the vial in a dose calibrator, which had been previously calibrated according to manufacturer specifications and tested with a ^{90}Y source.
- (b) Using a sterile 1 mL syringe, add to the vial containing the $^{90}\text{YCl}_3$, a 1.0M sodium acetate buffer at pH5.0 in a volume equal to the volume of 0.05M HCl, in which the ^{90}Y is dissolved. Shake the vial.
- (c) Using a sterile 1 mL syringe, add to the vial containing the buffered ^{90}Y , 1.0 mg of biotin DOTA dissolved in 0.5 mL of saline. Shake and incubate for 30 min at 95°C in a thermostatic bath.
- (d) Remove the vial from the bath and allow it to cool at room temperature and then shake again.

- (e) Determine the RCP as follows. Using a sterile 1 mL syringe, an aliquot (~0.05 mL) is removed and transferred to a conical tube containing 0.2 mL of a mixture of avidin and diethylenetetraminopenta acetic acid (DTPA) (0.4mM avidin and 2.5mM DTPA at pH6.0). The RCP is determined by spotting an aliquot of the mixture on an instant thin layer chromatographic (ITLC) silica gel (SG) strip and developing it with saline. Once developed, the strip is cut in the middle and each portion counted separately. The ⁹⁰Y DOTA biotin bound to avidin remains at the origin (bottom counts), whereas the unbound ⁹⁰Y, chelated by DTPA, migrates with the solvent front (top counts). Caution: The amount of radioactivity at the origin is expressed as a percentage of the total amount of radioactivity applied to the strip (RCP).
- (f) If the RCP is >98%, add to the reaction mixture 0.2 mL of a sterile solution of DTPA, 1mM, pH5.0, to bind any possible trace of free ⁹⁰Y not bound to the biotin DOTA and then 1 mL of saline.
- (g) Using a sterile 3 mL syringe, withdraw the required patient's dose and measure in a dose calibrator that has previously been calibrated for that counting geometry.

A-5. BIOTINYLATION OF IMMUNOGLOBULINS (CONTRIBUTION FROM EUROPEAN INSTITUTE OF ONCOLOGY)

A-5.1. Introduction

The biotinylation of monoclonal antibodies (MAbs) represents a useful tool to prepare in house MAbs containing a number of biotin molecules, which do not compromise the MAb immunoreactivity (see Section 6 of this Annex), and can be used as a first step in the pretargeting approach, which foresees as a final step the intravenous injection of radiolabelled biotin (see Section 4 of this Annex) [A-10, A-11].

A-5.2. Materials

2X AH biotin NHS (biotinyl aminocaproic acid N-hydroxysuccinimide ester) containing a six carbon atom spacer between the head of the biotin group and the activated carboxylic group can be purchased from SPA - Società Prodotti Antibiotici S.p.A.

A-5.3. Procedure

The technique was performed as described in the following steps:

- (a) Start with a solution of antibody in sodium bicarbonate buffer, 0.1M, pH8.5 (overnight dialysis at 2–8°C).
- (b) Prepare a solution of 2X AH biotin NHS in dimethyl sulphoxide at the same concentration of the antibody (e.g. antibody concentration = 3 mg/mL), and prepare the same concentration of the biotinylation agent).
- (c) Add 0.04 mL of the above biotinylation agent to every millilitre of antibody (molar ratio biotin:antibody = 10:1) under continuous and gentle stirring.
- (d) Keep the solution under slow stirring for 2 h at room temperature.
- (e) Dialyse overnight against phosphate buffered saline (PBS) (pH7.4) at 2–8°C (at least two changes of 5 L each).
- (f) Filter through a 0.22 µm Millipore filter, determine the titre and then make aliquots.
- (g) Store the aliquots of biotinylated antibody in refrigerator, and avoid the use of dry ice.
- (h) Determine the biotinylation yield (number of biotin per molecule of MAb) using the 2-(4-hydroxyphenyl-azo) benzoic acid (HABA) method after enzymatic digestion of the antibody (see Section 6 below).

A-6. DETERMINATION OF BIOTIN:ANTIBODY MOLAR RATIO (CONTRIBUTION FROM EUROPEAN INSTITUTE OF ONCOLOGY)

The determination of the biotinylation yield (number of biotin molecules per molecule of antibody) is important to ensure that the MAb has maintained its immunoreactivity.

A-6.1. Procedure

The technique was performed as described in the following steps:

- (a) Start with a solution of biotinylated antibody at a concentration ≤ 1.5 mg/mL (if the concentration is higher, dilute with saline);
- (b) Place, in an Eppendorf tube, 240 µL of antibody and heat at 60°C for 10 min;
- (c) Add 8 µL of protease (Sigma catalogue No. P-6911) solution previously prepared at 5% in water and stir;
- (d) Leave for 4 h at 37°C to allow digestion of the protein;

- (e) Titre the biotin by the HABA (Fluka catalogue No. 54791) method using a biotin standard curve previously obtained by plotting known amounts of biotin against the change in absorbance at 500 nm.

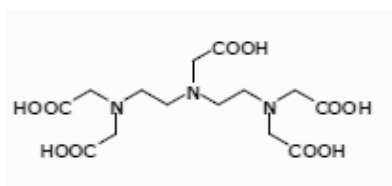
A-6.2. Conclusion

If the biotinylation of the MAb is carried out with a molar ratio of biotin:antibody $\sim 10:1$, then the number of biotins per MAb usually ranges between 6 and 8.

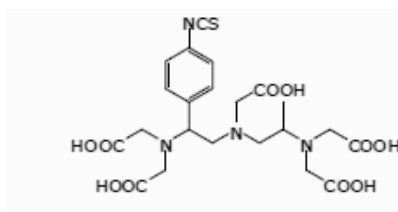
A-7. CONJUGATION OF A CHELATOR TO ANTIBODY (CONTRIBUTION FROM UNIVERSITY OF COLOGNE, DEPARTMENT OF NUCLEAR MEDICINE, GERMANY)

A-7.1. Introduction

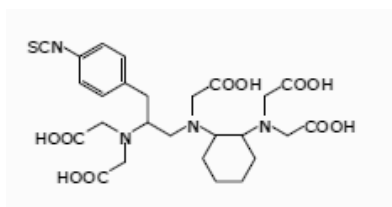
As a rule, the labelling of antibodies with trivalent radioactive metal ions such as ^{90}Y as trivalent Y^{3+} ion requires chelating agents. Derivatives of DTPA and DOTA are the chelators most commonly used (see Fig. A-1).



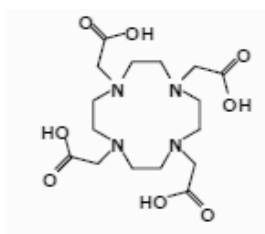
DTPA



MX-A''-DTPA



CHX-A''-DTPA



DOTA

FIG. A-1. Various ligands used for coupling ^{90}Y to antibodies.

Although acyclic chelators offer many of the necessary features required of a chelating agent, such as low temperature and short reaction time, they are seldom used, as the complexes formed have a lower in vivo stability than those produced with cyclic chelators such as DOTA. For example, with unmodified DTPA as the chelator, the only complexes stable enough for in vivo applications are the ^{111}In conjugates. To increase the stability of the complexes formed, DTPA derivatives have been developed in which the backbone of the molecule is modified to allow preconformation of the carboxyl groups. This reduces the entropy of the chelator molecule and increases the stability of the final conjugate. Binding with ^{90}Y ions is then also possible. However, the rigid conformation of these chelating agents also prolongs the reaction time needed for complex formation. Examples of such DTPA derivatives are MX-A'' DTPA and CHX-A'' DTPA.

Extremely stable complexes with some clinically relevant metallic radionuclides can be produced using the cyclic chelating agent DOTA, although the conjugation process takes much longer than with acyclic chelators.

The key point here is that the selected chelators are bifunctional, acting not only as chelators, but also as coupling agents. The latter capability can be achieved by insertion of a reactive ester group (e.g. tetrafluorophenol). Addition of cyclic acid anhydride groups enables coupling via primary amino groups such as lysine side chains on an antibody to occur. Coupling to primary amino groups can also be achieved using a chelator with an isothiocyanide function. If this is replaced by a maleimide function, coupling proceeds via a thiol group (cysteine or free sulphydryl groups).

A whole series of bifunctional chelating agents are commercially available (<http://www.chematech-mdt.com/>, <http://macrocylics.com/shop/>). The procedure for conjugation of the bifunctional chelator p-isothiocyanatobenzyl DOTA (p-NCS-Bz DOTA) via binding of ϵ amine functions of lysine on the antibody with the isothiocyanate (NCS) group of the chelating agent is presented below as a standard protocol for DOTA conjugation to rituximab.

A-7.2. Methods

A-7.2.1. Synthesis of the DOTA antibody

For coupling of NCS-Bz-DOTA, 3 mg of antibody is transferred by centrifugal filtration (molecular weight cut-off = 30 000, for ~10 min at 3000 rev./min) from a PBS buffer into a 0.2M sodium carbonate buffer (pH9). A 30-fold molar excess of NCS-Bz-DOTA (dissolved in sodium carbonate buffer) is subsequently added to the solution and left to incubate for 2 h at 37°C. To stop the reaction, the reaction mixture is transferred by centrifugal filtration, first into

0.25M ammonium acetate buffer (pH5.5), then into 0.25M ammonium acetate buffer (pH7.5) and finally concentrated down to 500 μ L.

A-7.2.2. Yttrium-90 labelling of the DOTA modified antibody

An activity of 100 MBq of (^{90}Y) yttrium chloride (carrier free) is added to 3 mg of the DOTA antibody in ammonium acetate buffer (pH7.5) and incubated for 1–2 h at 42°C. This is followed by purification through an NAP-5 column (GE Healthcare, formerly Amersham Biosciences, 0.5 mL, prepacked with Sephadex G-25 deoxyribonucleic acid grade in distilled water containing 0.15% Kathon CG/ICP biocide, sample volume 0.5 mL) and quality control using high performance liquid chromatography (Tosoh Bioscience LLC, TosoHaas SW 2000 column silica, 10 and 13 μm , pore size (mean) 125 \AA).

A-7.3. Conclusion

The described procedure allows preparation of ^{90}Y rituximab with RCP >90% and a sufficient affinity for CD20 positive tumour cells.

A-8. IN VITRO STABILITY TESTING OF RADIOCOLLOIDS IN SYNOVIAL LIQUIDS (CONTRIBUTION FROM UNIVERSITY OF COLOGNE)

A-8.1. Introduction

Yttrium-90, ^{169}Er and ^{186}Re colloids are used for radiation synovectomy. The method below can be used to measure the in vitro stability of radiocolloids for radiosynovectomy. This is important because there is the widespread use of radiation synovectomy throughout the world on the one hand, but a surprising lack of reliable data on the in vivo stability of radiocolloids on the other hand, if X ray contrast agents, anaesthetics and glucocorticoids are co-injected.

A-8.2. Methods

The technique was performed as described in the following steps:

- (a) Vials of 1 mL synovial fluid and 0.02 mL radioactive colloid suspension of ^{90}Y citrate, ^{169}Er citrate or ^{186}Re sulphide with initial activities of between 0.56 and 3.6 MBq were prepared. Positive controls are generated by adding 1.0M DTPA in a first series and 0.37% HCl in a second series to the ^{169}Er

and ^{90}Y colloids, both series with a volume ratio of 1:10. For the ^{186}Re colloid, radionuclide mobilization is achieved by admixing 65% HNO_3 . The extent of release of low molecular species from the radiocolloids is determined using thin layer chromatography (TLC) and ultrafiltration after incubation times of 1 h, 4 h, 24 h, 48 h, 6 d, 9 d, 13 d and 15 d.

- (b) TLC is performed using 20 cm \times 20 cm ITLC SG strips (Varian). The distribution of radioactivity is measured using a linear radioactivity scanner.
- (c) For ultrafiltration, the Ultrafree MC filter with 5000 nominal molecular weight limit (Millipore) is used. After filtration, probe volumes of 200 μL are centrifuged for 7 h at 5000 U/min (2250g) using the ultracentrifuge Optima L-70K (Beckman Coulter) and the rotor model 70 Ti. Thus, the free or low molecular radionuclides ^{90}Y , ^{186}Re or ^{169}Er released from the radiocolloids are detected. Subsequent measurements of both filter and filtrate are performed after centrifugation in a well counter (such as ISOMED 100, Nuklear-Medizintechnik).

A-8.3. Conclusion

The two independent methods, TLC and ultrafiltration/ultracentrifugation, can differentiate between intact radioactive colloids and mobilized radionuclides with good conformity.

REFERENCES TO ANNEX

- [A-1] NATIONAL BUREAU OF STANDARDS, "Maximum permissible body burden and maximum permissible concentrations of radionuclides in air and water for occupational exposure", National Bureau of Standards Handbook, Vol. 69, NBS, Gaithersburg (1959) 38.
- [A-2] EUROPEAN MEDICINES AGENCY, Ytracis: European Public Assessment Report (EPAR), EMEA/H/C/470, European Medicines Agency (2008), http://www.ema.europa.eu/docs/en_GB/document_library/EPAR_-_Summary_for_the_public/human/000460/WC500045979.pdf
- [A-3] UNITED STATES PHARMACOPEIAL CONVENTION, Yttrium (Y-90) ybritumomab tiuxetan injection, United States Pharmacopeia 30 NF 25, USP Convention, Rockville (2007) 3487.
- [A-4] PANDEY, U., DHAMI, P.S., JAGESIA, P., VENKATESH, M., PILLAI, M.R.A., A novel extraction paper chromatography (EPC) technique for the radionuclidic purity evaluation of ^{90}Y for clinical use, *Anal. Chem.* **80** (2008) 801.
- [A-5] INTERNATIONAL ATOMIC ENERGY AGENCY, Therapeutic Radionuclide Generators: $^{90}\text{Sr}/^{90}\text{Y}$ and $^{188}\text{W}/^{188}\text{Re}$ Generators, Technical Reports Series No. 470, IAEA, Vienna (2009) 33-35.

- [A-6] MARWAH, U.R., "Synthesis of organophosphorous extractants for solvent extraction of metals", Proc. Natl Symp. Organic Reagents–Synthesis and Use in Extraction Metallurgy (ORSEUM-94), BARC, Mumbai (1994).
- [A-7] INTERNATIONAL COMMISSION ON RADIOLOGICAL PROTECTION, Radiation Dose to Patients from Radiopharmaceuticals (Addendum to ICRP Publication 53), Publication 80, Pergamon Press, Oxford and New York (1998).
- [A-8] BONARDI, M.L., MARTANO, L., GROPPI, F., CHINOL, M., Rapid determination of ^{90}Sr impurities in freshly "generator eluted" ^{90}Y for radiopharmaceutical preparation, *Appl. Radiat. Isot.* **67** (2009) 1874.
- [A-9] HORWITZ, E.P., McALISTER, D.R., BOND, A.H., BARRANS, R.E., Jr., Novel extraction of chromatographic resins based on tetraalkyldiglycolamides: Characterization and potential applications, *Solvent Extr. Ion Exch.* **23** (2005) 319.
- [A-10] URBANO, N., et al., Evaluation of a new biotin-DOTA conjugate for pretargeted antibody-guided radioimmunotherapy (PAGRIT), *Eur. J. Nucl. Med. Mol. Imaging* **34** (2007) 68.
- [A-11] PAGANELLI, G., et al., Intraoperative avidination for radionuclide therapy: A prospective new development to accelerate radiotherapy in breast cancer, *Clin. Cancer Res.* **13** Suppl. 18 (2007) 5646s.

CONTRIBUTORS TO DRAFTING AND REVIEW

Blower, P.	St Thomas' Hospital, United Kingdom
Chinol, M.	European Institute of Oncology, Italy
De Rosales, R.T.M.	St Thomas' Hospital, United Kingdom
Djokić, D.	Vinča Institute of Nuclear Sciences, Serbia
Fischer, T.	University of Cologne, Germany
Hernandez Gonzalez, I.	Nuclear Energy Agency and Advanced Technologies, Cuba
Kameswaran, M.	Bhabha Atomic Research Centre, India
Mikołajczak, R.	POLATOM, Poland
Oso, J.A.	Nuclear and Energy Research Institute, Brazil
Park, S.-H.	Korea Atomic Energy Research Institute, Republic of Korea
Pasquali, M.	University of Ferrara, Italy
Poramatikul, N.	Ministry of Sciences and Technology, Thailand
Sangsuriyan, J.	Thailand Institute of Nuclear Technology, Thailand
Schomäcker, K.	University of Cologne, Germany
Thu, N.T.	Nuclear Research Institute, Viet Nam
Yassine, T.	Atomic Energy Commission of Syria, Syrian Arab Republic

Technical Meeting

Vienna, Austria: 16–20 November 2009

Consultants Meeting

Vienna, Austria: 4–8 February 2013



IAEA

International Atomic Energy Agency

No. 23

ORDERING LOCALLY

In the following countries, IAEA priced publications may be purchased from the sources listed below or from major local booksellers.

Orders for unpriced publications should be made directly to the IAEA. The contact details are given at the end of this list.

AUSTRALIA

DA Information Services

648 Whitehorse Road, Mitcham, VIC 3132, AUSTRALIA

Telephone: +61 3 9210 7777 • Fax: +61 3 9210 7788

Email: books@dadirect.com.au • Web site: <http://www.dadirect.com.au>

BELGIUM

Jean de Lannoy

Avenue du Roi 202, 1190 Brussels, BELGIUM

Telephone: +32 2 5384 308 • Fax: +32 2 5380 841

Email: jean.de.lannoy@euronet.be • Web site: <http://www.jean-de-lannoy.be>

CANADA

Renouf Publishing Co. Ltd.

5369 Canotek Road, Ottawa, ON K1J 9J3, CANADA

Telephone: +1 613 745 2665 • Fax: +1 643 745 7660

Email: order@renoufbooks.com • Web site: <http://www.renoufbooks.com>

Bernan Associates

4501 Forbes Blvd., Suite 200, Lanham, MD 20706-4391, USA

Telephone: +1 800 865 3457 • Fax: +1 800 865 3450

Email: orders@bernan.com • Web site: <http://www.bernan.com>

CZECH REPUBLIC

Suweco CZ, spol. S.r.o.

Klecakova 347, 180 21 Prague 9, CZECH REPUBLIC

Telephone: +420 242 459 202 • Fax: +420 242 459 203

Email: nakup@suweco.cz • Web site: <http://www.suweco.cz>

FINLAND

Akateeminen Kirjakauppa

PO Box 128 (Keskuskatu 1), 00101 Helsinki, FINLAND

Telephone: +358 9 121 41 • Fax: +358 9 121 4450

Email: akatilaus@akateeminen.com • Web site: <http://www.akateeminen.com>

FRANCE

Form-Edit

5 rue Janssen, PO Box 25, 75921 Paris CEDEX, FRANCE

Telephone: +33 1 42 01 49 49 • Fax: +33 1 42 01 90 90

Email: fabien.boucard@formedit.fr • Web site: <http://www.formedit.fr>

Lavoisier SAS

14 rue de Provigny, 94236 Cachan CEDEX, FRANCE

Telephone: +33 1 47 40 67 00 • Fax: +33 1 47 40 67 02

Email: livres@lavoisier.fr • Web site: <http://www.lavoisier.fr>

L'Appel du livre

99 rue de Charonne, 75011 Paris, FRANCE

Telephone: +33 1 43 07 50 80 • Fax: +33 1 43 07 50 80

Email: livres@appeldulivre.fr • Web site: <http://www.appeldulivre.fr>

GERMANY

Goethe Buchhandlung Teubig GmbH

Schweitzer Fachinformationen

Willstätterstrasse 15, 40549 Düsseldorf, GERMANY

Telephone: +49 (0) 211 49 8740 • Fax: +49 (0) 211 49 87428

Email: s.dehaan@schweitzer-online.de • Web site: <http://www.goethebuch.de>

HUNGARY

Librotrade Ltd., Book Import

PF 126, 1656 Budapest, HUNGARY

Telephone: +36 1 257 7777 • Fax: +36 1 257 7472

Email: books@librotrade.hu • Web site: <http://www.librotrade.hu>

INDIA

Allied Publishers

1st Floor, Dubash House, 15, J.N. Heredi Marg, Ballard Estate, Mumbai 400001, INDIA
Telephone: +91 22 2261 7926/27 • Fax: +91 22 2261 7928
Email: alliedpl@vsnl.com • Web site: <http://www.alliedpublishers.com>

Bookwell

3/79 Nirankari, Delhi 110009, INDIA
Telephone: +91 11 2760 1283/4536
Email: bkwell@nde.vsnl.net.in • Web site: <http://www.bookwellindia.com>

ITALY

Libreria Scientifica "AEIOU"

Via Vincenzo Maria Coronelli 6, 20146 Milan, ITALY
Telephone: +39 02 48 95 45 52 • Fax: +39 02 48 95 45 48
Email: info@libreriaaeiou.eu • Web site: <http://www.libreriaaeiou.eu>

JAPAN

Maruzen Co., Ltd.

1-9-18 Kaigan, Minato-ku, Tokyo 105-0022, JAPAN
Telephone: +81 3 6367 6047 • Fax: +81 3 6367 6160
Email: journal@maruzen.co.jp • Web site: <http://maruzen.co.jp>

NETHERLANDS

Martinus Nijhoff International

Koraalrood 50, Postbus 1853, 2700 CZ Zoetermeer, NETHERLANDS
Telephone: +31 793 684 400 • Fax: +31 793 615 698
Email: info@nijhoff.nl • Web site: <http://www.nijhoff.nl>

SLOVENIA

Cankarjeva Založba dd

Kopitarjeva 2, 1515 Ljubljana, SLOVENIA
Telephone: +386 1 432 31 44 • Fax: +386 1 230 14 35
Email: import.books@cankarjeva-z.si • Web site: http://www.mladinska.com/cankarjeva_zalozba

SPAIN

Díaz de Santos, S.A.

Librerías Bookshop • Departamento de pedidos
Calle Albasanz 2, esquina Hermanos García Noblejas 21, 28037 Madrid, SPAIN
Telephone: +34 917 43 48 90 • Fax: +34 917 43 4023
Email: compras@diazdesantos.es • Web site: <http://www.diazdesantos.es>

UNITED KINGDOM

The Stationery Office Ltd. (TSO)

PO Box 29, Norwich, Norfolk, NR3 1PD, UNITED KINGDOM
Telephone: +44 870 600 5552
Email (orders): books.orders@tso.co.uk • (enquiries): book.enquiries@tso.co.uk • Web site: <http://www.tso.co.uk>

UNITED STATES OF AMERICA

Bernan Associates

4501 Forbes Blvd., Suite 200, Lanham, MD 20706-4391, USA
Telephone: +1 800 865 3457 • Fax: +1 800 865 3450
Email: orders@bernan.com • Web site: <http://www.bernan.com>

Renouf Publishing Co. Ltd.

812 Proctor Avenue, Ogdensburg, NY 13669, USA
Telephone: +1 888 551 7470 • Fax: +1 888 551 7471
Email: orders@renoufbooks.com • Web site: <http://www.renoufbooks.com>

United Nations

300 East 42nd Street, IN-919J, New York, NY 1001, USA
Telephone: +1 212 963 8302 • Fax: 1 212 963 3489
Email: publications@un.org • Web site: <http://www.unp.un.org>

Orders for both priced and unpriced publications may be addressed directly to:

IAEA Publishing Section, Marketing and Sales Unit, International Atomic Energy Agency
Vienna International Centre, PO Box 100, 1400 Vienna, Austria
Telephone: +43 1 2600 22529 or 22488 • Fax: +43 1 2600 29302
Email: sales.publications@iaea.org • Web site: <http://www.iaea.org/books>



IAEA

International Atomic Energy Agency

RELATED PUBLICATIONS

THERAPEUTIC RADIONUCLIDE GENERATORS:

$^{90}\text{Sr}/^{90}\text{Y}$ AND $^{188}\text{W}/^{188}\text{Re}$ GENERATORS

Technical Reports Series No. 470

STI/DOC/010/470 (233 pp.,2009)

ISBN 978-92-0-111408-2

Price: €45.00

A key requirement for the effective implementation of the therapeutic approach, based on the intravenous administration of radiolabelled compounds (radionuclide therapy), is the sufficient availability of radionuclides with appropriate physical characteristics. Based on their nuclear properties, ^{188}Re and ^{90}Y are considered among the most interesting radionuclides for therapy. Furthermore, they are produced through portable generators, which provide a crucial advantage toward ensuring a worldwide distribution of these radionuclides. This publication illustrates recent studies aimed at investigating efficient quality control methods to ensure both the radionuclidic purity of generator eluates, and the proper preparation of new target specific ^{188}Re and ^{90}Y radiopharmaceuticals for various clinical applications.